Vibrational Performance of Pedestrian Bridges Due to Human-Induced Loads

by

Roberto Leal Pimentel, MSc

A Thesis submitted to the Faculty of Engineering of the University of Sheffield for the degree of Doctor of Philosophy

September, 1997

Department of Civil & Structural Engineering
University of Sheffield

Abstract

The vibrational performance of footbridges due to human-induced loads has been investigated, based on modal and pedestrian tests carried out on three prototype footbridges. Analyses using calibrated finite element models of these structures were also conducted. All test structures presented natural frequencies within the range of excitations produced by pedestrians and were therefore suitable for investigating the applicability of some current guidelines for vibration performance. In addition, the inclusion of a footbridge made of glass reinforced plastic in the test programme enabled the performance of this new type of footbridge construction to be investigated.

The techniques of ambient excitation, impulse response using an instrumented hammer, and free-vibration decay were employed to obtain the modal properties of the test structures. The practicalities of using these techniques are discussed and improvements in their application are suggested.

Very good agreement was obtained between the experimental and the numerical results. The calibrated numerical models were employed to investigate ways of removing the natural frequencies of the structures from the common range of pedestrian excitation, thereby improving their vibration performance. The handrails were identified as a potential way to increase the stiffness and thus the natural frequencies of a structure. In addition, use of a catenary shape or pre-camber in combination with horizontal restraint at the bearings were also shown to be useful for increasing natural frequencies since beneficial axial effects are introduced. In the case of the glass reinforced plastic footbridge, it was shown that a selective distribution of mass, that could be conveniently added within the cells of the deck, was the best strategy for frequency tuning.

Guidelines for vibration performance are suggested, focusing on the definition of the pedestrian load and frequency ranges of interest, acceptability limits to vibration, treatment of multi-frequency component vibrations and vandal loading.

To my parents

To my wife

Acknowledgements

The author wishes to express his sincere gratitude to Professor Peter Waldron for his valuable supervision, continuous support, and constructive criticism throughout this study.

Having worked with site tests of pedestrian bridges, a task that is feasible only if carried out in group, the author would like to thank to several people for their help and participation in the tests: Professor W. J. Harvey, Mr G. Ripley and Mr T. Sullivan, from the University of Dundee; Mr A. Pavic, Mr M. Petkovski, Mr P. Reynolds and Mr D. Smith, from the University of Sheffield; and I. Makeev, Professor I. Gosav and Miss G. Michelatti, visitors at the University of Sheffield.

The financial support of the Conselho Nacional de Desenvolvimento Científico e Tecnológico - CNPq (Brazil), and the Universidade Federal da Paraíba (Brazil), sponsor and employer, respectively, is gratefully acknowledged, as well as the Engineering and Physical Sciences Research Council (UK), for financial support of one of the site tests.

The author would like to thank the Aberfeldy Golf Club, Blue Circle Industries plc, and Mosedale Construction Ltd for providing access to the test footbridges and permission for the tests.

Special thanks to my colleagues A. Pavic, M. Petkovski, P. Reynolds and M. Hartley from the Dynamics Research Group of the Department for the fruitful discussions and friendly support, which greatly contributed for this study to be concluded.

The assistance of T. Robinson, S. Waters and the technical and secretarial staff of the Department is also acknowledged.

Thanks are also due to Mrs Una Pierce for her patient correction of the thesis.

Finally, I am greatly indebted to my wife Marcia for her support, encouragement and patience throughout the years.

Table of Contents

List of Abbreviations

ACCS - Advanced Composite Construction System

ACM - Advanced Composite Materials

ANPSD - Average Normalised Power Spectral Density

AVS - Ambient Vibration Survey

CEB - Comite Euro-International du Beton

COMAC - Coordinate Modal Assurance Criterion

DFT - Discrete Fourier Transform

DTA - Dynamic Testing Agency

FE - Finite Element

FFT - Fast Fourier Transform

FRF - Frequency Response Function

GRP - Glass Reinforced Plastic

IDFT - Inverse Discrete Fourier Transform

MAC - Modal Assurance Criterion

MDOF - Multi-Degree of Freedom

PC - Personal Computer

PSD - Power Spectral Density

RMS - Root Mean Square

SDOF - Single Degree of Freedom

TMD - Tuned Mass Damper

VDV - Vibration Dose Value

List of Figures

List of Plates

List of Tables

Notation

| | - Indicates absolute value / amplitude of a complex variable

a(*t*) - Acceleration time response signal

a_{lim} - Acceleration limit

a_{max} - Maximum vertical acceleration

a_o, a_n and b_n - Fourier coefficients

a_{RMS} - Root mean square acceleration

A_c - Cross sectional area of a cable

$A_{jk}(f)$ - FRF inertance between points j and k

A_{RMS} - Root mean square of a signal

$b[\hat{\varphi}]$ - Bias error

B_e - Bandwidth of a discrete spectral function

B_r - Half-power bandwidth of the resonant peak **r**

C - Number of correlated mode shapes

C_{mf} - Crowd magnification factor

$E[\hat{\varphi}]$ - Expected value

E_c - Young's modulus of elasticity of the concrete

E_{cab} - Elastic modulus of the cable material

E_{eq} - Equivalent modulus of elasticity

E_s - Young's modulus of elasticity of the steel

f - Frequency

f_c - Non-aliased frequency range

f_{cab} - Estimated fundamental frequency of a cable

f_{nyq} - Nyquist or Folding frequency

f_o - First natural frequency of a footbridge in the vertical direction

f_p - Pacing rate

f_r - Natural frequency of the r^{th} mode

$f_{r_{cal}}$ - Calculated natural frequency of the r^{th} mode

$\bar{f}_r$ - Undamped natural frequency of the r^{th} mode

$\bar{f}_{r_{cal}}$ - Calculated undamped natural frequency of the r^{th} mode

f_s - Frequency range

f_v - Generic frequency of vibration of a structure

F_c - Cable Tension

$F_p(t)$ - Pedestrian forcing function

$F(t)$ - Notional pedestrian forcing function

g - acceleration of gravity

G - Weight of a pedestrian

G_{ff} - One-sided Power Spectral Density of the excitation

G_{xx} , G_{yy} - One-sided Power Spectral Density of the signals x and y, respectively

G_{xy} , G_{yx} - One-Sided Cross Spectral Densities

H - Frequency Response Function (FRF)

H1 and H2 - Estimators of the FRF

i - Square root of minus one

k_a - Configuration factor

k_l - Load distribution factor

k_p - Dynamic impact factor

K_{HL} , K_{HR} - Elastic stiffnesses of the bearings in the horizontal direction

K_{VL} , K_{VR} - Elastic stiffnesses of the bearings in the vertical direction

l - span length

ln - Natural logarithm

L_c - Cable length

L_{ch} - Horizontal projected length of the cable

m - Mass of a SDOF system

m_c - Mass per unit length of a cable

M - Total mass of a footbridge

n_d - Number of estimates in the averaging process

n_p - Number of pedestrians

n_s - Number of steps to cross the span

N - Number of samples of a discrete signal / number of frequency lines

$\ddot{q}_r(t)$ - Generalised acceleration modal coordinate function of the r^{th} mode

$\ddot{Q}_r(f)$ - Fourier Spectrum of $\ddot{q}_r(t)$

p - Number of mode shape ordinates

P - Amplitude of the sinusoidal excitation

P_r - Modal Force of the r^{th} mode

$P_s(a_{max})$ - Probability of synchronisation

R - Number of modes of vibration

S - Multiplying factor for footbridge response

S_{xx} - Power Spectral Density

S_{xy} - Cross Spectral Density

t - Time

t_p - Contact duration

T - Acquisition time / period of a signal or function

T_p - Period of the pedestrian load ($= 1/f_p$)

T_t - Total record length

$u_h(t)$ - Hanning window

v - Speed of the load

Var $[\hat{\varphi}]$ - Variance of an individual estimate $\hat{\varphi}$

W - Total weight of a footbridge

x , y - Generic (discrete) time signals

x_m - m^{th} component of the discrete time signal x

x(*t*)- Generic time domain function

$\ddot{x}_j(t)$ - Acceleration response time signal at coordinate j

X_n , Y_n - Generic component of the discrete Fourier spectrum of the signals x and y, respectively

X_n^* - Complex conjugate of X_n

X_{h_n} - Hanning-windowed n^{th} component of the discrete Fourier spectrum of a signal

X(f) - Generic (continuous) Fourier spectrum

$X^*(f)$ - Complex conjugate of X(f)

χ_n - Another version of a generic term of the discrete Fourier spectrum of the signal x

$\chi(f)$ - Another version of a generic (continuous) Fourier spectrum

X_o - Static or DC component (at f=0) of a discrete Fourier Spectrum

$\ddot{X}_j(f)$ - Fourier Spectrum of $\ddot{x}_j(t)$

y_s - Static deflection

$\alpha_{jk}(f)$ - FRF receptance between points j and k

α_n - Dynamic load factor of the n^{th} harmonic of the pedestrian load

δ - Logarithm decrement (damping)

Δf - Frequency increment or resolution (=1/T)

Δt - Time interval or sampling time

ε_{rd}- Normalised random error

ε_b - Normalised bias error

${}_r\phi_j$ - j^{th} ordinate of the r^{th} mass-normalised mode shape

γ^2_{xy} - Coherence function

γ_{cab} - Specific weight of the cable

γ_e - Decay coefficient of the exponential window

$\hat{\varphi}$ - Individual estimate

φ - True value of a variable

φ_n - Phase angle between harmonics of the pedestrian load

$\sigma[\hat{\varphi}]$ - Random error

Ω_d - Dynamic amplification factor

ψ_d - Dynamic response factor

ζ - Damping ratio

$\zeta_{r_{cor}}$ - Corrected equivalent viscous damping ratio of the r^{th} mode

$\zeta_{r_{cal}}$ - Calculated equivalent viscous damping ratio of the r^{th} mode

ζ_r - Equivalent viscous damping ratio of the r^{th} mode

Dummy indices:

k, j - indicates the coordinate / indicates the measurement point

m - indicates the component of a discrete function

n - indicates the term of a summation / indicates the component of a discrete function

r - indicates mode shape

Chapter 1

Introduction

1.1 Definition of the Problem

Engineers have been aware of vibration problems in bridges since the introduction of cast iron in the 18th century for the construction of such structures. One of the earliest cases reported in the literature refers to the collapse of a cast iron bridge in 1831 when it was crossed by soldiers marching in step (Tilly *et al.*, 1984). Another milestone in failures caused by vibrations was in 1940, with the collapse of the Tacoma Narrows bridge due to the effects of a moderate wind (Ross, 1984; BENCHmark, 1994). The solution for the first problem was simply to require troops to break step. In the second problem the excitation source obviously cannot be removed, and new design methods have been developed to prevent the collapse of bridges due to the dynamic effects of wind loading. Despite the two different sources of loading, both are examples of the same problem, that is the closeness between the frequencies of the excitation and the natural frequencies of the structure. This problem may also exist in low natural frequency bridges and footbridges due to excitation under normal pedestrian usage.

Highway bridges are unlikely to be subject to any serious vibrations caused by pedestrians since they are designed to support the much heavier loads associated with vehicular traffic. The research presented here therefore concentrates on footbridges, which are structures designed solely for the conveyance of pedestrians. The coincidence between the frequencies of excitation and the natural frequencies of the structure together with the low damping ratios normally associated with such structures may cause larger vibrations. On the other hand, since the human body is very sensitive to vibrations (Wright and Green, 1959; Smith, 1988), the level which causes disturbance to pedestrians is unlikely to be sufficient to cause structural damage. This is corroborated by several cases of users expressing concern over the vibration of footbridges reported in the literature, in which no damage to the structure occurred. Pedestrian induced vibrations may therefore be characterised as a serviceability issue, although it should be

noted that other actions such as deliberate excitation (i.e. vandalism) could cause risk to the integrity of the structure.

The load produced by a pedestrian walking has a static component, which is his weight, and a fluctuating component caused by the way the load is applied by each foot and by the load transfer mechanism between the feet. Similar patterns also occur for running or jumping. It is this fluctuating component which can cause significant vibrations in footbridges. Although the intensity of the load varies among pedestrians, the cadence or pacing rate has well defined frequency ranges, which makes it possible to identify the footbridges that can potentially be subject to vibration problems.

A comment by Smith (1969) related to pedestrian sensitivity to vibrations is worth mentioning: " *...and it seems that one of the most important factors is the psychological one of fear that a vibrating bridge is in danger of collapse. Experience and conditions would probably help to convince the public eventually that this is not necessarily true. However, it is recognised that, in view of the possibility of very slender and flexible structures being built, an upper limit of vibration should be suggested*". Opinions may diverge on how onerous the vibration serviceability recommendations should be. However, despite the fact that the presence of a pedestrian on a footbridge is a short term event and the problem is based on comfort issues, a criterion should be established; otherwise the structure may have its primary function compromised.

Attention is paid to this problem by various codes of practice and guidelines. However, their approaches diverge not only in adopting different limits for sensitivity to vibrations but also in how the problem should be tackled. This is an indication of continuing uncertainty in dealing with the pedestrian-induced vibration problem. In some of the codes, such as UK (BS5400, 1978) and Ontario (OHBDC, 1991), more detailed recommendations are presented. These include the definition of limits for sensitivity to vibrations, which are based on peak accelerations, a definition of the pedestrian load and a procedure for calculating accelerations due to the application of such a load. The maximum acceleration produced must be within the proposed limits. Nevertheless, discrepancies between the calculated accelerations using these codes and measured

accelerations in footbridges from controlled pedestrian tests have been reported (Cheung, 1984; Eyre and Cullington, 1985).

In addition, recent lightweight footbridges have been constructed using advanced composite materials (ACM) such as glass or carbon-fibre reinforced plastic. One of the advantages of ACM is its high strength to weight ratio, which reduces the self weight of the structure and makes handling and installation much easier (Mufti *et al.*, 1991). However, this much reduced self weight requires that attention should be paid to the dynamic performance since such ACM structures may be more susceptible to vibrations. Investigating the applicability of the present vibration serviceability guidelines to this type of structure is necessary mainly due to the lightness of the construction material when compared to footbridges made of conventional materials.

Recent advances in instrumentation have facilitated investigations into the dynamic behaviour of structures. Obtaining natural frequencies, mode shapes and damping values from tests and using these results to calibrate analytical models is the subject area of modal testing, which encompasses several test techniques and has been used for testing civil engineering structures, including footbridges. These techniques are based on the well established theory of modal analysis, which assumes a linear behaviour of the structure. Since the serviceability problem under investigation is related to low level vibrations, such an assumption is generally satisfied and modal testing provides a powerful tool in the investigation. However, there is still little experience in applying some of these techniques to testing open space footbridges reported in the literature.

1.2 Objectives and Implementation

The general aim of this thesis is to contribute to a better understanding of the vibrational performance of pedestrian bridges due to human-induced loads, including a revision of present guidelines on the vibration performance of these structures. The dynamic behaviour of newly constructed ACM footbridges is also investigated. The specific objectives are as follows:

- To analyse the present guidelines for the vibration serviceability limit state of pedestrian bridges due to human-induced loads, based on a literature review of the recent research developments in this area, tests carried out on pedestrian bridges and simulations using numerical models of these test structures.

- An investigation into the dynamic behaviour of ACM footbridges, by testing a prototype ACM footbridge. This includes checking the applicability of the present vibration serviceability guidelines to the design of such structures and an assessment of the feasibility of designing ACM footbridges considering their vibrational behaviour.

- An investigation into general aspects of modelling footbridges and ways of improving the design of the test structures in terms of vibration performance by using their numerical models calibrated against test data.

- An assessment of the applicability of modal test techniques, namely the ambient vibration survey, the impulse response technique using an instrumented hammer, and the free-vibration decay, for obtaining the dynamic properties of the test structures.

These objectives are pursued by site tests and numerical analyses of three pedestrian bridges. The test structures comprise a single span composite footbridge, a single span stressed ribbon concrete footbridge and a three span ACM cable-stayed footbridge. These structures were found very suitable for this investigation since they have natural frequencies within the range of frequencies of the excitations produced by pedestrians. The numerical models of the structures, calibrated against these test data, will make it possible to suggest methods for improving their present vibrational performance.

The equipment available for the site tests included accelerometers, an instrumented hammer as a source of excitation, a spectrum analyser for data acquisition and initial processing, and a PC notebook. The data collected was further processed using Modent/Modesh software (ICATS, 1995), spreadsheets and digital filters, and their application will be discussed throughout the thesis. For the numerical analysis, the finite element (FE) package ANSYS 5.0 was employed. This software enables various

dynamic analyses to be performed, including the calculation of natural frequencies and mode shapes, and also modal and time response analysis (ANSYS, 1992). Furthermore, it also enables the pedestrian load to be modelled for those analyses requiring the response of the structure to such loads.

1.3 Outline of the Thesis

A literature review regarding the pedestrian load and general aspects of vibration serviceability of footbridges is carried out in Chapter 2, to provide background knowledge about the subject. A characterisation of ACM footbridges is also included. The literature review is extended into Chapter 3, in which the principal details regarding signal processing and the experimental techniques adopted for the modal testing of pedestrian bridges are described. The procedures for applying these techniques are detailed, based on the literature review and also on experience acquired during the tests.

The following chapter deals with the tests, data processing and preparation of the calibrated numerical models of the three test footbridges, each being treated in a separate section. Experience acquired in modelling the structures is discussed. The vibrational performance of each footbridge is analysed and methods for improving their dynamic performance are investigated using the calibrated models where applicable.

An analysis of the present vibration serviceability guidelines is carried out in Chapter 5, based on the test results and the current state of knowledge identified in Chapter 2. The applicability of such guidelines to lightweight footbridges is subject to particular attention.

Conclusions and suggestions for further work are presented in Chapter 6. An Appendix is added, describing in more detail the equipment used for testing.

Chapter 2

Human-Induced Loads and Vibration Performance

2.1 Introduction

Vibration problems in footbridges can be caused either by wind or human action. Due to the former, long span lightweight footbridges may be subject to stability problems or experience excessive displacements that can cause disturbance to the pedestrians. Due to the latter, a risk of compromising structural integrity caused by vandalism or vibration serviceability caused by human footfall are the principal design issues. These issues are the subject of this study and are covered in a literature review carried out in this chapter. The subject is interdisciplinary by nature, involving studies of human locomotion, sensitivity to vibrations and structural dynamics.

Initially, a review of human-induced loads is carried out in Section 2.2, focusing attention on the human motions of interest for footbridges. The vibration performance of footbridges is analysed in Sections 2.3 and 2.4, covering the issues of vibration serviceability and vandal loading, respectively. In Section 2.5, several measures which can be employed to limit excessive vibrations in footbridges are described. Concluding remarks are presented in the final Section summarising the topics in which further research was found to be necessary.

2.2 Human-Induced Loads

In this Section, human activities are characterised and suitable mathematical models are established to represent them. Attention is first focused on the characterisation of the motions and loads produced by a single person, followed by loads produced by groups of people.

2.2.1 Characterisation and Modelling of Human Activities

Human activities of walking, running, jumping, bouncing in contact with the surface and lateral swaying are the motions of interest as sources of dynamic excitation in footbridges. Walking is the most common activity considered in design since it is related to the normal use of a footbridge. Running, on the other hand, could generally be seen as a peripheral activity, whereas the motions of jumping, bouncing and lateral swaying are related principally to deliberate excitation. A high variability in human movements among individuals is to be expected and a characterisation and modelling of such movements is most meaningful if seen as an average of results obtained from several individuals.

Walking

According to Inman *et al.* (1994), there are two basic requisites to characterise the act of walking: continuous reaction forces to support the body (i.e., there is always at least one foot in contact with the ground), and periodic movement of each foot from one supporting point to the next in the direction of the movement. This involves a brief stage when both feet are on the ground, during the period when the support of the body is transferred between the legs. These requisites are always observable and are the key point in investigating and modelling the forces produced by this motion.

The magnitude of these forces is modest when compared to static design loads. However, their fluctuating components generated by specific motions of the body may cause significant vibrations. The forces are actually generated in three axial directions. In the vertical direction, they are due to up and down movements as the body passes over a supporting leg and descends as this leg passes behind. Wyatt (1989) mentioned body accelerations of the order of 3 m/s^2 and typical displacements of 50 mm related to this rise and fall. In the lateral direction, the forces are caused by the periodic sway of the body weight from one leg to the other. These two aforementioned forces are the ones of most interest as sources of excitation in footbridges although there are also forces applied in the longitudinal direction. Inman *et al.* (1994) gives a good example of how to notice the latter in the case of a person carrying a shallow pan of water. The water

moves backward and forward as a result of the alternating accelerations and decelerations of the body in the longitudinal direction.

The early studies in measuring the aforementioned forces were carried out with purposes other than investigating their effect on structures. Using an instrumented force plate installed in a rigid platform, Harper (1962) measured vertical and longitudinal forces from a footstep, to investigate the slipperiness of floor finishes. Galbraith and Barton (1970) used a similar test device to measure the vertical footstep load-time history, in order to obtain data as part of a study to improve detection of intruders by sensing signals from footsteps. The latter carried out a more detailed investigation regarding the effects of shoe type and wearing surface on the load, and concluded that they had a minor influence. The load was shown to have a typical saddle shape, where the first peak corresponded to the heel strike, the trough was related to a lowering of the trunk as the swinging leg passes the supporting one, and the second peak corresponded to the toe lift-off (Fig. 2.1). For a given pacing rate, this shape was found to be similar for different subjects, but the amplitude increased with the subject's weight. The similarity in shape is due to the basic mechanisms of walking common for all subjects as already discussed.

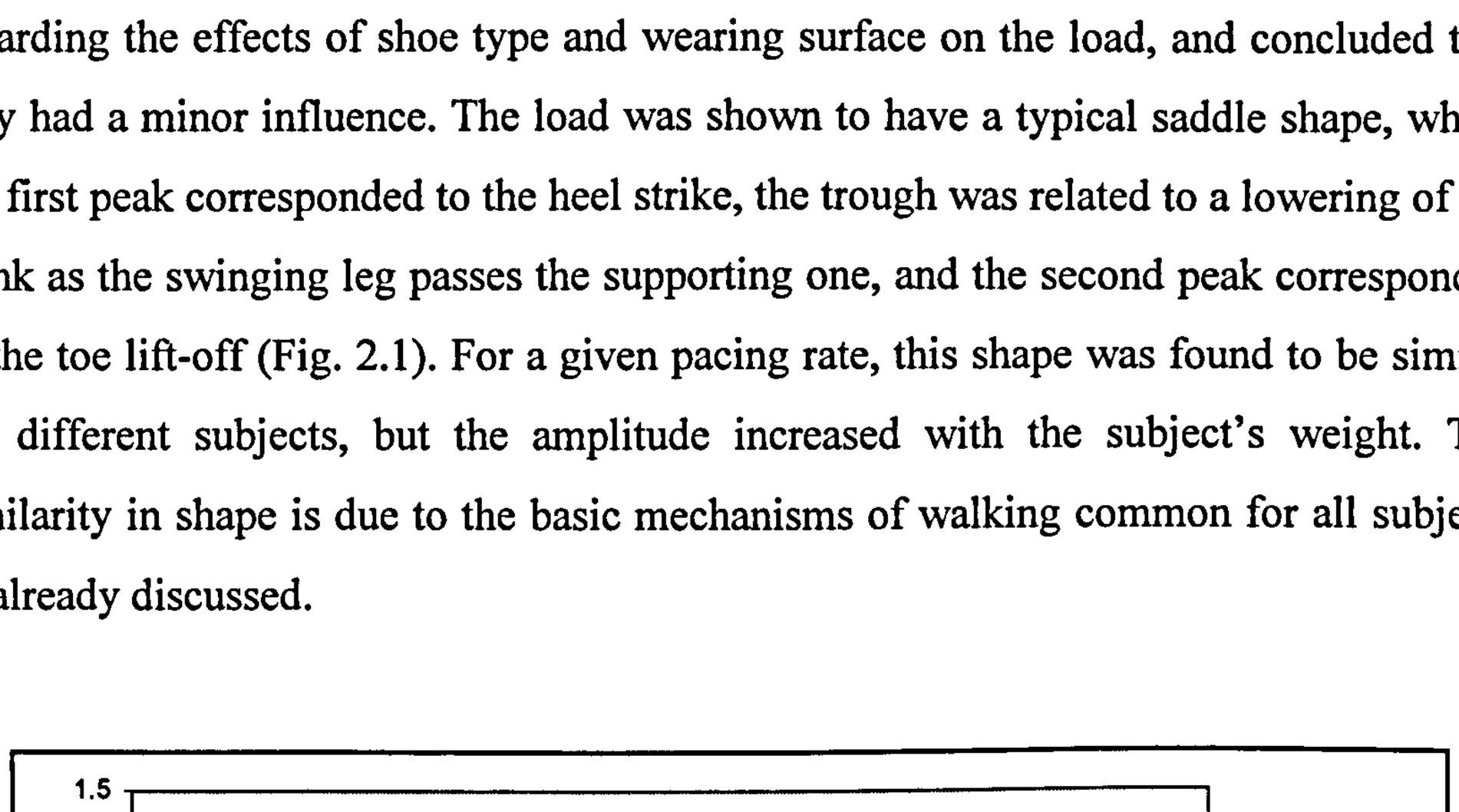

Figure 2.1 - Illustration of the vertical load from footsteps (after Bachmann and Ammann, 1987)

Galbraith and Barton (1970) showed that the pacing rate also influenced the shape of the load. For slow pacing rates of the order of one step per second, or 1.0 Hz, there was no fluctuation of the load around the static weight of the subject. With increasing pacing rates, a point is reached at which only one foot is in contact with the ground at any time. At this stage, the two peaks of the saddle degenerate into one and the subject is said to have started running. An investigation into typical pacing rates of pedestrians was conducted by Matsumoto *et al.* (1972), using more than 500 randomly chosen test subjects. The pace distribution was found to have an almost Normal distribution[1] with a mean value of 2 Hz and a standard deviation of 0.178 Hz. A practical range for pacing rates can be set from 1.6 to 2.4 Hz (Figure 2.2). Similar results from other studies were cited by Eyre and Cullington (1985) and by Bachmann and Ammann (1987), and the effect of pacing rate on other parameters such as forward speed and stride length were presented by Wheeler (1982).

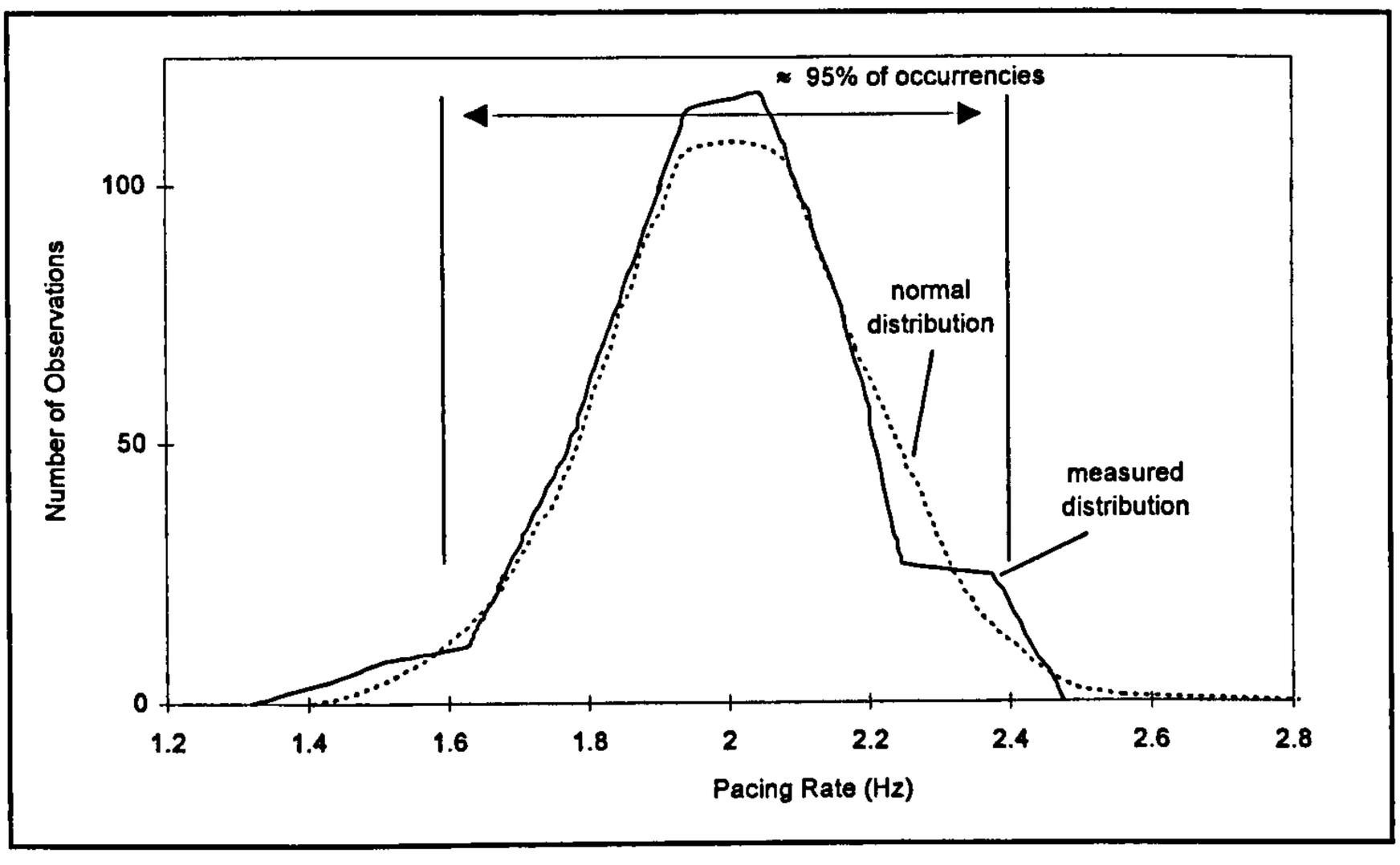

Figure 2.2 - Distribution of pacing rates of pedestrians (after Matsumoto *et al.*, 1972)

The walking load is a summation of the load produced by continuous paces and may be simulated by creating pulse trains of single footstep loads. This assumes that the load from each footstep is approximately the same and that the time the feet overlap is kept

---

[1] The Normal distribution is a probability density function associated with random processes having a finite mean and deviation. Any distribution having a finite mean and deviation is essentially Normal if the number of samples is sufficiently large (Gray and Odell, 1970). In this particular case, the pacing rate of the pedestrians is the random process.

constant for a given pacing rate, i.e. the load has a periodic nature. The first assumption was shown to hold true from measurements done by Ohlsson (1982). Furthermore, Inman *et al.* (1994) described the walking cycle as having a reasonable periodic nature and presented a chart in which the duration of the overlap stage was shown in terms of a percentage of the duration of two successive footsteps. Recent results from Ebrahimpour *et al.* (1996) have also shown that the ratio between the duration of overlap and footstep remains somewhat constant for the typical range of pacing rates of pedestrians, enabling the pulse train for any given pacing rate to be created.

However, the determination of the walking load has usually been carried out indirectly, by measuring vibrations caused by it on structures with well-known dynamic properties. It should be noted that in this case the load from each footstep cannot be determined; instead, it is the total load that is established, although such a load is not actually applied at a single position at a time, i.e. the gradual transferring of load applied by each foot at successive positions cannot be represented.

The fact that the walking load satisfies the Dirichlet conditions (Sneddon, 1969) enables its representation by means of Fourier series. Briefly, these conditions state that a function (e.g. the walking load) must have a finite number of maxima and minima, and a finite number of (finite) discontinuities within its interval of periodicity. Use of the Fourier series requires the load to be decomposed into distinct harmonic components. The predominant first harmonic has a frequency equal to the pacing rate. The addition of a few higher harmonics, the frequencies of which are multiples of the pacing rate, was found to be sufficient for an accurate representation. The nature of the load, being a summation of a static component, which is the weight of the pedestrian G, plus a fluctuating component, enables it to be expressed in terms of a Fourier series as:

$$F_p(t) = G + G\alpha_1 \sin(2\pi f_p t) + G\alpha_2 \sin(4\pi f_p t + \varphi_2) + G\alpha_3 \sin(6\pi f_p t + \varphi_3) + \ldots \quad (2.1)$$

where t is the time, f_p is the pacing rate, α_n is the so called dynamic load factor of the n^{th} harmonic of the load, and φ_n is a phase angle that can be seen as representing a time shift with respect to the first harmonic. The determination of the dynamic load factors is usually carried out by analysing the response signals in the frequency domain, where the

contribution of each harmonic can be identified and isolated. Details about this procedure will be further discussed in Section 5.2, and values obtained from several sources are presented in Table 2.1 .

Dynamic Load Factors for the First Harmonics										
α_1								α_2		
1.5	1.6	1.75	1.8	2.0	2.2	2.4	2.5	2.0	2.3	← Pacing Rate (Hz)
			0.257							Smith (1996): tests on a gait machine.
0.18+	0.2	0.32+	0.33+	0.4+	0.48+	0.52		0.15+	0.24	Rainer and Pernica (1986); Pernica (1990): tests on a 17 m long platform. Average from 3 subjects.
				0.4		0.5		0.1		Bachmann and Ammann (1987): reported values from previous work.
0.18*		0.25		0.34*			0.51*			Ebrahimpour *et al.* (1996): forces directly estimated from tests on a platform. Average of 40 tests.

+ - values taken from a chart
* - values obtained from simulations

Table 2.1 - Dynamic load factors for the walking load in the vertical direction

The results in Table 2.1 show that the load factors vary with the pacing rate. The results from Rainer and Pernica (1986) are compatible with those reported by Bachmann and Ammann (1987); both of these are generally a bit higher than those from the other reported tests.

Eriksson (1994) also conducted tests for determining forces from walking in the vertical direction using a 10-metre long platform having a fundamental frequency of 8 Hz. His approach was to represent the forces as a function in the frequency domain instead of a time domain representation as in Eq. 2.1. Although based on some assumptions, a comparison is possible between his results and those compiled in Table 2.1, but will be left for discussion in Section 5.2. His results were also useful to show that the amplitudes of the first and second harmonics of the load varied with the pacing rate in a different fashion. Whereas an increase on the amplitude was observed for the first harmonic with increasing pacing rate, somewhat constant values for the amplitudes of the higher harmonics were observed for different pacing rates. This latter observation is however in disagreement with the variation of the load factor α_2 observed in Table 2.1 .

A disagreement also exists on the evaluation of the phase angles φ_2 and φ_3 (Eq. 2.1). Rainer and Pernica (1986) evaluated these angles as 90° and 0°, respectively. On the other hand, Bachmann and Ammann (1987) reported the phase angles exhibiting a large scatter and suggested a value of 90° for each as a reference for computations. Beyond the immediate discrepancy in the numerical value of φ_3 , they also defined these angles as subtractive terms instead of the additive terms adopted by Rainer and Pernica and presented in Eq. 2.1. This implies that the evaluations of the angle φ_2 were also in disagreement. However, if the analysis is such that the interest is on the effect of only one harmonic at a time, the phase angles become unimportant.

Plots of the walking load using Eq. 2.1, adopting the first two load factors from Table 2.1 and the aforementioned values for the angle φ_2 , are shown in Fig. 2.3. Another plot of the load arising from individual footsteps is also shown for comparison. Representations of the load using other Fourier series are possible like the half-range cosine series adopted by Allen and Murray (1993); however, Eq. 2.1 is the representation usually employed in practice.

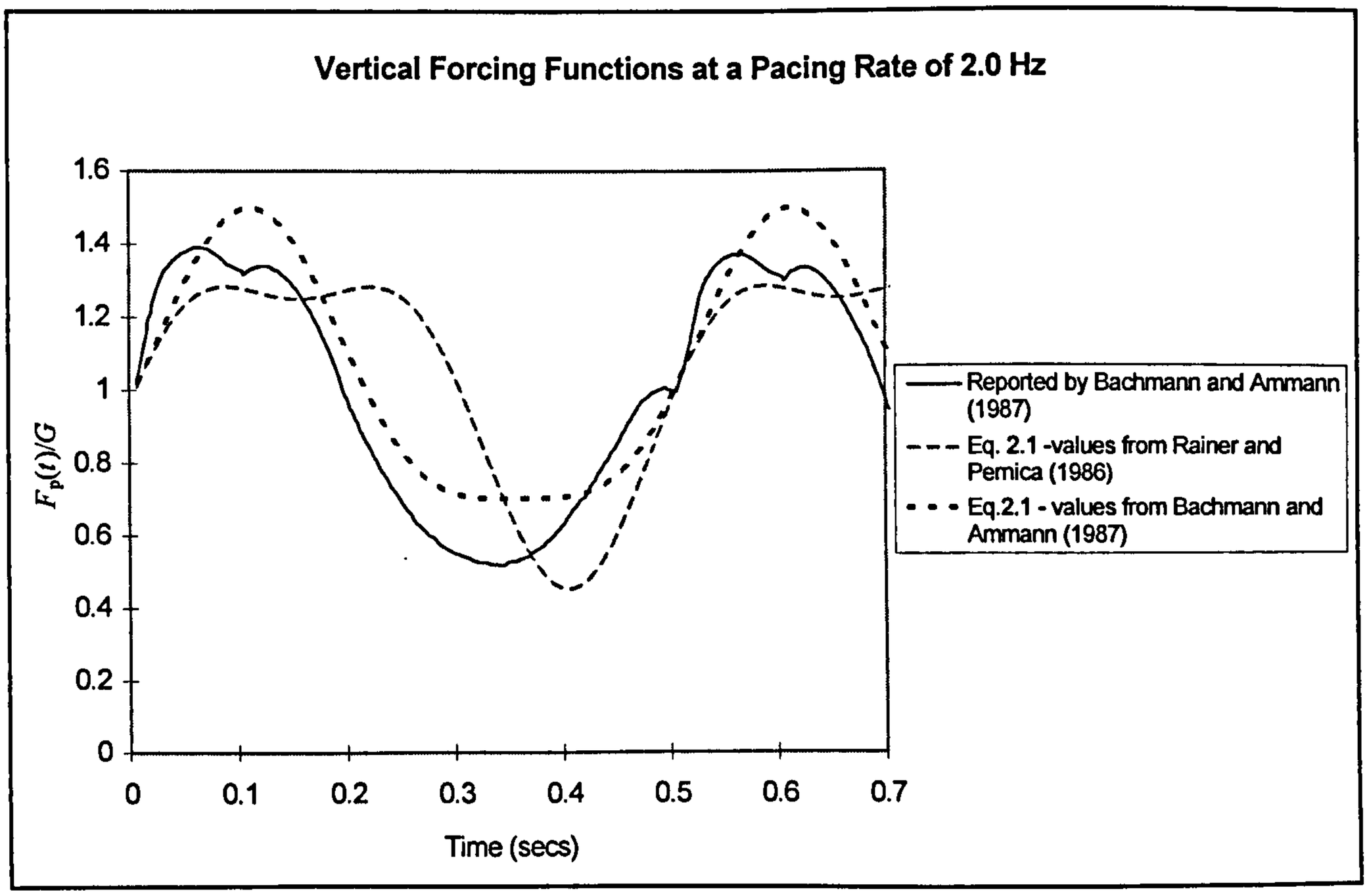

Figure 2.3 - Representation of the walking load in the vertical direction

The typical motions of the body during walking also produce periodic forces in the lateral direction. The basic frequency associated with this motion is half of the person's pacing rate, since two steps are necessary for a cycle of the body in the lateral direction to be completed. The typical frequency range for the first harmonic of the lateral load is thus from 0.8 to 1.2 Hz.

Investigations of the forces exerted in the lateral direction are much scarcer than in the vertical direction. The only reference found was the work of Schulze, reported by Bachmann and Ammann (1987). The latter mentioned that tests were carried out using one test subject walking at a pacing rate of 2.0 Hz. The magnitude of the first harmonic of the lateral load was smaller by one order of magnitude than that of the first harmonic in the vertical direction.

Running

Running is a motion related to a higher pacing rate than walking. Transferring from walking to running does not occur at a precise pacing rate since activities such as brisk walking and jogging (slow running) could be developed at the same pacing rate. However, a point is reached at which the load transfer mechanism between the feet is such that there is a discontinuous ground contact characterising a running movement. Galbraith and Barton (1970) showed that at this stage the footstep load changes to a typical sharp peak, resembling a half-sine sinusoidal function (Fig. 2.4).

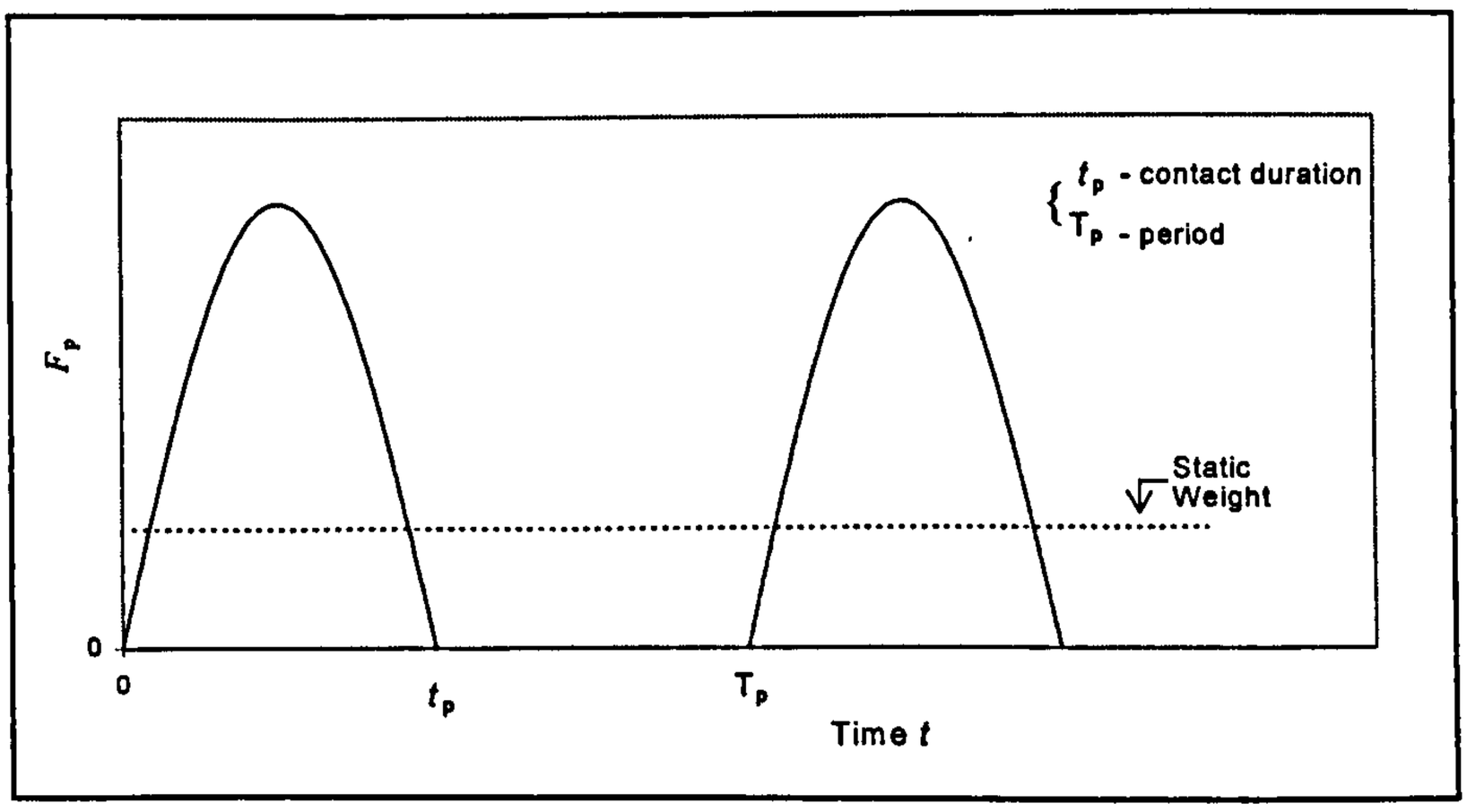

Figure 2.4 - Sketch of the forces due to running (after Wheeler, 1982)

Typical distributions of pacing rates for running are not explicitly mentioned, perhaps due to the fact that people do not naturally choose this motion as their usual way of locomotion. Wheeler (1982) reported that pacing rates as high as 5.0 Hz, related to forward speeds of 7 to 8 m/s, are unlikely to be attained by an untrained runner. Eriksson (1994) cited Baumann and Bachmann as suggesting ranges from 2.4 to 2.7 Hz for normal running and up to 3.2 Hz for intensive running. Tilly *et al.* (1984) reported that pacing rates higher than 3.5 Hz are rare on public footpaths.

A general mathematical representation of the pedestrian load as a half-sine model was proposed by Wheeler (1982), which can be adopted to represent the load due to running. In a similar way, Bachmann and Ammann (1987) defined a function as a sequence of semi-sinusoidal pulses, which, for one period, was given by:

$$F_p(t) = \begin{cases} k_p\, G\, sin(\pi\, t/t_p) & \text{for } t \le t_p \\ 0 & \text{for } t_p < t \le T_p \end{cases} \qquad (2.2)$$

where k_p is a dynamic impact factor, t_p is the contact duration, T_p is the period being equal to the inverse of the pacing rate (see Fig. 2.4), and the other parameters are as defined in Eq. 2.1. The dynamic impact factor and contact duration can be obtained from a chart presented by Wheeler(1982) as a function of the pacing rate (Fig. 2.5). Bachmann and Ammann (1987) also developed a theoretical relation between the dynamic impact factor and the ratio t_p/T_p , based on the condition that the integral of the load-time function over one period should equalise the integral of the static weight over the same period (i.e., the impulse of the resultant force is nil). This expression is shown in Fig. 2.6 but agreement with data from Wheeler's curves (Fig. 2.5) was found only for pacing rates around 3.0 Hz.

Alternatively, a Fourier series similar to that used to represent the walking load (Eq. 2.1) could be employed to represent the running load. Rainer and Pernica (1986) showed that the load also contained distinct frequency components which are multiples of the pacing rate, although it would be expected that a higher number of harmonics would be needed to represent the sharp variations of the load within the period. Rainer and Pernica also mentioned that the phase angles of each harmonic were not as clearly defined as those

for walking and, indeed, they did not report them. However, as was mentioned in the discussion of the walking load, the phase angles are only of importance if the simultaneous effect of more than one harmonic is needed for the analysis. The dynamic load factors were evaluated in a similar way to those for the walking load, the load factor for the first harmonic varying approximately from 1.3 at a frequency of 2.5 Hz, to a maximum of 1.5 at a frequency of 3.6 Hz. It can be noted that such a variation is not as significant as that reported for the load factor of the first harmonic of the walking load, this trend being in agreement with measurements carried out by Eriksson (1994).

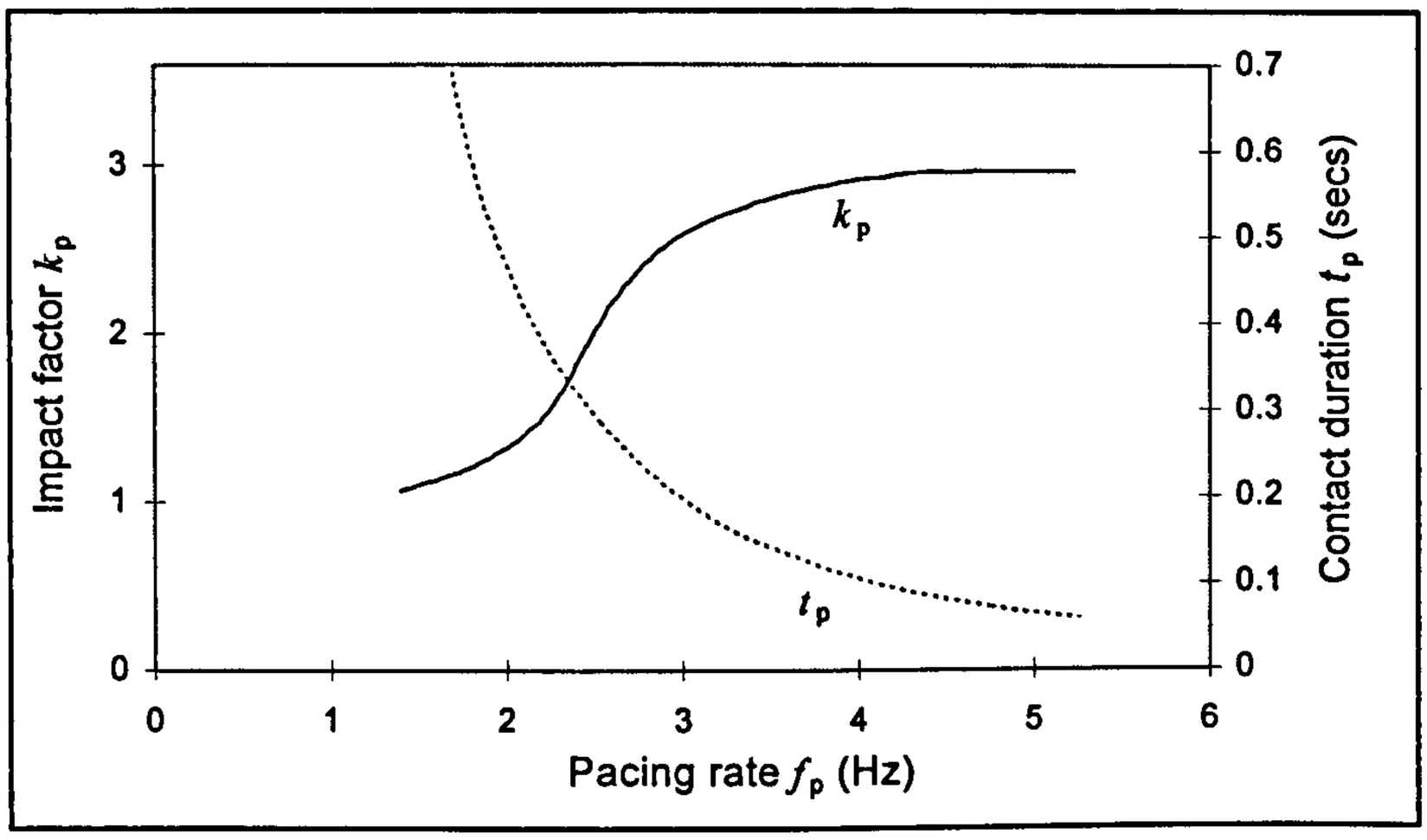

Figure 2.5 - Impact factor k_p and contact duration t_p as a function of the pacing rate (after Wheeler, 1982)

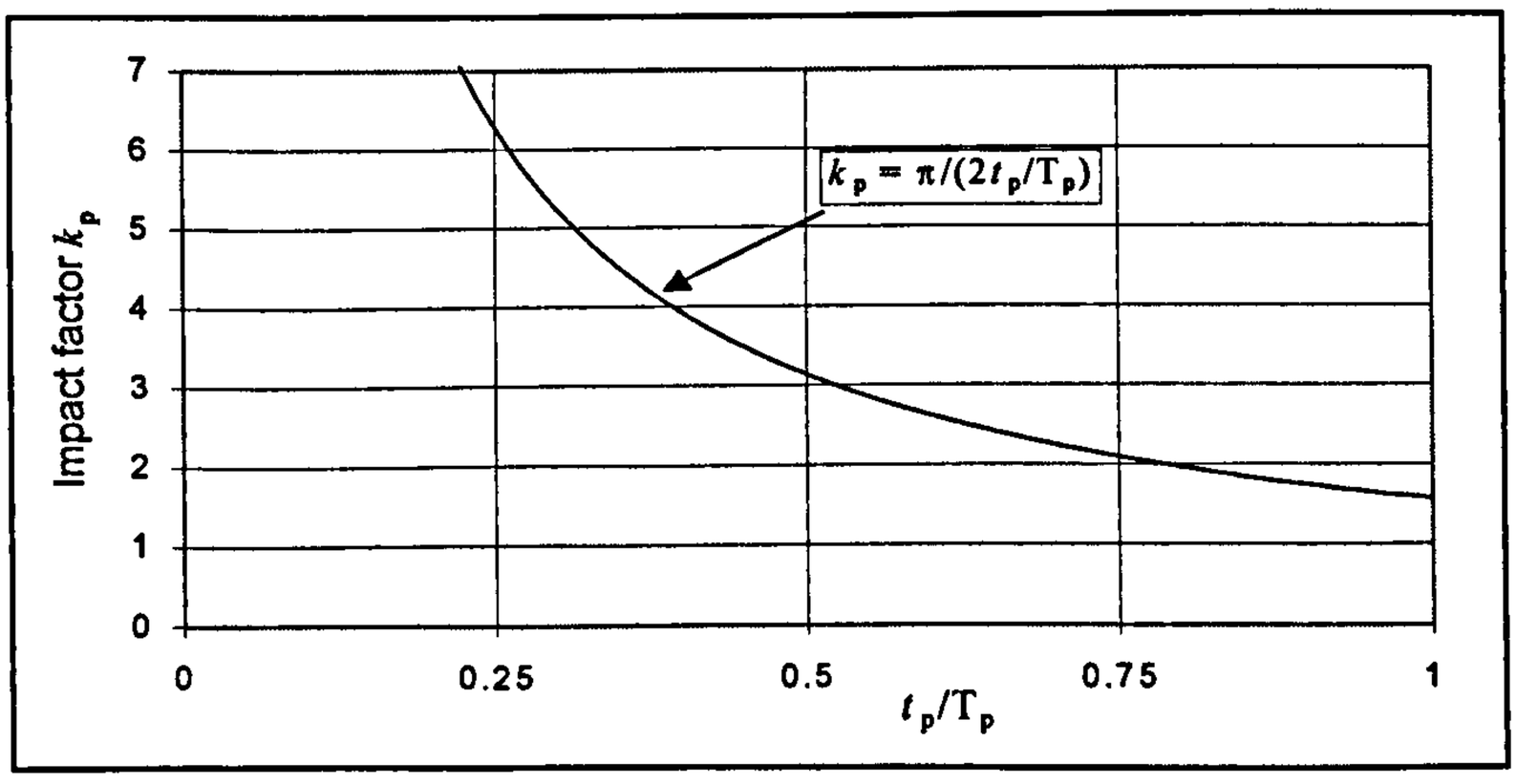

Figure 2.6 - Theoretical impact factor as a function of the ratio t_p/T_p (after Bachmann and Ammann, 1987)

Bachmann and Ammann (1987) also suggested a Fourier series expression for the load, based on cosine functions, the frequency of each being a multiple of the pacing rate, and having equal phase angles expressed as a function of the contact duration t_p . This would again make the use of Wheeler's chart (Fig. 2.5) necessary in order to obtain this value for a given pacing rate.

Other activities

Jumping is a human motion extensively studied due to the fact that it produces forces of high magnitude, and its consideration is essential in floors and other structures subjected to rhythmic activities. In the case of footbridges, however, this motion is related to deliberate excitation.

The amplitude of the body motion and the duration of what Wyatt (1985) called the "*free flight*" phase of jumping is controlled by the force of gravity and the muscular strength of the jumper, and this somehow establishes practical limits for jumping rates. Wyatt referred to rates between 1.5 to 2.5 Hz for reasonable jumps while Bachmann and Ammann (1987) suggested a range between 1.8 to 3.4 Hz for calculation purposes, mentioning that it is unlikely human physiology permits rates higher than 3.5 Hz.

Forces due to rhythmic jumping have the same pattern as those for running (Fig. 2.4) and can be mathematically represented in the same way (Eqs. 2.1 or 2.2). However, the different nature of the motion demands specific evaluations of dynamic load factors and phase angles if using Eq. 2.1, or dynamic impact factor and contact duration if using Eq. 2.2.

With regard to applying Eq. 2.1, tests carried out by Pernica (1990) showed that the first dynamic load factor had an average value of around 1.7, this value being reasonably constant for jumping rates between 2.0 and 3.0 Hz and reducing beyond these limits. Values of about 1.0 were determined for the second dynamic load factor, but phase angles, however, were not reported.

For applying Eq. 2.2, the contact duration t_p needs first to be defined for different jumping rates, although this has been rarely reported. Values for a few jumping rates

were reported by Bachmann and Ammann (1987) and measured by Ellis and Ji (1994). With regard to the dynamic impact factor k_p, the latter authors in a companion paper (Ji and Ellis, 1994) mentioned experimental evidence to support, for rhythmic jumping, the use of the theoretical expression presented by Bachmann and Ammann (Fig. 2.6). Furthermore, and taking this expression into account, they developed a theoretical parallel between the Eqs. 2.1 and 2.2, obtaining formulae for the dynamic load factors and phase angles as a function of the period of the load and contact duration, which held true against jumping tests carried out by them.

Beyond the practical frequency range mentioned for jumping, a person would have difficulty in sustaining continuous movement. In these outer frequency ranges, a similar source of excitation might come from bouncing up and down without losing contact with the surface, by flexing the knees. Although the previous expressions for jumping have not been checked for this motion, the fact that the person does not leave the surface implies lower forces being applied. Consequently, expressions developed for jumping could be conservatively employed.

To conclude the survey of human motions of interest, another motion related to deliberate excitation can be identified, which is lateral body swaying. Not to be mistaken for the natural lateral sway of the body when walking, the mathematical representation of this motion has not been fully investigated. The only similar reference found is related to the body swaying while being seated or standing, actually applicable for human motions in concerts or social events (Bachmann *et al.*, 1995).

Human-Structure Interaction

As was mentioned before, an indirect determination of the characteristics of the human motions described may be carried out by measuring the response of platforms or structures subjected to them. These test structures are usually constructed in order to have natural frequencies higher than those of the human activity to be measured, the idea being to avoid the vibrations of the test structure interfering significantly with the measurements. This enables the applied loads to be treated as quasi-static and thus to associate them directly to the measured response without need of including the

dynamics of the test structure in the analysis. However, correction factors have been employed to account for the small distortions caused by the vibrations of the structure (Rainer and Pernica, 1986; Pernica, 1990). The dynamics of the test structure were also taken into account by Eriksson (1994); however, the test platform employed by him had a fundamental frequency of 8 Hz, which was also higher than the frequencies of the first harmonics of the excitation. These test platforms were intentionally of sufficient stiffness to experience vibrations of only negligible amplitude, being an alternative to the direct measurement of the load by means of force plates.

However, these loads are studied and modelled so they may be applied in the design of structures in order to investigate their dynamic performance. These structures may have natural frequencies closer to the first harmonics of the load and experience vibrations of significant amplitude. How this would modify the loads determined from tests on rigid surfaces is still unclear. This question, raised since the early tests to determine dynamic load factors (Blanchard *et al.*, 1977), has also been discussed by other researchers. Tests carried out by Ohlsson (1982) on floors having natural frequencies above 20 Hz showed a drop in the force components at frequencies near to the resonance of the structure. He explained this by looking at the mechanics of the footfall force, in which the initial part of a footfall force pulse would be caused by the human system, which is 'falling' at the surface. The late part of the force pulse would probably be more dependent on the muscle forces. Low stiffness and resonant frequencies of the structure would change the contact force. It is possible that this could also happen in resonance conditions at lower natural frequencies, which would imply reductions in the forcing function.

Another aspect of the problem comes from the potential disturbance that the vibration of the structure may cause to the movement of the pedestrian. In practice, this may cause difficulty in keeping a rhythmic step rate, the outcome of which would be a reduction of the vibrations caused by the pedestrian. Bachmann and Ammann (1987) mentioned that vertical vibration displacements of more than 10 or 20 mm appeared to cause difficulty in keeping to one's usual step rate but they did not relate this to modifications on the mathematical representation of the load.

A final aspect to call attention to is the full interaction between humans and the structure, considering the former not only as the source of applied load but also as a dynamic system. In investigations on floor vibrations, Eriksson (1994) pointed out that for low frequency floors this effect can probably be ignored as the weight of the floor system is large compared to the weight of the pedestrian. On the other hand, Eyre and Cullington (1985) reported that test subjects standing on a bridge contributed to the damping of the system, from which interaction could be inferred. However, the interaction for moving individuals was not investigated in their work.

Other research involving measurements on a lightweight beam having a natural frequency of 18.68 Hz identified the human presence as an additional mass-spring-damper (dynamic) system (Ellis and Ji, 1994). However, these researchers only showed that this holds for standing subjects, always in contact with the structure. When people were jumping, stamping and running on the spot, their mass was not vibrating with the structure and they were found to act as a load only. This leaves for further discussion the case of walking, in which the subject is always in contact with the structure.

Conversely, in a subsequent paper, Ellis and Ji (1997) mentioned the walking pedestrian as also acting as a load only. Their tests were again carried out on the aforementioned beam, in which the test subject was asked to walk on the spot at mid span. Measuring the natural frequency of the structure with and without the test subject performing the activity resulted in the same figure, from which the authors concluded that the pedestrian was acting as a load only. To some extent, this contradicts the idea that the permanent contact between subject and structure would imply an interaction between the two dynamic systems. Nevertheless, their test set-up may not be representing adequately the actual situation of a pedestrian walking along on a low natural frequency footbridge, in which higher vibration amplitudes could induce pedestrian-structure interaction.

2.2.2 Effect of Groups of People

The presence of several pedestrians on a footbridge is a common situation. Two cases need to be considered in the design: the effects of large groups of people walking (crowd loading), and a smaller group of people deliberately trying to excite the

structure. Early studies on the effects of groups of people have shown that, in general, evaluating the total load as the load due to a single person multiplied by the number of people involved is a rather conservative approach.

Walking

Several factors need to be considered with regard to the walking load produced by a crowd: variability in pedestrian weight and pacing rate; phase differences among the pedestrians, even for those who walk at the same pacing rate; density effects, which can prevent a free walk; and synchronisation among the pedestrians, due to their proximity to each other and vibration of the structure. These individual factors are also interrelated, e.g. density effects and pacing rate, or synchronisation and phase differences. The complexity of the problem is usually tackled by taking simplifications and adopting a stochastic analysis since some of these factors can be described in terms of probabilities.

The investigations into crowd loading usually depart from the load due to an individual and attempt to relate to it the load produced by the crowd. One of the first results of practical significance was published by Matsumoto *et al.* (1978). The probability of pedestrians arriving at a footbridge was investigated as a first step to a stochastic analysis of the response of the structure to several pedestrians. The number of people who crossed a prototype footbridge during one day was taken as a basis for considering the arrival as a random phenomenon, following a Poisson distribution[2]. It was shown that, for a common given pacing rate and pedestrian weight, the theoretical mean vibration amplitude in the vertical direction due to several pedestrians could be determined by multiplying the mean vibration amplitude due to one pedestrian by the square root of the number of pedestrians n_p on the structure at any time. This coefficient of magnification is called here a crowd magnification factor C_{mf}, being given by:

$$C_{mf} = \sqrt{n_p} \tag{2.3}$$

---

[2] The Poisson distribution is cited as a satisfactory probability density function in processes involving counting, to represent the distribution of the number of events in a given interval (Gray and Odell, 1970).

The process can be seen as one where the assumed identical load applied by each pedestrian is shifted in time by the introduction of a phase angle which follows the Poisson distribution. The summation of the effects on the vibration amplitude of the simultaneous application of these identical individual loads shifted in time would have the aforementioned relationship with the effect of an individual load.

Some simplifications in Eq. 2.3 for calculating the crowd magnification factor C_{mf} are evident. On the one hand, it may be conservative to consider that all pedestrians would be walking at the same pacing rate. On the other hand, it may not be conservative to consider the phase differences between the load of each pedestrian as being entirely random (no synchronisation is considered). Furthermore, all pedestrians are considered to have a common weight.

Further insight into these simplifications came from the work of Mouring and Ellingwood (1994), who did simulations on floors submitted to walking loads from individuals arriving at random. Such floors had fundamental frequencies from 5 to 10 Hz, and the simulations considered both a common pacing rate of 2 Hz and random pacing rates between 1.7 and 2.3 Hz. In addition, another set of simulations considered both a constant weight of 700 N for all pedestrians and random weights following a normal distribution taken from other studies. The conclusion of the authors was that considering pacing rate and weight as constants did not appear to affect the response of the system to the level of accuracy required for the serviceability evaluations investigated. In terms of the response, they also found the relation between peak accelerations due to one pedestrian and those due to several pedestrians to be in accordance with Eq. 2.3. The same conclusion regarding the insignificant difference between common or random pacing rates was obtained previously by Wheeler (1981), from simulations on footbridges.

Tests with several pedestrians were carried out by Pernica (1990) and Eriksson (1994). The former did tests with groups of 2 and 4 people for several controlled pacing rates. The latter did tests with groups of 7 and 11 people for coordinated walking at pacing rates of 1.7 and 2.0 Hz, and also for uncoordinated walking. Both works focused on analysing the behaviour of the forces applied by a group and by individuals in the

group. Following Eriksson, these results are comparable to the aforementioned of Mouring and Ellingwood (1994) and with Eq. 2.3, both established in terms of response. The rationale for this is that if only one mode of vibration is considered, magnifications of force and response would have been the same. Eriksson showed his results for larger groups to follow the trend of Pernica's results for small groups. Significant conclusions could be drawn from these results (Eriksson, 1994):

(a) A different trend was found with regard to the magnification of the harmonics of the load in the case of coordinated walking. The first harmonic, the frequency of which is the pacing rate, was found to experience greater magnification than the higher harmonics, increasing almost linearly with the number of pedestrians. On the other hand, the higher harmonics were shown to follow Eq. 2.3 .

(b) The magnification factors for uncoordinated walking were shown to follow Eq. 2.3 for all harmonics.

It can be noted that the test results show a difference in behaviour for coordinated and uncoordinated walking in contrast to what was found in the previous simulations. In practical terms, the results verified Eq. 2.3, except for the situation when pedestrians walked in a coordinated fashion. In this case, higher magnifications would be expected for the first harmonic, the frequency of which is the common pacing rate.

Other tests and simulations with groups of pedestrians were carried out by Ebrahimpour *et al.* (1996). Their investigations concentrated on the first harmonic of the walking load, which was shown to decrease with the number of pedestrians n_p in a logarithmic fashion. The tests themselves were conducted for a group of four pedestrians only, resulting in a dynamic load factor per individual in the group smaller than that reported in the aforementioned work of Pernica (1990). The simulations considered an Exponential distribution[3] of phase lag between the individuals instead of the Poisson distribution that resulted in Eq. 2.3. The justification for this came from observing that

[3] The Exponential distribution is often employed in reliability studies and can also be used to represent the distribution of time intervals between events (Gray and Odell, 1970). This latter application may be the motivation for using this distribution to represent the time delay (phase lag) among pedestrians.

test subjects consciously made changes in their footstep frequency to synchronise with the movement of the others. This phenomenon had also been observed in previous work (Ebrahimpour and Sack, 1989), in which the Exponential distribution for the phase was proposed as a best fit for the time shifts in peak forces of two people jumping in a coordinated fashion. This proposal was checked experimentally for a group of four coordinated jumpers. However, its validity for several uncoordinated walkers seems to deserve further investigation.

A further point of interest is the degree of synchronisation that uncoordinated pedestrians may experience when crossing a vibrating structure. According to the previous test results, this would contribute to an increase in the crowd magnification factor since the pedestrians would tend towards coordinated motion. Very few investigations have been conducted to date with respect to this subject. Grundmann *et al.* (1993) reported this phenomenon as occurring only for groups of pedestrians whose pacing rates are closer to a natural frequency of the structure. This is because synchronisation was shown to be dependent on vibration level, which is higher when the natural frequencies of the structure are within the frequency range of common pacing rates. Based on previous work in which the probability of synchronisation was investigated, these authors proposed the following crowd magnification factor:

$$C_{mf} = k_l \; n_p \; P_s(a_{max}) \tag{2.4}$$

where n_p is the number of pedestrians as previously defined in Eq. 2.3, $P_s(a_{max})$ is the probability of synchronisation as a function of the acceleration amplitude a_{max}, and k_l is a factor to account for the spatial distribution of the load along the structure, which depends on the mode shape associated with the natural frequency under consideration. Eq. 2.4 was meant to be applied to situations in which a stream of pedestrians in free walking were crossing a footbridge. In addition, it can only be formally applied if the frequency of vibration is within the pacing rate range (i.e., it is not certain if Eq. 2.4 would apply for vibrations with a frequency within the range of the higher harmonics of the walking load).

A chart was also presented by Grundmann *et al.* (1993) from which the values of P_s can be obtained for several acceleration levels. A typical value was suggested by the authors as 0.225, corresponding to an acceleration amplitude of 0.7 m/s^2, which is the acceptable limit value adopted by the British code of practice (BS5400, 1978) for vibrations at a frequency of 2.0 Hz. In addition, if the load factor k_l is taken as 0.6, as the authors did for the first mode shape of a simply supported beam, a comparison is possible between Eq. 2.4 and the previous proposals (Fig. 2.7). It can be seen that Eq. 2.4 does not reduce to the value of one in the case of a single pedestrian crossing the structure as do the other proposals.

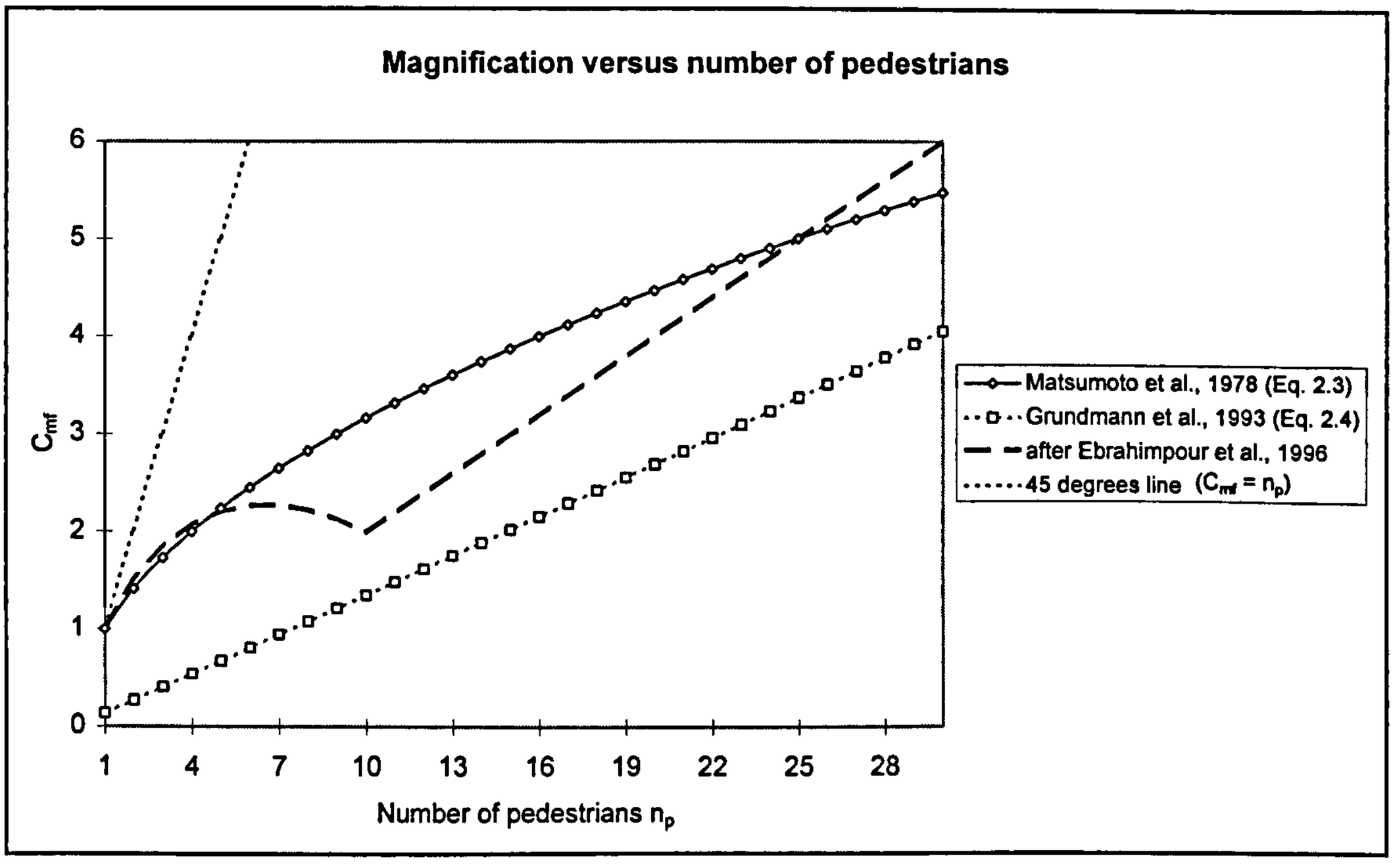

Figure 2.7 - Magnification factors for vertical vibration amplitude

Up to now, a common variable in all proposals has been the number of pedestrians on the structure at any time, which is the product of the area of the deck and the density of pedestrians. It so happens that this latter parameter also affects the magnitude of the load applied by an individual in a crowd. The higher the density, the more 'packed' are the pedestrians who are therefore prevented from walking freely. This causes a reduction in the pacing rate and, as was shown in Section 2.2.1, a commensurate reduction in individual applied loads. On the other hand, a higher density would

enhance the synchronisation, which would contribute to increasing the overall load. These opposing effects have not been fully investigated. What has been reported, based on previous studies of pedestrian traffic, is that densities of up to 0.25 (Ebrahimpour *et al.*, 1996) or 0.3 pedestrians/m^2 (Grundmann *et al.*, 1993) represent a condition of unrestricted choice of speed and pacing rate by an individual in a group. This can be used to identify the maximum number of pedestrians that can be on a footbridge without reductions on an individual's pacing rate and load.

The load effects of a group of pedestrians in the lateral direction have been subject to very little investigation. In principle, Eq. 2.3 would also apply to sum up random distributed lateral loads, although there is no experimental evidence to confirm this. In terms of synchronisation, Bachmann and Ammann (1987) suggested that this phenomenon was more pronounced in this direction. According to them, a pedestrian, having noticed the lateral displacements, would attempt to re-establish his balance by moving his body in the opposite direction; however, the load he thereby exerts on the pavement would be directed so as to enhance the structural vibration. Conversely, Grundmann *et al.* (1993) considered the possibility of synchronisation being lower in the lateral than in the vertical direction, since the phase range and consequently the phase spread among the pedestrians is higher for vibrations in the lateral direction. They therefore recommended the application of Eq. 2.4 as a conservative solution for the lateral direction.

A case study by Fujino *et al.* (1993) of a footbridge experiencing large lateral vibrations in a congested situation gave some insight into the application of crowd magnification factors in this direction. Calculations carried out by the authors using Eq. 2.3 produced displacement amplitudes much smaller than the ones measured on the structure. They explained this by considering that a pedestrian would take a larger step in the lateral direction in order to walk in a stable manner on a laterally vibrating deck, causing each individual's load to increase. A study by Okamoto *et al.* was mentioned by Fujino *et al.* to corroborate this hypothesis, and which apparently also showed that synchronisation began to appear for lateral amplitudes of the order of 1 to 2 cm. Studies of the pedestrians' head motion showed that about 20% of them had their motions

synchronised, and taking this as a crowd magnification factor ($C_{mf} = 0.2\ n_p$) produced a much closer fit with the measured displacements than that obtained by applying Eq. 2.3.

A last point to discuss is the interaction between pedestrians and the structure. As was observed previously, the interaction between a person walking and the structure is not completely clear, although it has been shown that the level of interaction, if existent, would be much reduced when compared with that for a standing subject. The effect of interaction would, however, be enhanced by the presence of several pedestrians but no investigation was found in this area.

Jumping

Investigations of the effect of groups of people jumping have relevance to the design of structures subject to rhythmic movements, like those in aerobic or dancing classes, pop concerts, etc. There is usually an auditory effect (music) that enhances the synchronisation among the participants, causing a high magnification of the applied load. However, the point of interest in this study of footbridges is restricted to deliberate excitations, usually due to a small number of people. The participants intend to be coordinated, and this effort produces a similar effect as the aforementioned auditory effect.

Tests involving a small number of people jumping in unison have been carried out by Pernica (1990). His results showed that there was negligible reduction on the load factors per person in a group of up to 4 people, i.e. the load would increase linearly with the number of participants.

2.3 Vibration Serviceability of Pedestrian Bridges

Controversy among the engineering community over serviceability provisions is motivated by various factors. In a general review of the subject, Ellingwood (1996) highlighted issues of safety, as being thought of by some as the sole purpose of codes of practice, and issues of economics, as the concern that mandatory serviceability

requirements would increase costs. A typical comment cited by him reflects this latter view: *"Serviceability is where I save my client money"*.

It is likely that vibration serviceability is often considered in this way since it involves only issues of comfort in using the structure. In the particular case of footbridges, the tendency to disregard the problem of vibration serviceability would be more pronounced. This is because sensitivity to vibrations has been shown to be time dependent (Griffin, 1990), and the duration that a subject is exposed to vibrations while crossing a footbridge would be considered to be a relatively short term event. On the other hand, public concern caused by fear of crossing a lively footbridge would bring more attention to the problem. Case reports of footbridges have occurred in practice in which remedial measures to reduce excessive vibrations had to be taken due to complaints, and this not only costs money but also results in significant inconvenience to those involved.

The problem of vibration serviceability of footbridges is addressed in several codes of practice and is reviewed in this Section. First, footbridges which are prone to experience vibration serviceability problems are identified, bearing in mind the peculiarities of the human-induced loads previously discussed. This will be followed by two separate discussions, in which sensitivity to vibrations and current design recommendations to tackle the problem are analysed.

2.3.1 Footbridges Susceptible to Vibration Serviceability Problems

In almost all books about structural dynamics, the steady state response of a single degree of freedom (SDOF) system to a sinusoidal loading is well covered. The dynamic amplification is shown to be dependent on frequency (actually, on the ratio between the frequency of the excitation and the natural frequency of the system) and on damping of the system. Higher amplifications occur when such a ratio approaches one, characterising a resonance condition.

As has been described in the previous Section, the moving loads from walking or running are characterised by typical frequency ranges, according to the type of motion

in question. These loads could also be considered to induce a sort of steady-state response since several footsteps are necessary to cross a footbridge. Consequently, by reducing the behaviour of the structure to that of a SDOF system, it could be concluded that the critical frequency ranges for vibration serviceability would be those coincident with the frequency ranges of the excitation.

Several case reports of lively footbridges confirm this fact and are presented in Table 2.2. This reveals the presence of lively footbridges with natural frequencies within the first harmonic of the walking load in the lateral direction and the first two harmonics in the vertical direction. Looking in more detail into each of these frequency ranges, we have:

- A frequency range from 0.8 to 1.2 Hz in the lateral direction, related to the first harmonic of the walking load. As described in Section 2.2.1, despite the fact that the amplitude of the excitation is lower by one order of magnitude than that of the first harmonic in the vertical direction, significant vibrations have been reported. This may be explained by the enhanced effect of synchronisation among pedestrians in the lateral direction, as previously discussed. Another factor that may contribute to explain the reported large vibrations is that there is no requirement for footbridges to be stiff in this direction in order to support static dead and live loads.

- A frequency range from 1.6 to 2.4 Hz in the vertical direction, related to the first harmonic of the walking load or pacing rate. Several of the cases reported had fundamental frequencies around the most common value of the excitation of 2.0 Hz (Fig. 2.2). However, some footbridges had natural frequencies close to the upper limit of 2.4 Hz, one of them having a fundamental frequency of 2.46 Hz, marginally outside the upper limit. The incidence of lively structures with frequencies close to and above this limit deserves further investigation.

- A frequency range from 3.2 to 4.8 Hz in the vertical direction, for the second harmonic of the walking load. In this frequency range, only one case report has been found. The fact that the magnitude of the harmonic of the walking load for this frequency range is lower than the magnitude of the first harmonic may explain the much lower incidence of lively footbridges in this frequency range.

Footbridge Description	Dynamic Properties	Reference
Two span steel box girder cable stayed bridge, with a main span of 134 m. Large vibrations in congested situations.	Lowest lateral frequency of 0.9 Hz	Fujino *et al.*, 1993
Reinforced concrete multi-span footbridge with a hollow box section, the central spans being each 15.5 m long; considerable lateral vibrations causing panic **	Fundamental lateral frequency of 1.0 Hz	Bachmann, 1992
Steel Box girder footbridge with a 110 m main span suspended from an angular arch; strong lateral movements during opening. **	Lowest lateral frequency of 1.1 Hz	Bachmann and Ammann, 1987
Steel multi-span cable-stayed footbridge, with a main span of 38 m **	Fundamental vertical frequency of 1.80 Hz; damping ratio of 1.5%	Wheeler, 1982
Simply supported beam-like footbridge with a 40 m span	Fundamental vertical frequency of 1.92 Hz; damping ratio of 2.2%	Bachmann and Ammann, 1987
Steel box girder cable-stayed, with a main span of 48 m **	Fundamental vertical frequency of 1.92 Hz	Tilly *et al.*, 1984
35 m single span steel suspension footbridge with a wooden deck.	Vertical frequencies of 2.07 Hz related to an asymmetric mode, and 2.15 Hz related to a symmetric mode	Brownjohn, 1997
Steel footbridge with a span length of 48.5 m **	Fundamental vertical frequency of 2.09 Hz; damping ratio of 0.8%	Matsumoto *et al.*, 1978
36 m single span composite (steel/concrete) box girder bridge **	Fundamental vertical frequency of 2.23 Hz; damping ratio of 0.5%	Eyre and Cullington, 1985
34 m single span prestressed concrete box girder footbridge **	Fundamental vertical frequency of 2.30 Hz	Bachmann and Ammann, 1987
Steel overpass, having a 43.3 m main span	Fundamental vertical frequency of 2.40 Hz	Pan, 1992
3-span continuous beam-like steel footbridge, with a mid-span of 25 m **	Fundamental vertical frequency of 2.46 Hz; damping ratio of 0.0025	Bachmann, 1992
Steel-girder footbridge. Noticeable vertical vibrations for a peak traffic flow of 30 to 55 people/minute	Fundamental vertical frequency of 4.0 Hz	Bachmann, 1992a

** - indicates cases where remedial measures to reduce excessive vibrations were reported

Table 2.2 - Case reports of excessive vibrations in footbridges

These case reports suggest that only in special situations would other excitation forces need to be considered apart from the forces produced by walking. It is also appropriate to note that some of the reports explicitly mention that the excessive vibrations occurred due to crowd action, and therefore this load case should deserve particular attention.

A chart containing the vertical natural frequencies of several footbridges was published (CEB, 1991), in which some of the aforementioned lively footbridges (Table 2.2) have been added (Fig. 2.8). The critical frequency ranges are also indicated in the chart and it can be noted that is common to find footbridges having natural frequencies within these critical ranges. However, it should be recognised that having frequencies within the critical ranges does not necessarily mean that the structure is lively, rather it is potentially lively.

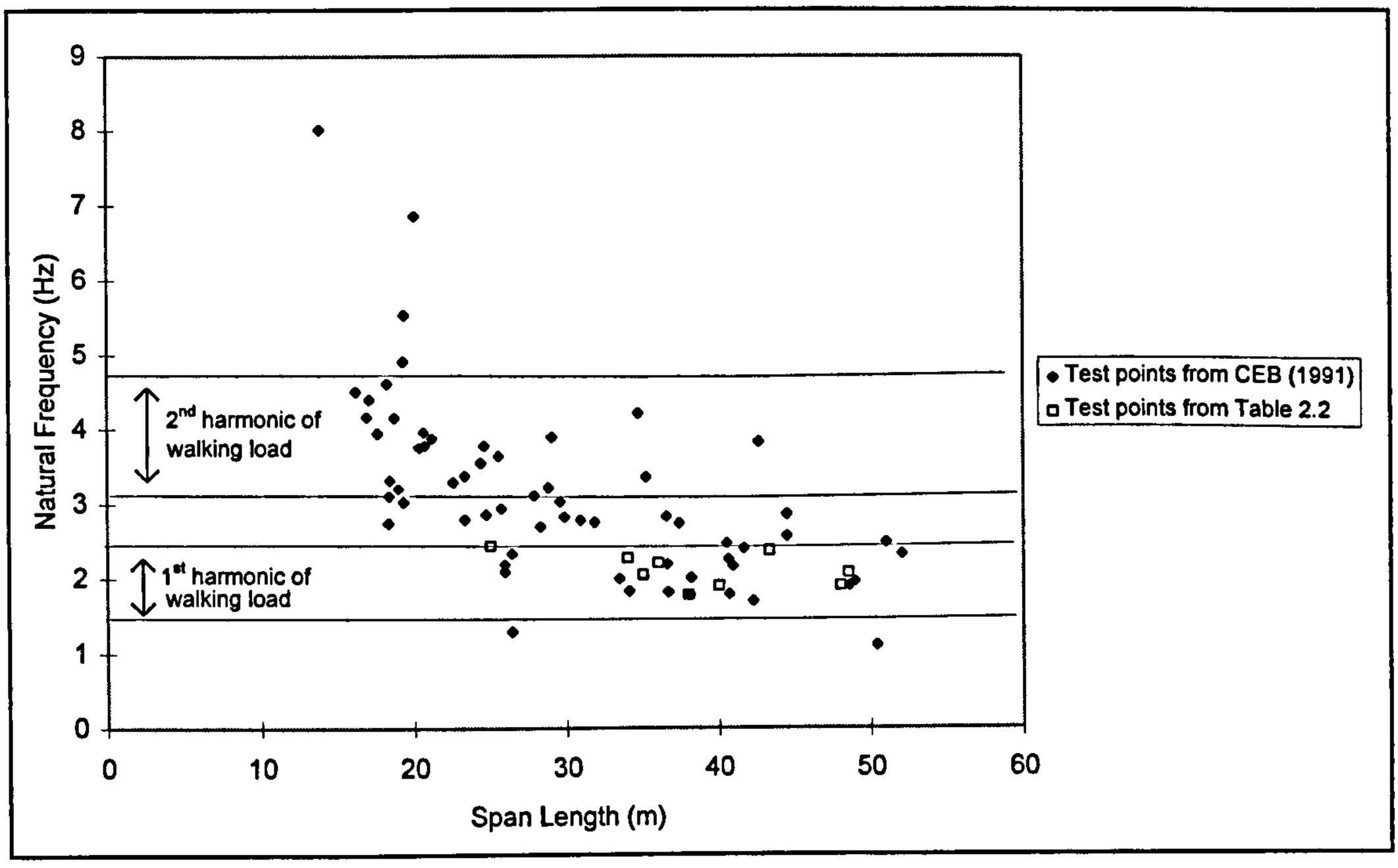

Figure 2.8 - Vertical fundamental frequencies of footbridges

In the initial discussion, damping was the other factor identified as having a significant role in vibration levels. A survey of damping values for several footbridges (Tilly *et al.*, 1984) showed that it is common to find footbridges having equivalent viscous damping ratios lower than 1% of critical damping. If this value of 1% is used in a SDOF model in a resonance condition (Rao, 1995), a ratio of fifty is obtained between the amplitude of

the dynamic oscillation and the static deflection. Taking this high ratio as a reference would be conservative if simplifying the dynamic behaviour of a footbridge to a SDOF model. This is because the pedestrian load does not induce a pure steady state response since it moves along the structure. This will be discussed in more detail in Section 2.3.3 but, for now, it can be said that footbridges may be subjected to significant human-induced vibrations because of the potential coincidence between the frequencies of excitation and the natural frequencies of the structure, and due to the low damping values usually present.

Advances in footbridge design resulting in the construction of more slender footbridges and by the introduction of ACM as a construction material have increased the awareness of vibration problems in these structures. Several prototype footbridges have been constructed with ACM (Meier, 1991), although most of them are still in areas of restricted access.

Properties of ACM provide some insight into expected design challenges. Two main types of fibre have been adopted for the construction of civil engineering facilities: glass and carbon. Despite the higher strength of the latter, its higher cost has restricted its application to cables, and the use of glass fibre has become predominant in all the other structural elements (Erki *et al.*, 1994). The glass fibres are usually embedded into a resin matrix constituting a final material called glass reinforced plastic (GRP). The relatively low stiffness of this material means the desired rigidity of the structural element is governed principally by the cross-sectional shape (Meier, 1992). On the other hand, this material also has a low density, resulting in lighter structures, and that is the reason why attention is drawn to the dynamic performance of such structures. These peculiarities of ACM structures raise the question as to whether vibration serviceability guidelines developed for structures made of conventional materials would fully apply to them.

2.3.2 Thresholds for Sensitivity to Vibrations

Acceleration has been adopted as a parameter for evaluating the degree of vibration to which pedestrians are exposed on footbridges. Its adoption as the limiting parameter has a double benefit: its limiting value does not vary significantly within the frequency

range of the excitation (Smith, 1988), and it is more easily measured than other parameters when assessing the serviceability of existing footbridges.

Considerable research on the sensitivity of human beings to vibrations in various environments has been conducted to date. However, comparatively little research has been found in the literature setting sensitivity limits for acceleration related to disturbance or discomfort during walking on footbridges.

Walking is the most appropriate condition when establishing human acceptability limits for the vibration serviceability of footbridges, since:

(i) Tests with pedestrians walking revealed an increase in tolerance levels over pedestrians standing still (Leonard, 1966). Since footbridges are designed for the movement of pedestrians, evaluating the vibration serviceability using standing subjects would result in a conservative solution;

(ii) The flexing of knees in the process of walking changes the amount of movement transmitted to the human body (Leonard, 1966). On the other hand, the self-induced movement of the body as a result of walking would be superimposed on the vibration of the bridge deck, affecting the human perception of the vibration of the structure (Smith, 1969).

Some proposed acceptability limits applicable to footbridges are plotted in Figure 2.9, adopting the peak acceleration as the reference parameter for comparison. Each line shown limits the regions of acceptable and unacceptable vibration, the latter region standing above the respective line.

The acceptability limit adopted in the UK (BS5400, 1978) was proposed by Blanchard *et al.*, (1977), based on the works of Leonard (1966) and Smith (1969). Leonard did experiments where test subjects crossed a footbridge set vibrating by electro-hydraulic means in order to establish a threshold of unpleasantness for walking. Smith conducted tests using a flexible plank so that the oscillations set by a pedestrian walking across it were great enough to cause disturbance. Despite the different set-ups, both tests produced curves for acceptability to vibrations varying similarly as a function of the

frequency of the vibration. The BS 5400 curve was chosen to lie approximately midway between the curves proposed in those works, being defined by the expression:

$$a_{lim} = 0.5\sqrt{f_v}\ (m/s^2) \tag{2.5}$$

where f_v (Hz) is the frequency of vibration of the structure. As it will be seen later, the evaluation of vibration serviceability is carried out by exciting the structure at its first natural frequency in the vertical direction (f_o), which will be the frequency of vibration. This is taken into account in BS 5400 by writing Eq. 2.5 directly as a function of f_o.

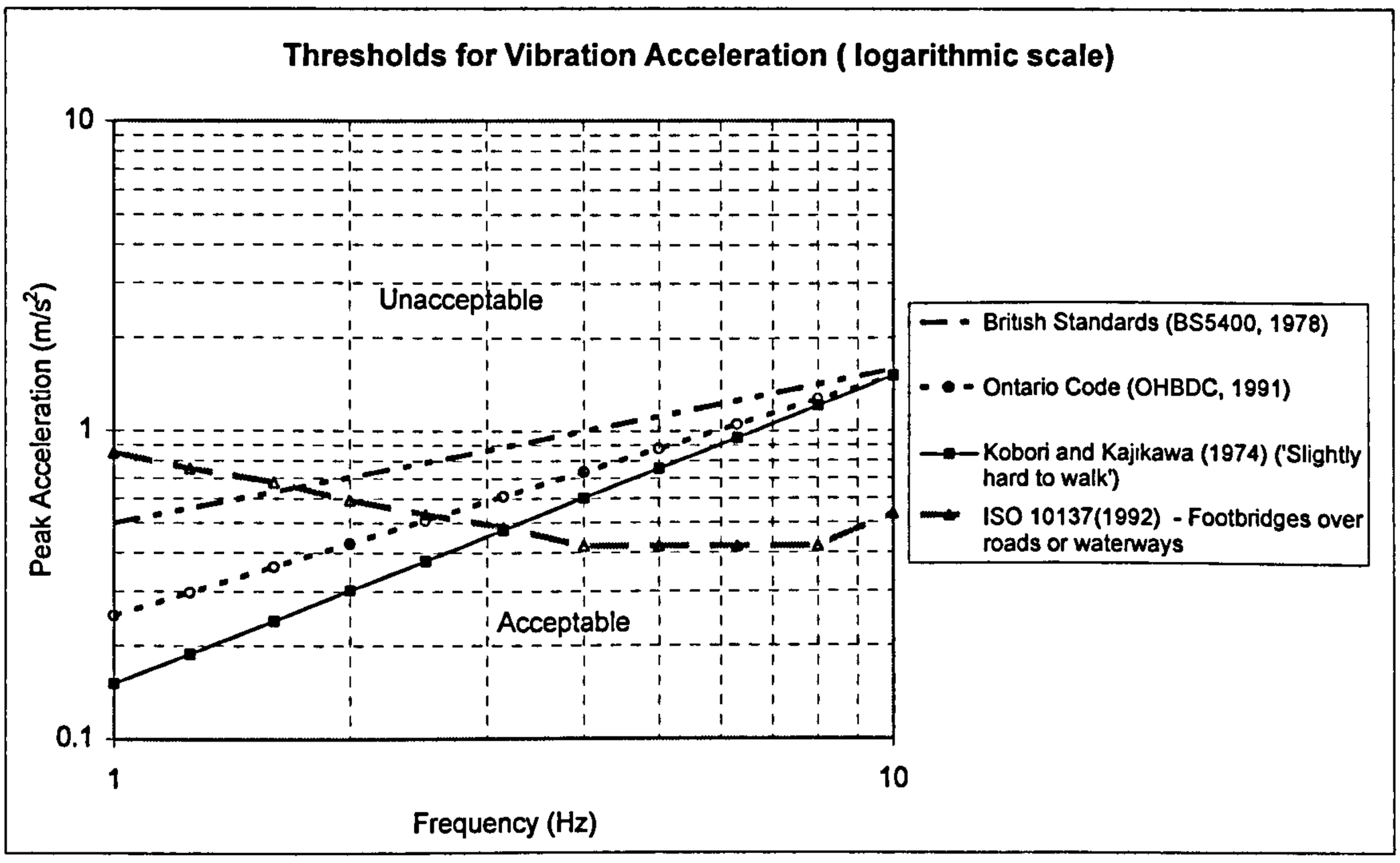

Figure 2.9 - Acceptability curves for vertical vibration acceleration of footbridges

The acceptability limit curves adopted in the Ontario code (OHBDC, 1991) and by Kobori and Kajikawa (1974) are similar to the UK code recommendations (BS5400, 1978). Kobori and Kajikawa's tests were carried out asking test subjects to walk on a shaking table set vibrating at different frequencies under sinusoidal excitation, this set-up being similar to that adopted on Leonard's tests. The curves for acceptability to vibration were, in fact, originally expressed in terms of velocity of vibration, but they

can easily be converted to acceleration since the vibration had only a single frequency component at a time.

In spite of having different limit values, the acceptability curves increase with frequency in the same fashion in all the aforementioned proposals. This similarity strengthens the idea that sensitivity varies with frequency. However, there have been suggestions for adopting a constant limiting peak acceleration of 0.7 m/s^2 for the whole frequency range (Bachmann *et al.*, 1995).

The acceptability curve proposed in the ISO code 10137 (1992) is also presented in Fig. 2.9, but it shows a variation with frequency that differs from all the other proposals. Instead of peak acceleration, the parameter adopted by the ISO code to define acceptable vibration levels is the root mean square (RMS) acceleration, which is given by:

$$a_{RMS} = \sqrt{\frac{1}{T}\int_0^T a^2(t)\,dt} \tag{2.6}$$

where a(t) is the acceleration time response signal and T is the time the measurement was taken. However, there is a straightforward relation between peak (i.e. amplitude) and RMS values for a steady state sinusoidal vibration given by the square root of two. This enabled the plotting of the ISO curve in terms of peak acceleration.

Unlike the other curves, the ISO curve was not obtained from walking tests. In fact, it is an adaptation, using a multiplying factor, of a curve obtained for a standing subject. The ISO code itself recognises that its limit curve is only applicable in the absence of more definitive data regarding vibrations in footbridges.

A different approach is adopted by both the Comite Euro-International du Beton (CEB) (1993) and the Swiss code (1989). These are not shown in Figure 2.9 since acceleration limits are not defined in either code. Instead, pedestrian bridges with natural frequencies between 1.6 and 2.4 Hz and also between 3.5 and 4.5 Hz shall be avoided. Such limitations are based on the fact that the walking frequency range (pacing rate) is normally within the range from 1.6 to 2.4 Hz, as was discussed in Section 2.2.1. In

addition, these codes also consider as critical the (reduced) frequency range for excitations caused by the second harmonic of the walking load, ranging from 3.5 to 4.5 Hz. Therefore, the rationale of these codes is to design footbridges not prone to vibrations by banning these critical frequency ranges.

It may be noted that the acceptability curves plotted in Fig. 2.9 enable the evaluation of vibrations containing a single frequency component. However, it is possible for a footbridge to have more than one of its natural frequencies within the specified frequency ranges of the harmonics of the walking load. The suspension footbridge reported by Brownjohn (1997), included in Table 2.2, and also two of the test structures discussed in Chapter 4, are typical examples of structures falling into this category. In cases like these, more than one natural frequency may be simultaneously excited by harmonics of the walking load, and thus the response signal is composed of more than one frequency component. Recent procedures for evaluating transient multi-frequency component vibrations have been adopted in the UK as evaluation criteria for vibrations in buildings (BS 6472, 1992). In general, this requires first the application of a frequency weighting to the response signal in order to consider properly the significance of each frequency component. Using this frequency weighted response signal, calculations are made of the RMS acceleration or alternatively of a vibration dose value (VDV) for comparisons with acceptability limits. This latter parameter is reported to incorporate the effect of time exposure to vibration (Griffin, 1990), and is given by:

$$\mathrm{VDV} = \left[\int_0^T a^4(t)\,dt \right]^{1/4} \tag{2.7}$$

where a(t) and T are as previously defined in Eq. 2.6. Nevertheless, developments of this multi-frequency component criterion for footbridges are still to come since the frequency weighting and acceptability limits do not apply to walking subjects.

There is also the question of whether acceptability curves established in the laboratory or under special test conditions, such as those curves in Fig. 2.9, would be appropriate for use for the assessment of actual footbridges. This is because these proposed curves account for comfort issues during the crossing but do not account for psychological

reactions of panic or fear when crossing a vibrating footbridge. Motions resulting in a suspicion of structural inadequacy can be disturbing even if they are just perceptible, particularly in the case of open air footbridges over roads or rivers (Leonard, 1966). In such cases, a vibration level stated as *acceptable* in laboratory conditions could turn out to be *annoying* on an actual footbridge. However, this is difficult to quantify in order to be included in assessment criteria and, when adopting one of the proposed curves (Fig. 2.9), it should be borne in mind that in some circumstances this may not result in a conservative evaluation.

Regarding the definition of sensitivity limits in the lateral direction, no studies have been found dealing with these limits for walking subjects. Applicability of the available studies for standing subjects would be questionable at the very least considering the differences in perception which occur between standing and walking subjects in the vertical direction.

2.3.3 Design Procedures for Vibration Serviceability

The response to dynamic loads depends on factors such as stiffness, damping and frequency. Suggested limit values for such factors leading to a lesser likelihood of lively behaviour in footbridges were suggested by Tilly *et al.*(1984), based on tests on several footbridges. As a general approach, accelerations either need to be calculated during the design stage or measured on the actual footbridge in order to assess the structure for vibration serviceability. The UK (BS5400, 1978) and Ontario (OHBDC, 1991) codes have similar guidelines regarding this subject. In the British code, the maximum vertical acceleration is calculated by representing the load produced by one pedestrian as a dynamic pulsating load $F(t)$ which moves along the footbridge. Such a load has a frequency f_p (the pedestrian pacing rate) which is to coincide with the first natural frequency f_o of the unloaded footbridge in the vertical direction, given by:

$$F(t) = 180 \sin(2\pi f_o t) \quad \text{(N)} \tag{2.8}$$

where t is the time (secs) and the pedestrian moves with a speed $v = 0.9\ f_o$ (m/s). In Eq. 2.8, the term 180 N is the amplitude of the first harmonic of the walking load, being

the product of the weight of the pedestrian (assumed to be 700 N) by a dynamic load factor α = 0.257 (Blanchard *et al.*, 1977). The calculated peak acceleration must be smaller than the specified limit value in Eq. 2.5, discussed in the previous Subsection.

Eq. 2.8 is to be applied to footbridges having a fundamental vertical frequency below 5 Hz. The vibration serviceability requirement is deemed to be satisfied if the fundamental frequency is above this limit. It may be noted that this limit is confirmed by the absence of case reports of lively footbridges having fundamental frequencies above 5 Hz (Table 2.2). According to the description of the walking load in Section 2.2.1, the limit of 5 Hz also limits the range of interest to the first two harmonics of the walking load. A reduction factor to be applied to the calculated acceleration is proposed in the code for the range of frequencies between 4 and 5 Hz, since no pedestrian could walk at such a high pacing rate. The reduction is zero at 4 Hz and varies linearly to a 70% reduction at 5 Hz.

The Ontario code (OHBDC, 1991) presents minor differences with respect to the aforementioned procedure. Apart from having a stricter limit for maximum accelerations (see Fig. 2.9), an upper limit for the speed of the pedestrian is also considered. Accordingly, this code considers that a notional pedestrian walks with a frequency that is the lesser of the fundamental frequency f_o or 4 Hz. There is also no explicit reference to an upper limit for the frequency range of interest.

Recent research developments and the design of new slender and lightweight footbridges have created situations in which some drawbacks are becoming apparent regarding the application of these general rules:

(a) Discrepancies between the calculated accelerations using the guidelines of the British code (BS 5400, 1978) and measured accelerations in footbridges from controlled pedestrian tests (Cheung, 1984; Eyre and Cullington, 1985) have called attention to the definition of the pedestrian load. A comparison between the pedestrian load as defined in the code (Eq. 2.8) and the Fourier series representation (Eq. 2.1) shows that the code considers only the term related to the contribution of the first harmonic of the load. In addition, the adopted dynamic load factor of 0.257,

also reported in Table 2.1, was obtained from pedestrian tests at a pacing rate of 1.8 Hz. This load factor actually underestimates the pedestrian load if taken as a representative value for the frequency range between 1.8 and 2.4 Hz. It should be noted that studies about human-induced loads were limited at the time the British code was written; only afterwards were analytical expressions for the representation of walking, jumping and running movements including higher harmonics proposed. Nevertheless, in its new edition, the Ontario code (OHBDC, 1991) has retained the load factor of 0.257 .

(b) As was seen in Section 2.2.1, pedestrians normally walk using a pacing rate of about 2 Hz, with a small standard deviation around this value. Even taking into account the reduction factor proposed by the codes for the range of frequencies between 4 and 5 Hz, the frequency range between 2.4 and 4 Hz remains improperly addressed.

(c) Attention is concentrated only on the first natural frequency of the footbridge in the vertical direction. A single frequency component excitation is also considered, by reducing the pedestrian load to only one harmonic component, the frequency of which is made equal to the aforementioned structure's fundamental frequency. Therefore, it would not be possible to evaluate the effects of a vibration signal containing more than one discrete frequency component. This would certainly be the case for footbridges having more than one natural frequency within the normal range of pacing rates for pedestrians and/or within the higher harmonics of the pedestrian load.

(d) Vibrations in the lateral direction are not considered in the British code. In the Ontario code, the problem is partly treated in a qualitative manner, recommending avoidance of slender piers for those footbridges which are supported on such elements. This aims to avoid lateral flexural modes of vibration in the frequency range of pedestrian footfalls. Bearing in mind the need to avoid coupling between vertical, lateral and longitudinal modes, it is also stated that the frequencies of the modes in these last two directions should be such that they are not less than 1.5 times the first vertical frequency nor less than 4 Hz. These restrictions for lateral frequencies would definitely avoid footbridges such as those reported in Table 2.2

being lively in this direction. However, these rules seem too restrictive for the purpose of avoiding vibration serviceability problems and could result in perfectly serviceable and economic structural solutions being disallowed.

(e) Reference is made in the Ontario code for consideration of significant torsional modes of vibration, for footbridges presenting similar torsional and flexural frequencies. However, no procedure was specifically defined to check the structure for vibration serviceability in this situation.

Beam-Like Footbridges

In this particular (common) case, the simplicity of the structure makes it possible to introduce some simplifications in the general procedure, and several alternative formulae have been suggested for assessing vibration serviceability.

A simplified expression for the calculation of peak accelerations produced by a notional pedestrian is also presented in both UK (BS5400, 1978) and Ontario (OHBDC, 1991) codes for simply supported, single span or two- or three-span continuous, beam-like superstructures of constant cross section. It was obtained from numerical exercises applying Eq. 2.8 (Blanchard *et al.*, 1977). The maximum vertical acceleration a_{max} is given by:

$$a_{max} = 4 \pi^2 f_o^2 y_s k_a \psi_d \tag{2.9}$$

where the first natural frequency f_o is expressed in Hz, y_s is the static deflection (in meters) at the midpoint of the main span due to the assumed weight of the pedestrian (700 N) applied at this point, and ψ_d is a dynamic response factor, which is taken from a chart and is a function of the length of the main span and the damping of the footbridge. The configuration factor k_a depends on the number of spans and the ratio between side and main spans. A more extensive table of values for k_a and more entries for damping in the chart for obtaining ψ_d are presented in the Ontario code. The same reduction factors for fundamental frequencies higher than 4 Hz discussed for the general loading case are adopted here by the British code and, in this case, are also adopted by the Ontario code.

Another expression to calculate peak accelerations was proposed by Rainer *et al.* (1988), obtained by modelling the structure as an equivalent single-degree-of-freedom (SDOF) oscillator. A sinusoidal excitation having an amplitude $P = \alpha_n G$ is applied, where G is the weight of the notional pedestrian. The dynamic load factor α_n is chosen in accordance to what harmonic of the walking load is employed to excite the fundamental mode of the structure. The excitation is enveloped by the fundamental mode shape of the structure to simulate the variation in vibration amplitude during the crossing. In doing this, the moving load is reduced to a stationary load of varying amplitude. The number of cycles of vibration is also taken into account and the final expression for the maximum acceleration is given by:

$$a_{max} = \Omega_d \frac{2\alpha_n G}{M} \tag{2.10}$$

where M is the total mass of the footbridge, and Ω_d is a dynamic amplification factor taken from a chart as a function of both the number of cycles of vibration (i.e., the number of steps to cross the span) and the damping ratio. The advantage of this proposal is the flexibility of choosing the appropriate load factor according to the harmonic of the walking load (e.g., a footbridge having a fundamental frequency of 4 Hz may be excited by the second harmonic of the load produced by a pedestrian walking at about 2 Hz). However, this proposal is valid only for single span simply supported footbridges.

A design criterion is proposed by Allen and Murray (1993), having as starting points the expression proposed by Rainer *et al.* (1988) and the ISO (ISO 10137, 1992) limit curve for acceptability of vibrations both discussed previously. After some modifications, a criterion for walking vibrations was established in terms of a minimum vertical natural frequency f_o that is acceptable for footbridges:

$$f_o = 2.86 \ln\left(\frac{8.0}{\zeta W}\right) \tag{2.11}$$

where ζ is the equivalent viscous damping ratio and W is the weight of the footbridge.

Another proposal was presented by Grundmann *et al.* (1993) to be applied to single span footbridges, based on an analogy with a SDOF system. A completely analytical expression (i.e. no chart is needed to obtain parameters) for the maximum acceleration produced by a notional pedestrian of weight *G* was proposed, and can be written as :

$$a_{max} = \frac{2G}{M}\frac{0.75}{\delta}(1-e^{-n_s\delta}) \qquad (2.12)$$

where M is the mass of the structure as previously defined, δ is the damping in terms of logarithm decrement ($\delta \approx 2\pi\zeta$) and n_s is the number of steps to cross the span. The applicability and accuracy of Eq. 2.12 depends on some simplifications considered in its deduction. Initially, a dynamic load factor of 0.4 was assumed, corresponding to the first harmonic of the walking load. The term $(1- e^{- n_s\delta})$ was taken from the theoretical harmonic response of a SDOF to a sinusoidal load of constant amplitude (Clough and Penzien, 1975). In order to consider the effect of the load movement, a multiplying factor of 0.6 was introduced, which is actually a conversion factor adopted to obtain a SDOF approximation for vibrations in the fundamental mode of a simply supported beam subject to a distributed load.

Eq. 2.12 would be applicable to vibrations caused by the first harmonic of the walking load. In order to generalise its validity for higher harmonics and also to consider the effect of a few pedestrians simultaneously walking on the bridge (see Eq. 2.4 also proposed by Grundmann *et al.* (1993) for footbridges subjected to crowd loading), a multiplying factor *S* to be applied to a_{max} was introduced (Fig. 2.10), being a function of the frequency. This factor aimed to: a) compensate for taking a constant peak acceleration of 0.7 m/s^2 as the limit for the whole frequency range (this limit was obtained from applying Eq. 2.5 for a frequency of 2 Hz); b) compensate for considering the dynamic load factor of the first harmonic constant for the whole frequency range; and c) consider a minimum of three fully synchronised pedestrians walking along.

Apart from this last proposal, in all the aforementioned procedures in this Subsection, only one notional pedestrian is taken into account in the design procedures. This has been reported as appropriate, based on either a limited number of tests carried out on

some footbridges or in numerical developments of the effects of crowd loading (Blanchard *et al.*, 1977; Wheeler, 1982). Eyre and Cullington (1985) mentioned that using only one person is not an unreasonable compromise when account is taken of the short duration of vibrations experienced during the crossing, the occasional incidence of perfect resonance, and the fact that the maximum discomfort is only partially experienced around the points of maximum displacement.

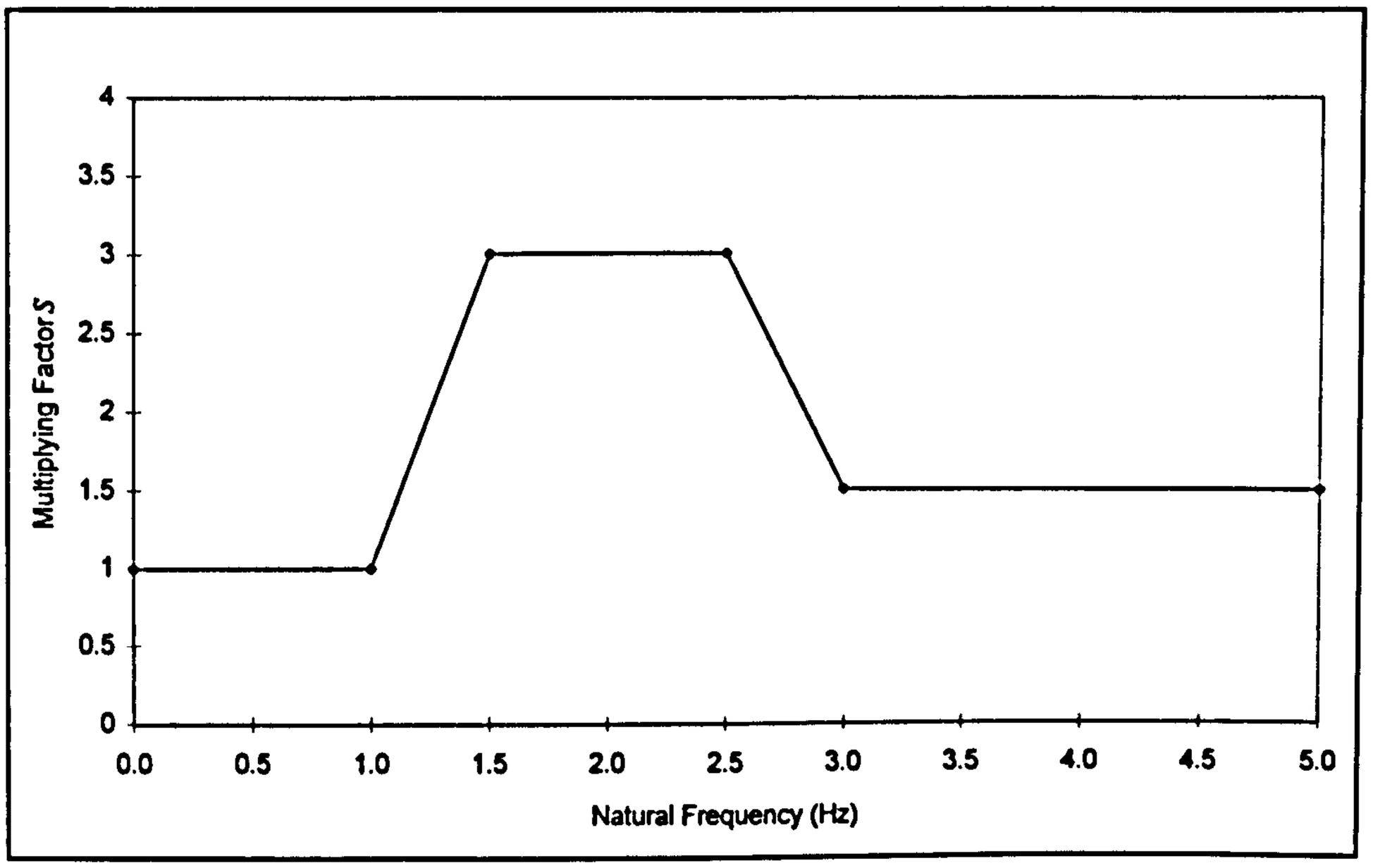

Figure 2.10 - Multiplying factor for footbridges as a function of frequency (after Grundmann *et al.*, 1993).

Conversely, it has been shown in Section 2.2.2 that experimental data have provided evidence for the validity of a crowd magnification factor (Eq. 2.3) for uncoordinated pedestrian movements. An expression has also been proposed for coordinated crowd effects taking into consideration the synchronisation which occurs among pedestrians due to the presence of structural vibration (Eq. 2.4). It may be noted that adopting such crowd magnification factors will significantly increase the response levels. On the other hand, complaints regarding excessive vibrations in footbridges have occurred when the structure is being crossed by streams of pedestrians. How reasonable the design load is in predicting actual vibration levels by using a single notional pedestrian deserves investigation.

2.4 Deliberate Excitation

Since vandals do not usually have any background in structural dynamics, their action is likely to be motivated by experiencing the potential liveliness of a structure, which motivates them to deliberate excitation. Indeed, vandals might be delighted to produce high excitations, and this problem is therefore not really a vibration serviceability issue since what is in question is the integrity of the structure.

As was seen in Section 2.2.1, the activities of jumping and bouncing in contact with the structure have usual frequency rates that can be broadly taken from 1.5 to 3.5 Hz. On the other hand, footbridges may have natural frequencies within this range (Fig. 2.8), and can potentially be set vibrating, deliberately. There is also the possibility of the footbridge being deliberately excited in the lateral direction. However, the lack of information regarding appropriate excitation functions in this direction makes further investigations into this matter difficult.

The problem of structural damage due to human action has been reported in a few cases (Ellingwood and Tallin, 1984). However, no case reports have been found of damage to footbridges explicitly caused by deliberate excitation. This may explain why the words *"general precaution"* are adopted by the British code (BS 5400, 1978) with regard to defining recommendations against deliberate excitation. A recommendation is made in this code indicating that bearings should be of a robust construction in order to resist upward or lateral movements. There is also a recommendation that there should be a minimum amount of unstressed reinforcement in prestressed concrete footbridges, so as to prevent cracking due to load reversal caused by oscillation. Actually, studies to quantify the jumping load were not available at the time the code was launched (Blanchard *et al.*, 1977). This may explain the lack of a clearer reference in the code to critical frequency ranges for deliberate excitations or to procedures for applying vandal loading and for evaluating the response of the structure.

2.5 Measures to Reduce Human-Induced Vibrations

Some possible solutions to improve the vibrational performance of lively footbridges have been identified (Bachmann and Ammann, 1987). These may be applied either

during the design stage or retrospectively to reduce the lively behaviour of an existing footbridge Basically, they can be grouped in two categories: frequency tuning and special measures.

Frequency tuning

This takes into consideration the very characteristic frequency ranges of human motion, and aims to keep the natural frequencies of the structure outside of these ranges. In the case of footbridges, this would imply avoiding the frequency ranges of the harmonics of the walking load, since this is the normal source of excitation. Based on the case reports of lively footbridges, the critical situations are those in which the fundamental frequency of the structure is within the frequency range of the first harmonics of the walking load in the vertical and lateral directions. The fundamental natural frequency of the structure can be either increased (high tuning) or lowered (low tuning) in an attempt to avoid these critical frequency ranges.

It should be noted that the small damping values usually associated with footbridges have here a positive effect. As Tilly *et al.* (1984) mentioned, small shifts in the fundamental frequency with respect to a resonance condition will significantly decrease the dynamic amplifications. This is because the small damping is related to a narrow resonance peak, in which higher dynamic amplifications can be attained only in a respective narrow frequency range in the neighbourhood of the resonant frequency.

Low Tuning - achieved by adding mass to the structure. Taking as a reference the dynamic response of a SDOF system, 'adding mass' implies an increase in the time in which the resonance condition is reached when the structure is excited at its fundamental frequency. It also implies a direct reduction in acceleration levels since acceleration is inversely proportional to the mass of the system for a steady state excitation (Clough and Penzien, 1975). On the other hand, if the requirements of the British (BS 5400, 1978) or Ontario (OHBDC, 1991) code are applied to the letter, the whole frequency range should be subject to examination and two drawbacks would occur when adopting this solution:

- The code acceleration limit decreases (Eq. 2.5), as the frequency of vibration will be equal to the fundamental frequency of the structure.

- The time a pedestrian takes to cross the footbridge would increase as it is assumed that he walks at a slower pacing rate equal to the reduced fundamental frequency. This compensates for the increase in time taken for the resonance condition to be reached.

High Tuning - achieved by increasing the stiffness of the footbridge. This would directly improve the static behaviour by reducing the structural deflections. If again a SDOF system is employed for a qualitative examination of dynamic behaviour, the dynamic magnification would be reduced since the fundamental frequency of the structure would be removed from the critical range where resonance occurs. Conversely, according to the aforementioned codes, the structure should always be checked in resonance conditions and therefore no reduction in the magnification of acceleration would apply. However, since the frequency of vibration would increase, a benefit of high tuning would come from an increase in the acceptability limits for vibration (see Eq. 2.5).

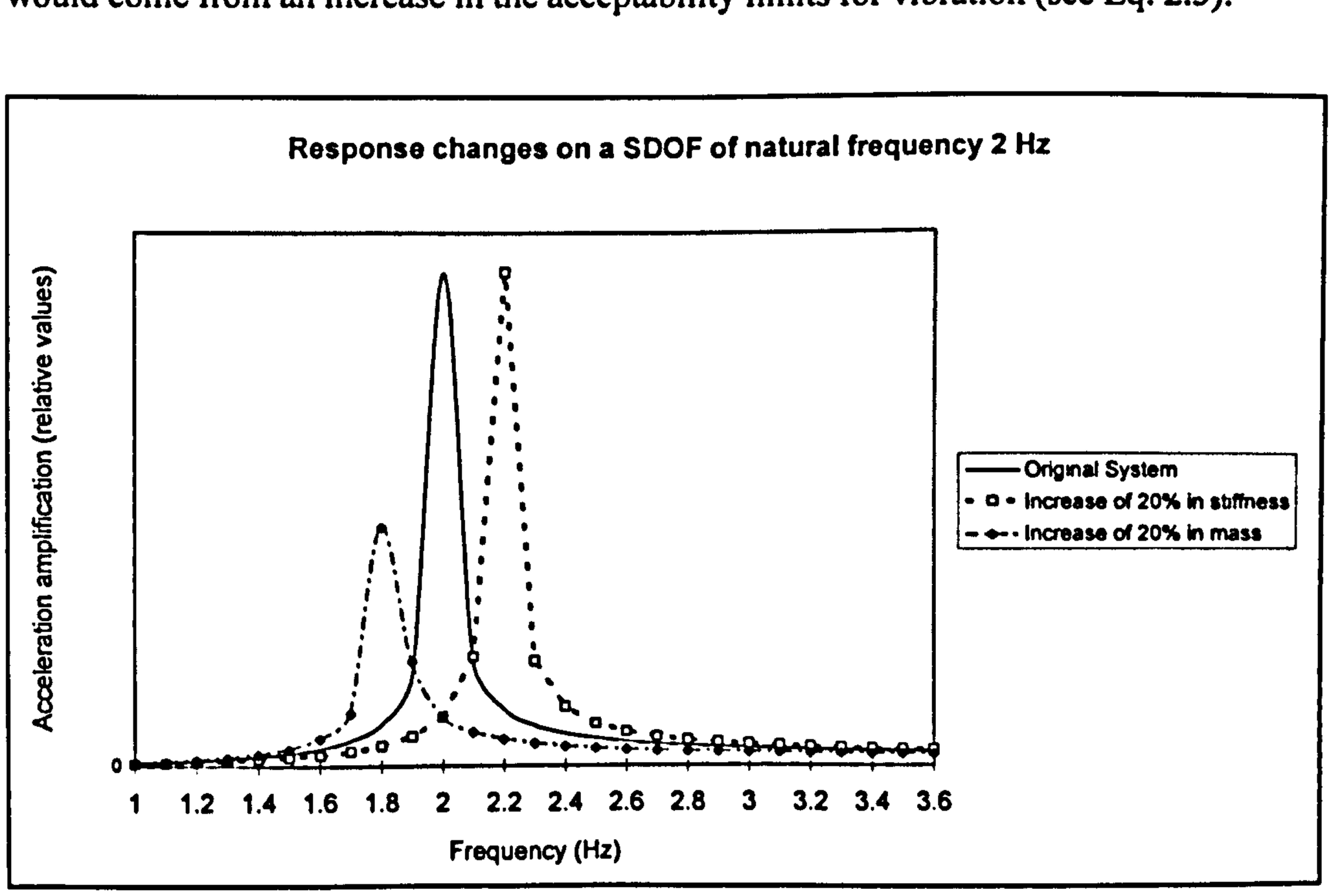

Figure 2.11 - Acceleration frequency response of a SDOF system with an arbitrary damping ratio of 1%

The effect of low and high tuning on the acceleration frequency response of a SDOF system can be visualised in Fig. 2.11, where arbitrary increases of 20% were applied independently to the mass and stiffness to simulate low and high tuning, respectively. For a given excitation frequency in resonance with the original system, the beneficial effect of both changes in reducing acceleration levels is visible. However, it can be seen that, if the response at resonance is sought in each of the systems, no beneficial effect is achieved by high tuning in terms of reducing the acceleration response.

Special Measures

These include measures intended to improve the dynamic performance at resonance. One of the solutions is the installation of a vibration absorber on the structure, the most popular type being a tuned mass damper (TMD). Its working principle is that the TMD's induced inertial forces will counteract the vibration of the structure (Bachmann and Ammann, 1987). This solution has been used successfully in practice to damp vibrations of lively footbridges (Tilly *et al.*, 1984; Eyre and Cullington, 1985; Bachmann and Ammann, 1987; Bachmann, 1992).

The TMD can be modelled as a SDOF system, which is attached to the structure at the point of maximum displacement of the target structural mode of vibration. It should be noted that, once it is attached, a new structural system is obtained with different natural frequencies. But the actual benefit of the TMD does not come from this frequency change; instead, it comes from an overall reduction in the dynamic response (Fig. 2.12).

By reducing the structure to a SDOF system, the calibration of the TMD is carried out by investigating the dynamics of a two degrees of freedom system composed of the structure plus the TMD. Optimum values have been suggested in the literature for the TMD calibration according to the structure's properties (Jones and Pretlove, 1979). However, it has been pointed out that the actual effectiveness of a TMD is strongly dependent on the accuracy with which the structural properties are determined, and particularly on the accuracy of estimating or measuring the structure's natural frequency of interest. This usually prevents the use of TMDs during the design stage since the estimation of natural frequencies of a footbridge may be significantly affected by the

presence of non-structural elements, uncertainties in material properties and the actual structural behaviour of joints and supports.

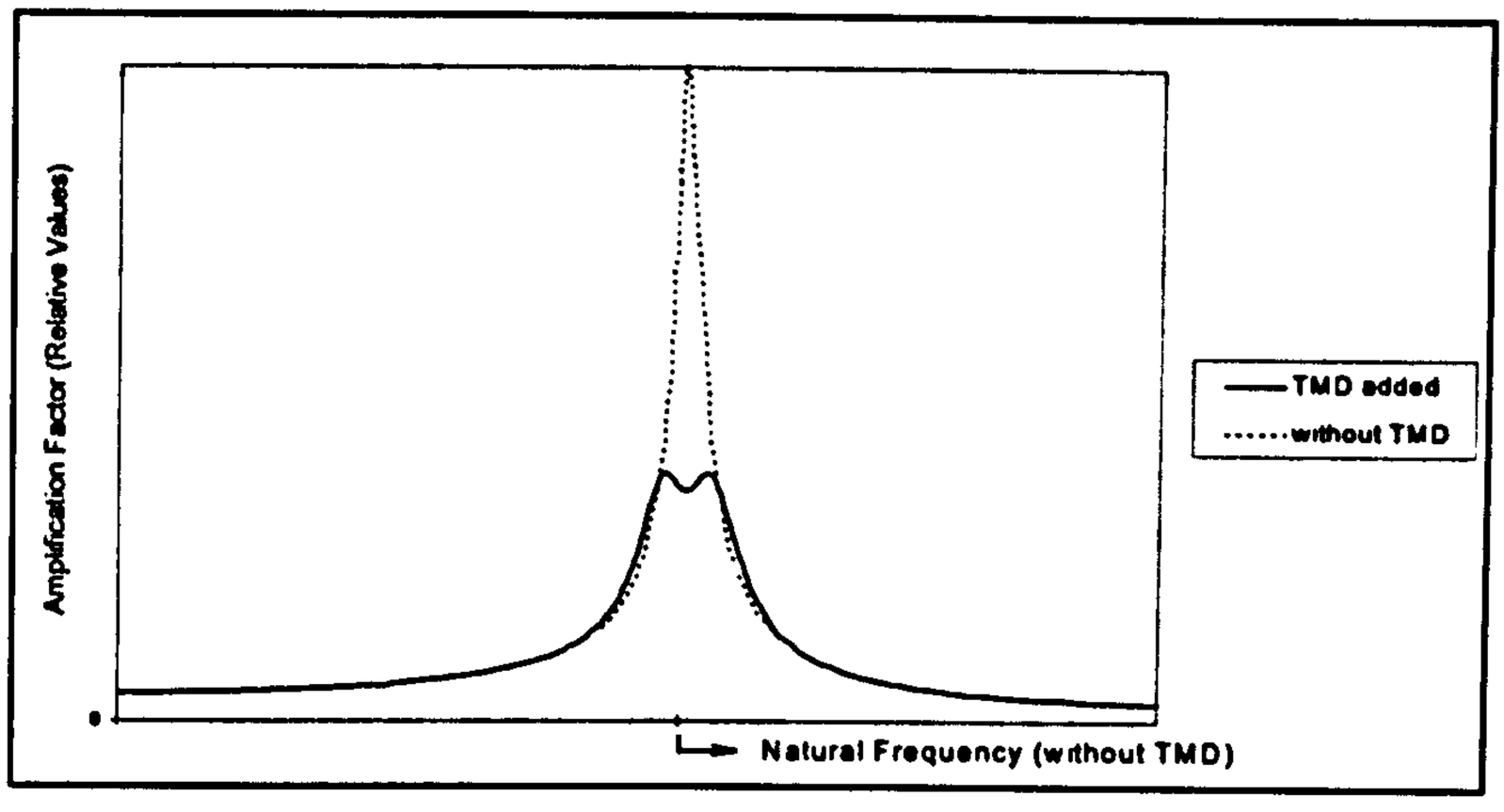

Figure 2.12 - Sketch of the effect of a TMD in reducing response levels (after Bachmann and Ammann, 1987).

2.6 Concluding Remarks

The topics discussed in this Chapter take into consideration the three aspects necessary to evaluate vibration levels: the definition of an appropriate excitation, the definition of permissible vibration levels, and a procedure to evaluate the response of the structure when subjected to the specified excitation.

The review carried out on these three aspects has shown that, in general, the codes of practice are not following the research advances in this area and a revision of the codes would be appropriate. There is also a degree of uncertainty in dealing with the problem, evidenced by divergent procedures to calculate or assess vibration performance. In addition, some issues were found to require further investigation and are summarised below:

(a) Investigations into the pedestrian load were carried out on rigid surfaces and it is not certain to what degree this load is modified when applied to a vibrating footbridge tested in resonance conditions. In addition, these structural vibrations may also cause interaction between pedestrians and the structure, which would make it questionable to treat the former as a load only.

(b) There is a lack of harmonisation between the codes in terms of assessing the human sensitivity to vibrations in civil engineering facilities. Whereas peak accelerations are adopted by the UK (BS5400, 1978) and Ontario (OHBDC, 1991) codes for footbridges, RMS acceleration and VDV are adopted for assessing vibrations in buildings (BS 6472, 1992). Furthermore, the latter code also presents a procedure for assessing multi-frequency component vibrations, a matter not explored in the footbridge codes.

(c) In the UK code (BS 5400, 1978), attention is concentrated on the first natural frequency of the footbridge in the vertical direction only, with no evaluation being made of vibrations in the lateral direction. There is a reference to vibrations in the lateral direction in the Ontario code (OHBDC, 1991), although only in terms of avoidance of a frequency range. Moreover, such a range is much broader than that in which vibration problems in the lateral direction have been reported (Table 2.2).

(d) Present investigations into the effect of crowd loading have shown discrepancies in results. Investigations into the crowd loading effect for vibrations at higher harmonics of the walking load have not been found in the literature.

(e) The applicability of the current vibration serviceability guidelines to the new generation of ACM footbridges deserves investigation since their relatively light weight may make them more susceptible to vibrations than footbridges made of conventional materials.

(f) Vandal loading should be further investigated considering the research advances made on modelling pedestrian load.

Thirteen case reports of lively footbridges have been presented (Table 2.2) and they confirm that only footbridges which have low natural frequencies are of interest in terms of vibration serviceability. Specifically, the frequency ranges of the first harmonics of the walking load could be taken as critical since it is there that all reported cases of lively footbridges are concentrated.

Chapter 3

Aspects of Modal Testing Applied to Pedestrian Bridges

3.1 Introduction

Okubo (1994) cited Brown's definition of the term *Modal Analysis*, which is the analytical or experimental analysis of the dynamic characteristics of a mechanical system in terms of its modal properties, i.e. natural frequencies, mode shapes and damping values. Taking the experimental route, the term *Modal Testing* encompasses the processes involved in testing a structure to obtain its modal properties and a mathematical description of its dynamic behaviour (Ewins, 1984). It may be noted that in either case the mechanical system is assumed to behave linearly and, when taking the experimental route, this assumption should be checked as part of the test procedure.

The experimental route to modal analysis encompasses a sequence of operations. To begin with, the structure is set vibrating and measurements are made. Raw (unprocessed) data consisting of time domain signals are initially obtained and, in a second step, the data collected are processed. There are several techniques in the time and frequency domains available for this latter task. In either case, the data processing involves the calculation of functions from which the modal properties can be obtained.

The availability of equipment and software has made the frequency domain techniques the prime choice for the processing of data. This involves a conversion of the acquired time domain signals to the frequency domain, by means of mathematical operations called Fourier Transforms. Although the time domain approach is more straightforward since it does not involve a conversion to another domain, it is from data processed in the frequency domain that modal properties of a structure, like the natural frequencies, are evident from visual inspection. Knowing the natural frequencies of the test structure during data acquisition is necessary in order to adjust parameters of the data acquisition system related to the acquisition itself. Another advantage of having the acquired signals converted to the frequency domain is that it is in this domain that an initial (on site)

evaluation of the quality of the data is possible. Therefore, independent of the group of techniques adopted for processing the data, conversion to the frequency domain is usually necessary. In practice, since algorithms have been developed for rapid application of the Fourier Transform, conversion to the frequency domain does not create difficulties in terms of delaying the signal processing. However, there are potential problems caused by applying this Transform to real (collected) data and several measures are necessary to ensure that the frequency domain functions (spectral functions) are accurately calculated.

Once these experimental spectral functions are calculated, a mathematical model to represent the structure is chosen and its modal properties are determined by curve-fitting the experimental functions to their theoretical counterparts. The final product is a mathematical model calibrated against test data and able to describe the dynamic behaviour of the structure.

The variety of techniques available for obtaining the modal properties of a structure is such that there are entire books devoted to the subject, some even concentrated on just a few of these techniques. This Chapter concentrates on specific issues of Modal Testing, in order to establish a basis for the understanding of the techniques adopted for the modal testing of prototype footbridges. It is divided into two Sections, the first being dedicated to a description of the Fourier Transform and several spectral functions that can result from its application, and the problems and measures that need to be taken for an accurate calculation of such functions. The second Section is dedicated to a description of the three different techniques adopted for the modal testing of prototype footbridges and the respective extraction of modal properties: ambient excitation, impulse response technique and free-vibration decay. Although a general description and application of these techniques for testing structures is covered in the literature, the experience acquired in applying them to the structures tested in this project has enabled suggestions to be made for improving their application.

3.2 Spectral Analysis

The heart of the analysis in the frequency domain is the Fourier Transform, which is a mathematical operator applied to time domain functions. The latter are actually sampled

signals of the excitation (applied forces) and/or responses (displacements, velocities or accelerations) of a test structure, and the advent of algorithms like the Fast Fourier Transform (FFT) has made it possible to speed up the conversion to the frequency domain. Several spectral functions can be calculated in this way by combining excitation and/or response signals. Details about the mathematics of the Fourier Transform and the definition of several spectral functions of interest are described in Section 3.2.1.

However, the signals being sampled in the field tests are not actually continuous as they are in the theoretical Fourier Transform formulae. The sampling is usually carried out at equally spaced time intervals and the acquired (discrete) signal is digitised i.e., converted from an analogue electrical quantity produced by a transducer to a digital value that can be processed by a computer. In addition, each acquired signal is of finite duration, which is also in conflict with the theoretically infinite signals used in the Fourier Transform formulae. Sampling and finite duration create the appearance of several sources of errors when obtaining spectral functions. This is the object of the discussion in Section 3.2.2, in which several sources of errors are described and measures to overcome them are presented. To conclude, the technique of zooming is described in Section 3.2.3, this being a way of improving the resolution of the calculated spectral functions.

3.2.1 Fourier Transforms and Spectral Functions

The Fourier Transform can be understood as an extension of the Fourier Series, which was employed to represent the pedestrian load (see Chapter 2). As was mentioned in Section 2.2.1, the Fourier Series can be used to represent periodic functions which satisfy the Dirichlet conditions. These conditions are satisfied by the signals of limited duration that are acquired from vibration tests. Looking now at the Fourier Series in a more general way, the representation of a periodic function $x(t)$ in terms of a Fourier Series is given by (Newland, 1993):

$$x(t) = a_o + \sum_{n=1}^{n=+\infty} \left(a_n \cos\left(\frac{2\pi n t}{T}\right) + b_n \sin\left(\frac{2\pi n t}{T}\right)\right) \tag{3.1}$$

where t is the time, n indicates the n^{th} term of the summation, T is the period of the function $x(t)$, and a_o, a_n and b_n are Fourier coefficients, given by:

$$a_o = \frac{1}{T}\int_{-T/2}^{T/2} x(t)\,dt$$

$$a_n = \frac{2}{T}\int_{-T/2}^{T/2} x(t)\cos\left(\frac{2\pi n t}{T}\right) dt \qquad (3.2)$$

$$b_n = \frac{2}{T}\int_{-T/2}^{T/2} x(t)\sin\left(\frac{2\pi n t}{T}\right) dt$$

A mathematical proof of the validity of Eq. 3.1 and deductions for Eqs. 3.2 are described in books on the subject (e.g. Sneddon, 1969). The limits of integration in Eqs. 3.2 can be changed, however, bearing in mind that the integration is to be carried out over a single period T (Newland, 1993). The choice of these limits is a matter of convenience.

Using Euler's relation to express trigonometric functions in complex exponential form, Eq. 3.1 can be rewritten as (Ewins, 1984):

$$x(t) = \sum_{n=-\infty}^{n=+\infty} X_n\, e^{i(2\pi n t/T)} \qquad (3.3)$$

where $i = \sqrt{-1}$ and the complex Fourier coefficient X_n is given by:

$$X_n = \frac{1}{T}\int_{-T/2}^{T/2} x(t)\; e^{-i(2\pi n t/T)}\, dt \qquad (3.4)$$

in which the previous discussion regarding the integration limits also applies. A consequence of the complex representation is that the Fourier coefficients X_n occur in complex conjugate pairs, i.e. $X_{-n} = X_n^*$, the term on the right hand side being the complex conjugate of X_n. Such coefficients have the same units as the function $x(t)$ and

each coefficient X_n is related to a frequency component the value of which is n times the frequency increment $\Delta f = 1/T$, this also being called frequency resolution.

It should be noted that if the period of the function x(*t*) tends to infinity, non-periodic functions could also be represented. Taking the period T to infinity in Eqs. 3.3 and 3.4, a new pair of equations can be obtained (Bendat and Piersol, 1993):

$$x(t) = \int_{-\infty}^{+\infty} X(f)\, e^{i(2\pi f t)}\, df \tag{3.5}$$

$$X(f) = \int_{-\infty}^{+\infty} x(t)\, e^{-i(2\pi f t)}\, dt \tag{3.6}$$

where X(f) is usually called the Fourier spectrum, being a complex continuous function containing amplitude and phase information. In obtaining Eq. 3.5 from Eq. 3.3, X_n was replaced by $X(f)\Delta f$, and so X(f) has the unit of spectral density. Eqs. 3.5 and 3.6 are called the Fourier Transform pair, Eq. 3.6 being the (forward) Fourier Transform and Eq. 3.5 the Inverse Fourier Transform. The Fourier spectrum X(f) also occurs in conjugate pairs ($X(-f) = X^*(f)$), leading to a common representation of a one-sided (positive side) spectrum. Knowledge of either of the functions x(*t*) or X(f) does allow the other to be regained using as appropriate Eq. 3.5 or 3.6. Application of Eqs. 3.5 and 3.6 is however limited by the condition that the function x(*t*), when having its modulus integrated over the limits $-\infty$ to $+\infty$, produces a finite value (Newland, 1993).

Eqs. 3.5 and 3.6 are not, however, the way the Fourier Transforms are applied in practical applications. As was mentioned in Section 3.2, the continuous function x(*t*) (e.g., a measured acceleration or input force) is actually represented by a sampled signal of finite duration, and this will imply that the signal will have a discrete representation in the frequency domain. Calling the duration of the acquired time signal T, by analogy with the Fourier Series, the frequency lines of the Fourier Spectrum will be equally spaced at intervals of (1/T). For a periodic signal x_m consisting of N equally spaced samples (at discrete points $t=t_m$, m= 0, N-1), acquired at a rate of (N/T) samples per unit of time, Eq. 3.4 can be replaced by the following summation, taking conveniently the

integral limits from zero to T and making substitutions to introduce the number of samples N in the expression (Newland, 1993):

$$X_n = \frac{1}{N}\sum_{m=0}^{N-1} x_m\, e^{-i(2\pi nm/N)} \tag{3.7}$$

Eq. 3.7 allows all discrete values x_m to be regained, this being given by an inverse formula obtained making similar changes into Eq. 3.3, to take into account the finite number of Fourier coefficients X_n (n=0 to N-1):

$$x_m = \sum_{n=0}^{N-1} X_n\, e^{i(2\pi nm/N)} \tag{3.8}$$

Eqs. 3.7 and 3.8 form a pair having the same properties as their continuous counterparts Eqs. 3.6 and 3.5, being their discrete version. Accordingly, Eqs. 3.7 and 3.8 are called Discrete Fourier Transform (DFT) and Inverse Discrete Fourier Transform (IDFT), respectively. As Randall (1987) observed, for convenience, Eqs. 3.7 and 3.8 have not been made symmetrical at the origin, but since they are periodic, the second half represents the negative half period to the left of the origin, and the 'conjugate even' property of the Fourier coefficients also applies ($X_{N-s} = X_s^*$). It may be noted that Eq. 3.7 actually calculates discrete Fourier coefficients X_n having the same unit of x_m, in contrast to the units of spectral density of the spectrum X(f). A slightly different definition of the Discrete Fourier Transform pair is given by Bendat and Piersol (1993):

$$\chi_n = \frac{T}{N}\sum_{m=0}^{N-1} x_m\, e^{-i(2\pi nm/N)} \tag{3.9}$$

$$x_m = \frac{1}{T}\sum_{n=0}^{N-1} \chi_n\, e^{i(2\pi nm/N)} \tag{3.10}$$

For obtaining Eq. 3.9, a finite version of Eq. 3.6 is defined, in which a Fourier Spectrum χ(f) is obtained integrating the function x(t) over one period:

$$\chi(f) = \int_0^T x(t)\, e^{-i(2\pi f t)}\, dt \tag{3.11}$$

Substitution of the integral in Eq. 3.11 by a summation (since x(t) is a sampled function of finite duration) leads to Eq. 3.9. The difference between Eqs. 3.9 and 3.10 and the previously defined DFT pair (Eqs. 3.7 and 3.8) occurs because Eqs. 3.9 and 3.10 are obtained starting from the definition of the Fourier Transform pair (Eqs. 3.5 and 3.6) whereas Eqs. 3.7 and 3.8 were obtained starting from the Fourier Series Eqs. 3.3 and 3.4. It may be noted that the discrete Fourier coefficient χ_n in Eq. 3.9 has units of spectral density and that it is related to the coefficient X_n by (Bendat and Piersol, 1993):

$$\chi_n = T X_n = \frac{X_n}{\Delta f} \tag{3.12}$$

These different definitions of the DFT are worth mentioning since each DFT pair will lead to different definitions of other derived spectral functions in order to obtain the same values for them. The DFT pair of Eqs. 3.7 and 3.8 was adopted for the subsequent definitions because they are in agreement with the way the DFT operations are performed by the test instrumentation (see Appendix A.1). For the sake of clarity, the Fourier coefficients X_n will be further referred to as a Fourier Spectrum and each individual value as a Fourier component.

The DFT is calculated by algorithms referred to by the general name of Fast Fourier Transform (FFT), this name being given by Cooley and Tukey, who are acknowledged as having first conceived of one such algorithm that made possible a most efficient calculation of the DFT on computers. The FFT algorithms most commonly employed require the number of samples of the input (i.e. the signal) to be a power of two (Newland, 1993).

An important relation between the time and frequency domain representations of a signal is the Parseval theorem, which states that the mean *power* of a signal can be obtained either by integrating the squared signal amplitudes x(t) with respect to time and dividing this by the acquisition time, or by adding up the squared amplitudes of all

frequency components of the Fourier Spectrum. The term *power* actually comes from an analogy to electrical quantities but here means simply the square of a variable (Randall, 1987). Denoting the root mean square of the time signal by A_{RMS} , the application of the Parseval theorem gives:

$$A_{RMS}^2 = \sum_{n=-\infty}^{n=+\infty} \left|X_n^2\right| = X_o^2 + 2\sum_{n=0}^{n=+\infty} \left|X_n^2\right| \tag{3.13}$$

the last identity on the right hand side being based on the fact that $X_{-n} = X_n^*$ whereas X_o indicates the component at the origin (f = 0), sometimes called static or DC component and being related to the mean value of the time signal. It should be noted that, for a single sinusoidal excitation of frequency f and zero mean value (the latter implying that $X_o = 0$), only two lines or frequency components appear in the spectrum, and the respective Fourier components X_{-f} and X_f have an amplitude of $A_{RMS} / \sqrt{2}$. If only one side of the spectrum is represented, and it is usually the positive side, the amplitude of the Fourier coefficient X_f is multiplied by $\sqrt{2}$ (i.e. the square of the amplitude is doubled) in order to keep the *power*. This will imply that the one-sided spectrum will have a Fourier component having a value equal to the root mean square of the sinusoidal excitation. This conclusion can be extended to each frequency component of a multi-frequency component signal.

Several spectral functions can be defined based on the Fourier Transform of signals. These functions are theoretically defined for signals of infinite duration but are actually calculated based on signals of finite duration through the use of the Discrete Fourier Transform. The spectral representation of a discrete signal is based on the assumption that such a signal is periodic within the acquisition time, and consequently repeatable for successive acquisition frames throughout the whole duration of the signal. Actually, as will be seen in more detail later in this Chapter, each acquired signal is related to a repeatable process of excitation of the structure and measurement of its response, in which the same excitation conditions are either attempted to be applied or assumed. There is also the presence of noise which is added to the signal during its acquisition, which is due to the electronics of the test equipment and measurement conditions. This

causes variations among individual spectral calculations and the phrase spectral estimate properly refers to spectral functions obtained in this way, inducing the use of averaging for increasing their reliability. In doing this, each acquired signal of finite duration is converted to the frequency domain, and the individual spectral calculations are averaged out resulting in a final estimate.

The following is a brief definition of the spectral functions of interest, together with a description of some of their properties. The index n indicates the n^{th} term of each discrete spectral function.

Power Spectral Density or Autospectral Density

The Power Spectral Density (PSD) or simply Autospectral Density, as estimated by the DFT, is defined by (see Appendix A.1):

$$G_{xx_n} = 2S_{xx_n} = 2T\left|X_n^2\right| = 2\frac{X_n^* X_n}{\Delta f} \tag{3.14}$$

bearing in mind that $\Delta f = (1/T)$, where T is the acquisition time. S_{xx} is a real valued function and G_{xx} its one-sided representation. One of the most useful properties of the PSD is the immediate identification of the predominant frequencies of vibration of the signal. For a structure in free vibration, for example, the PSD of a response signal will have peaks at the natural frequencies of the structure.

It may be convenient simply to plot the amplitude of the Fourier spectrum of X_n ($|X_n|$) or its square $\left|X_n^2\right|$, the latter being called Power Spectrum or Autospectrum. A plot of a one-sided amplitude of the Fourier spectrum of a response signal measured on one of the test footbridges can be seen in Fig 3.1, in which the frequencies of vibration appear as peaks. In all of these spectra, the phase information is lost and consequently the original time domain signal cannot be regained.

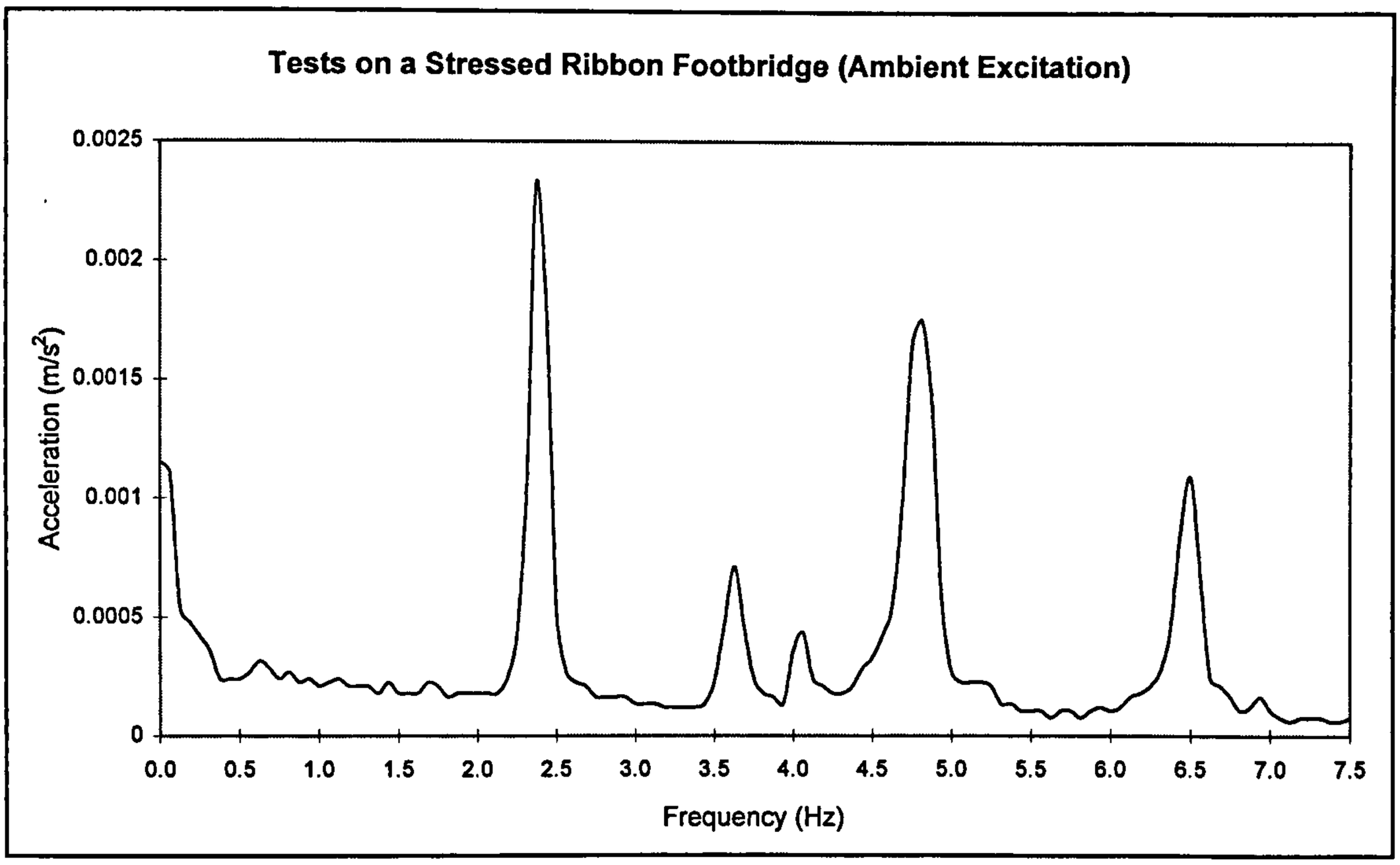

Fig. 3.1 - Fourier amplitude spectrum of an acceleration response signal

Cross Spectral Density

The Cross Spectral Density of two signals x and y is defined as:

$$G_{xy_n} = 2S_{xy_n} = 2\frac{X_n^* Y_n}{\Delta f} \tag{3.15}$$

where G_{xy} is the one-sided version of S_{xy}. The cross spectral density is a complex spectral function, the amplitude of which, for each frequency line, being obtained by multiplying the amplitudes of each individual Fourier spectra and dividing this product by the frequency resolution Δf. The Cross Spectral Density phase is the difference of phase angles between the individual Fourier spectra. In a similar way, the cross spectral density G_{yx} would have the same amplitudes but opposite phases, i.e. it is the complex conjugate of G_{xy}. This spectral function is useful for calculations of phase differences and time shifts between two given signals (Randall, 1987). However, it is mainly used for calculating other spectral functions like the Frequency Response Function (FRF).

Similarly to the Power Spectrum function, the Cross Spectrum is defined as the spectral function obtained by simply calculating the product of the two spectra X_n^* and Y_n (Randall, 1987).

Frequency Response Function

The Frequency Response Function (FRF) is the most complete spectral function for obtaining the response characteristics of a structure. It is a complex function defined in terms of a single input/single output system as the ratio of the Fourier spectrum Y_n of the system output or response (displacements, velocities or accelerations), to the Fourier spectrum X_n of the system input or excitation (applied force) (Halvorsen and Brown, 1977):

$$H_n = \frac{Y_n}{X_n} \tag{3.16}$$

As mentioned by Halvorsen and Brown (1977), there are two requirements for the calculation of the FRF. The first one is that both signals are Fourier transformable, and this was already seen as a condition that is usually met for the signals of finite duration dealt with in vibration testing. The second requirement is that X_n is non-zero at the frequency range of interest, implying that appropriate excitation sources need to be sought.

The FRF can be expressed as a function of other spectral functions (Ewins, 1984). Using the one-sided Power and Cross Spectral Density functions and departing from Eq. 3.16, multiplying both its numerator and denominator by the complex conjugate of X_n gives:

$$H_n = \frac{Y_n}{X_n} = \frac{Y_n X_n^*}{X_n X_n^*} = \frac{G_{xy_n}}{G_{xx_n}} \tag{3.17}$$

Alternatively, multiplying both the numerator and denominator of Eq. 3.16 by the complex conjugate of Y_n, the following expression is obtained:

$$H_n = \frac{Y_n}{X_n} = \frac{Y_n Y_n^*}{X_n Y_n^*} = \frac{G_{yy_n}}{G_{yx_n}} \tag{3.18}$$

The FRF estimations using Eqs. 3.17 and 3.18 are called H1 and H2 estimators of the FRF, respectively. By combining these two equations, a third expression can be obtained for the amplitude of the FRF, losing, however, the phase information (Ewins, 1984):

$$\left|H_n^2\right| = \frac{G_{yy_n}}{G_{xx_n}} \tag{3.19}$$

The choice of the estimator depends on the application, since they are influenced by signal noise in different ways. Noise is originated from the electronics of the test equipment and from ambient sources, and its presence in both input and output signals are considered to be uncorrelated to each other. This concept can be understood as these signal components, i.e. the noise, not having any relationship between each other, and this can be seen by plotting them one against another, from which no pattern or relation can be inferred. Bearing this in mind, it is shown that by averaging, it is possible to remove the noise effects from the Cross Spectral Density functions, and only the Power Spectral Density functions are left as being potentially contaminated by noise (Ewins, 1984). Consequently, the H1 estimator (Eq. 3.17) is affected by noise present only on the input signal whereas the H2 estimator (Eq. 3.18) is affected by noise present only on the output signal.

In any of the Eqs. 3.17 to 3.19, use of the auto and cross spectrum instead of the respective spectral densities is possible since the term Δf present in the spectral densities will cancel out as it is appearing in both the numerator and denominator of the expressions.

For a given steady-state sinusoidal excitation of unit amplitude, the magnitude of the FRF indicates the amplification factor on the response at the frequency of the excitation. The FRF phase represents the phase difference between excitation and response, which appears due to the structure's damping. As to the excitation sources, they are chosen in

such a way that they are ideally able to excite the structure equally over the whole range of frequencies of interest. This will cause the appearance of peaks on the FRF at the natural frequencies of the structure, for which the aforementioned amplification factors are higher. The condition of equal excitement of all frequencies of interest implies a flat Autospectrum of the excitation, a condition that occurs, for example, when applying an impact to the structure, as it will be seen in Section 3.3.2.

Being a function based on excitation and response signals, the relative positions between the points where the excitation is applied and the response is measured distinguish two types of FRF: point FRF or driving point FRF, in which the excitation and response stations are coincident; and transfer FRF in the other situations. The driving point FRF has an important role in the measurement chain, and this will be discussed in Section 3.3.2. The selection of this point should ideally be such that it is not coincident or closer to a node of a vibration mode of interest for the analysis; otherwise the identification of such a mode will be compromised when further processing the data.

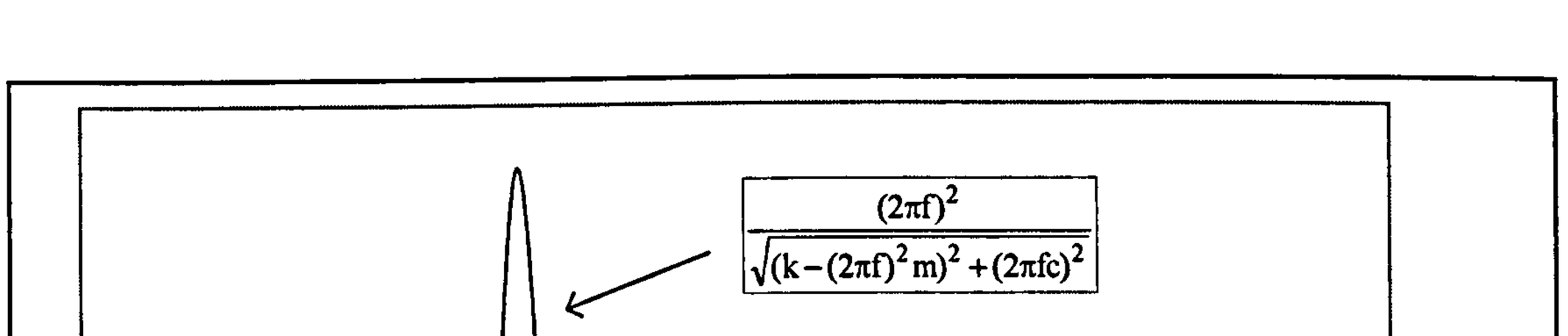

Figure 3.2 - Typical plot of the amplitude of a FRF inertance of a SDOF system

The FRFs also receive different names according to which output signal is being measured: for displacement signals, the FRF is called receptance; for velocities or accelerations, they are called mobility or inertance, respectively. These FRFs are converted from one to another using the relationships between displacement, velocity and acceleration for sinusoidal signals (Ewins, 1984). Typical plots of the amplitude of a FRF inertance for a SDOF system and a FRF point inertance for a multi-degree of freedom (MDOF) system are shown in Fig. 3.2 and 3.3 respectively.

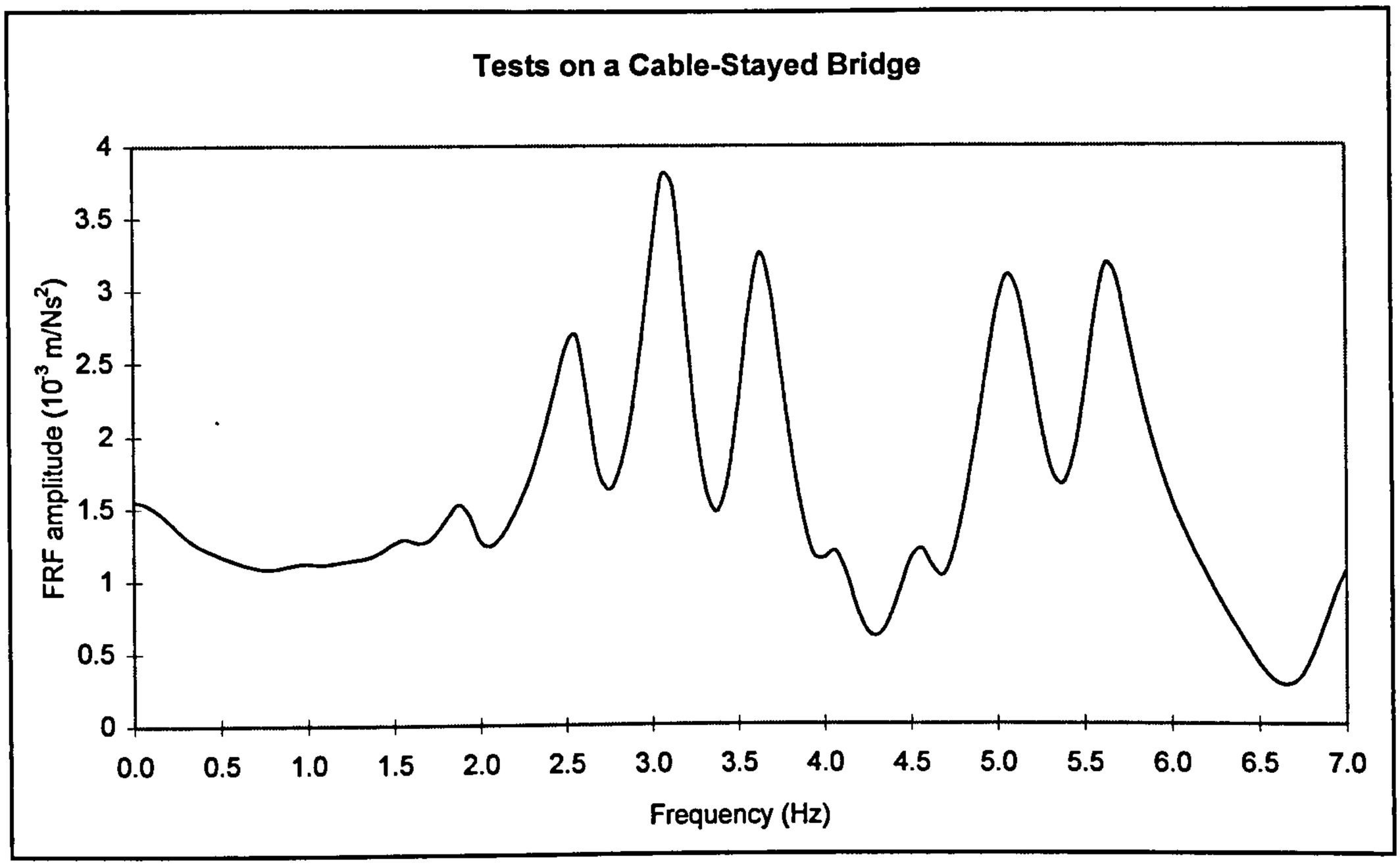

Figure 3.3 - Typical plot of the amplitude of a FRF point inertance of a MDOF system

An important theoretical relation between the FRF and the modal properties of the structure makes it possible to obtain the latter from the former. For a system with proportional viscous damping, this is given by (Ewins, 1984):

$$A_{jk}(f) = -(2\pi f)^2 \alpha_{jk}(f) = -(2\pi f)^2 \sum_{r=1}^{R} \frac{{}_r\phi_j \; {}_r\phi_k}{(2\pi \bar{f}_r)^2 - (2\pi f)^2 + i 2\zeta_r (2\pi f)(2\pi \bar{f}_r)} \qquad (3.20)$$

where $A_{jk}(f)$ and $\alpha_{jk}(f)$ are the FRF inertance and receptance, respectively, between the response at coordinate j due to the excitation of frequency f applied at coordinate k. In

the right-hand side of Eq. 3.20, a summation is carried out over R modes of vibration, where ${}_r\phi_j$ and ${}_r\phi_k$ are the respective ordinates of the mass-normalised mode shape[4] r at coordinates j and k; the product of the mode shape ordinates is called modal constant. $\bar{f}_r$ and ζ_r are the respective r^{th} undamped natural frequency and equivalent viscous damping ratio of the system. Further details about the FRF and its properties are fully covered in textbooks about the subject (e.g. see Ewins, 1984).

Coherence

Coherence is a measure of identifying how signals are correlated with each other. As was mentioned before, the correlation, or lack of it, between two signals can be inferred by plotting them one against the other, from which a relation between the two signals can be identified. As examples of the application of Coherence, if two signals are the excitation applied and response of a structure to it, Coherence measures how much the response signal of the structure is due to the excitation. In another situation in which, for a common excitation, two response signals are measured, Coherence would be a measure of the degree to which the two output signals appear to be caused by the same input.

The Coherence function is defined as (Bendat and Piersol, 1993):

$$\gamma^2_{xy_n} = \frac{\left|G_{xy_n}\right|^2}{G_{xx_n}\, G_{yy_n}} \tag{3.21}$$

being a real valued spectral function varying between zero and one, the higher value indicating that the two signals x and y are fully correlated. Recalling the definitions of the Power and Cross spectral densities (Eqs. 3.14 and 3.15), it turns out that the quotient in Eq. 3.21 will theoretically always have a unit value. However, as was mentioned before, the presence of noise, which can be averaged out on the numerator of Eq. 3.21

---

[4] Mass-normalised mode shapes are those which diagonalise the mass matrix [M] of the structure: $[\Phi]T[M][\Phi] = [I]$, where $[\Phi]$ is a matrix the columns of which are the mass-normalised mode shapes and [I] is the unit matrix (Thomson, 1993).

but not on the denominator, where it is actually added up, leads to Coherence values of less than one.

Based on this, Coherence is a way of identifying the effects of noise on the spectral evaluations and consequently their quality. However, it must be borne in mind that Coherence only makes sense as an indicator of correlation between signals within an averaging process, in which the uncorrelated noise is averaged out from the Cross Spectral Density estimates. Indeed, Coherence could be used to help in determining how much averaging is required to reduce the effects of measurement noise.

Eq 3.21 can also be expressed as a quotient of the FRF estimators H1 and H2 (Eqs. 3.17 and 3.18) as (Ewins, 1984):

$$\gamma^2_{xy_n} = \frac{\left|G_{xy_n}\right|^2}{G_{xx_n} G_{yy_n}} = \frac{G_{xy_n} G^*_{xy_n}}{G_{xx_n} G_{yy_n}} = \frac{G_{xy_n} G_{yx_n}}{G_{xx_n} G_{yy_n}} = \frac{H1}{H2} \qquad (3.22)$$

from which it can be seen that the H1 estimator produces estimations of the FRF which are smaller than those obtained using the H2 estimator. This can be understood considering that the H1 estimator has the term in which noise is added up (i.e. G_{xx}) on the denominator whereas the H2 estimator has the noise affected term (G_{yy}) on the numerator.

However, noise is not the only effect that can cause low coherence. McConnell (1995) cited three other sources of low coherence: non-linear structural response, poor frequency resolution, and time delay between signals. Having such a variety of sources, Coherence is generally taken as a qualitative parameter for immediate (on site) evaluation of collected data, varying from very bad quality (coherence approaching zero) to very good quality (coherence approaching unity).

Although a scale of quality has not been suggested, coherence values of 0.9 or higher have been recommended as an indication of the good quality of a spectral estimate (DTA, 1995).

It has been mentioned that low coherence is an indication of a poor measurement. However, there is one situation in which this may not necessarily be the case. This is when measurements are taking place with the presence of measured and unmeasured excitations, and these different excitation sources are uncorrelated with each other. This situation arises, for example, when testing open space civil engineering structures using the impulse response technique (see details in Section 3.3.2), in which case the measured excitation signal consists of an impact of a hammer on the structure, whereas the wind acts as a source of unmeasured excitation. The response signal is actually due to both excitation sources.

It has been shown (McConnell, 1995) that only the estimator H2 is affected (augmented) due to the contribution of the unmeasured excitation (which is not to be mistaken for noise) since H2 includes the Power Spectral Density of the response signal, this being due to both sources of excitation. The H1 estimator is not affected by the presence of the unmeasured excitation since the effect of the wind on the response is averaged out of the Cross Spectral Density between the measured excitation signal and the response. Therefore, a low coherence value would not necessarily mean that the quality of the data is poor if the H1 estimator is used to calculate the FRFs in these conditions. A corollary of this discussion is that the H1 estimator is recommended for testing open space structures.

A typical plot of coherence is shown in Fig. 3.4 together with the magnitude of a FRF obtained using the H1 estimator from an impact excitation test on one of the test footbridges. It can be seen that coherence is high in the regions of the peaks (resonances) of the FRF, which correspond to the natural frequencies of the structure, whereas it may be low in the regions of the troughs or anti-resonances. This pattern can be understood by considering that, for an excitation which possesses a flat amplitude spectrum like that produced by a hammer impact (see Section 3.3.2), the response of the structure is magnified at frequencies close to resonance, the responses being higher in these regions when compared to the noise levels.

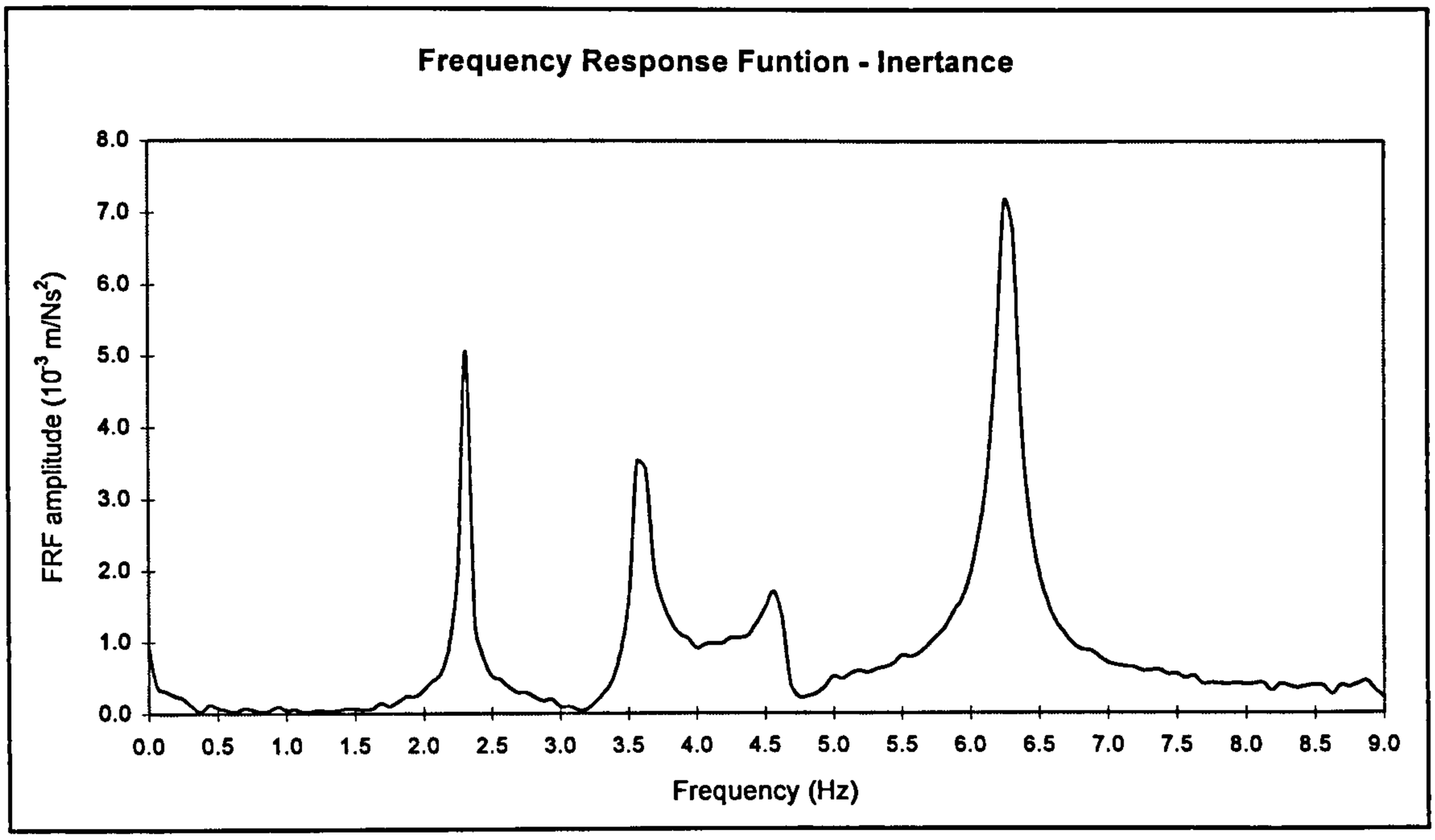

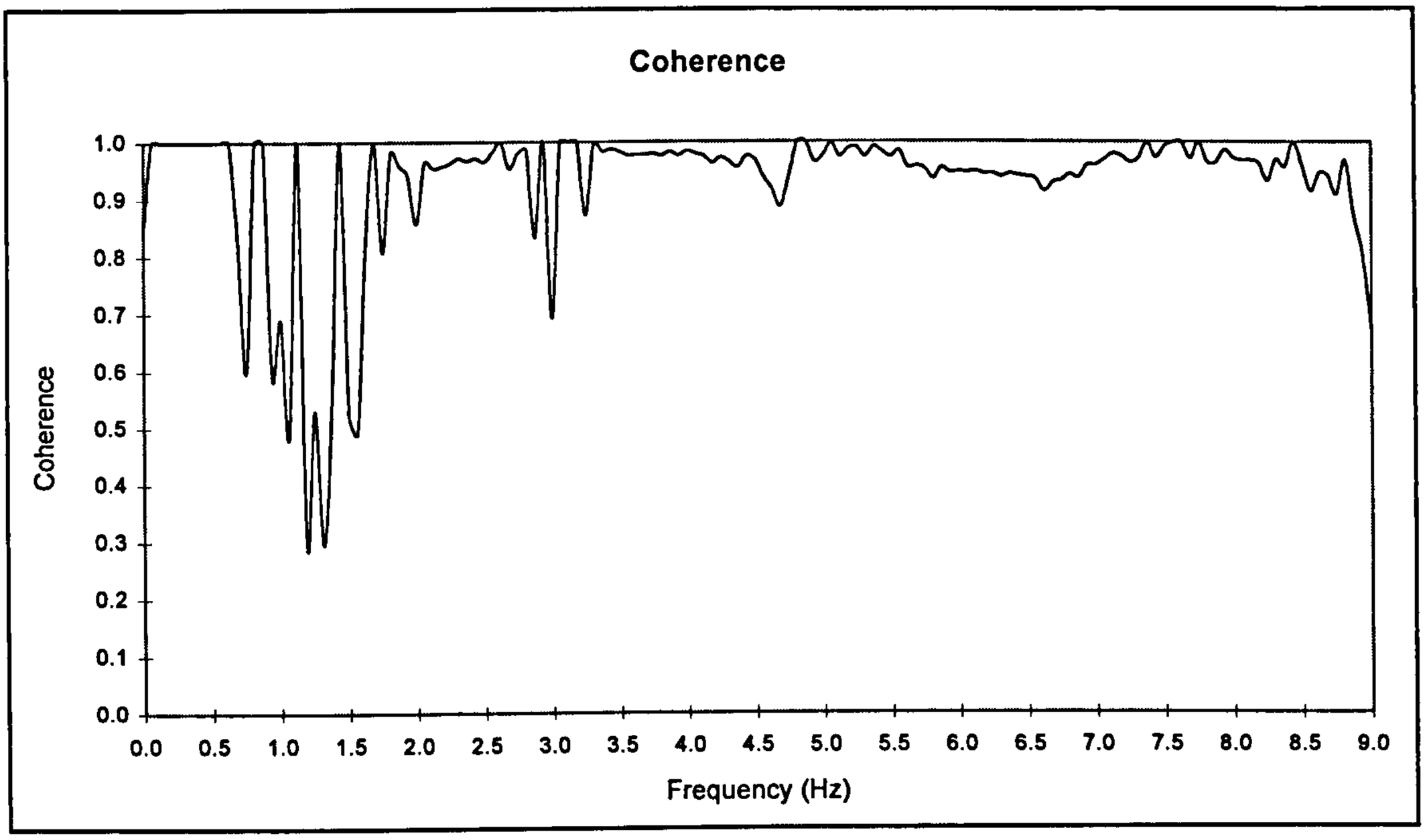

Figure 3.4 - FRF amplitude and coherence

3.2.2 Errors in Spectral Evaluations

There are a number of features of digital Fourier Analysis based on the DFT which can give rise to errors when evaluating spectral functions. As a reminder, the parameters related to the acquisition of discrete signals are:

- the constant time interval or sampling time Δt between two consecutive samples. For acquiring N samples, the duration of the acquired record is $T= N\Delta t$. The number of samples N is generally restricted to powers of two in order to use FFT algorithms for obtaining Fourier spectra, and the signal is assumed to be periodic within the acquisition time.

- the frequency increment or resolution Δf, given by the inverse of the period T. The frequency increment also defines the frequency components of the discrete signal, which are multiples of Δf. The frequency range f_s is given by the inverse of the time interval Δt, containing N frequency components or lines on the spectrum. The frequency range f_s actually coincides with the numerical value of the maximum frequency component that can be represented since the frequency range is initiated from zero.

Discretisation, acquisition of signals of finite duration and lack of periodicity of the signal within the acquisition time cause the following errors when obtaining spectral estimates: aliasing, leakage, bias (due to frequency resolution) and random errors, which are described as follows.

Aliasing

This phenomenon is caused by the discretisation of a continuous signal. For a given sampling rate, the signal may contain high frequency components which are erroneously acquired, being actually mistaken as low frequency components. This can be seen in Fig. 3.5 where, for a sampling time of 1 sec, a sinusoidal signal of frequency 1.2 Hz is sampled, being 'aliased' as a signal of frequency 0.2 Hz. The aliased signal will be indistinguishable from an actual low frequency component that may be present in a signal, causing distortions on the Fourier spectra.

Aliasing is indeed a folding back of high frequency components, resembling signals of lower frequency, and it is caused by an insufficient sampling rate to represent properly the high frequency components. The frequency up to which the aliasing phenomenon

does not occur is called the Nyquist or Folding frequency, being given by (Bendat and Piersol, 1986):

$$f_{nyq} = \frac{1}{2\Delta t} \tag{3.23}$$

For a component of frequency f in the range from zero to f_{nyq}, the Nyquist theorem shows that such a frequency component is aliased with components of frequencies ($2nf_{nyq} \pm f$, n=1,2 ...) (Bendat and Piersol, 1986). The effect will depend on how significant is the component of frequency f with respect to the others.

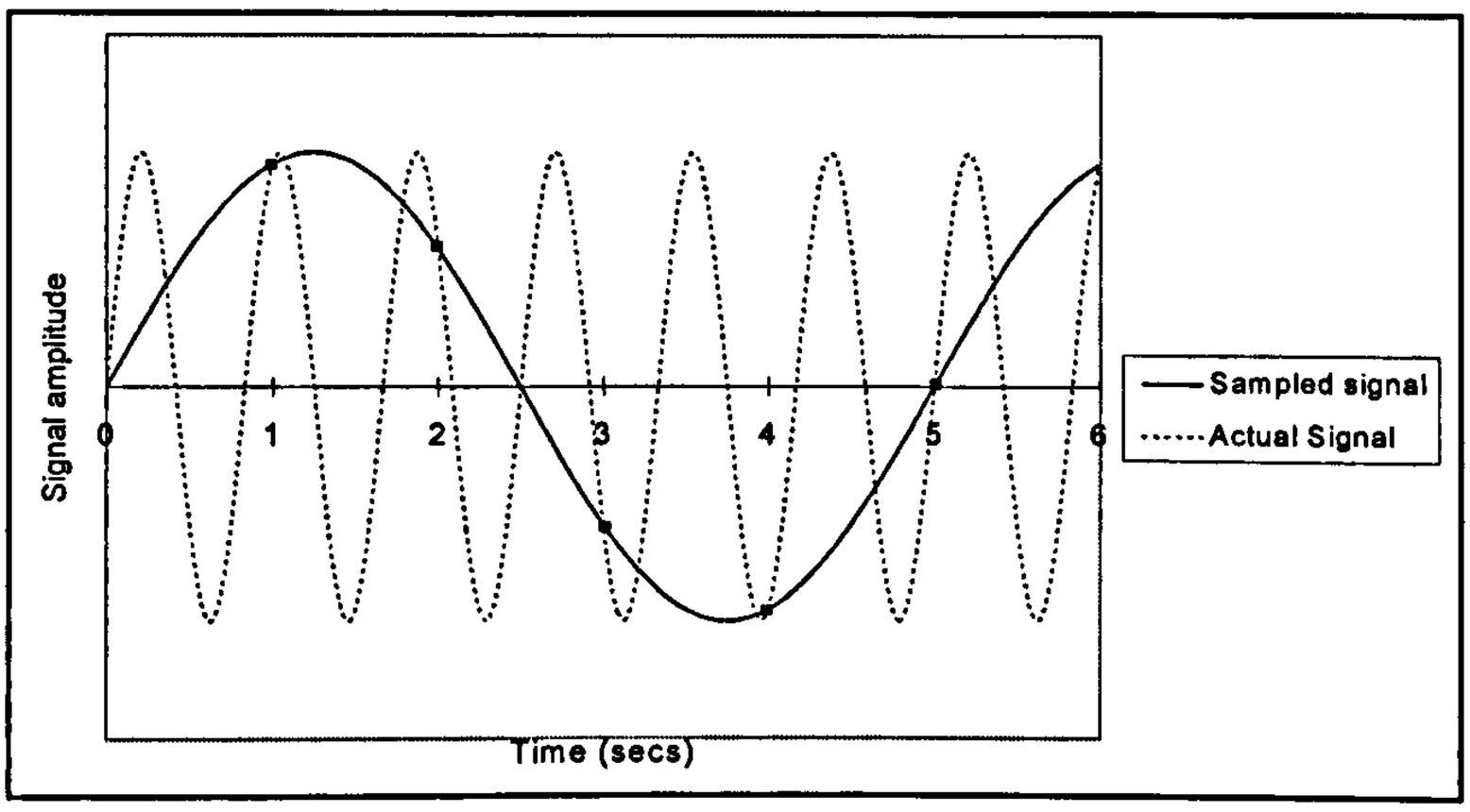

Figure 3.5 - Illustration of aliasing of a sinusoidal signal (after Randall, 1987)

An immediate solution for the aliasing problem would be reducing Δt as much as is necessary to avoid any significant frequency components being aliased. However, this could lead to large amounts of data being acquired, requiring more storage space and increasing the time for processing data (i.e., for obtaining spectral functions). The usual solution for sorting out the aliasing problem is to use anti-aliasing (a/alias) filters to remove undesirable higher frequencies from the signal. These filters are low-pass filters and are usually included as part of the hardware of the test instrumentation. They remove frequency components above a given frequency from the signal. However, an a/alias filter, like any filter, cannot cut off abruptly undesirable frequency components, since it presents a slope in the frequency domain. This varies from zero (no removal) up to a frequency from which all subsequent frequencies are removed, this being called the cut-off frequency.

In order to have an unaffected frequency range, it is customary to limit the upper frequency to a value which is below the beginning of the slope of the filter (Bendat and Piersol, 1986). By taking the filter cut-off frequency as the Nyquist frequency, Randall (1987) pointed out that, for the high slope filters usually employed in anti-aliasing operations, the upper frequency is usually taken at about 80% of the Nyquist frequency. Furthermore, bearing in mind that the FFT algorithms usually demand a number of samples N which is a power of two, and that this number N is also the total number of frequency lines, the search for an unaffected frequency range with an entire number of frequency lines leads to a choice of the upper frequency (or frequency range) f_c given by:

$$f_c = \frac{1}{2.56\,\Delta t} = \frac{N}{2.56\,T} = (\frac{N}{2.56})\,\Delta f \qquad (3.24)$$

where the number 2.56 makes $f_c \approx 0.8\ f_{nyq}$ and gives an entire number of frequency lines within f_c , since the powers of two above 2^6 can be divided exactly by 2.56. Table 3.1 gives some typical values for data acquisition parameters taking into account the relations presented in Eq. 3.24.

Acquisition time T = 8 secs ($\Delta f = 1/T = 0.125$ Hz)		Number of Frequency Lines within f_c	Acquisition time T = 16 secs ($\Delta f = 1/T = 0.0625$ Hz)	
Number of Samples N	Frequency Range f_c (Hz)		Number of Samples N	Frequency Range f_c (Hz)
256	12.5 Hz	100	256	6.25 Hz
512	25 Hz	200	512	12.5 Hz
1024	50 Hz	400	1024	25 Hz
2048	100 Hz	800	2048	50 Hz
4096	200 Hz	1600	4096	100 Hz

Table 3.1 - Typical values for data acquisition parameters

It should be noted that the absence of anti-aliasing filters does not necessarily mean that the spectral calculations are affected by aliasing. This will depend on the frequency content of the signal, i.e. if the signal has frequency components above the Nyquist frequency and if such components are significant. However, a word of caution: application of this filter must be done before the analogue to digital conversion. This is to say that the signal should enter the analogue to digital (A/D) converter free of

frequency components above the Nyquist frequency because, once the signal is digitised, aliased high frequency components can no longer be removed (McConnell, 1995).

Leakage

This is an error in the spectral evaluations caused by truncating a signal which is non-periodic within the acquisition time. As a reminder, the Fourier Transform assumes that the signal is periodic within the frame (acquisition time) in which the calculations are carried out. If the signal is non-periodic, it is misrepresented in the frequency domain since it will contain frequency components other than the frequencies of the discrete spectrum obtained by applying the DFT. Therefore, the power contained in each of the actual misrepresented frequency components of the signal will spread or 'leak' over the frequency components of the discrete spectrum (Randall, 1987).

This phenomenon can be understood by observing the effect of applying a rectangular window in an infinite periodic signal. This window is actually what is applied on the signal for selecting a portion of it for spectral calculations, its application being sometimes referred to as absence of window. It has a unit value in the selected region and a value of zero anywhere else. Taking such a window as a function which is multiplied by the time domain signal, it is shown that a multiplication in the time domain results in convolution in the frequency domain and vice versa (Randall, 1987). Therefore, the Fourier spectrum of the signal is convoluted with the Fourier spectrum of the applied rectangular window. The amplitude spectrum of the latter is shown to be given by $|T \sin(\pi f T)/\pi f T|$ (Bendat and Piersol, 1993), where T is the acquisition time. This function is shown in Fig. 3.6a,b , and it can be seen that it contains lobes, with zero crossings at intervals of 1/T.

If the signal is periodic within the acquisition time, its frequency components are multiples of the frequency increment (1/T). Convoluting the two spectra, each frequency component of the signal will coincide, at a time, with the peak of the main lobe of the window. All other frequency lines are coincident with the zeros of the window, leaving the Fourier spectrum of the signal unaltered (Fig. 3.6a). This is also the case for

transient signals which are entirely contained within the acquisition time. Such signals can be seen as a periodic function fully described by the discrete frequency components multiples of (1/T). Conversely, in the other cases, each frequency component (frequency line) does not coincide with the peak of the main lobe and leakage occurs (Fig. 3.6b).

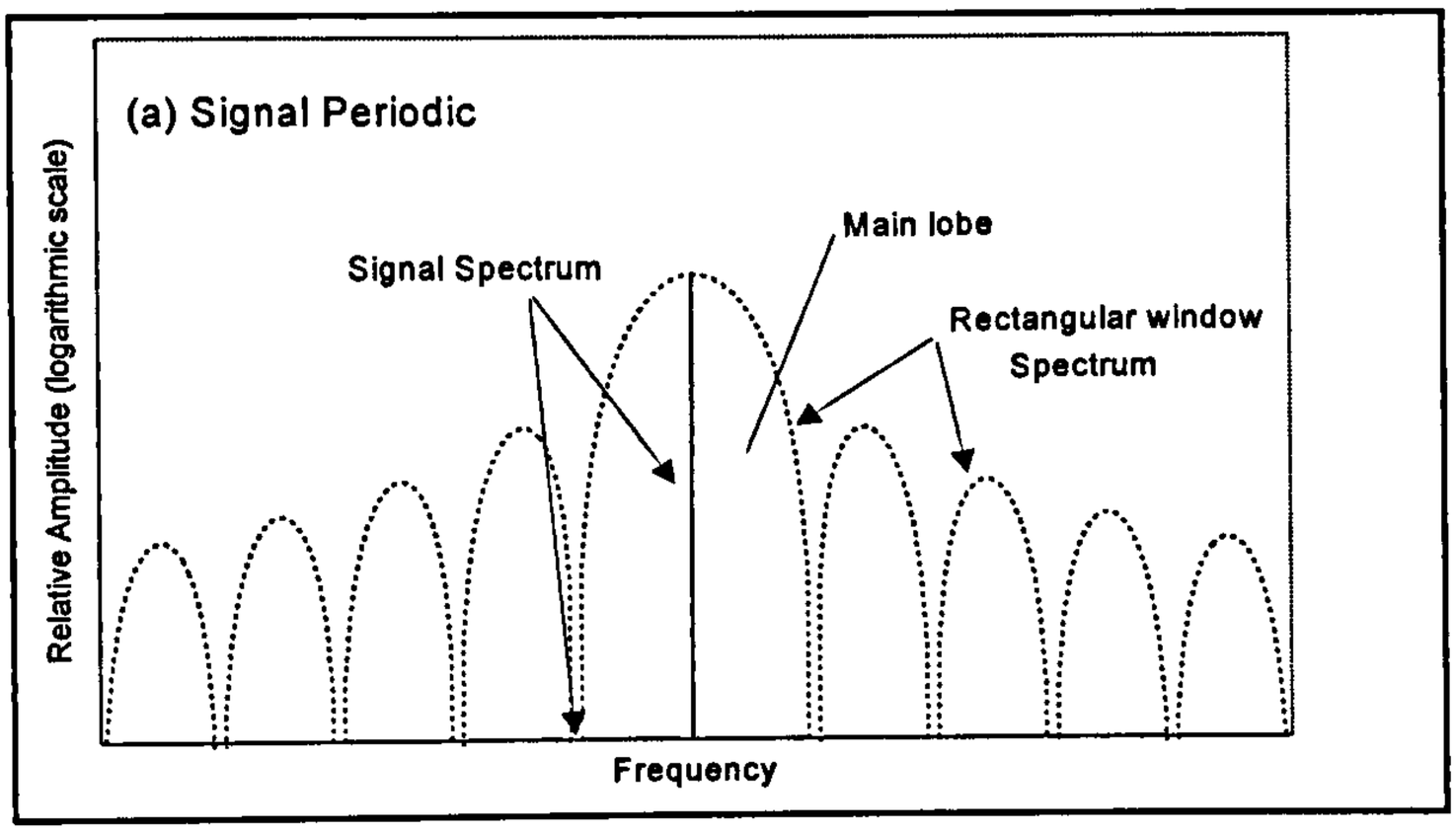

Figure 3.6 - Application of a Rectangular window: (a) signal periodic within the window; (b) signal non-periodic within the window (after Randall, 1987)

Fig. 3.6b does not actually represent the situation as it occurs for an individual spectrum of a signal of finite duration. However, the averaged spectra of the finite signals would converge to the spectrum of the signal of infinite duration shown in the Figure. Fig. 3.6b also shows that leakage is governed by the width of the main lobe and presence of side lobes on the spectrum of the applied window.

Leakage can either be eliminated or reduced. Eliminating leakage is accomplished by adjusting the acquisition time to the period of the periodic signal being acquired. In the

case of a transient signal, the strategy is to extend the duration of the acquisition in order to include the whole signal.

In the case where leakage cannot be avoided, the usual solution is to employ special windows as a substitute for the rectangular window, the selection of the window depending on the characteristics of the signal. In general, these windows are introduced to eliminate the discontinuities at the beginning and end of an acquired signal (Bendat and Piersol, 1986), forcing it to be periodic within the acquisition time. In the frequency domain, this results in reduced side lobes when compared to those of the rectangular window, although usually at the expense of enlarging the central lobe. This implies that the windowed signal may have a larger bandwidth[5] B_e in comparison to that of the original rectangular windowed signal ($B_e = \Delta f$).

The change caused by the application of the window in attenuating the original signal may be compensated for by introducing scale factors in order to retain its power (Gade and Herlufsen, 1987). Two windows were adopted for the tests of prototype footbridges:

- *Hanning Window*, recommended as a general window to be applied in most cases where continuous signals are analysed, the term 'continuous' meaning that the signal extends beyond each individual acquisition time. The Hanning window has side lobes much reduced than those in the rectangular window. Nevertheless, its application results in a signal bandwidth of $B_e = 1.5\ \Delta f$ (Gade and Herlufsen, 1987). A practical example of an application of this window is when obtaining the spectrum of the response of a structure subjected to ambient excitation. The Hanning window is defined by (Bendat and Piersol, 1986):

$$u_h(t) = \frac{1}{2}\left(1 - \cos\left(\frac{2\pi t}{T}\right)\right) \qquad , 0 \le t \le T \tag{3.25}$$

For the DFT calculations, Eq. 3.25 changes into:

$$u_{h_n} = \frac{1}{2}\left(1 - \cos\left(\frac{2n\pi}{N}\right)\right) \qquad , n = 0, 1, 2, \ldots N\text{-}1 \tag{3.26}$$

---

[5] The (effective noise) bandwidth is the width of a rectangle with the same area of the squared spectrum of the window function. The wider the main lobe, the wider the frequency range encompassed by each frequency line (McConnell, 1995).

As an alternative to applying Eq. 3.26 to a discrete signal, an equivalent expression that could be applied on the Fourier Spectrum of the signal obtained without applying any window is given by (Bendat and Piersol, 1986):

$$X_{h_n} = 0.5X_n - 0.25X_{n-1} - 0.25X_{n+1} \tag{3.27}$$

where X_{h_n} is the Hanning windowed n^{th} component of the Fourier spectrum. Bendat and Piersol (1986) also showed that the scale factor to be applied to each of these windowed spectral lines is $\sqrt{8/3}$, in order to keep the power of the original signal.

Gade and Herlufsen (1987) defined the Hanning window in a different way, multiplying the right hand side of Eq. 3.25 by two. However, adopting an appropriate scale factor ($\sqrt{2/3}$) will produce the same windowed spectrum. The scale factor may or may not be applied by the instrumentation used to acquire and process data, and, also taking into account these different definitions for the Hanning window, a correct interpretation of the results produced by the instrumentation requires awareness of how the calculations are performed. Appendix A.1 provides some details regarding this subject for the equipment adopted to acquire and process data.

• *Force/Exponential Window*, which has been applied in transient single impact tests, in which the significant part of the record occurs at its beginning, after a hit is applied to the structure.

It is a double window, applied selectively on both excitation and response signals. In order to have an idea about the beneficial effects of this window, two typical signals from an impact test are shown in Figs. 3.7a,b. Fig. 3.7a shows the excitation signal, produced by an impact applied to the structure by a hammer, which generates a sharp peak. A theoretical signal should contain only the sharp peak and, to improve its quality, a force window is applied on it, consisting of a function that preserves the value of the original signal near the peak and reduces the fluctuation of the signal, due to noise, for the rest of the acquisition time. This is done by applying a rectangular window only around the peak area and, since the signal is transient and entirely contained within the

acquisition time, no leakage occurs. Noise present on the signal in areas away from the peak is removed, leading, in general, to a smoother spectrum (McConnell, 1995).

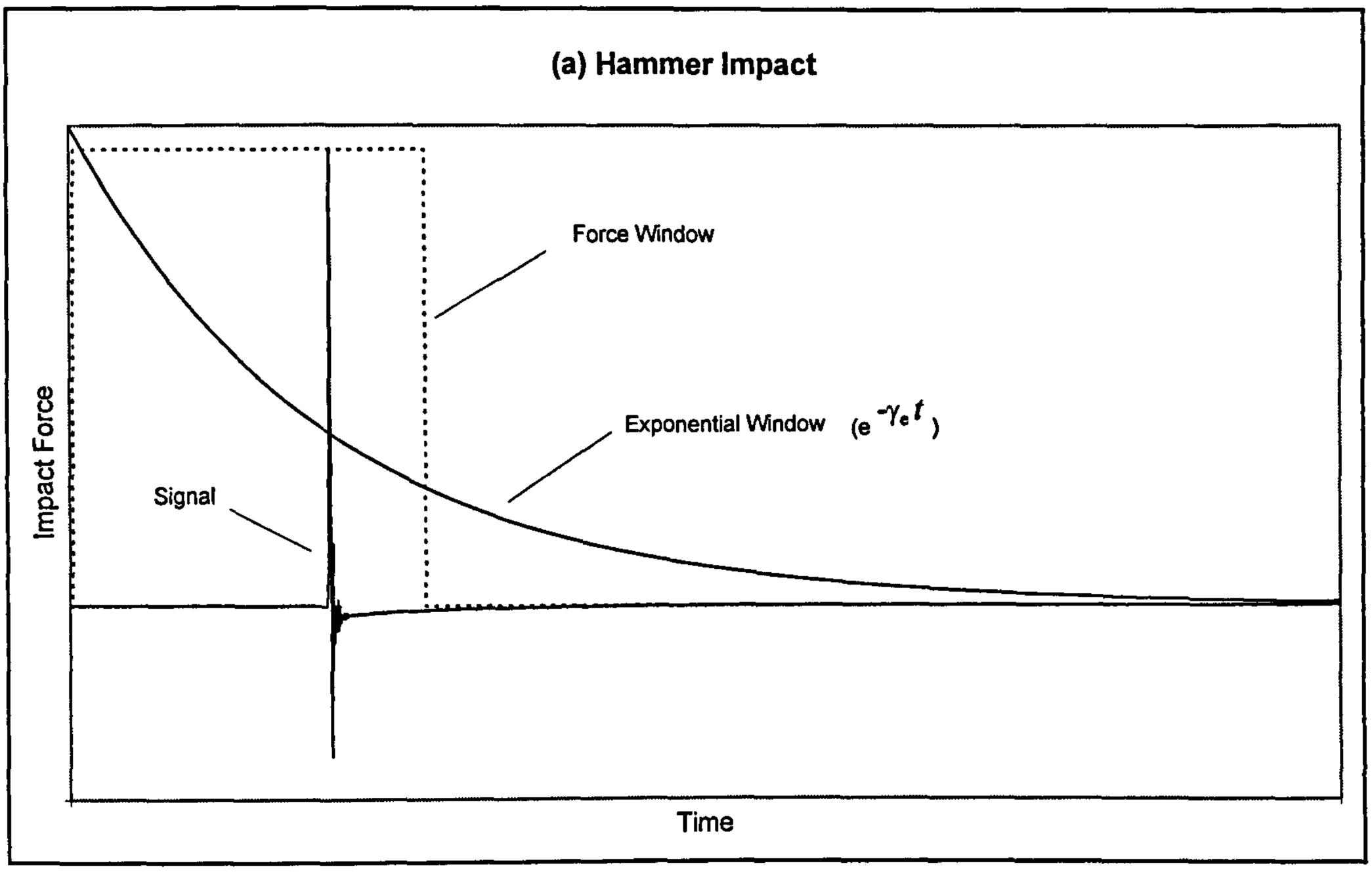

Fig 3.7 - Application of the Force/Exponential window on signals from an impact test: a) force and exponential window on excitation; b) exponential window on response

On the other hand, the response signal may not finish within the acquisition time, being a source of leakage. Following the decay pattern of the signal (due to damping) after the impact, an exponential window is applied, in order to speed up the decay, aiming to reduce the ending of the signal to a negligible value within the acquisition time (Fig. 3.7b). It simultaneously preserves the strong signal at the beginning of the acquisition time. However, for those signals which decay substantially before the end of the acquisition time, such a window is also beneficial in improving the signal to noise ratio by reducing the significance of the tail end of the signal, where this ratio is low (Halvorsen and Brown, 1977).

To ensure consistency in post-processing of these signals for calculating FRFs, this same exponential window is also applied to the excitation signal, on top of the force window. Guidance in selecting the parameters for defining this window is presented by McConnell (1995).

A scale factor is not usually employed for this window. This is because it is applied in signals when the aim is usually to obtain a FRF, and since this is a ratio between spectral functions, the scale factor would be cancelled provided the window is being applied in both excitation and response signals (Ewins, 1984). As will be discussed in Section 3.3.2, the application of this window will not affect the obtaining of correct modal properties from the windowed FRFs apart from damping, which is artificially increased. This is related to a spread of the power of each frequency line, linked to leakage which is not efficiently reduced by applying this window.

Frequency Resolution (Bias) Error

This error occurs when frequencies of the signal are not represented in the spectral function since only discrete frequency components are available, which may not include the former if the signal is not periodic within the acquisition time. Each line of a discrete spectral function is representative of a bandwidth and has a value which is an average of the power of the signal on that bandwidth (McConnell, 1995). Consequently, the resolution of a discrete spectral function and the change of the spectral function in the neighbourhood of a frequency line lead to a difference between the actual value of the

spectral function at that frequency line and the estimated value, called bias error (Fig 3.8). This denomination may be a bit confusing since the term *bias error* means a general systematic error. However, it has usually been adopted to indicate the error caused by poor frequency resolution.

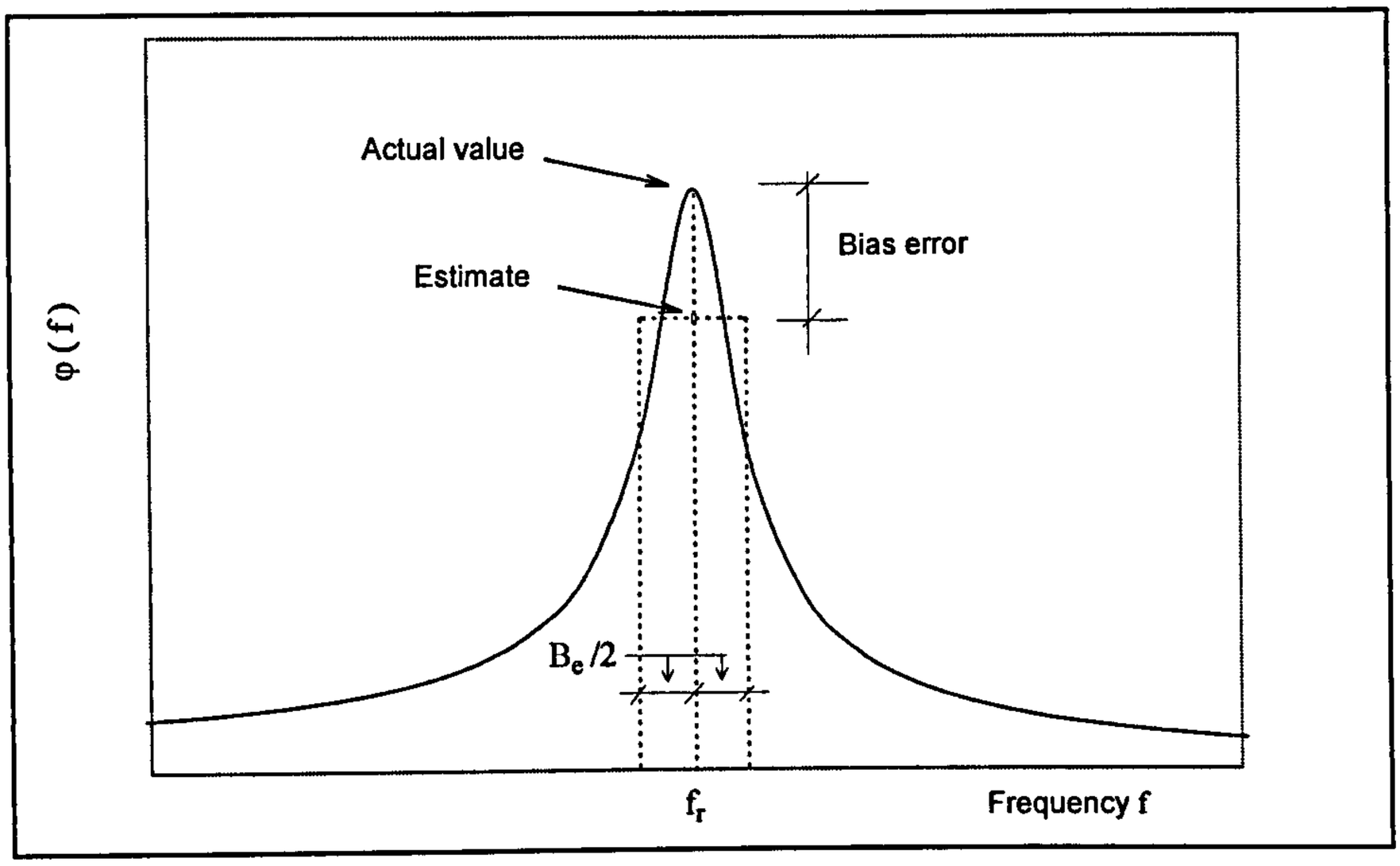

Figure 3.8 - Bias error in a spectral function (after Bendat and Piersol, 1986)

The bias error of an individual estimate is given by (Bendat and Piersol, 1986):

$$b[\hat{\varphi}] = E[\hat{\varphi}] - \varphi \tag{3.28}$$

where $E[\hat{\varphi}]$ is the expected value (mean value from an averaging process), $\hat{\varphi}$ is an individual estimate and φ is the true value of the spectral function. A normalised bias error is also defined as:

$$\varepsilon_b = \frac{b[\hat{\varphi}]}{\varphi} = \frac{E[\hat{\varphi}]}{\varphi} - 1 \tag{3.29}$$

It can be noted from the aforementioned discussion that the bias error is related to the spread of power from the true frequency components of a signal into the discrete frequency components of the calculated spectral function. This leads to an underestimation of spectral peaks and an overestimation of spectral troughs, the

difference between estimated and corrected values depending on the frequency resolution.

Bendat and Piersol (1986) presented an approximated formula to calculate the normalised maximum bias error for the resonance peaks of the Power Spectral Density function, based on a truncated expansion of the Taylor series of the theoretical expression of the error. The normalised bias error is given by:

$$\varepsilon_b [G_{xx_n}] \approx -\frac{1}{3}\left(\frac{B_e}{B_r}\right)^2 \tag{3.30}$$

where B_r is the half-power bandwidth of the resonant peak r ($B_r \approx 2\zeta_r f_r$, where ζ_r is the equivalent viscous damping ratio and f_r is the natural frequency), and B_e is the bandwidth of the spectral estimate.

Schmidt (1985a,b) in a series of papers showed the dependence of the bias error on the window applied on the signal to reduce leakage, which affects the bandwidth around each frequency line. Formulae are presented in these papers establishing bias errors for several spectral functions when rectangular or Hanning windows are applied. However, his formulae for the Power Spectral Density function are not in agreement with Eq. 3.30, although it shows the same dependence on the square of the ratio B_e/B_r for the Hanning window.

With regard to bias errors in FRFs when force/exponential windows are applied on transient signals (e.g. from impact tests), no references have been found. Related studies comparing the performance of the different FRF estimators in terms of bias error for random excitation and application of rectangular and Hanning windows were conducted by Cawley (1984) and Schmidt (1985c). Ewins (1984) showed that the bias error in this case leads to drops in the Coherence function in the vicinity of the resonance peaks, this being an indication that the adopted frequency resolution is unsatisfactory. However, in a subsequent paper, Cawley (1986) showed that this trend in coherence does not occur for transient impact tests. His tests using a rectangular window presented high

coherence in the region of the resonances, in spite of having underestimated spectral estimates in these regions.

Improving the frequency resolution is the way to reduce the bias error, which is achieved by increasing the acquisition time.

Variance and Random Error

Random error (the root square of Variance) is the error that arises in spectral estimates from the assumption that a spectral estimate, obtained by taking a single segment of a continuous signal, is equally obtained by taking any other segment of the signal. This error is meaningful when the system is subject to random excitations (e.g. from the wind) in which there is a statistical uncertainty in each individual estimate, and its study derives from statistical properties of random signals. It does not apply, for example, to signals from transient tests when sources of deterministic excitation like those from the impact of a hammer are employed.

The variance of an individual estimate $\hat{\varphi}$ is defined as the expected value of the squared differences from the mean value (Bendat and Piersol, 1986):

$$Var[\hat{\varphi}] = E[(\hat{\varphi} - E[\hat{\varphi}])^2] \tag{3.31}$$

The square root of the variance yields the random error $\sigma[\hat{\varphi}]$, this being the standard deviation of the estimate. A normalised random error is also defined, and is given by:

$$\varepsilon_{rd} = \frac{\sigma[\hat{\varphi}]}{\varphi} \tag{3.32}$$

where φ is the true value of the variable. Bendat and Piersol (1986) also showed that, for the Power Spectral Density function, the normalised random error is given by:

$$\varepsilon_{rd}[G_{xx_n}] \approx \frac{1}{\sqrt{B_e T_t}} \tag{3.33}$$

where B_e is the bandwidth of the spectral estimate and T_t is the total record length. Usually $T_t = n_d T$, where n_d is the number of estimates in the averaging process, each individual record being of duration T. On the other hand, the bandwidth B_e is affected by the window applied to the signal. Taking the frequency resolution $\Delta f = 1/T$ as a lower limit for B_e and introducing these into Eq. 3.33, leads to:

$$\varepsilon_{rd}[G_{xx_n}] \leq \frac{1}{\sqrt{n_d}} \tag{3.34}$$

The solution to this error is achieved by averaging an adequate number of individual spectral estimates throughout the whole time history of the signal. It is shown (Bendat and Piersol, 1986) that averaging increases the statistical reliability of the spectral estimates in random processes and Eq. 3.34 gives an indication of the number of estimates required to reduce the random error to a certain level. For example, an average of 100 estimates are necessary to have a normalised random error less than 10%. Expressions for the normalised random error of other spectral estimates are also presented by Bendat and Piersol (1986).

It may be noted that whereas the bias error always tends to produce smaller estimates for the points around a resonance peak (see Eq. 3.30), the random error indicates a variation around the expected value, which can be either an overestimation or an underestimation.

3.2.3 Zooming

The Fourier Transform is based on a frequency range f_s extending from zero up to an upper frequency nominally equal to f_s, given by $f_s = 1/\Delta t$. The number of frequency lines is equal to the number of samples N, and the frequency resolution is given by the inverse of the acquisition time. The upper frequency is usually limited to $1/2.56\Delta t$ due to the application of anti-aliasing filters, as was discussed previously in Section 3.2.2. The analysis based on this frequency range is called baseband analysis. Zooming is a technique to obtain finer frequency resolution over a portion of the baseband frequency range. This will lead to a reduction in bias error and a better definition of the spectral

function for obtaining the dynamic properties of the structure. Zooming is particularly important at the lower end of the frequency range, in which a high ratio $\Delta f/f$ implies fewer frequency lines within the half-power bandwidth of the resonant peaks. It is also important for distinguishing closely spaced modes of vibration and on lightly-damped systems (Ewins, 1984).

Considering that the frequency resolution Δf is given by:

$$\Delta f = \frac{1}{T} = \frac{f_s}{N} \tag{3.35}$$

two ways of improving the frequency resolution are by reducing the frequency range f_s (and so losing the high frequency information) or by increasing the number of samples N (equal to the number of frequency lines). Zooming enables the increased resolution to be obtained without losing the high frequency information or increasing the number of samples processed at a time. This is achieved at the expense of being able to analyse only a small part of the original frequency range at a time. Thrane (1980) presented two zoom techniques, called real-time (or destructive) zoom and non-destructive zoom, and both imply that operations are carried out on the signal to avoid the limitations imposed by the baseband analysis on the definition of the spectral parameters. These techniques are briefly summarised as follows, and further details can be found in the work of the aforementioned author or alternatively in Randall (1987).

- *Real-Time (Destructive) Zoom* - The name of this technique comes from the fact that the operations carried out on the time signal modify it. It can be summarised in the following steps:

  - the centre frequency of the frequency range is changed from $f_s/2$ to a chosen frequency f_b. This is achieved by applying a rotating vector $e^{-i2\pi f_b t}$ to the time signal, creating a complex time signal, the spectrum of which has a centre frequency f_b and the same frequency range as that of a signal processed using baseband analysis, subsequently referred to as baseband signal.

- a digital low-pass filter is applied to remove all frequency components except those in a narrow range of interest around f_b. This avoids aliasing occurring in the reduced frequency range since the other frequency components were removed. To comply with the reduced frequency range, the sampling interval Δt is increased, by decimating (i.e. selecting samples) the acquired signal. It may be noted that in order to have the same number of samples of the baseband signal, which will keep constant the number of frequency lines, a longer acquisition time is required than that of a baseband analysis.

- the low-pass filtered complex samples are FFT transformed, producing the required 'zoomed' spectrum.

- *Non-Destructive Zoom* - this is carried out by acquiring a longer signal at a given sampling rate and applying successive Fourier transforms on selective ensembles of the acquired data. The long signal will be called the extended signal to differentiate it from a baseband (shorter) signal. Both signals have the same sampling rate and consequently a different number of samples. The following steps are carried out:

- An assembly of several time series is carried out by decimation of the extended signal. Each derived time series has a constant sampling rate, the l^{th} time series beginning with the l^{th} sample of the extended signal. This implies that there will be a time shift among the series. Since the total record length is the same, the frequency resolution of each derived time series is the same as that of the extended signal. However, the number of samples in each time series is made equal to that of a baseband signal.

- A rotation is applied to compensate for the time shift in each derived time series. This does not apply to the first time series, in which the first sample is also the first sample of the extended signal. These selected rotations will induce small changes in the position of the frequency lines in the spectrum of each data series, in a similar way to that described in the previous technique.

- Each derived and rotated time series is Fourier transformed. Since the Fourier Transform is a linear operation, the sum of the transforms of the undersampled series is equal to the transform of the sum of the series. Summing up will lead to a high frequency resolution spectra in comparison to those obtained from a baseband analysis.

Any of the two zooming techniques actually implies extending the duration of acquisition, which may be undesirable for transient tests if the transient signals have a short duration compared to the acquisition time adopted for the baseband analysis. Extending the acquisition time would capture more noise, thus reducing the quality of the spectral calculations.

3.3 Modal Testing Techniques

The aim of a Modal Test is to obtain the modal properties of a structure, which are the natural frequencies, mode shapes and damping values. This information can be used to validate a theoretical model of the structure which involves several assumptions regarding support conditions, specification of material properties and behaviour of the structural elements. Once calibrated, the theoretical model can be used to simulate load conditions that are not possible to apply during the tests and it can also be used to investigate the effect of design changes on the vibration performance.

Since the aim is to obtain dynamic properties, a test structure must be somehow set vibrating, and a classification of the Modal Testing techniques can be based on whether or not the source of excitation is measured. This is because only with the measurement of the excitations is it possible to obtain frequency response functions (FRFs), and the availability or not of this important spectral function leads to different ways of processing the test data. FRFs are the most powerful spectral functions for obtaining modal properties and, in order to obtain them, special excitation devices are employed. Nevertheless, it is not only the availability of such devices that can determine if FRFs can be obtained or not, as for example in the case of massive structures which are difficult to excite by artificial means. Following this classification, the two groups of Modal Testing techniques are:

- *Techniques without Measurement of Excitation* - In this case, only response signals are measured, and there may or not be the application of sources of artificial excitation. Use of excitation devices like a non-instrumented shaker or an impact hammer, or simply applying heel drops exemplify the case in which sources of artificial excitation are applied. A special case is the one regarded as Free-Vibration Decay, in which the structure is set vibrating and the excitation is halted prior to the beginning of the measurements. On the other hand, there is the case of large scale structures like long span bridges, in which the application of any source of artificial excitation is not feasible. A technique called Ambient Vibration Survey is the only one available in this case, in which the excitation sources are the in-service dynamic loads of the structure, such as wind or traffic.

- *Techniques with Measurement of Excitation* - In this case both excitation and response signals are measured, and FRFs can be obtained. There is control over the forced excitation, which is usually applied by means of an instrumented shaker or hammer. Use of a shaker makes it possible to apply a variety of excitation signals, each characterising a technique. Some examples are Stepped-Sine, Random and Slow-Sine Sweep techniques, and the description of them and of other techniques using a shaker can be found in Ewins (1984). On the other hand, if a hammer is employed, the excitation applied is an impact force, which produces a sharp response being followed by a free decay. This technique is referred to as the Impulse Response Technique.

In principle, any of these aforementioned techniques are applicable for testing short and medium sized pedestrian bridges. The availability of testing equipment and peculiarities of the test structures led to the use of the Ambient Vibration Survey and the Impulse Response Technique. Free-Vibration Decay was also employed for obtaining natural frequencies and damping values for some modes of vibration. These techniques and the respective procedures to obtain the modal properties are discussed in the following three Sections. The author's experience in applying them to the test footbridges has made it possible to suggest some practical guidelines for their application and for the subsequent data processing, which are discussed in the respective Sections.

3.3.1 Ambient Vibration Survey

Ambient Vibration Survey (AVS) is applied mainly to structures which would require powerful sources of artificial excitation to provide signals that could be distinguishable from those generated by ambient excitation. The latter are actually taken as excitation sources in this technique, which is based on the following assumptions:

- The ambient excitation sources are considered to provide excitation for the whole frequency range of interest. This is actually a requirement for using any technique but since the excitation sources are not controlled in this case, one has to rely on the fact that they 'naturally' fulfil this requisite.

- The excitation sources are also assumed to have a reasonably flat Fourier spectrum over the frequency range of interest. This assumption is necessary for response-only measurement techniques with no control of the excitation, since, having a (reasonably) flat spectrum, the unmeasured excitation source will equally excite the whole frequency range of interest. Therefore, the response is magnified on those frequencies which correspond to the natural frequencies of the structure, which can be identified as peaks in the respective spectrum.

- The response of the structure at each natural frequency is assumed to be solely due to the mode of vibration related to such a frequency, the contribution of other modes being considered negligible. This is illustrated in Figs. 3.9a,b, which shows the Fourier spectrum of the response of a two degree of freedom system having natural frequencies f_1 and f_2. Fig. 3.9a shows the situation in which these two modes are well separated and the assumption holds true. Conversely, in Fig. 3.9b these modes are closely spaced and the total response at each natural frequency is due to contributions of the two modes. The assumption of mode separation is regarded as a SDOF approximation since each mode is treated as an isolated one, and it is due to the lack of techniques for extracting modal properties of MDOF systems from response-only measurements based on spectral functions (i.e., on a frequency domain approach). Techniques for extracting modal properties of MDOF systems in these measurement

conditions based on time domain data can be found in the literature (James *et al.*, 1992; Desforges *et al.*, 1995).

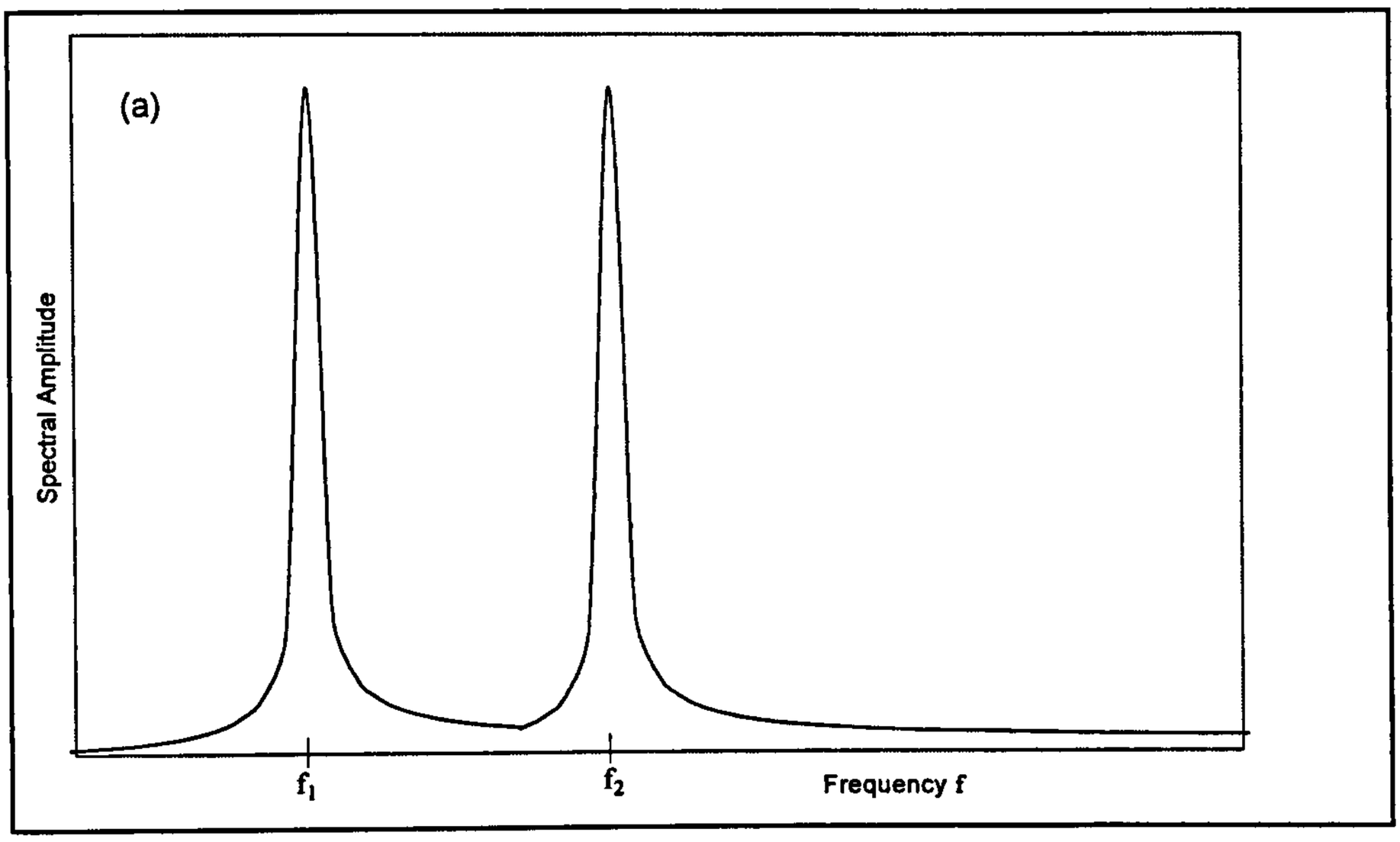

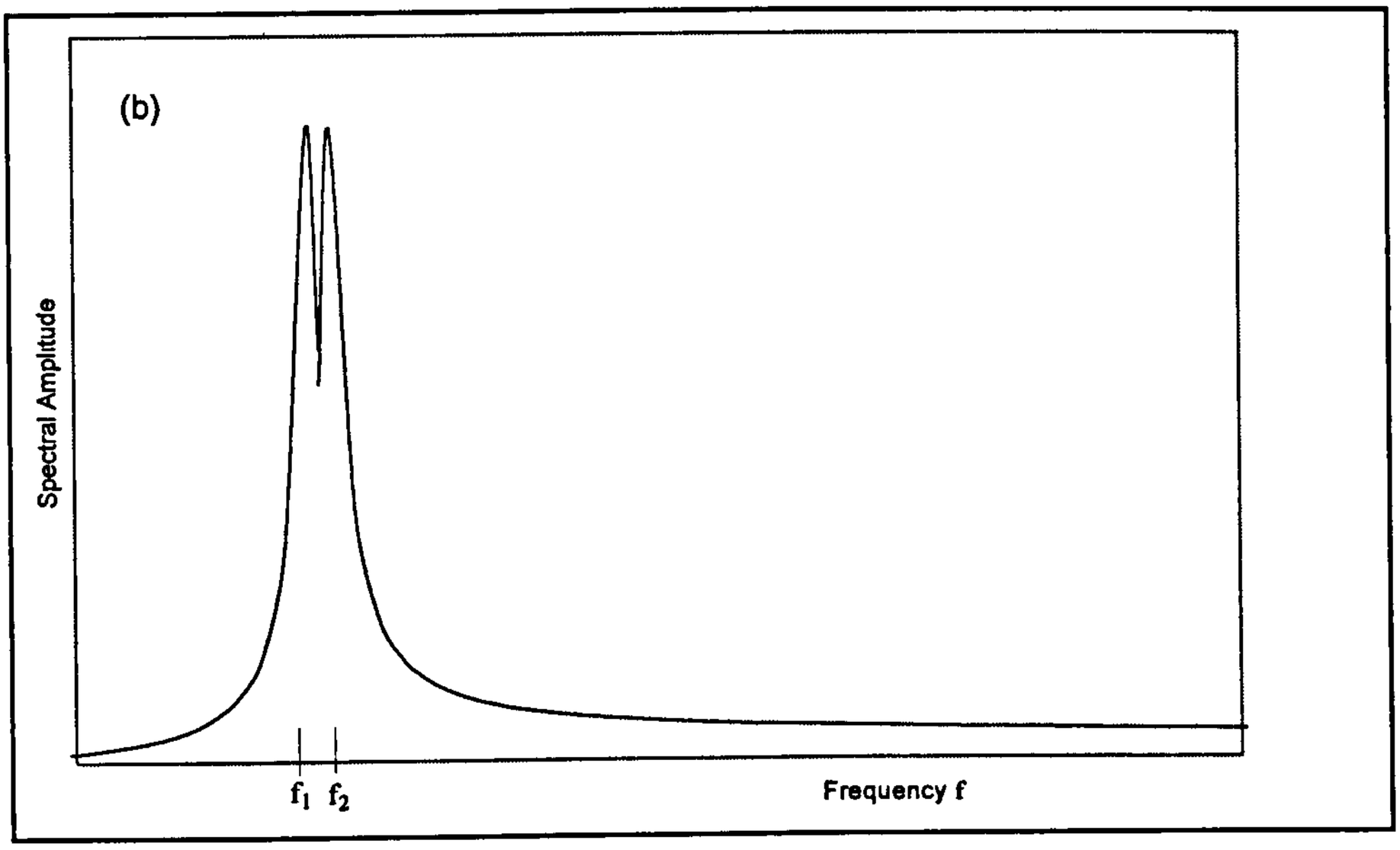

Figure 3.9 - Illustration of Fourier spectrum of a two degree of freedom system: a) separated modes; b) closely spaced modes

Although at first sight these hypotheses are too restrictive, AVS has been applied in several modal tests of large scale structures (Abdel-Ghaffar and Housner, 1978; Abdel-Ghaffar and Scanlan, 1985; Brownjohn *et al.*, 1987, 1992), resulting in good agreement with numerical calculations. Application of AVS in testing pedestrian bridges has also

been carried out using wind as the source of excitation (Brownjohn *et al.*, 1994). The low natural frequencies of these structures are excitable by sources of ambient excitation and their usual low damping values generate tiny peaks in the response spectra, contributing to the assumption of separated modes being verified. An advantage of using this technique is that it does not usually prevent use (during the tests) of the structures as is recommended in tests using controlled sources of artificial excitation. However, in the case of pedestrian bridges, the frequency content of the excitation produced by pedestrians, as seen in Section 2.2.1, is in contradiction with the requirement of a flat excitation spectrum. Consequently, pedestrian bridges should be closed for AVS testing, the wind being taken as the sole source of excitation in this case.

In terms of instrumentation, AVS does not require excitation devices. On the other hand, sensitive transducers are necessary for detecting the low vibration levels usually induced by ambient excitation.

3.3.1.1 Procedures for Collecting and Processing Data

In the absence of FRFs, obtaining modal properties from AVS is based on Power and Cross Spectrum functions or their respective spectral density functions. Each spectrum is obtained by averaging several individual measurements at points on the structure (actually, at degrees of freedom in the directions of interest). A window (e.g., Hanning) is applied to reduce leakage, with a respective scale factor to keep the power of each spectral estimate (see Section 3.2.2). Natural frequencies and damping values can be obtained from the Power Spectrum or Power Spectral Density (PSD) of a given point whereas obtaining each ordinate of a mode shape envelope requires two simultaneous measurements. This is carried out by fixing one of the transducers (say, accelerometers, since these were the transducers employed in the tests) at a reference station whereas the other is placed at different locations along the structure. Each pair of simultaneous measurements for each position of the traveller accelerometer will provide an ordinate of the mode shape envelope for each mode of vibration.

A summary of the steps for obtaining the modal properties follows:

• *Natural Frequencies and Damping* - The natural frequencies will all appear as peaks in the Power Spectrum or PSD, provided the measurement station is not at, or too close to, a node of a mode shape of interest. The simple choice is taking the PSD of the reference station, in which all natural frequencies of interest should appear as peaks. The search for a suitable reference station on site is based on experience but can be informed by an initial finite element (FE) model of the structure. Some trials to locate the best reference station are the usual practice, and there may be cases in which more than one reference station is necessary if one is not enough to identify all the modes of interest. Having more than one reference station may also be due to practicalities when testing very long structures, due to a limiting length of the cables (Brownjohn *et al.*, 1987). For revealing all natural frequencies of interest, Felber and Ventura (1996) suggested the use of Average Normalised Power Spectral Density (ANPSD). This function is defined as the average of PSDs from several points on the structure.

Another advantage of taking the PSD of the reference station for evaluating natural frequencies and damping values is that a very high number of averages can be obtained by combining several sets of averaged PSDs. Each of these sets is obtained when taking measurements to obtain an ordinate of a mode shape envelope. A high number of averages at the reference station is thus available, reducing the random error present on the spectrum to a negligible value (see Section 2.3.2).

Spurious peaks on the PSD which are not related to natural frequencies can be discarded by checking the consistency of the appearance of such a peak over all the measurement points, by observing the shape of the resulting mode shape related to this peak, and by correlating the experimental data with numerical results obtained from an FE model of the structure. The identified peaks related to natural frequencies are selected and each peak is associated with a theoretical expression of the PSD which, in terms of acceleration, is given by:

$$G_{xx}(f)_j = \frac{(2\pi f)^4 ({}_r\phi_j \; {}_r\phi_k)^2 G_{ff}(f)_k}{((2\pi \bar{f}_r)^2 - (2\pi f)^2)^2 + (2\zeta_r \, 2\pi f \, 2\pi \bar{f}_r)^2} \tag{3.36}$$

Eq. 3.36 is obtained by combining Eqs. 3.19 and 3.20, in which only the mode related to the peak natural frequency $\bar{f}_r$, identified by the subscript r, was taken into account. $G_{xx}(f)_j$ is the PSD of the response, evaluated at a generic measurement point j, whereas $G_{ff}(f)_k$ represents the PSD of the excitation applied at a point k although this latter point is not actually relevant. This is because the product ${}_r\phi_k^2\, G_{ff}(f)_k$ is assumed constant over the frequency range in the neighbourhood of the peak, according to one of the hypotheses on which AVS is based. Grouping the squared mode shape ordinates and $G_{ff}(f)_k$ together in a variable F_j, Eq. 3.36 is rewritten as:

$$G_{xx}(f)_j = \frac{(2\pi f)^4 F_j}{((2\pi \bar{f}_r)^2 - (2\pi f)^2)^2 + (2\zeta_r 2\pi f 2\pi \bar{f}_r)^2} \tag{3.37}$$

where the subscript j in F_j indicates that this parameter varies according to the point in which $G_{xx}(f)$ is evaluated.

Eqs. 3.36 and 3.37 are based on the hypothesis of separated modes previously discussed since the contribution of only one mode is considered for each peak. The natural frequencies and damping values can be estimated by one of the following procedures:

- Peak estimation - This is simply to take the natural frequency as the frequency corresponding to the maximum ordinate of each peak of the PSD. The respective equivalent viscous damping ratio is obtained by the so called Half-Power method (Clough and Penzien, 1975), which calculates the damping ratio based on a combination of the values of the frequencies related to ordinates of half of the value of the peak. The accuracy of these estimates depends on how close the maximum ordinate of the peak is to the correct peak, this being dependent on the frequency resolution of the PSD. A poor frequency resolution also implies in significant bias errors, as discussed in Section 3.2.2.

- Curve-fitting - This is carried out by adjusting (by a least-squares technique) the theoretical expression of the PSD (Eq. 3.37) to the points around the maximum value of the peak. The natural frequency, damping value and the variable F_j are taken as variables to be obtained in the curve-fitting process. Since there are three unknown

variables, a minimum of 3 points is required. According to Brownjohn *et al.* (1987), this procedure is intended to reduce the errors that can arise by using the Peak estimation. Fig 3.10 shows a curve-fitting applied to a PSD having a coarse frequency resolution, obtained from tests on a cable-stayed footbridge. The curve-fitting was carried out by developing the expression of the error between the theoretical PSD and the experimental values, and seeking for optimum values of the variables that minimised this error using a least squares solution.

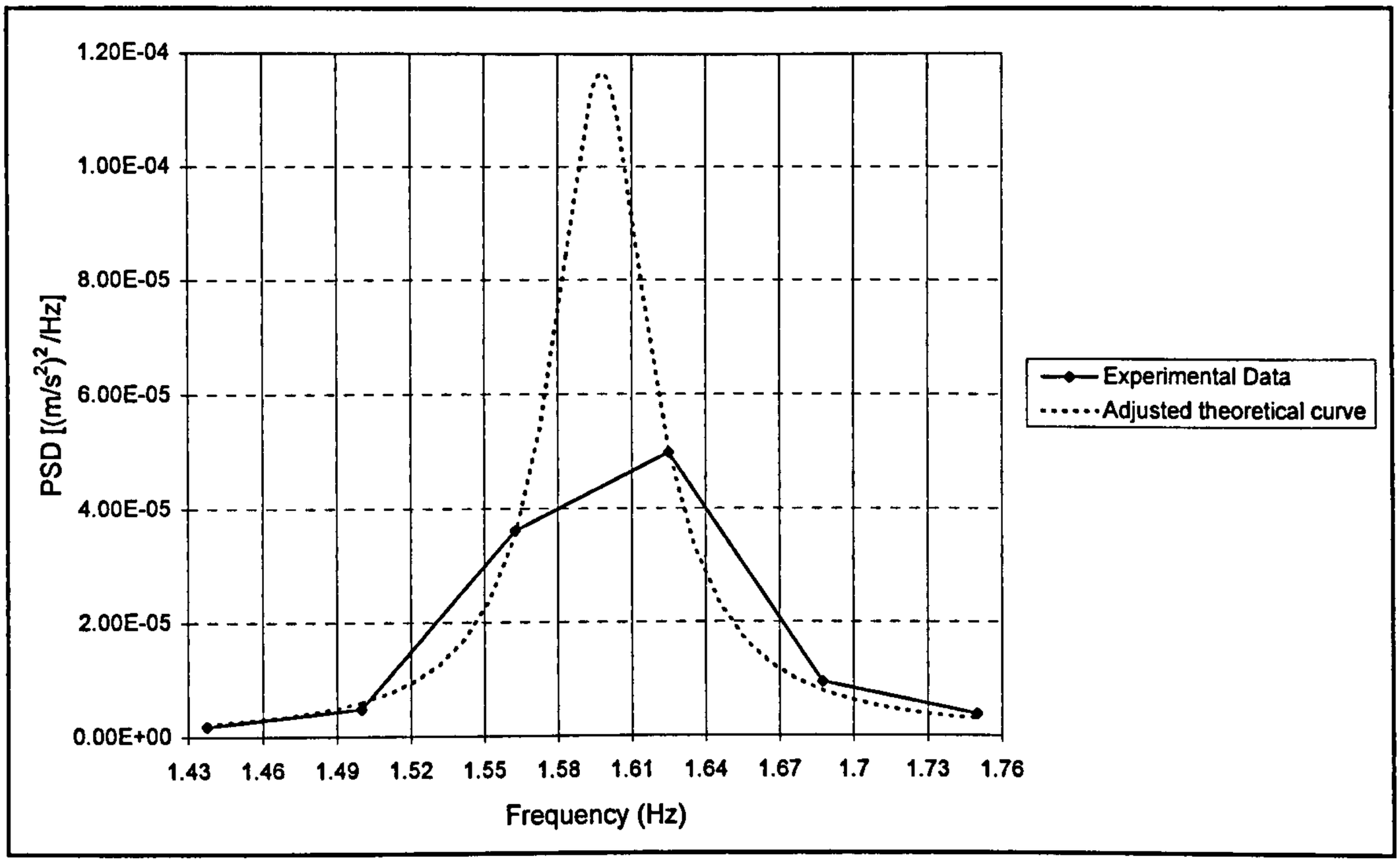

Figure 3.10 - Curve-fitting of the PSD of an acceleration response

• *Mode Shapes* - As already mentioned, these are obtained by successive simultaneous measurements of pairs of responses, each pair providing a mode shape ordinate. To obtain an expression for a coordinate of a mode shape, initially the response of a MDOF system in terms of acceleration, at a generic point *j*, is expressed using modal superposition (Clough and Penzien, 1975) as:

$$\ddot{x}_j(t) = {}_1\phi_j\,\ddot{q}_1(t) + {}_2\phi_j\,\ddot{q}_2(t) + \cdots + {}_r\phi_j\,\ddot{q}_r(t) + \cdots + {}_R\phi_j\,\ddot{q}_R(t) \qquad (3.38)$$

where the $\ddot{x}(t)$ is the acceleration response signal, ${}_r\phi_j$ is the mass-normalised mode shape ordinate of the r^{th} mode at point j and $\ddot{q}_r(t)$ its respective generalised acceleration

modal coordinate function. The mode shape ordinates do not have an absolute value; they represent only what the shape of a mode of vibration is like. Other relative values for the mode shape ordinates could be used in Eq. 3.38, requiring appropriate changes to the functions $\ddot{q}_r(t)$. Conversion of Eq. 3.38 to the frequency domain gives:

$$\ddot{X}_j(f) = {}_1\phi_j \ddot{Q}_1(f) + {}_2\phi_j \ddot{Q}_2(f) + \cdots + {}_r\phi_j \ddot{Q}_r(f) + \cdots + {}_R\phi_j \ddot{Q}_R(f) \qquad (3.39)$$

where $\ddot{X}_j(f)$ and $\ddot{Q}_r(f)$ are the respective Fourier Spectra of the acceleration response and generalised modal coordinate. For a given natural frequency f_r, if the contributions of the modes other than ${}_r\phi_j$ are disregarded (SDOF approximation), Eq. 3.39 can be simplified into:

$$\ddot{X}_j(f_r) \approx {}_r\phi_j \ddot{Q}_r(f_r) \qquad (3.40)$$

It can be noted that each $\ddot{X}_j(f_r)$ is a complex function containing amplitude and phase information. By taking two simultaneous measurements at points j and k, the ratio between the mode shape ordinates at these two points, for the natural frequency f_r, is given by:

$$\frac{\left|\ddot{X}_k(f_r)\right|}{\left|\ddot{X}_j(f_r)\right|} = \frac{{}_r\phi_k}{{}_r\phi_j} \qquad (3.41)$$

Taking the point j as a reference station and varying the point k along the structure will produce the desired mode shape, the magnitude of each of its ordinates being related to the ordinate of the reference station. It may be noted that Eq. 3.41 does not allow the individual (mass-normalised) mode shape ordinates to be obtained, and the ordinate at the reference station is assumed to have an arbitrary value (usually equal to unity). The mode shapes may also be obtained from the PSDs (see Eq. 3.36) as:

$$\sqrt{\frac{G_{xx}(f_r)_k}{G_{xx}(f_r)_j}} = \frac{\left|\ddot{X}_k(f_r)\right|}{\left|\ddot{X}_j(f_r)\right|} = \frac{{}_r\phi_k}{{}_r\phi_j} \qquad (3.42)$$

The phase difference between each point and the reference station can be obtained from the Cross Spectrum between these points, in which 0 deg. indicates that the point vibrates in phase with the reference point and 180 deg. indicates the opposite. If the phase difference is either 0 deg. or 180 deg., there is no imaginary component and the respective mode shape is said to be a real mode. Conversely, for other phase differences, the mode shape is said to be complex. However, existence of complex modes in structural systems is associated with the occurrence of closely spaced modes (Imregun and Ewins, 1995), and this is in conflict with the hypothesis of separate modes. Therefore, the mode shapes will be assumed real and the Cross Spectrum is also useful for confirming this assumption.

The mode shapes obtained by this procedure are called operating deflection shapes. The closeness between each of them and the mode shape associated with a respective natural frequency of the structure relies on the assumption of separation between the modes. This procedure for obtaining mode shapes has been extensively reported in the literature; however, scarce information can be found with respect to its accuracy, taking into account the errors introduced when obtaining the spectral functions (see Section 3.2.2).

3.3.1.2 Accuracy of the Estimates

The modal properties are estimated by using Power and Cross Spectra and/or their respective spectral functions. The accuracy of the estimates is related not only to the validity of the assumptions on which AVS is based but is also related to intrinsic errors that can be made when calculating the spectral functions.

The variability of the (uncontrolled) excitation sources may constitute a problem, demanding a high number of averages for obtaining stable spectral estimates. Littler (1992) suggested including anemometers as part of the test instrumentation in a case in which the wind is taken as the sole source of excitation. This would enable selecting response signals measured under the same wind speed and direction, thereby reducing the variability of the measurements included in the averaging process.

Measures such as using anti-aliasing filters, the Hanning window, proper frequency resolution and averaging can be taken to avoid the spectral errors. These were discussed in Section 3.2.2, where it was shown that the latter two measures are related to bias and random errors, respectively. These errors may be avoided by setting appropriate parameters for the data acquisition, and this is discussed in more detail for each of the estimated modal properties.

• *Errors in Natural Frequencies and Damping* - As has been discussed, use of the reference station for estimating natural frequencies and damping values leads to a high number of averages, and consequently the random errors are reduced to negligible values. With regard to bias errors, Eq. 3.30 gives some insight into the required frequency resolution for a given resonance peak.

As Littler (1992) pointed out, Eq. 3.30 cannot be considered as providing absolute values for the bias error if estimated biased natural frequencies and damping values are used in it. However, it provides awareness of the error committed and the level of improvement obtained by increasing the frequency resolution. Since the normalised error varies with the square of the ratio B_e/B_r (see Eq. 3.30), increasing the acquisition time of each record reduces the bandwidth B_e by the same proportion and consequently reduces the bias error by the square. Littler (1992) suggested taking ratios B_e/B_r around 1/4 for obtaining accurate estimates with less than 2% of bias error. He also showed that significant errors can be committed in damping estimates for higher B_e/B_r ratios.

However, Eq. 3.30 gives the normalised bias error of the PSD and not of the estimated natural frequencies and damping values. A straightforward relation between these errors is not readily available, and some approximation formulae for the error in determining damping as a function of the frequency resolution are presented by Brownjohn (1988), based on simulations using a SDOF system.

Another aspect is to quantify the amount of improvement obtained by the curve-fitting procedure with respect to the peak estimation. If the amount of bias error is considered to be such that the convex shape of the peak is not affected (i.e. the maximum biased value is related to a maximum non-biased value and so on), the curve-fitting procedure

is expected to produce reasonable estimates of the natural frequencies even for relatively poor frequency resolutions. The same does not seem to apply to damping, which is more sensitive to the broadening that occurs on the biased spectral peak. Although some intuition is present in this discussion, the results obtained from AVS tests in a cable-stayed footbridge confirmed this trend. These results are shown in Table 3.2, where the estimations obtained from Free-Vibration Decay are also shown for reference. Table 3.2 shows that reasonable estimates for natural frequencies were obtained using curve-fitting for ratios of B_e/B_r greater than one. Conversely, estimations for the equivalent viscous damping ratios did not present the same level of accuracy.

	B_e/B_r [+]	Estimations Based on Peak Values		Estimations Based on Curve-Fitting		Results from Free-Vibration Decay	
		Natural Frequency	Damping Ratio*	Natural Frequency	Damping Ratio	Natural Frequency	Damping Ratio
1st Vertical Mode	3.5	1.63 Hz	4.02 %	1.59 Hz	1.47 %	1.56 Hz	0.84 %
2nd Vertical Mode	2.6	1.94 Hz	3.15 %	1.92 Hz	2.27 %	1.88 Hz	0.94 %

[+] estimated using data from Free-Vibration Decay

* from Half-Power bandwidth

Table 3.2 - Estimations of modal parameters from tests on a cable-stayed footbridge

The use of curve-fitting tends to contribute to better estimations of natural frequencies and damping. This is particularly useful for the first natural frequencies of a test structure, which tend to have lower half-power bandwidths B_r, increasing the ratio B_e/B_r and consequently the bias error.

• *Errors in Mode Shapes* - Bias errors affect mode shapes in a different way to that discussed for natural frequencies and damping. This is because these estimates are obtained by the ratio of two simultaneously measured spectral functions, which may help in alleviating the effect of the spectral errors. Random errors are also of importance here since the number of averages taken to obtain each mode shape ordinate is much less than that available for estimating natural frequencies and damping.

Since the mode shape ordinates are related to the same natural frequency and damping, the respective PSDs evaluated at different measurement points present the same normalised bias error (Eq. 3.30), which is independent of the magnitude of each individual peak. Combining Eqs. 3.29 and 3.42, it can be readily shown that the ratio between the (biased) mode shape estimates is the same as that between the unbiased estimates. Therefore, the ratio in Eq. 3.42 would not be subject to bias errors. This holds if bias is the sole source of error in the spectral estimates, as represented in Eq. 3.29. Since random errors are also present, it can be said that bias errors in mode shape estimates tend to cancel out when using Eq. 3.42.

With regard to the random errors, Eq. 3.34 shows that, for each spectral estimate, this error varies with the inverse of the square root of the number of averages. A similar line of thought adopted for investigating the effects of the bias error could be applied for investigating the effect of random errors on the ratio Eq. 3.42. However, as was discussed in Section 3.2.2, whereas bias errors always produce underestimated estimates for points around a peak, the random error indicates a plus or minus variation of the estimation in relation to the respective expected value, this latter value having been obtained by taking a very high number of averages. The variations of the two estimations in Eq. 3.42 may occur in opposite directions, and do not necessarily tend to cancel out, as was the case for the bias error. Eq. 3.34 may thus be taken only as a reference to give some insight into the number of averages required.

Nevertheless, if Eq. 3.34 is to be followed, a high number of averages would be necessary for evaluating each ordinate of a mode shape envelope, a condition that may be difficult to fulfil due to the usual limitations in testing time. As an alternative, the strategy adopted in the tests was to observe the behaviour of the estimated PSDs throughout the averaging process. For the on site conditions during the tests, it was realised that for the majority of the measurements taken, an average of 10 spectral estimates led to very stable PSDs, i.e., after this averaging, only very small changes could be visually observed around each resonance peak of the averaged PSDs. Although a figure of 10 averages would theoretically imply normalised random errors of the order of 32% if applying Eq. 3.34, the visual inspection of the PSDs was taken as the basis for defining the number of averages.

Curve-fitting of each spectral peak of the PSDs could help in reducing the fluctuations of the ratios between the measured discrete spectral estimates around each peak, caused by noise. The ratio of the spectral estimates would be obtained using the maximum ordinates of the fitted curves. However, experience in applying the curve-fitting procedure for obtaining natural frequencies and damping revealed that the selection of points around each peak affects the final curve-fitted estimates, and usually some trials are involved observing the level of adjustment obtained by each fitted curve before a final decision is made. This means that the process of curve-fitting involves a reasonable amount of 'manual' labour and it would be cumbersome to apply for all peaks of all PSDs.

In order to avoid this significant additional work, the procedure adopted was to calculate a few mode shape ordinates (Eqs. 3.41 or 3.42) for each test point. These ordinates were calculated by taking spectral estimates in the neighbourhood of a resonance peak. The final ordinate of the (experimental) mode shape envelope was obtained by the average of the calculated ordinates. Table 3.3 shows the experimental mode shape ordinates of one of the mode shapes of a test footbridge, obtained by the average of the values calculated from two spectral estimates close to the resonance peak. It is also shown the ordinates of the numerical mode shape from the calibrated FE model of the structure.

This procedure for obtaining the mode shapes may contribute to reducing the effects of the random error, which can affect the spectral lines around the neighbourhood of a peak in different ways. Additional information regarding the quality of the spectral functions adopted for determining the mode shapes can be obtained by determining the Coherence function for at least some pairs of measurements.

The correlation between the experimental and numerical modal properties, the latter being obtained from an FE model of the test structure, is a final assessment of the quality of the measurements and the appropriateness of the model. The two sets of natural frequencies can be plotted one against the other and should ideally lie on a 45° line.

Station Number*	Experimental Mode Shape Ordinates (f = 1.56 Hz)	Experimental Mode Shape Ordinates (f = 1.63 Hz)	Experimental Mode Shape (average)	Numerical Mode Shape Ordinates from a FE Model
12 (support)	0	0	0	0.02
13	0	0.11	0.06	0.13
14	0.17	0.27	0.22	0.31
15	0.48	0.48	0.48	0.52
16	0.57	0.71	0.64	0.74
17 (Reference)	1.01	1.00	1.01	1.00
18	1.35	1.34	1.35	1.36
19	1.79	1.78	1.79	1.87
20	2.52	2.60	2.56	2.58
21	3.50	3.44	3.47	3.49
22	4.25	4.20	4.23	4.19
23	4.44	4.26	4.35	4.65
24	4.29	4.40	4.35	4.33
25	3.51	3.83	3.67	3.71
26	2.67	2.69	2.68	2.79
27	2.0	2.24	2.12	2.04
28	1.34	1.54	1.44	1.48
29	1.01	1.00	1.01	1.00
30	0.75	0.72	0.74	0.79
31	0.58	0.63	0.61	0.56
32	0.40	0.39	0.40	0.36
33	0.19	0.21	0.20	0.18
34 (support)	0	0	0	0.01
50 (tower top)	0.59	0.64	0.62	0.63

* - points on the deck at main span unless otherwise specified

Table 3.3 - Obtaining experimental mode shape ordinates from tests on a cable-stayed footbridge

Correlation checks between experimental and numerical mode shapes can be carried out by using the Modal Assurance Criterion (MAC) (Allemang and Brown, 1982) and/or Coordinate Modal Assurance Criterion (COMAC) (Lieven and Ewins, 1988). These well established parameters vary from zero to one. The MAC is a general parameter for checking the independence of pairs of experimental and numerical modes. Correlated pairs produce MAC values close to one. For a pair of modes a and b, ${}_e({}_a\phi)$ being an experimental mode and ${}_c({}_b\phi)$ a numerical mode, the MAC value is given by:

$$MAC_{ab} = \frac{\left(\sum_{j=1}^{p} {}_{e}(_{a}\phi_{j})\ {}_{c}(_{b}\phi_{j}) \right)^{2}}{\left(\sum_{j=1}^{p} {}_{e}(_{a}\phi_{j})\ {}_{e}(_{a}\phi_{j}) \right)\left(\sum_{j=1}^{p} {}_{c}(_{b}\phi_{j})\ {}_{c}(_{b}\phi_{j}) \right)} \tag{3.43}$$

where p is the total number of mode shape ordinates. The COMAC is applied to the identified pairs of correlated mode shapes, and makes it possible to check the quality of data at each measurement point. COMAC values close to one indicate high quality data at a given point. For a measurement point j, the COMAC is given by:

$$COMAC_{j} = \frac{\left(\sum_{r=1}^{C} {}_{e}(_{r}\phi_{j})\ {}_{c}(_{r}\phi_{j}) \right)^{2}}{\sum_{r=1}^{C} {}_{e}(_{r}\phi_{j})^{2} \sum_{r=1}^{C} {}_{c}(_{r}\phi_{j})^{2}} \tag{3.44}$$

where C is the total number of correlated mode shapes. Eqs. 3.43 and 3.44 can be modified in order to include complex mode shapes (Ewins, 1984) and can be used independently of the scaling of the mode shapes.

3.3.2 Impulse Response Technique Using an Instrumented Hammer

Due to its advantages in being faster and easier to use, requiring less equipment than other forced excitation techniques, the impulse response technique using an instrumented hammer, or simply the hammer test, is frequently employed in site tests of open space civil engineering facilities. This technique makes it possible to obtain FRFs since both excitation and response signals are measured. However, limitations in the excitation energy that can be applied have restricted applications to so called 'medium sized' structures like floors, short span road bridges, and short and medium span footbridges. Some examples can be found on tests on chimneys and elevated tanks (Maguire and Severn, 1987), footbridges (Gardner-Morse and Huston, 1993; Brownjohn *et al.*, 1994), and floors (Caverson, 1992; Caetano and Cunha, 1993; Pavic *et al.* ,1994).

Simultaneous measurements of excitation and response are taken to obtain the FRFs. Excitation consists of a hammer blow applied to the structure, which induces an immediate response, followed by a decay. The acquisition time should conform with the duration of the response, which ideally would be sufficiently attenuated at the end of the acquisition time. Shorter acquisition times induce leakage; on the other hand, if the acquisition time is too long, significant noise is added.

Efforts have been directed to the development of techniques to improve the quality of the acquired data from hammer tests. One example of this is the adoption of the exponential window, as discussed in Section 3.2.2, which gives some flexibility for defining the acquisition time since such a window helps in reducing the distortions caused by too long or too short acquisition times. However, the presence of unmeasured excitations (e.g. wind) and a much lower frequency content create challenges for applying this technique to open space civil structures. Another aspect worthy of attention is setting-up of the test equipment, which is well recognised as a laborious task. Apart from that, the choice of the test parameters (and there are several) during this setting-up stage affects tremendously the quality of the results, and there is no single solution which can be applied to all cases. Instead, a trial and error procedure using different settings is the usual practice to achieve good quality results.

Several publications about hammer tests can be found in the literature. Articles by Halvorsen and Brown (1977), Corelli and Brown (1984), Trethewey and Cafeo (1992), McConnell and Varoto (1995), Fladung and Rost (1997) among others presented discussions and guidelines for setting parameters and conducting hammer tests. A recent publication by the Dynamic Testing Agency (DTA) (DTA, 1995) is also worth mentioning, in which a detailed procedure for conducting hammer tests is presented and discussed. The discussion here aims to point out the peculiarities and challenges of applying hammer tests to low natural frequency footbridges, based on the experience acquired from site tests and the extraction of modal properties in three such structures. The discussion is centred on the sequence of steps taken in conducting such a test, beginning with the setting-up of equipment and data acquisition. This is followed by the procedures for obtaining the modal properties.

3.3.2.1 Setting-up and Data Quality

As mentioned in the guidelines of the DTA (DTA, 1995), the setting of the parameters for hammer tests is often a compromise between adequate frequency resolution (Δf) and an adequate sampling interval (Δt). In order to investigate this subject for the case of low natural frequency footbridges, it is necessary to understand first the peculiarities of the excitation, i.e., the hammer blow. An illustration of a hammer blow and its respective Fourier spectrum is shown in Fig. 3.11. The impact applied on the structure resembles a dirac delta function, the spectrum of which is a flat line. Halvorsen and Brown (1977) investigated the effects of the duration of the impact on the hammer spectrum, showing that the spectrum decays to zero more quickly in the case of longer impacts. On the other hand, longer impacts concentrate the energy of the impact in the lower frequency range, which is the range of interest in civil engineering structures.

The duration of the hammer impact can be controlled by the tip attached to the hammer head, which should preferably be soft for testing civil structures since this will contribute to lengthening the duration of the impact on the structure. The typical duration of an impact, obtained during the tests on prototype footbridges, was about 3 to 4 $*10^{-3}$ secs, when using the softest tip available.

A typical measured signal of a hammer blow presents a high peak corresponding to the impact on the structure, followed by undershooting and ringing. The former is caused by the discharge of electronics within the hammer head (McConnell, 1995). This produces a small negative peak which returns to zero in the form of an exponential decay. The latter consists of small fluctuations of the signal over the zero position. The rest of the signal is composed of noise, the effects of which can be removed by applying the force window discussed in Section 3.2.2.

An important aspect when measuring the hammer blow is to have an appropriate time interval to get the peak. Pavic and Waldron (1996) showed that inappropriate (long) time intervals Δt may lead to an inaccurate spectrum of the excitation and consequently in deterioration of the quality of the FRF measurements. This happens because, being imperfectly detected, the hammer peak will not significantly differ from the undershoot

and ringing parts of the signal. The consequence is that the resulting spectrum will diverge from a theoretical flat line produced by a dirac delta function, to which an accurately detected peak would resemble.

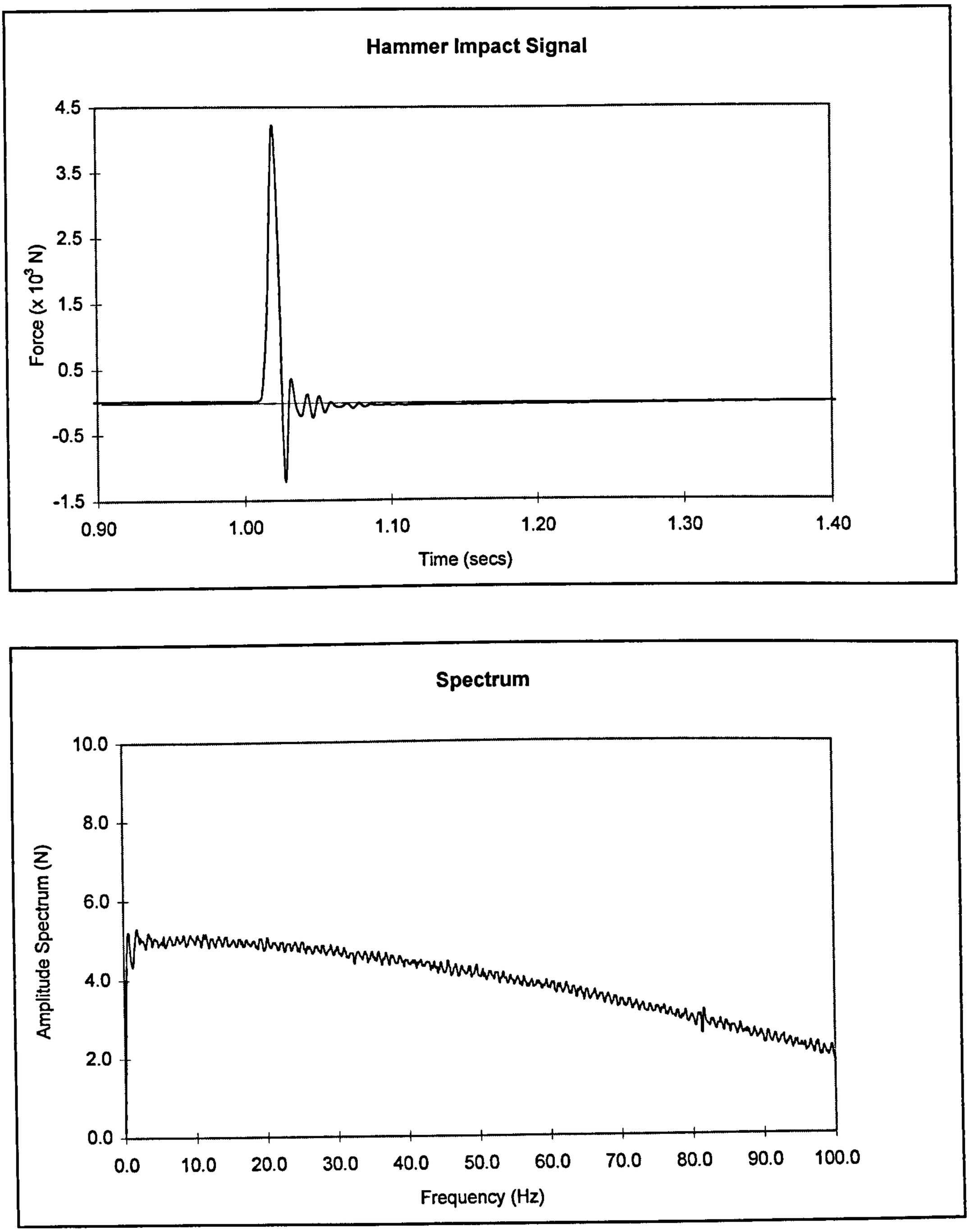

Figure 3.11 - Hammer impact signal and Fourier Spectrum

Although the magnitude of the time interval Δt, and consequently the proper detection of the peak, is not an issue when testing high frequency structures, care should be taken in this respect when testing low natural frequency civil structures. In order to explain why, it is necessary to bear in mind the relations between time domain parameters (time interval Δt and record duration T) and frequency domain parameters (frequency resolution Δf and frequency range f_c) when processing data using Fourier Transforms. These relations, presented in Eq. 3.24 and in Table 3.1, also include the number of data points N of the signal as a parameter.

Looking first at expected values of the frequency resolution for low natural frequency civil engineering structures, these can be inferred from the expected values of the half-power bandwidth of the fundamental frequency f_o of one of such structure. Since the half-power bandwidth is defined by $B_r = 2\zeta f_o$, if reasonable figures of 1% for the damping ratio ζ and 2 Hz for f_o are assumed (not unusual for medium span footbridges, see Fig. 2.8), this leads to a bandwidth $B_r = 0.04$ Hz. In order to have at least one frequency line within this bandwidth, the frequency resolution Δf should be of this order of magnitude. This naturally varies depending on damping and fundamental frequency; increases in damping or frequency leading to a higher half-power bandwidth. Based on these figures, as an initial reference value for testing footbridges, a frequency resolution of 0.0625 Hz could be adopted, which is related to an acquisition time of 16 secs.

On the other hand, when seeking time intervals Δt compatible with the duration of a hammer impact (note: the lesser the time interval the higher and more undesirable is the frequency range of the analysis), two values can be suggested: $\Delta t = 7.8125*10^{-3}$ secs, related to a frequency range of 50 Hz; and $\Delta t = 3.90625*10^{-3}$ secs, related to a frequency range of 100 Hz. In order to keep the frequency resolution at 0.0625 Hz, the necessary number of data samples is 2048 and 4096, respectively (see Table 3.1), the latter number of samples being actually quite high for FFT processing. It should be noted that smaller values for Δt would require a larger number of data points so as to keep constant the aforementioned frequency resolution. For obtaining frequency resolutions smaller than 0.0625 Hz, an even larger number of samples would be necessary.

The discussion in the previous paragraphs shows that an initial choice of parameters for testing low natural frequency civil structures, more specifically footbridges, may be to adopt a time interval $\Delta t = 7.8125*10^{-3}$ secs and an acquisition time of 16 secs, which implies that 2048 data samples are taken. The corresponding parameters in the frequency domain are a frequency resolution of 0.0625 Hz and a frequency range of 50 Hz, which results in 800 frequency lines on the calculated spectral functions.

However, it is important to note that the value of $7.8125*10^{-3}$ secs for the time interval Δt is actually larger than the aforementioned typical duration of a hammer impact. This means that the impacts could be undetected or improperly detected, and a general consequence of this is the deterioration of the FRF as already discussed. Signs of this problem during the data acquisition and processing can be noted by visually following the behaviour of the averaged FRFs throughout the application of successive hammer blows. An experienced hammer operator is able to apply uniform blows and, in ideal conditions, a small number of averages would produce stable FRFs, presenting very little fluctuation among individual blows. A sudden change in this trend when applying a subsequent hammer blow is an indication of a problem in properly detecting the peak.

A typical change on the FRF due to improperly detected peaks is a 'jump', i.e. as if the averaged FRF had been multiplied by a constant greater than one. This was observed during the tests and sometimes led to a repetition of the whole series of blows applied at a certain point. The reason for this behaviour can be explained by looking at Eq. 3.17, in which the so called FRF H1 estimator is defined. It can be seen that the PSD of the excitation is placed on the denominator of the expression. If the peak is not properly detected but a still reasonable flat spectrum is produced, the PSD of the measured signal will have a reasonably constant value although inferior to the value that corresponds to the applied impact. This causes the aforementioned jump, the magnitude of which will depend on the difference in magnitude between the estimated and the actual PSDs.

The phenomenon of a jump of the FRF is illustrated in Fig. 3.12, taken from the tests of one of the footbridges. A stage is reached in which the misrepresentation of the peak is such that the estimated PSD loses its flat characteristic and the changes on the FRF are

more dramatic, which will surely lead to the necessary repetition of the series of measurements.

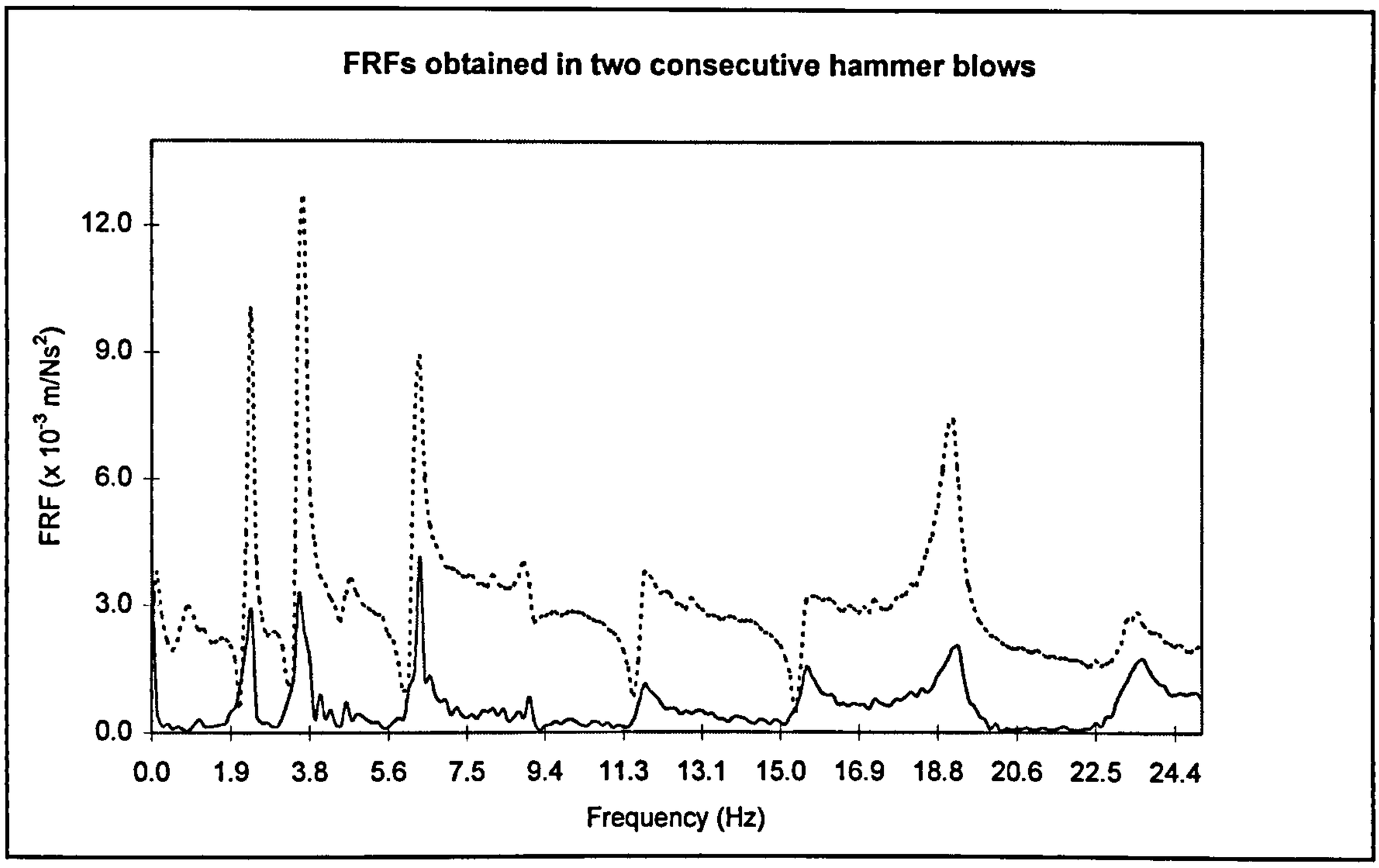

Figure 3.12 - Illustration of a 'jump' on the FRF

Regarding the frequency resolution, care is necessary since the suggested initial frequency resolution of 0.0625 Hz may lead to no frequency line within the half-power bandwidth of the first resonance peak. This would affect the accuracy in determining the modal properties. Ideally, the number of spectral lines within the half-power bandwidth of each resonance should be five to six, according to the guidelines of the DTA (DTA, 1995). However, as can be seen in these last paragraphs, obtaining even one spectral line may be a difficult task when testing low natural frequency footbridges.

If the aim is to improve the frequency resolution, zooming (see Section 3.2.3) does not seem a feasible solution in this case. This is because zooming extends the duration of the acquisition and consequently, for a given number of samples, the sampling time Δt would be increased accordingly. This in turn would further complicate detection of the hammer peak.

Indeed, few suitable options for setting the parameters are available. It can also be seen that it is increasingly difficult to test footbridges or other similar structures having fundamental frequencies lower than 2.0 Hz using the instrumented hammer technique.

One possible solution for improving the quality of the measured excitation is the possibility of rejecting badly detected peaks during the tests (i.e. not including them in the averaging process). This will prolong the testing time and the existence of this option will depend on the capabilities of the test equipment. However, it must be emphasised that visually following the behaviour of the (averaged) FRF throughout the averaging process is as important as having control over the quality of the excitation signal. Since plotting the FRF involves two diagrams, usually the amplitude and phase, the possibility of rejecting badly detected peaks would imply using equipment in which ideally four simultaneous plots could be displayed, two for the FRFs plus the time domain and spectrum of the excitation.

The spectrum analyser available for collecting and processing data from the hammer tests did allow the inspection of each applied hit and allowed the user to decide whether or not to include it in the averaging process. However, the equipment screen was limited to plotting two diagrams at a time, which meant that the visual inspection of the changes in the FRF would be impaired due to the successive changes on the screen between the FRF plots and the excitation response and respective spectrum. Alternatively, use could have been made of the equipment's trigger, which is used to initiate the data acquisition (see Appendix A.1). When properly adjusted, the trigger can help in selecting only the records in which a peak was reasonably detected.

Inspection or not of the hammer hits is therefore a factor which will influence the definition of the number of averages necessary to obtain stable FRFs. If such an inspection is carried out, fewer averages are necessary, which of course does not mean a reduction in the total number of hammer blows applied at each point. Instead, it means a reduction in the number of hammer blows included in the averaging process.

No references were found in the literature suggesting that the number of averages could depend on inspecting or not the quality of the measured excitation. This may be due to

the fact that very few applications of the hammer test can be found for testing structures with natural frequencies as low as 2.0 Hz, in which case a proper detection of the hammer peak becomes an issue. However, there are other factors that may compromise the quality of the FRFs like noise and the presence of unmeasured excitations, which are tackled by adjusting the number of averages.

This raises another important aspect of testing civil structures, which is their usual open space environment where they are subject to wind excitation. This is particularly significant in the case of footbridges, in which the expected low natural frequencies of the structure demanded long acquisition records to ensure that a proper frequency resolution is achieved. These long records intensify the effects of the wind, which may be an active source of excitation for the lower modes of the structure.

The wind is an unmeasured excitation, acting simultaneously with the measured hammer blows. As was discussed in Section 3.2.1, the effects of unmeasured excitations may be removed by averaging if the H1 estimator (Eq. 3.17) is employed. Indeed, this is the estimator usually adopted for obtaining FRFs from hammer tests, since it is not affected by noise on the output signal, and a reasonably flat input spectrum will provide FRFs with high signal to noise ratios in the region of the resonances.

Furthermore, and this is a point to be emphasised, it was also shown that, in the case of using the H1 estimator, a low value for Coherence does not necessarily mean that the quality of the data is compromised. Therefore, unless it presents high values, Coherence cannot be used with confidence as a qualitative parameter to help in adjusting the number of averages, as is generally stated in guidelines for hammer testing.

If searching for a parameter or procedure which enables a quick definition of the number of averages on site, it is suggested that the use of the repeatability check should be employed. As the name explains, the repeatability check aims to observe if identical FRFs can be obtained from two separate sets of averages for the same pair of points (actually, the same pair of DOFs). In the context here, the two sets of averaged FRFs are immediately obtained one after the other and superimposed to check similarities. A

repeatability check carried out on data from one of the test footbridges is shown in Fig. 3.13.

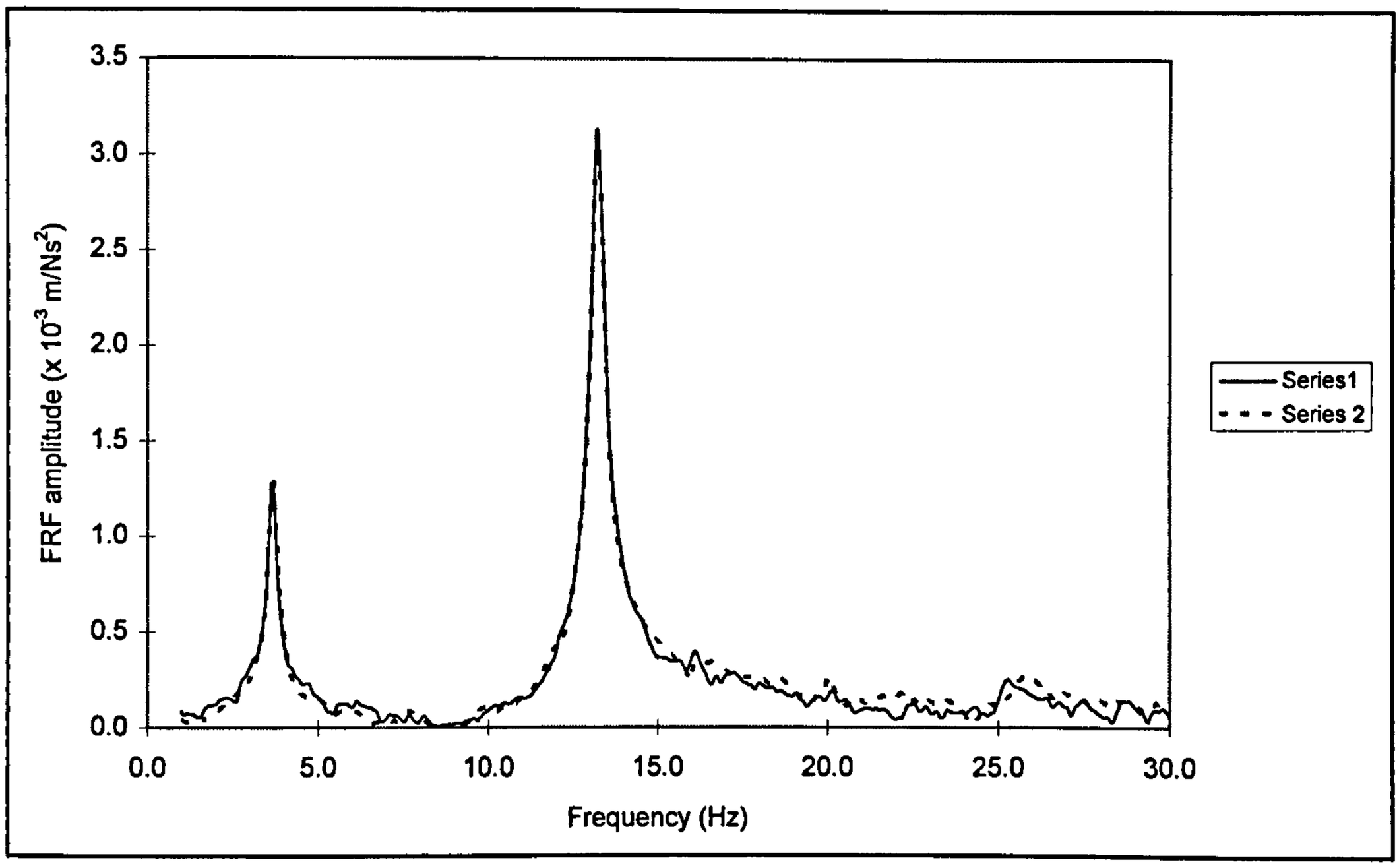

Figure 3.13 - Repeatability check.

If differences between the repeated estimations of the same FRF are significant, the behaviour of the FRFs during the averaging process can be observed to help in defining a higher number of averages for re-executing the repeatability check. Application of strong hammer hits is also recommended to push down the number of averages, since it increases the participation of the measured input on the response. A reference number of averages cannot be suggested as this depends on how significant the wind effects are during the tests. Its definition is part of the trial and error procedure usually followed for setting the particular test parameters.

Once a setting which reasonably satisfies the repeatability check is defined, two further checks are recommended to ensure that the structure behaves linearly to the level of excitation applied to it during the tests. These are the homogeneity and reciprocity checks (DTA, 1993a). In the former check, the structure is submitted to a series of soft and a series of hard hits applied at the same position. In the latter check, similar input

levels were applied but input and response were interchanged. In both cases, a good overlaying of the two FRFs is expected.

3.3.2.2 Obtaining Modal Properties

The procedure for obtaining the modal properties using the hammer technique is only similar to that adopted for ambient excitation in so far as simultaneous measurements at pairs of points are taken, in which one of the points is a reference station. All the other calculations are carried out in a different way.

The hammer operator usually stays on the structure to apply the hits, and either the accelerometer or the hammer (and so the hammer operator) stays at the reference station whereas the other moves along the structure. If the presence of the hammer operator is disregarded, there is no theoretical difference in both cases since the structure is assumed to behave linearly and so the Maxwell theorem (reciprocity) is valid (Thomson, 1993). However, the movement of the hammer operator along the structure can give rise to suspicions that alterations in modal parameters take place (Brownjohn, 1997). How significant this effect may be can be evaluated by observing the reciprocity check and also calculating the modal properties from individual FRFs at some points of the structure and observing whether they present significant variability.

The FRFs obtained for the several pairs of measurements taken are the basis for determining the modal properties. Considering that a FRF can be calculated between any two points of a structure, the complete set of FRFs can actually be represented as a matrix. The procedure detailed in the previous paragraph generates only one line or column of the FRF matrix. However, this provides enough information to make it possible to obtain the modal properties of the structure (Ewins, 1984).

Several algorithms have been developed for the extraction of the modal properties from FRFs, which are all based on curve-fitting of theoretical expressions to the experimental data. Algorithms of three levels can be identified: a) those that adjust SDOF theoretical expressions to individual resonance peaks of a single FRF; b) those which provide a MDOF extraction of modal properties of a single FRF; and c) those which provide a

MDOF extraction of several FRFs taken simultaneously. The advantage of the last group of algorithms is evident since these algorithms can take into account the (expected) small variations on the modal properties among different FRFs due to experimental errors. They are referred to as global curve-fitting algorithms.

Algorithms in all of the three aforementioned levels were available in the software employed here for extracting the modal properties of FRFs for the footbridge tests (ICATS, 1995). In group a) are the algorithms of Circle-fit (Kennedy and Pancu, 1947) and Line-fit (Dobson, 1987). An algorithm called Ident (Ewins and Gleeson, 1982) belongs to group b), and the algorithms Global-M (Fillod *et al.*, 1985), GRF-M (Richardson and Formenti, 1982) and NLLS-M (Gaukroger *et al.*, 1973) process simultaneously several FRFs using MDOF routines for modal extraction. A brief description of all algorithms can be found in the software manual (ICATS, 1995), together with suggestions regarding the performance of each algorithm according to the test case. An option of considering the effects of adjacent identified modes is available when using the SDOF algorithms.

At first sight, the algorithms of group c) are the natural first choice; however, the suggested procedures in the software manual discourage this. The user is first recommended to process some individual FRFs by combining the application of the algorithms of groups a) and b) which will give some confidence about the consistency of the modal properties extracted from different FRFs.

It is also possible to assess how close to each other are both sets of the experimental and theoretically estimated FRFs, since both are automatically superimposed on the computer screen. Several trials are recommended before a final choice is made.

The algorithms best suited for the processing of the measured FRFs from the footbridge tests were the Line-fit, Ident and Global-M. The Circle-fit proved unsuitable due to the small number of frequency lines within the half-power bandwidth of the first resonance peaks. The NLLS-M was not able to produce consistent estimations for some modes, and the GRF-M simply produced computer crashes for no apparent reason.

The modal properties will be obtained eventually by using a MDOF group c) algorithm (e.g., Global-M). Either real or complex modes can be obtained and a normalisation of the mode shapes with respect to the mass matrix of the structure is provided, dividing the modal constants calculated for each mode by the square root of the modal constant of the reference station (ICATS, 1995). This implies that the quality of the (reference) point FRF affects the whole series of results, and great care is necessary in carrying out this crucial measurement.

It should be noted that the modal properties thus obtained may be altered if an exponential window has been applied to the time domain signals. Corelli and Brown (1984) showed that there are no effects of the exponential window for obtaining frequency and mode shapes. This can be understood by thinking in terms of the physical nature of the response signal, which consists of a summation of damped sinusoids. The multiplication of such sinusoids by an exponential window function results in a new response function in which the decay coefficient of the exponential window is added to the decay coefficient of the sinusoidal response, with no changes on the frequencies of vibration. Since the exponential window is applied to all FRFs, obtaining mode shape envelopes is also not affected. However, the damping of the system is artificially increased.

Obtaining a corrected damping ratio for each mode can be carried out by subtracting the decay coefficient of the exponential function from that of the respective response at resonance. The development of this operation can be found in the literature (ISO 7626-5, 1994), resulting in:

$$\zeta_{r_{cor}} = \zeta_{r_{cal}} - \frac{\gamma_e}{2\pi f_r} \tag{3.45}$$

where $\zeta_{r_{cor}}$ and $\zeta_{r_{cal}}$ are respectively the corrected and (exponential window affected) calculated equivalent viscous damping ratios for the mode r, f_r is the natural frequency of mode r, and γ_e is the decay coefficient of the exponential window (see Fig. 3.7b). A slightly different version of Eq. 3.45 can also be found (Clark *et al.*, 1989), in which the

natural frequency f_r of the system with damping is substituted by the undamped natural frequency $\bar{f}_r$, the latter given by (Clough and Penzien, 1975):

$$\bar{f}_r = \frac{f_r}{\sqrt{1-\zeta_r^2}} \tag{3.46}$$

Substituting f_r by $\bar{f}_r$ in Eq. 3.45 leads to

$$\zeta_{r_{cor}} = \zeta_{r_{cal}} - \frac{\gamma_e}{2\pi \bar{f}_r} \tag{3.47}$$

The difference in using Eqs. 3.45 or 3.47 for estimating damping is actually negligible for the magnitude of damping values less than or around 1% as found in the test footbridges. However, Fladung and Rost (1997) have recently raised attention to the fact that it is the natural frequency of the system (the damped natural frequency f_r) and not the undamped natural frequency $\bar{f}_r$ that it is unaffected by the exponential window, i.e., $f_{r_{cal}} = f_r$. They also pointed out that Eq. 3.47 is an approximation (actually theoretically inconsistent) of the true expression, given by:

$$\zeta_{r_{cor}} = \left(\frac{\bar{f}_{r_{cal}}}{\bar{f}_r}\right)\zeta_{r_{cal}} - \frac{\gamma_e}{2\pi \bar{f}_r} \tag{3.48}$$

where $\bar{f}_{r_{cal}}$ is the calculated (window affected) undamped natural frequency, which can be obtained, in a similar way as $\bar{f}_r$, as:

$$\bar{f}_{r\,cal} = \frac{f_{r\,cal}}{\sqrt{1-\zeta_{r_{cal}}^2}} = \frac{f_r}{\sqrt{1-\zeta_{r_{cal}}^2}} \tag{3.49}$$

By comparing Eq. 3.47 and Eq. 3.48, it can be seen that the approximation in the former is to consider $\bar{f}_{r_{cal}} = \bar{f}_r$. Fladung and Rost (1997) showed that this approximation may lead to a considerable error, particularly for low damped systems.

Nevertheless, the application of Eq. 3.48 for obtaining corrected estimates of damping is not possible since the undamped natural frequency $\bar{f}_r$ is unknown. This may have been the motivation for using the approximation Eq. 3.45. However, for the case of lightly damped structures, like the test footbridges, the difference between the damped (unaffected) natural frequency f_r and the undamped natural frequency $\bar{f}_r$ is negligible. Therefore, substituting Eq. 3.49 into Eq. 3.48 and considering that $\bar{f}_r \approx f_r$, the following expression is obtained:

$$\zeta_{r_{cor}} \approx \frac{\zeta_{r_{cal}}}{\sqrt{1-\zeta_{r_{cal}}^2}} - \frac{\gamma_e}{2\pi f_r} \tag{3.50}$$

Use of Eq. 3.50 is suggested for correcting the effects of the exponential window on damping ratios as an alternative to Eqs. 3.45 and 3.47 found in the literature. Eq. 3.50 is consistent with the theoretical Eq. 3.48, and the only assumption is that $\bar{f}_r \approx f_r$, which leads to negligible errors in the case of lightly damped structures. The difference between Eq. 3.50 and Eq. 3.45 is the introduction in the former of the term $\sqrt{1-\zeta_{r_{cal}}^2}$ as the denominator of $\zeta_{r_{cal}}$. This term may be not negligible since $\zeta_{r_{cal}}$ may be significant because of the additional damping artificially introduced by the exponential window.

Some factors can cause uncertainty in damping evaluations from hammer tests in the low natural frequency structures currently discussed in this Section. The lack of a good definition of the FRF peaks due to low frequency resolution and the presence of the hammer operator on the structure, can both contribute to an increase on the estimated damping values.

As a final remark, the correlation between the measured and calculated modal properties from a numerical model is carried out in the same way as described in the previous Section for the ambient excitation tests.

3.3.3 Free-Vibration Decay Tests

In this group of tests, the measurements carried out on the structure are initiated after the load is removed from the structure or its application ceases. One of the techniques is

called step relaxation, in which a weight is usually attached to the structure by a wire or rope and then suddenly removed by cutting. Response-only measurements are taken and can lead to obtaining the modal properties of the structure.

However, in the context of this thesis, the free-vibration decay tests are restricted to evaluating natural frequencies and damping values of specific modes of vibration of the test structure. In this particular case, free-vibration decays can be induced by heel drops or from the tail end of jumping or walking tests.

Being an impulsive force, a heel drop excites all the modes of the structure which do not possess a node at the point in which the force is applied by the test subject. The application of a filter is necessary to isolate the contribution of the response caused by the mode of interest. This process can be repeated for several modes; however, its effectiveness will depend on how separate the modes are.

For obtaining responses containing only the contribution of the mode of interest, a better excitation source is found using the free decay part of jumping or walking tests. In these cases, a test subject, with the help of a metronome, jumps/walks along at a rate equal to the natural frequency of interest, generating responses dominated by the respective mode of vibration. Filtering is still recommended for obtaining a clearer decay containing only the mode of interest.

The procedure adopted to obtain the natural frequency and damping value of a filtered free-vibration decay follows the general guidelines of the DTA on the subject (DTA, 1993b). The (damped) natural frequency is calculated from the average time between zero crossings of the decay response. In this calculation, care is taken in determining each zero crossing by a linear interpolation of the discrete values of the measured signal around zero. The equivalent viscous damping ratio is calculated from the slope of a straight line adjusted to the curve defined by the logarithm of the peak values versus time (logarithmic decrement method).

References in the literature are found in which a full adjustment of a SDOF model is made to the free-vibration decay signal or parts of it (Littler, 1995; Ellis and Ji, 1996). However, the very small variation obtained in the modal properties of the test structures using discrete points of the free-decay signal, as detailed in the previous paragraph, assured the sufficiency of the adopted procedure.

Chapter 4

Modal Testing and Analysis of Prototype Footbridges

4.1 Introduction

This Chapter encompasses a description of the tests carried out on three prototype footbridges and the analysis of their vibration performance. The tests had two aims, the first one being to obtain the modal properties of the test structures, from which numerical FE models developed to represent them could be calibrated. Use was made of these numerical models to investigate the vibration performance of the test structures. The second aim of the tests was to assess the vibration performance of the prototype structures based on guidelines for vibration performance, and this was carried out by means of pedestrian tests.

The selected test footbridges were a single span beam-like composite (concrete and steel) footbridge, although with a small camber which introduced some arch action; a single span stressed ribbon concrete footbridge of catenary shape; and a three-span glass reinforced plastic cable-stayed footbridge. The variety of structural systems among the test footbridges provides a degree of generality in the analysis of their vibration performance. In addition, all test structures presented natural frequencies within the critical ranges of the harmonics of the walking load (see Chapter 2), which potentially makes them lively and makes them highly suited for an investigation into the applicability of the current guidelines of vibration performance. This latter investigation is discussed in the next Chapter.

The previous paragraph may indicate that it was a hard task to find suitable footbridges that would fulfil the aforementioned purposes. Indeed, each footbridge had a different story as to how it became to be included in the test programme, and it was more the availability for testing than any other factor that decided their selection. It was the fact that the test structures were potentially lively and the results obtained from the tests that

directed the research towards an examination of the present guidelines for vibration performance.

The organisation adopted in this Chapter is to describe the tests, the preparation and calibration of an FE model, and the analysis of vibration performance of each footbridge individually (Sections 4.3 to 4.5). These are preceded by the following Section, in which the general procedures adopted for the testing and analysis of the test structures are discussed. The sequence adopted for the presentation of the tests and respective analyses does not follow the chronological order in which the tests were carried out. Instead, it is based on the increasing complexity of the structural system that each structure represented.

4.2 General Procedures for Testing and Analysis

Vibration performance of footbridges is based on information obtained from dynamic tests. These tests can be divided into two groups: modal tests and pedestrian (serviceability) tests. The general procedures adopted in each of these two groups of tests and for the analysis of vibration performance of the test structures are detailed below.

Procedures for Modal Testing

Investigation of vibration performance of structures due to human-induced loads is mostly related to the behaviour of the structure in the vertical direction. However, initial trials were made to excite the test structures in different directions, to identify potential vibration serviceability problems and orientate the modal tests.

The modal testing techniques described in Chapter 3 were all used in the modal tests of the prototype structures, namely: the ambient vibration survey (AVS), hammer tests and free-vibration decay. Nevertheless, time restrictions for carrying out the site tests generally required a principal technique to be chosen in each case, between the first two aforementioned techniques. Attempts were made to use the hammer tests in the first

instance since this technique makes it possible to obtain FRFs and consequently a theoretically more consistent approach for obtaining the modal properties.

The calibration of the test equipment carried out by Pavic (1997), who was simultaneously using the equipment for testing floors, confirmed the nominal sensitivities of the components of the system instrumentation. However, a few additional tests were carried out in the laboratory, in order to check the accuracy of the accelerometers in detecting low frequency vibrations (see Appendix A.1).

Attention was paid to potential differences in terms of modal properties that could arise if different excitation levels were applied to the structure. What is meant by this is that the level of excitation due to wind, if using AVS, or due to a hammer blow, if using the hammer tests, was lower than that when the structures were excited by pedestrians. Since the object of carrying out the tests was to investigate the vibration performance of the test structures due to pedestrian excitation, a comparison was made between the modal properties obtained from free-vibration decay tests using pedestrians and those obtained by the other two techniques.

The procedures for obtaining natural frequencies and the equivalent viscous damping ratios from free-vibration decay tests were detailed in Section 3.3.3. Walking and jumping tests were used. In the former tests, the free-decay consisted of structural vibrations after the test subject had left the bridge, whereas, in the latter, the test subject initially jumped at a point on the bridge and stood still afterwards. Alternatively, application of heel drops were also employed. In all cases, the time domain decay response was filtered to isolate the contribution of the mode of interest. The software employed for this task was a band-pass digital filter (Petkovski, 1994), in which the user defines the frequency range that is intended to be preserved (the band-pass) and the slopes of the filter. By conveniently selecting the frequency range to include only the resonance peak of interest, all other frequency components are removed, producing a signal which more closely resembles that of a SDOF system.

Since footbridges are structures usually having a predominant dimension, simple FE models using beam elements were employed. Use was made of the computer package

ANSYS 5.0 (ANSYS, 1992) for developing the FE models and calculating the modal properties. The definition of the FE mesh in each case was based on the geometry of the structure, the length of the structural components, and also to provide a good resolution for representing the modes of vibration of interest. The subsequent use of the FE models for the investigation of the pedestrian load (see Chapter 5) was also considered to define the spacing among the nodes of the mesh. In order to check mesh size effects, a coarse FE mesh was prepared in each case, resulting in negligible differences in all calculated natural frequencies of interest.

The structural parameters selected for calibration varied according to the complexity of the structural system of the test footbridge. However, the material properties (e.g. Young's modulus of elasticity) and support conditions were usual choices due to uncertainty in their determination.

Procedures for Pedestrian Tests

For the purpose of assessing vibration serviceability, the guidelines of the UK code of practice (BS5400, 1978) were taken as a reference. In order to reproduce the design procedure adopted in this code, a single test subject was employed to walk along the structure, having a pacing rate such that the structure is set in resonance in its fundamental mode in the vertical direction. For an accurate detection of the amplitude of the time histories, a reference value for the sampling rate was taken to be 20 times the frequency of the vibration. This leads to an error a little over 1% in the determination of peak values of sinusoidal pulses (Griffin, 1990).

A metronome was employed to ensure the correct pacing rate was achieved. Furthermore, to ensure compatibility between the measurements and the procedure defined in BS 5400, the test results were filtered to contain only vibrations in the mode of interest.

A similar procedure was repeated for some natural frequencies other than the fundamental frequency but inside the frequency range of interest for vibration serviceability set by the code (frequencies up to 5 Hz). Further tests using pedestrians

for assessing the present guidelines of the codes of practice will be discussed in Chapter 5.

Procedures for Analysis of Vibration Performance

The test results and calibrated numerical models of the structures were subsequently used to investigate potential design improvements in terms of vibration serviceability.

4.3 Modal Testing of a Composite Footbridge

Tests were carried out in March 1996 on a single span pre-cambered footbridge of composite cross section, which consisted of a 2.16 m wide concrete deck connected to a steel box girder. The structure had a span with a horizontal projection of 19.90 m and was supported on elastomeric bearings of different type at the two ends. The small camber of 0.225 m created some arch action due to the partial restriction to horizontal movement provided by the elastic supports. Steel handrails, in the form of short independent panels made of hollow section components, were attached and followed the shape of the deck.

The footbridge was tested inside its construction shed, prior to removal to site for erection. The tests were carried out on two occasions with an interval of one week between them, giving the opportunity to carry out measurements on the structure before and after the installation of the handrails (Plate 4.1). Access restrictions to the structure limited each test to one day, more precisely for a period of about nine hours. This constituted a real limitation in exploring different test techniques. The following description applies to the tests on the structure with handrails unless otherwise specified. As will be seen, the handrails had a negligible influence on the dynamic behaviour of the structure.

Twelve test points, including one at each extreme, were marked on the centre of the deck along the longitudinal axis of the footbridge at approximately 1.80 m centres, being coincident with the positions where the handrails were attached to the deck. An

additional test point was marked at the central point of the span. This was thought to be enough for a good representation of the first modes of the structure. Attempts to excite the structure in the lateral and torsional direction produced oscillations that could be neither felt nor visually observed. Conversely, controlled jumps in the mid-span revealed a vertical natural frequency of at about 3.0 Hz and vibrations that could both be felt and visually observed. It was concluded that the possibility of vibration serviceability problems was restricted to the vertical direction.

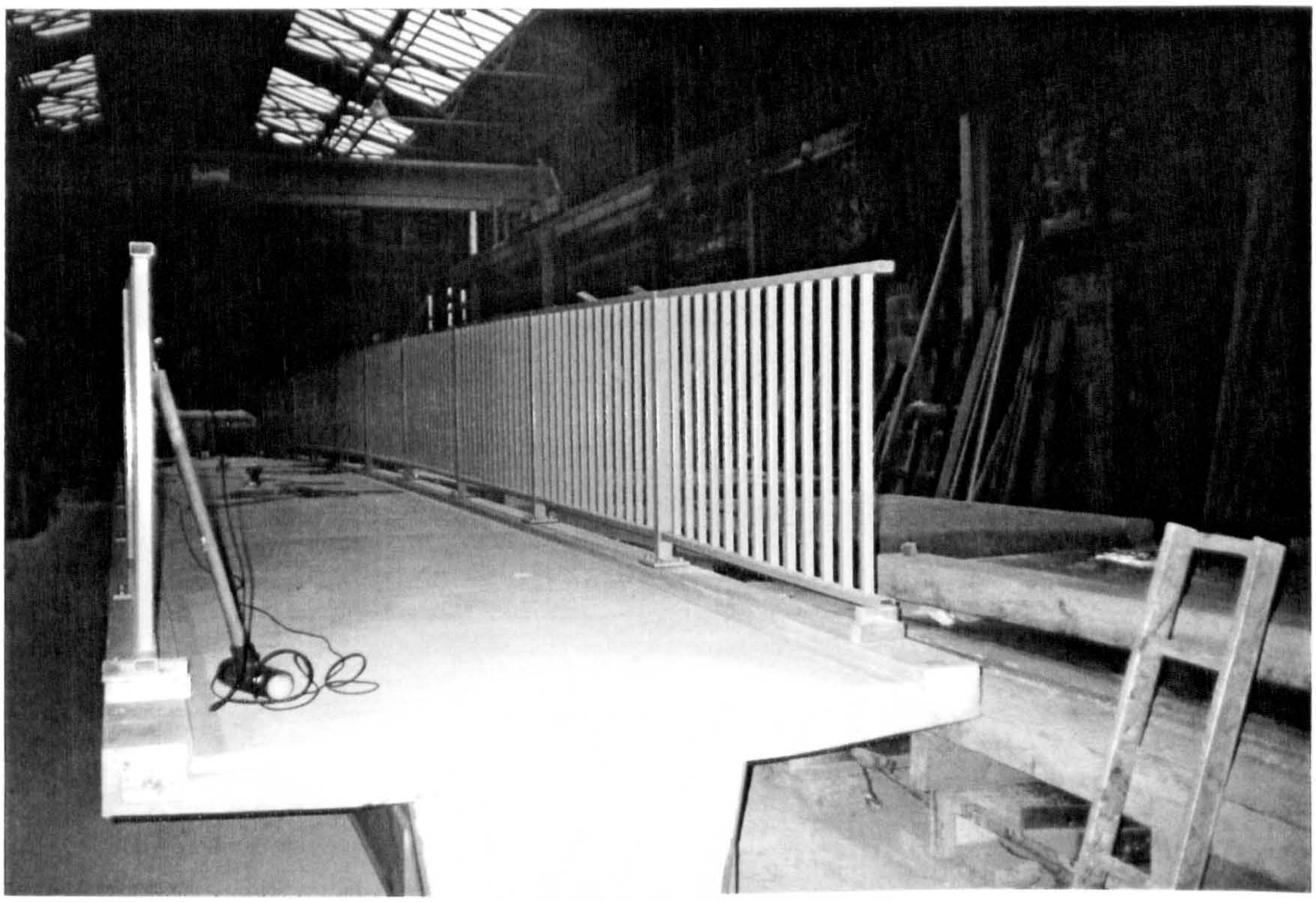

Plate 4.1 - Single span composite footbridge (handrails installed)

The impulse response technique using an instrumented hammer was the principal technique adopted. Additional measurements from the free-vibration decay response of pedestrian tests completed the modal survey of the structure, enabling the determination of the modal properties of the structure in the vertical direction.

The data was acquired using a spectrum analyser, to which a 5 kg instrumented hammer and an accelerometer having a sensitivity of approximately 1 Volt/g were connected (see more details about equipment in Appendix A.1). The preparation for the hammer

tests was a time consuming task involving the choice of the best position to place the fixed accelerometer and the selection of various test parameters. The final values selected for these parameters were based on the discussion presented in Section 3.3.2.1: a frequency resolution of 0.0625 Hz, related to an acquisition time of 16 seconds for each record, and a sampling interval Δt of $7.8125*10^{-3}$ secs related in turn to a frequency range of 50 Hz. Each record consisted of 2048 data samples. The decay coefficient of the exponential window was set at 10/16, where the numerator is defined by the user and the denominator is the acquisition time. More details about the setting of this window can be found in Appendix A.1.

It has been suggested (Pavic, 1996) that the use of a zoom from 1 to 51 Hz would be beneficial in removing the high static component (component at zero frequency) presented in the FRFs, and this was adopted in this test. However, it should be noted that since the zoomed frequency range of 50 Hz was kept the same as that of the baseband analysis, the acquisition time was also unchanged, the same applying to the other parameters. With regard to the number of averages at each point, it was found that five reasonably strong hammer blows at each point were enough to ensure repeatability of the frequency response function (FRF). However, the absence of wind excitation contributed to a smaller number of averages being adopted than in the other test cases of open space footbridges.

The reference station was chosen approximately at one third of the main span from one of the bearings. Initial checks revealed that the chosen frequency range of 50 Hz would make it possible to identify the first three vertical modes. It can be seen that the third mode of vibration is not clearly seen as a resonance peak in the FRF of the reference station as the other two modes are (Fig. 4.1a). A second FRF, obtained by applying the hammer blows at the reference station and measuring the accelerations at mid-span, confirmed the presence of the third mode at a frequency of approximately 26 Hz (Fig. 4.1b). These two FRFs indicated the first and third modes as resembling symmetric modes whereas the second mode, at a frequency of approximately 13 Hz, resembles an antisymmetric mode.

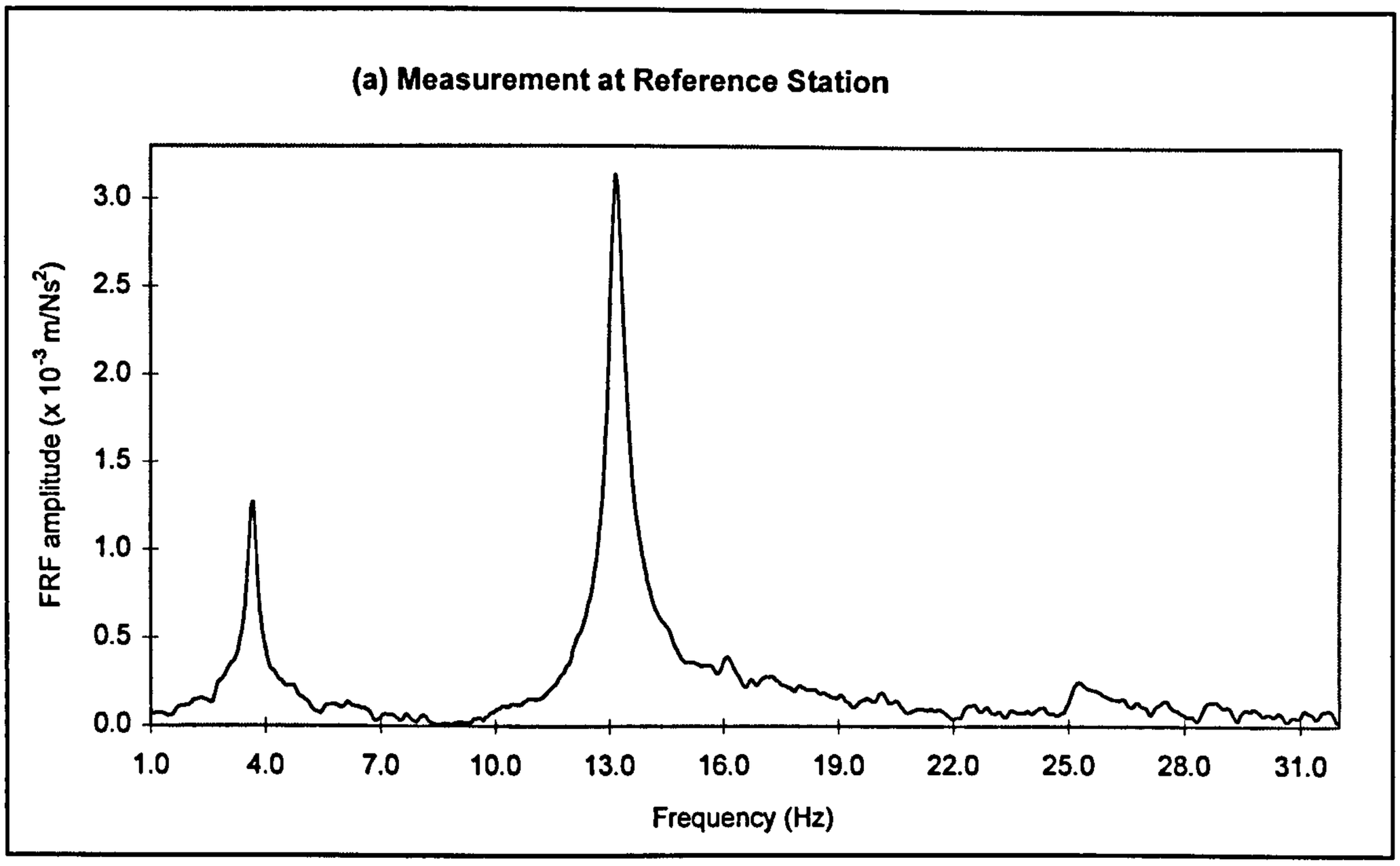

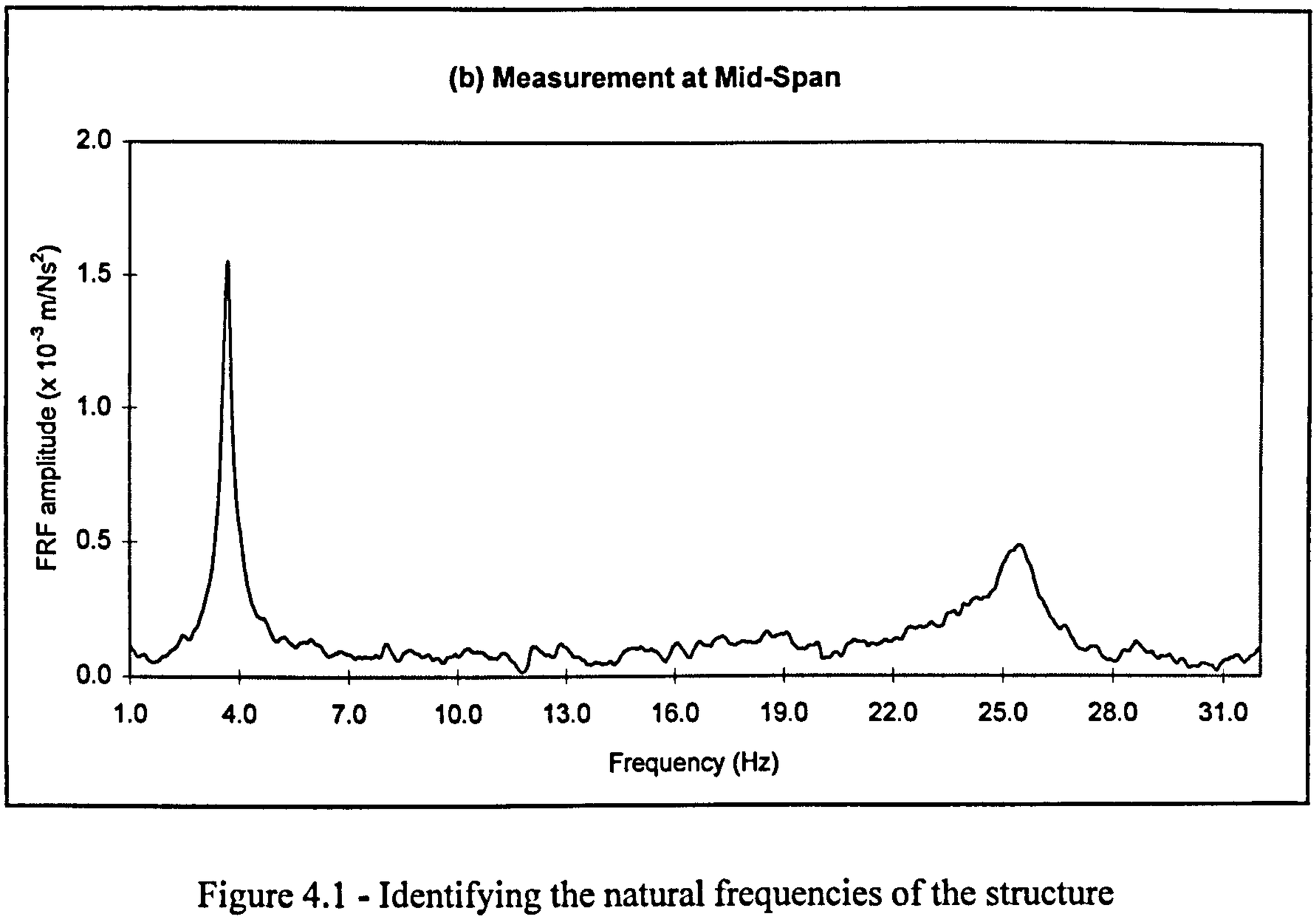

Figure 4.1 - Identifying the natural frequencies of the structure

Ideally, for identifying the three modes, more than one set of FRFs should be used, each set for a choice of a reference station. Fig. 4.1 shows that two reference stations could be selected, the first being the current choice, for identifying the first and second modes. The second reference station could be chosen at mid-span, for identifying again the first

mode and also the third mode. However, the spectrum analyser employed was limited to acquiring two channels at a time (see Appendix A.1), in this test one channel being for acquiring the excitation signal (hammer) and the other for acquiring the response signal (accelerometer). This would imply repeating the whole set of measurements for obtaining the two sets of FRFs, which was not possible due to the restricted testing time. The choice of the current reference station enabled the three modes to be identified despite the small participation of the third mode.

Linearity checks of the structure for the level of excitation applied by the hammer were carried out by means of homogeneity and reciprocity checks (DTA, 1993a), and a good overlaying of FRFs was obtained (Fig. 4.2).

The modal properties were obtained using Modent/Modesh software (ICATS, 1995), following the guidelines discussed in Section 3.3.2.2. The first identified mode was related to a frequency of 3.66 Hz, being the one of interest in this study since it is within the frequency range of interest for vibration serviceability. This fundamental frequency was also evaluated to be 3.67 Hz from the free-vibration decay of pedestrian tests. Close agreement with the value previously obtained showed that this natural frequency had negligible changes for different excitation levels, which is an indication that the structure is also behaving linearly for the level of excitation produced during the pedestrian tests.

The measurements of free-vibration decay for the walking and jumping tests were also used to evaluate the equivalent viscous damping ratio for the first mode of vibration. Almost pure exponential decays were observed in both cases, indicating that damping values were also not changing with amplitude of vibration (Fig 4.3a,b). Two damping factors were obtained, following the procedure described in Section 3.3.3 of adjusting a straight line to the plot of the logarithm of the peak values along the decay: 0.40 % and 0.53 %, from the walking and jumping tests respectively.

The actual damping value of the system during the crossing of pedestrians depends on the extent of the interaction between them and the structure, as was pointed out in Chapter 2. This is not a well understood phenomenon, particularly when the structure is

tested in resonance conditions. This is left for further discussion in Section 5.2. However, it is expected that the actual damping value of the system during the crossing lies between these two estimations since some interaction may exist between the walking subject and the structure, although to a much lesser degree than that occurring for a subject standing still.

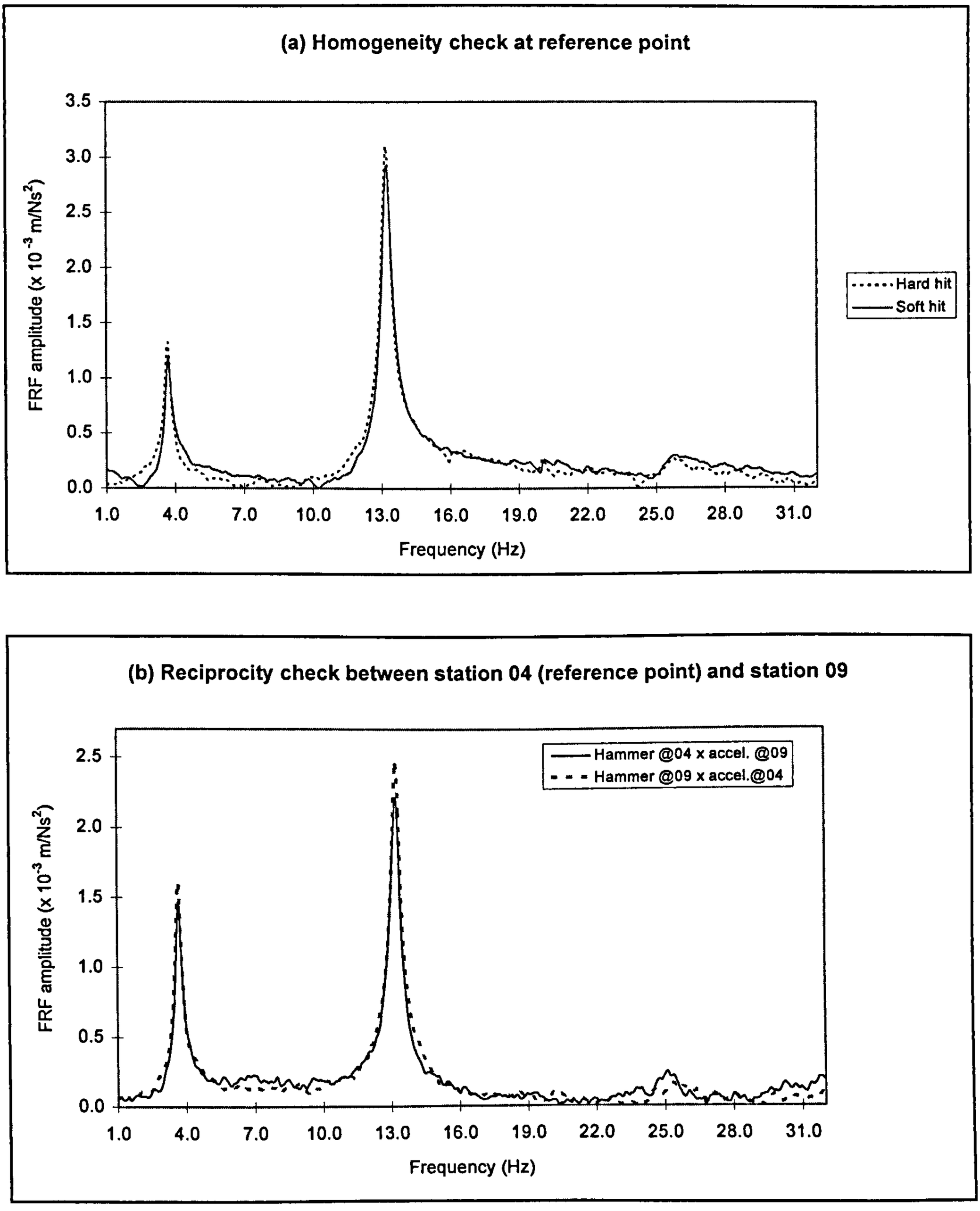

Figure 4.2 - Homogeneity and reciprocity checks

All experimental natural frequencies and damping ratios obtained from free-vibration decay and hammer tests are presented in Table 4.1, where the damping ratios from the hammer tests were obtained by applying Eq. 3.50 for correcting the effects of the exponential window. It can be seen that estimations for damping from this latter test produced higher values than those from free-vibration decay.

Figure 4.3 a) Filtered free-vibration decay from jumping tests; b) Logarithm of peak values versus number of cycles

Mode of Vibration	Hammer Tests		Free-Vibration Decay			
			Following Walking		After Jumping	
	Natural Frequency (Hz)	Damping Ratio (%)	Natural Frequency (Hz)	Damping Ratio (%)	Natural Frequency (Hz)	Damping Ratio (%)
Mode 1	3.66 Hz	0.73%	3.67 Hz	0.4%	3.64 Hz	0.53 %
Mode 2	13.20 Hz	0.65 %	-	-	-	-
Mode 3	25.45 Hz	1.78 %	-	-	-	-

Table 4.1 - Natural frequencies and equivalent viscous damping ratios

The finite element (FE) model of the structure was developed using the ANSYS 5.0 package (ANSYS, 1992). Since the investigations were focused only in the vertical direction, a two dimensional model was prepared, and beam elements were employed to model the deck. A total of 23 nodes were defined, being spaced at approximately 0.90 m centres. The mesh contained nodes coincident with all test points, being generally twice more refined. Handrails were included as an added uniformly distributed mass calculated as 65.18 kg/m, and the supports were modelled using spring elements in both the horizontal and vertical directions.

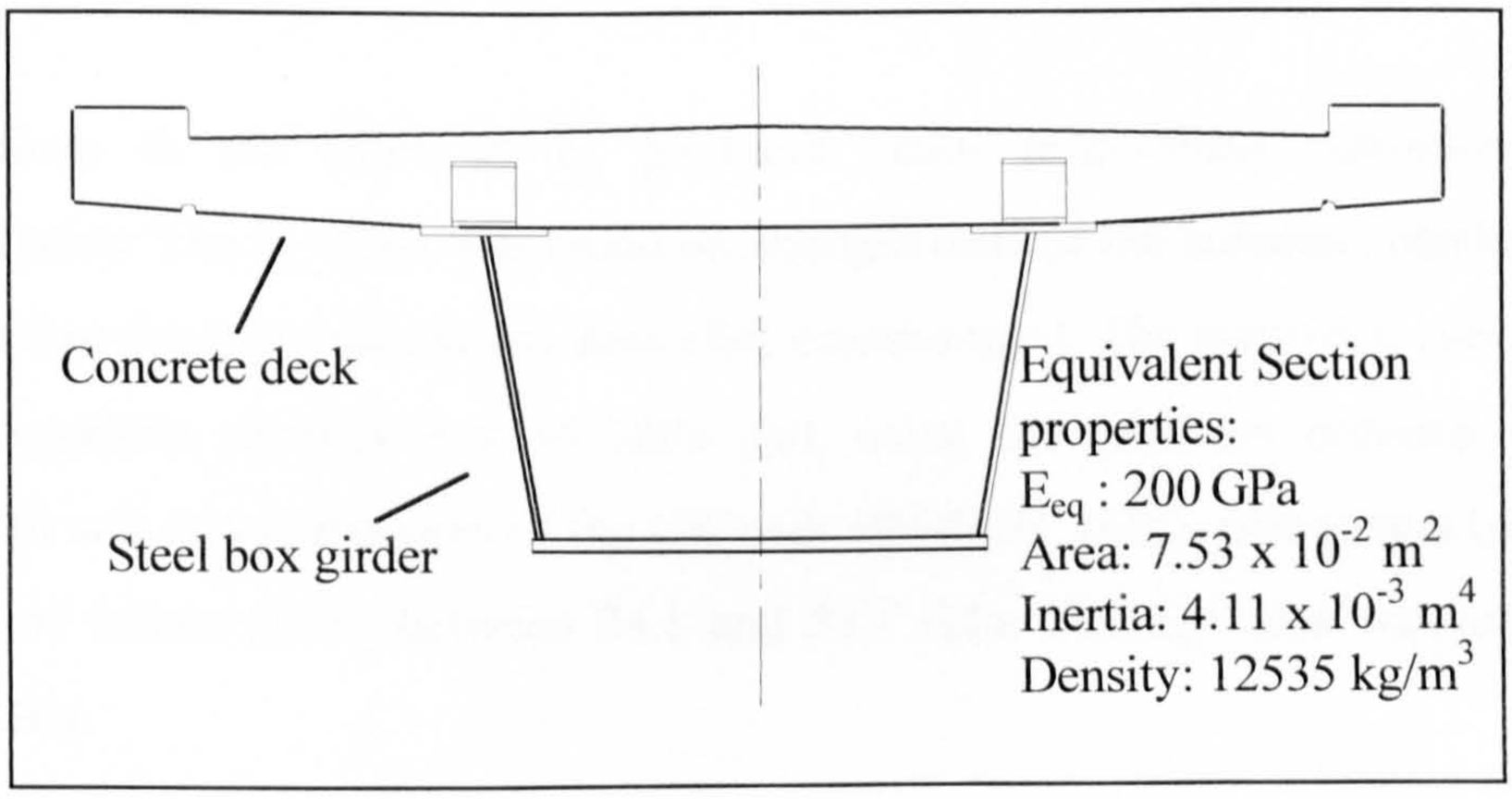

Figure 4.4 - Footbridge cross section and properties

The elastic modulus of the steel was assumed as 200 GPa and equivalent properties of the composite section were obtained from the properties of the cross section components (Fig. 4.4). Five parameters were considered as variables for correlation with the

experimental results: the Young's modulus of elasticity of the concrete (E_c), and the elastic stiffness of the elastomeric bearings at both the left and right hand supports in the horizontal (K_{HL}, K_{HR}) and vertical (K_{VL}, K_{VR}) directions. A sensitivity analysis was carried out using the FE model to help establish a final set of values which could provide a good correlation of numerical and experimental results. The outcome of this analysis is summarised as follows:

- Variations in K_{HL} and K_{HR} affected only the first mode. The ratio between the stiffness of these constants was assumed to be equal to the ratio between their manufacturer-based design values of $1.50*10^6$ N/m and $1.39*10^6$ N/m, respectively. The final adopted values for K_{HL} and K_{HR} were $4.25*10^8$ N/m and $3.94*10^8$ N/m, respectively.

- The ratio between the first and the higher natural frequencies were mainly affected by variations in K_{VL} and K_{VR}. Varying these parameters also directly affected the mode shape ordinates at the supports. The best values for K_{VL} and K_{VR} were found to be $9.20*10^7$ N/m and $1.43*10^8$ N/m respectively. The manufacturer-based design values were $8.0*10^6$ N/m and $1.50*10^8$ N/m, respectively.

- Variations in the value of E_c produced small proportional variations in all frequencies. The E_c value was based on strength tests of the concrete, carried out the day before the first tests (seven days after construction). The measured cube strength from concrete samples was 54 MPa and, using the relations between the cube strength and elastic modulus of the UK code (BS8110, 1985), this gave a (reference) range of values for E_c between 24.1 and 33.7 GPa. The E_c value was adjusted to 30.8 GPa.

Very good agreement between calculated and measured natural frequencies and mode shapes from the hammer tests was obtained. The first mode shapes are plotted in Fig. 4.5, and correlate well with the measured ones (Table 4.2 and Fig. 4.6). Both sets of natural frequencies are also shown in Table 4.2.

Natural Frequencies (Hz)		Modal Assurance Criteria (MAC) (%)
Calculated	Measured	
3.67	3.66	98
13.25	13.20	99
26.80	25.45	99

Table 4.2 - Natural frequencies and MAC values

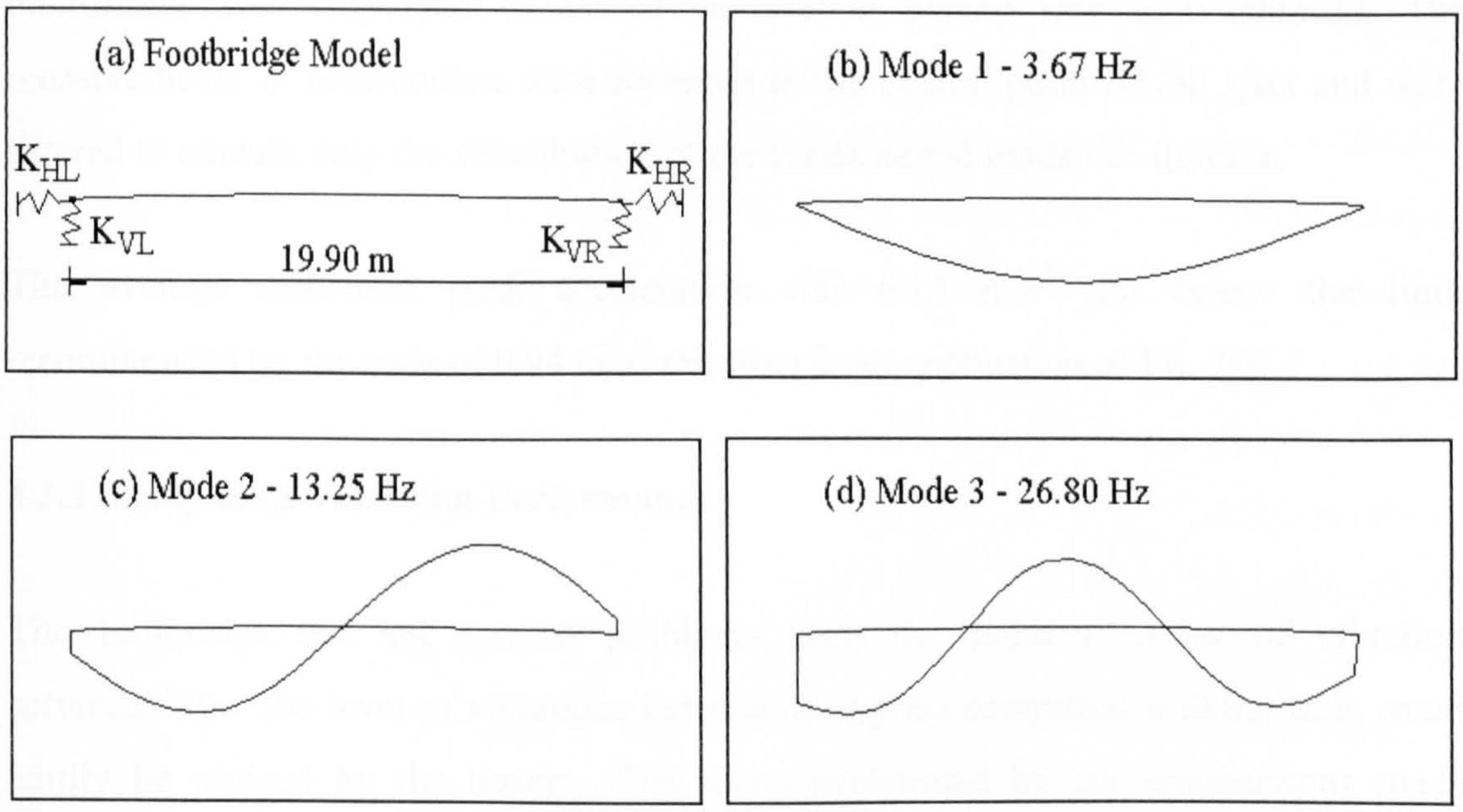

Figure 4.5 - Calculated mode shapes

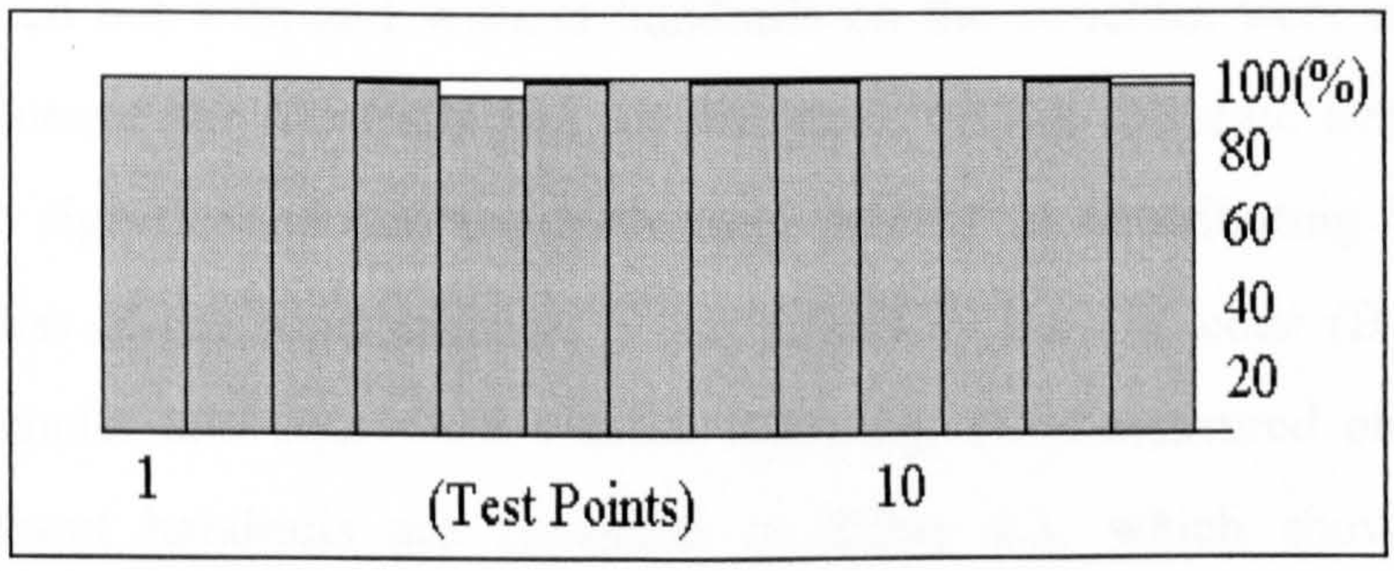

Figure 4.6 - Coordinate modal assurance criteria (COMAC)

For the purpose of assessing the vibration serviceability of the structure, tests were conducted using two pedestrians each weighing 740 N, walking at a pacing rate of 1.8 Hz. It may be noted that, in order to follow the guidelines of the BS 5400 (BS5400, 1978) to the letter, the test subjects should walk using a pacing rate of 3.6 Hz, equal to

the fundamental frequency of the structure. According to the discussion in Chapter 2 (see Fig. 2.2), this pacing rate is outside of the usual range for walking and, in any case, it is virtually impossible for anyone to walk at such a pacing rate. This was identified as one of the pitfalls in applying the guidelines of the BS 5400 in the earlier discussion.

The chosen pacing rate of 1.8 Hz implied that the second harmonic of the walking load would be approximately equal to the fundamental frequency of the footbridge, and a metronome was employed to ensure the correct pacing rate was achieved. The measurements of acceleration were recorded at the central point of the span and were filtered to contain only the contribution of the fundamental mode of vibration.

The average measured peak acceleration was 0.13 m/s^2, far below the limit recommended by the code of 0.94 m/s^2 resulting from application of Eq. 2.5.

4.3.1 Analysis of Vibration Performance

The footbridge did not present problems from the point of view of vibration serviceability. The level of vibrations induced during the controlled walking tests could hardly be noticed by the testers. This was corroborated by the comparisons made between the measured peak accelerations and the code provision limits.

The tests carried out with and without handrails on the structure were useful to show how little influence the handrails had, in this case, on the dynamic behaviour of the structure. The significance that handrails may present in contributing to the overall flexural stiffness of the superstructure is recognised by the UK code (BS5400, 1978). Natural frequencies and equivalent viscous damping ratios measured on the structure with and without handrails are presented in Table 4.3, which shows very small variations particularly in the fundamental frequency. The fact that the handrails were made of independent panels simply attached to each other contributed to nullify its potential structural function of increasing the stiffness of the structure. Increases in stiffness are one of the ways of promoting frequency tuning, which helps remove the natural frequencies of a structure from the critical frequency ranges of the walking load, as discussed in Section 2.5.

Case (Measured Results)	Natural Frequencies from Hammer Tests(Hz)			Damping from Free-Decay (%)*
	Mode 1	Mode 2	Mode 3	Mode 1
Measurements with Handrails	3.66 Hz	13.20 Hz	25.45 Hz	0.4 %
Measurements without Handrails	3.65 Hz	13.44 Hz	26.03 Hz	0.4 %

* following walking tests

Table 4.3 - Results from tests with and without handrails

The increase in stiffness and consequently on the natural frequencies that could come from the handrails if these were made continuous was investigated. This was carried out by modelling them as a continuous steel frame rigidly attached to the deck of the bridge. The Young's modulus of elasticity of the steel was taken as E_s = 200 GPa and the dimensions of the hollow cross sections of the handrail components were taken from the design calculations as being: a) top and bottom rails: 50x30x3.2 mm; b) posts: 60x60x4 mm; and c) infill bars (thirteen per panel): 30x30x3.2 mm. The height of the top rail was 1.07 m above the surface of the deck and 0.97 m above the bottom rail (see Plate 4.1 for reference). The infill bars were all grouped in a single beam element, centrally located in each panel. Finally, the contribution of the two handrails were added together into a single frame. The natural frequencies obtained in this analysis are presented in Table 4.4 together with the calculated natural frequencies for the as-built structure.

Case (Numerical Results)	Natural Frequencies (Hz)		
	Mode 1	Mode 2	Mode 3
Actual Structure (handrails are independent panels and included in the model as added mass)	3.67 Hz	13.25 Hz	26.80 Hz
Modified Structure (handrails are made continuous and modelled as a frame attached to the deck)	3.74 Hz	13.34 Hz	26.67 Hz

Table 4.4 - Effect of a continuous handrail system on natural frequencies

The results presented in Table 4.4 show that little contribution from the handrails occurs in this case, in terms of changing the natural frequencies of the structure.

The role of the elastomeric bearings in affecting the fundamental frequency of vibration was also investigated. Use of bearings to promote restraints to horizontal displacements was shown to be successful on the design of a footbridge which presented different abutment levels, aiming to detune its fundamental frequency (Willoughby, 1996).

In the case under study, the camber of the structure induced some arch action, and its influence depends on the amount of restriction to horizontal displacement that can be provided by the bearings. As was seen in the sensitivity analysis for correlating the experimental and numerical results, the predominant influence of the arch action is on the fundamental mode. This can be understood by the shape of this mode, implying that there are larger horizontal displacements, and consequently the mobilisation of the axial forces since the displacements are restricted to some degree by the bearings.

Natural frequencies obtained by changing the support conditions to the extreme situations of free horizontal displacements (i.e. $K_{HL} = K_{HR} = 0$) and complete restriction ($K_{HL} = K_{HR} = \infty$) are presented in Table 4.5 together with the natural frequencies calculated for the existing footbridge.

Case (Numerical Results)	Natural Frequencies (Hz)		
	Mode 1	Mode 2	Mode 3
Structure without horizontal constraints	3.51 Hz	13.25 Hz	26.80 Hz
Existing Structure	3.67 Hz	13.25 Hz	26.80 Hz
Structure fully constrained in horizontal direction	4.18 Hz	13.25 Hz	26.85 Hz

Table 4.5 Changes in natural frequencies due to different support conditions

Use of the horizontal stiffness of the bearings can be seen as a useful way of promoting frequency shifts from critical frequency ranges. However, one potential pitfall in using this during the design is the need to have reliable design data for the bearings. The bearings employed in the test structure are a good example. In this case, according to the information supplied by the designer, the elastic constants of the bearings were generally far inferior to the values obtained from the correlation with the numerical model. Use of the design values would actually lead to natural frequencies and mode

shapes in complete disagreement with the measurements. This discrepancy may be due to uncertainties in the material properties of the bearings and/or confinement conditions. However, in the case of the test structure, it should be noted that the bearings were not thought of as having any structural function in terms of restricting displacements in the horizontal direction.

The influence of the bearings discussed in the previous paragraph is associated with the amount of camber present on the structure. As a reference regarding the influence of the camber, Table 4.6 presents the calculated natural frequencies of the existing structure and those obtained by considering the structure as having twice the actual camber and also as being rectilinear. In the latter case, the calculated natural frequencies were the same of those obtained by removing the horizontal constraints from the current model (see Table 4.5).

Case (Numerical Results)	Natural Frequencies (Hz)		
	Mode 1	Mode 2	Mode 3
Numerical Model (camber of 0.45 m)	4.11 Hz	13.21 Hz	26.77 Hz
Existing Structure (camber of 0.225 m)	3.67 Hz	13.25 Hz	26.80 Hz
Numerical Model of the Structure without Camber	3.51 Hz	13.25 Hz	26.82 Hz

Table 4.6 - Changes in natural frequencies due to the camber of the structure

The conclusion from these numerical exercises is that the use of bearings having reliable elastic constants, in association with a pre-camber of the structure, are potential features that can be utilised during design to improve the vibration performance of beam-like footbridges.

4.4 Modal Testing of a Stressed Ribbon Footbridge

Series of tests were carried out on a stressed ribbon footbridge in June 1994 and June 1995, each lasting one day. The second series of tests complemented information missed in the first series and extended the investigations of the vibration performance of the structure by means of additional pedestrian tests. Both series of tests were carried

out under similar temperature conditions, and variations in modal properties between them were found to be negligible. A third series of tests was carried out specifically with the aim of investigating the interaction between walking pedestrians and the structure, and will be described in Chapter 5.

This stressed ribbon footbridge was reported to be the first of its kind in the UK (Butler, 1977). The superstructure of the footbridge consisted of a 34 m single span catenary shaped prestressed concrete slab fixed at the abutments (Plate 4.2). Steel handrails made of continuous hollow box sections were firmly attached which followed the catenary shape of the 1.8 m wide deck. The depth of the deck was 160 mm thickened locally towards the ends. Measurements carried out on site showed that the thickening of the deck was uniform along the first 3.6 m of the deck at each side, the depth starting from the value of 160 mm and reaching a value of 380 mm at the abutments. An asphalt topping of 12.5 mm was added. The actual geometry of the structure, including the non-structural elements, was determined by means of a site survey. A typical cross section of the footbridge is shown in Fig. 4.7.

Plate 4.2 - Single span stressed ribbon footbridge

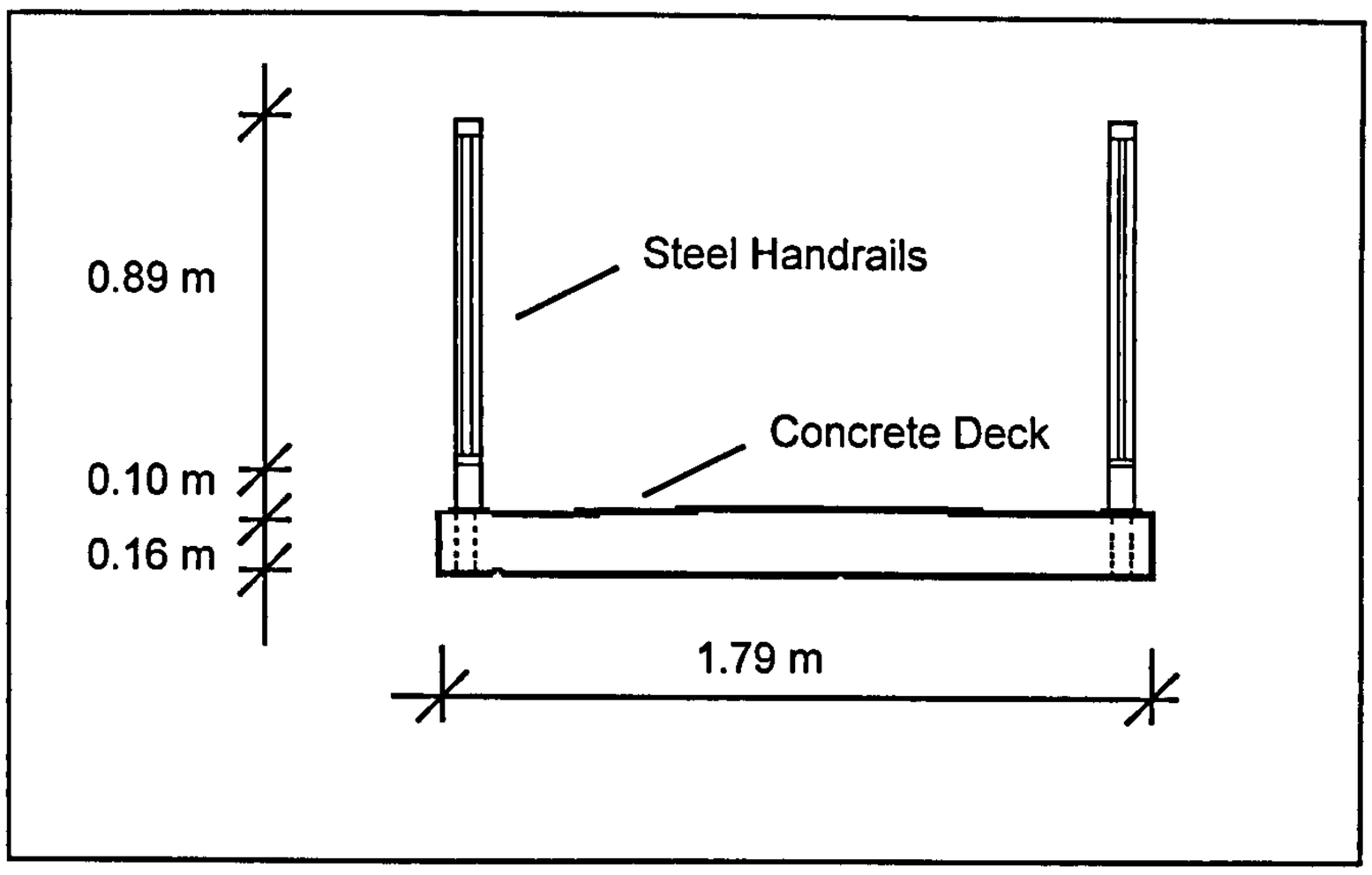

Figure 4.7 - Footbridge cross section

The tests comprised a modal survey for the determination of the natural frequencies, damping values and mode shapes of the structure, using the impulse response technique and additional measurements from ambient excitation, heel drop and free-vibration decay response from pedestrian tests. All the measurements were concentrated in the vertical direction since attempts to excite the structure in the lateral or torsional direction had failed in producing perceptible vibrations.

Twenty points were marked along the longitudinal axis of the footbridge, along the centre line of the deck. These points were selected to coincide with the nodes of a FE model being developed concurrently. The points were spaced approximately at 2.0 m centres, being located at both ends and at each connection between the deck and steel handrails.

The Impulse Response Technique using a hammer was the principal technique adopted. The set-up of the equipment for this test was the most laborious part, taking about 30% of the time spent on site. The procedures for determining the various test parameters are detailed below:

(a) Measurements from heel drop and ambient excitation tests were carried out to provide an initial site evaluation of the natural frequencies of the structure. The fundamental natural frequency was found to be about 2.2 Hz. Based on this value, the

frequency resolution chosen was 0.0625 Hz, according to the discussion in Section 3.3.2.1. This relates to an acquisition time of 16 seconds, which was already longer than the duration of the vibration decay due to an impulsive load. These measurements were also used to establish a reference point for the accelerometer, approximately one quarter along the span, which enabled the main modes of vibration of the structure to be identified.

(b) An exponential window was adopted to reduce the effects of wind, which would be intensified due to the relatively long acquisition time. Time domain responses due to preliminary hammer blows provided an estimate of the duration of the response signal and were used to select an appropriate decay constant γ_e of the exponential window. A value of γ_e equal to 1/16 was found to produce a good balance in eliminating the part of the signal mostly affected by wind and yet not over-damping the lower modes of vibration.

(c) In order to ensure repeatability of the tests, after some trials the number of hits at each point was set at 10.

Using this set of parameters and a frequency range of 50 Hz, the Coherence function was checked at several points. Values higher than 0.95 were found in the region of the peaks of the frequency response function (FRF) for the frequency range of interest, showing that the set-up of the equipment was satisfactory. A point of note is that the wind conditions during the tests were very calm, with no gusts, resulting in the appearance of high coherence values (see discussion about wind effects on Coherence in Sections 3.2.1 and 3.3.2.1). A plot of the FRF at the reference station is shown in Fig. 4.8, from which the natural frequencies of the structure can be identified.

Linearity of the structure for the level of excitation applied by the hammer was assured by a good overlaying of the FRFs (Fig. 4.9). To obtain the natural frequencies and mode shapes, the hammer tests were processed using Modent/Modesh software (ICATS, 1995). The first natural frequency of 2.3 Hz was identified, related to an antisymmetric mode shape.

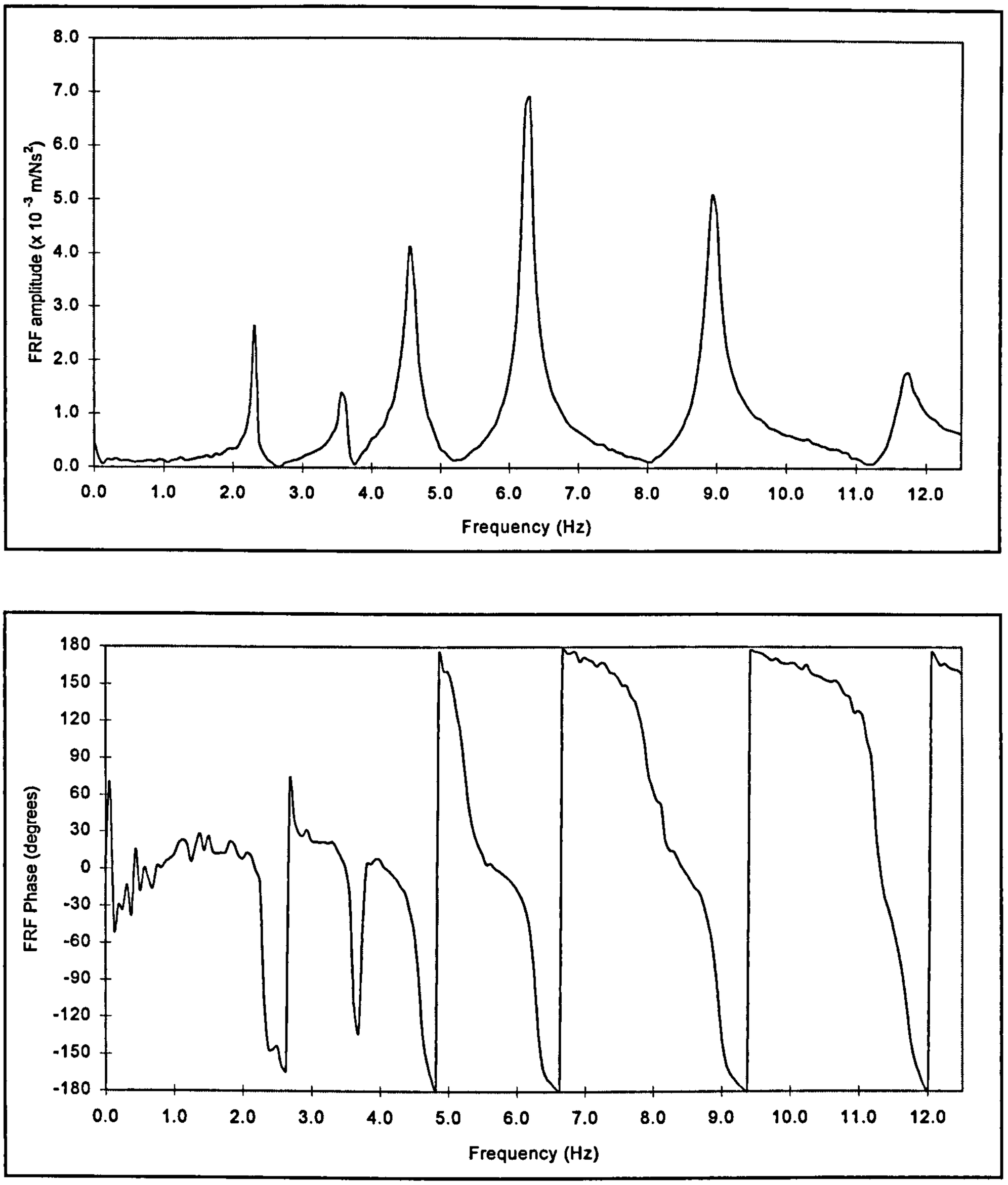

Figure 4.8 - FRF amplitude and phase at the reference point

The FE model of the structure was developed using ANSYS 5.0 software (ANSYS, 1992). A two dimensional model was prepared, in which deck and handrails were modelled using beam elements and the surfacing was included as an added mass. Tapered elements were adopted to account for the variation of the thickness of the deck. The modelling of the handrails followed the procedure described in Section 4.31 for modelling them as an attached frame. The mass of the surfacing was calculated as being 45 kg/m, obtained by the product of the measured width of 1.53 m in which the asphalt

topping was distributed and a mass per square metre of 29.41 kg/m^2, the latter obtained from typical values for asphalt (BS 648, 1964). With reference to the FE mesh, the nodes were spaced at approximately 1.0 m centres along the deck, half the distance adopted for the test points.

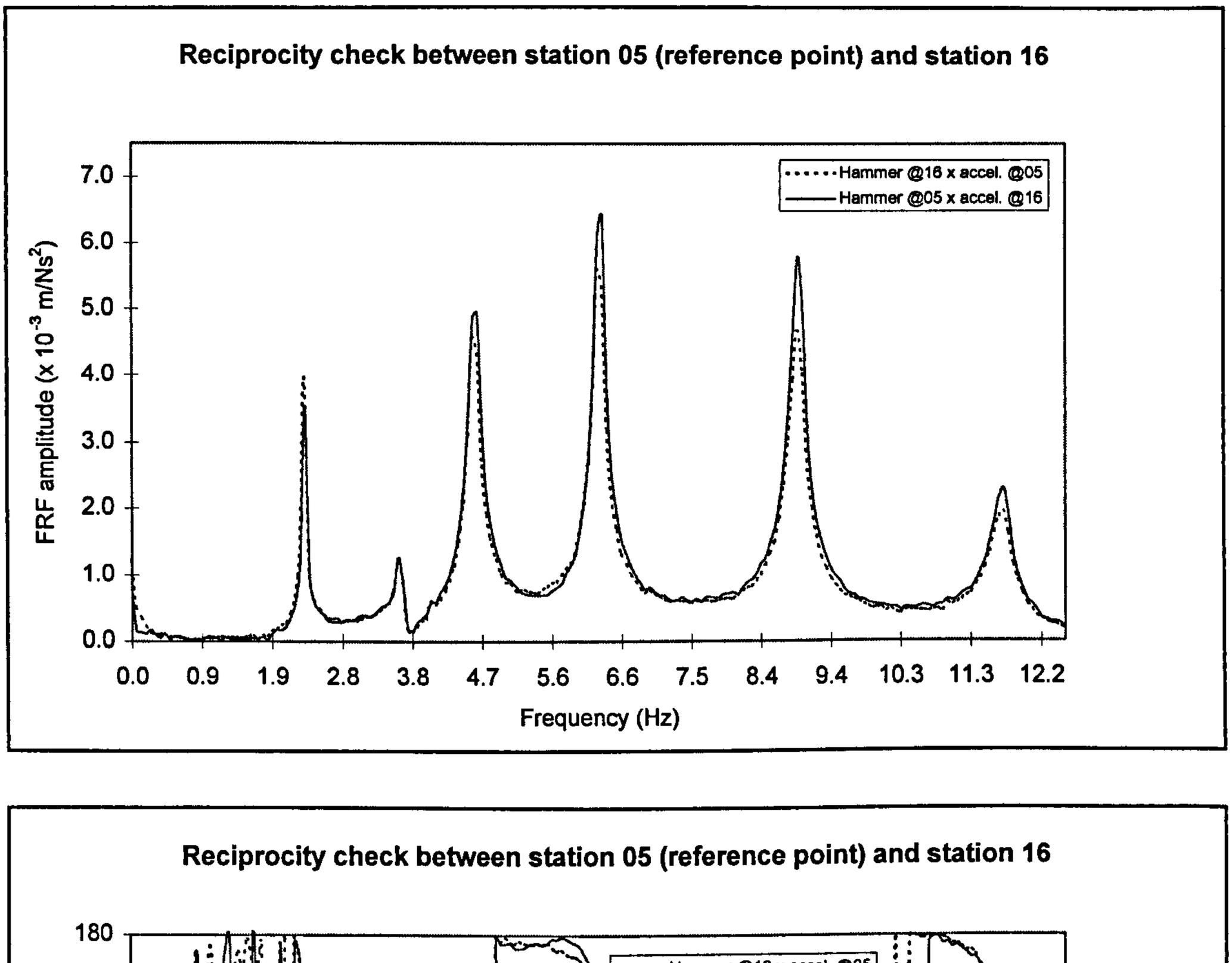

Figure 4.9 - Reciprocity check: amplitude and phase

Three parameters were initially considered as variables for the correlation with the experimental results: the Young's modulus of elasticity of the concrete; the elastic rotational stiffness of the deck at the abutments; and the unknown thickness of the hollow box components of the steel handrails. With regard to this last variable, a sensitivity analysis was carried out varying such a thickness within the commercial range of thicknesses for steel hollow box sections. This showed negligible changes in the mode shapes and small changes in the quotients of the natural frequencies. Similar small differences were found when varying the Young's modulus of the concrete. Consequently, variation in the Young's modulus would cover the uncertainty regarding the handrail thickness and a reference value of 4 mm was adopted for subsequent analyses. The other two remaining variables were adjusted for a good correlation to be obtained between the calculated and measured results.

The natural frequencies from both sets were compared and agreement of the mode shapes (Fig. 4.10) was evaluated by both the modal assurance criterion (MAC) and the coordinate modal assurance criterion (COMAC). The final values adopted were 42.5 GPa for the Young's modulus of the concrete (E_c) and $2.0*10^8$ Nm/rad for the elastic constant of rotation, which provided very good agreement between both measured and calculated natural frequencies and mode shapes (Table 4.7 and Fig. 4.11). Such a value for the Young's modulus is probably not the actual value due to the uncertainty in establishing the thickness of the handrails. However, this value is comparable with the results of similar research on concrete floors (Pavic *et al.*, 1995).

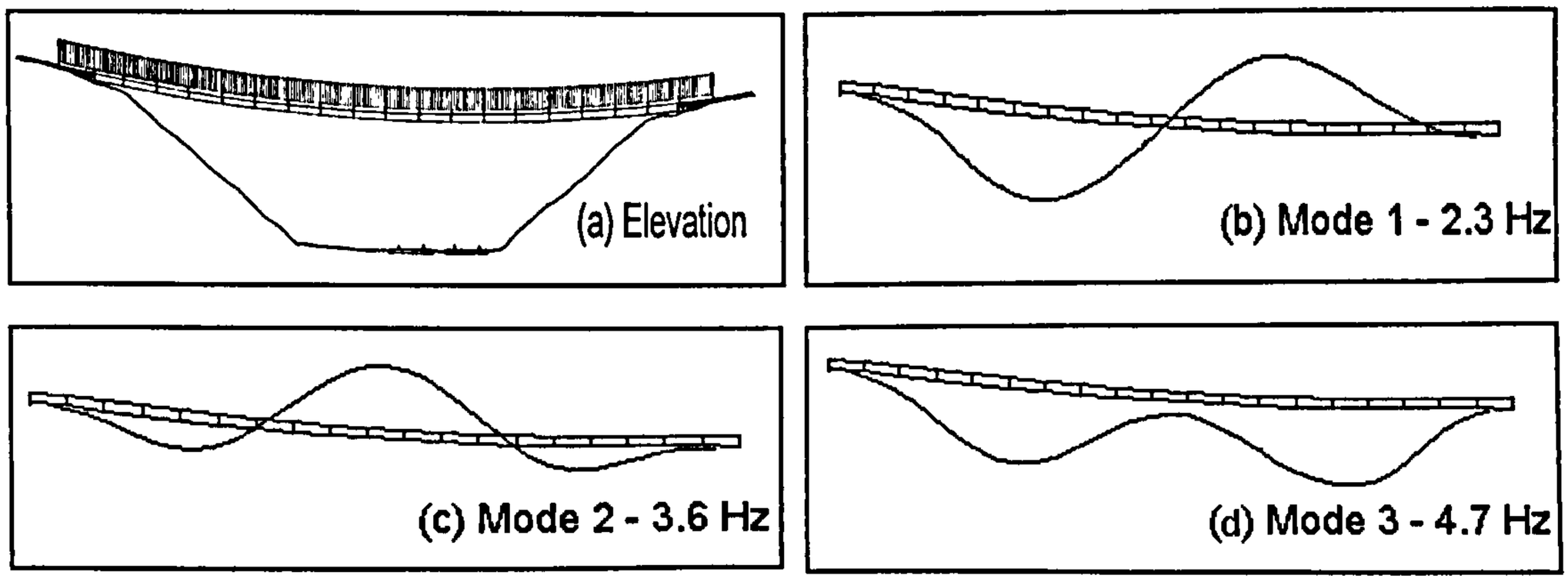

Figure 4.10 - First calculated mode shapes

Natural Frequencies (Hz)		MAC (%)
Calculated	Measured	
2.3	2.3	99
3.6	3.6	95
4.7	4.6	95
6.2	6.3	96
8.8	8.9	97
11.9	11.7	95

Table 4.7 - Natural frequencies and mode shape correlation

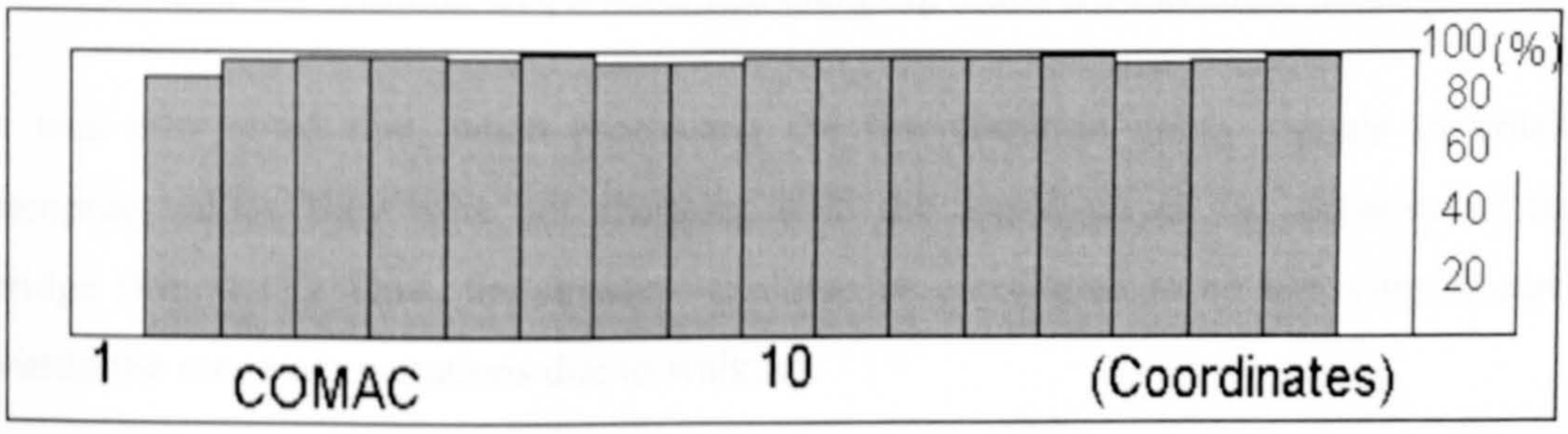

Figure 4.11 - Mode shape correlation (COMAC)

Equivalent viscous damping ratios for the lower modes were evaluated from the filtered free-vibration decay response of pedestrian tests using the logarithmic decrement technique (see Section 3.3.3). The evaluation was carried out considering the presence of the test subject standing on the bridge (after the jumping tests) and after the test subject left the bridge (following the walking tests). The difference in the results followed a similar pattern of the results described in the previous test footbridge. The damping values and also the natural frequencies of the structure evaluated with and without the presence of a test subject standing on it are presented in Table 4.8. In the former, the results from hammer tests and the average results from free-decay of jumping tests are presented. In the latter, the average results from the free-decay following walking tests and those from ambient excitation tests using the same data acquisition parameters and 20 averages are shown.

It can be noticed from Table 4.8 that the changes in damping values due to the presence of the test subject are generally more significant than the changes in natural frequencies. On the other hand, the agreement between the figures for natural frequencies in each group is evident. This shows that the natural frequencies of the structure obtained from different excitation levels are in close agreement with each other.

Bridge + Test Subject			Bridge (only)		
Natural Frequency		Damping Ratio (after jumping)	Natural Frequency		Damping Ratio (following walking)
Hammer	After Jumping		Ambient Excitation	Following Walking	
2.29 Hz	2.31 Hz	0.65 %	2.38 Hz	2.35 Hz	0.56 %
3.58 Hz	3.53 Hz	1.02 %	3.63 Hz	3.60 Hz	0.64 %
4.56 Hz	4.62 Hz	0.64 %	4.81 Hz	4.70 Hz	0.68 %

Table 4.8 - Natural frequencies and damping ratios (two decimal places)

It was also noted that, when processing the free-vibration decay signals to obtain damping values, they were not changing with the amplitude of the vibration of the bridge (Fig. 4.12). Thus, the structure can also be considered to be behaving linearly within the range of excitations due to walking.

The pedestrians tests, for the purpose of assessing the vibration serviceability of the test structure, were carried out using several test subjects of different weights. The tests were conducted following the procedures discussed in Section 4.2, and the pedestrians, one at a time, were walking with a pacing rate of 2.37 Hz. The measurements of acceleration were recorded at an antinode of the first mode shape and were filtered to contain only the contribution of this mode. A few additional tests were also conducted with pedestrians walking at a pacing rate of 1.8 Hz, approximately half of the second natural frequency of the structure. In this case, the accelerations were measured at the central point of the span and filtered to contain only the contribution of the second mode.

The average measured peak accelerations are presented in Table 4.9, together with the limits of the UK code (BS5400, 1978) for each frequency of vibration respectively. The average peak acceleration for the fundamental mode is marginally above the code limit.

Natural Frequency Excited (Hz)	Average Peak Acceleration (m/s^2)	Code Limit (BS5400, 1978)
Mode 1 - 2.3 Hz	0.84	0.76
Mode 2 - 3.6 Hz	0.27	0.95

Table 4.9 - Measured peak accelerations in controlled pedestrian tests

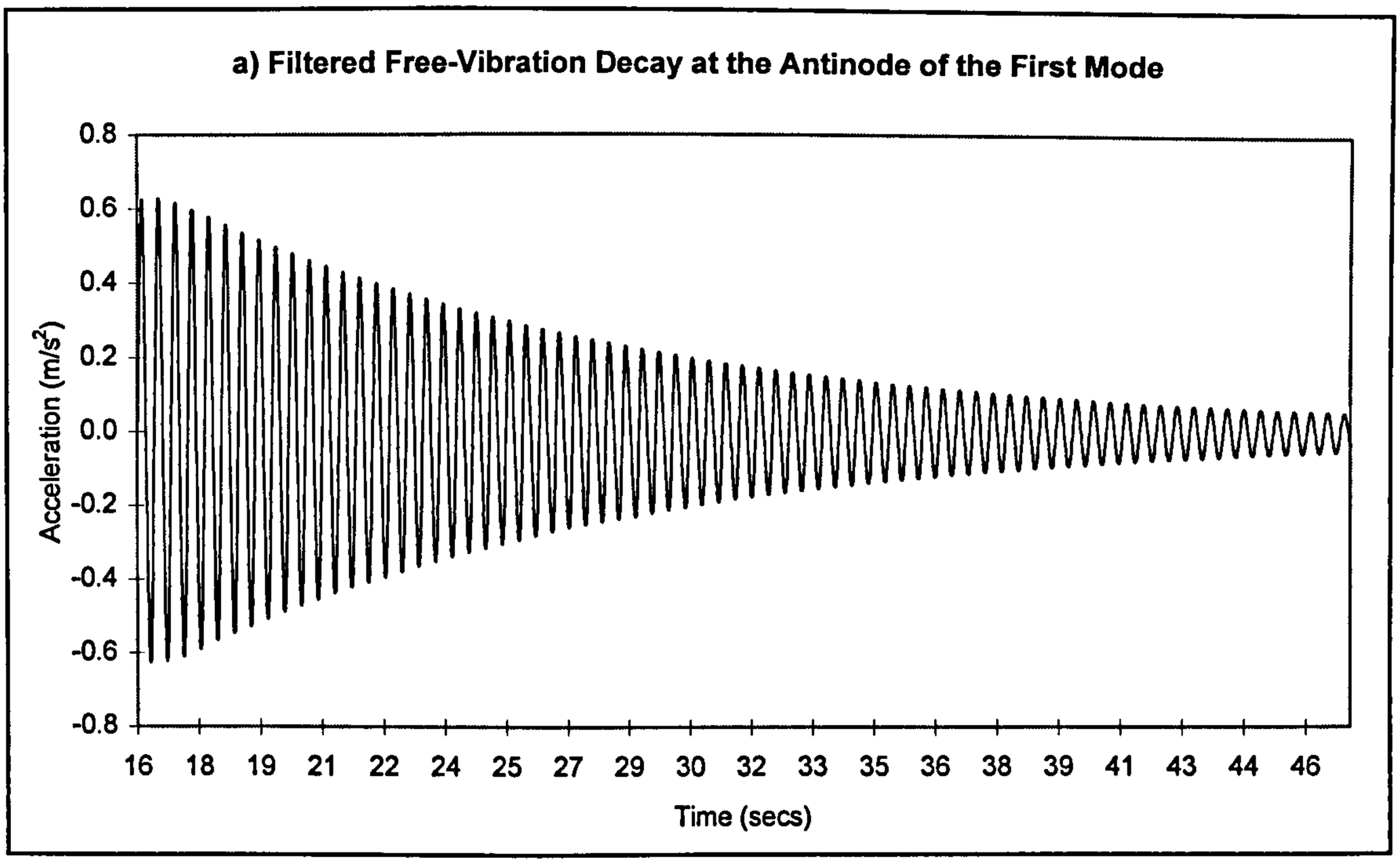

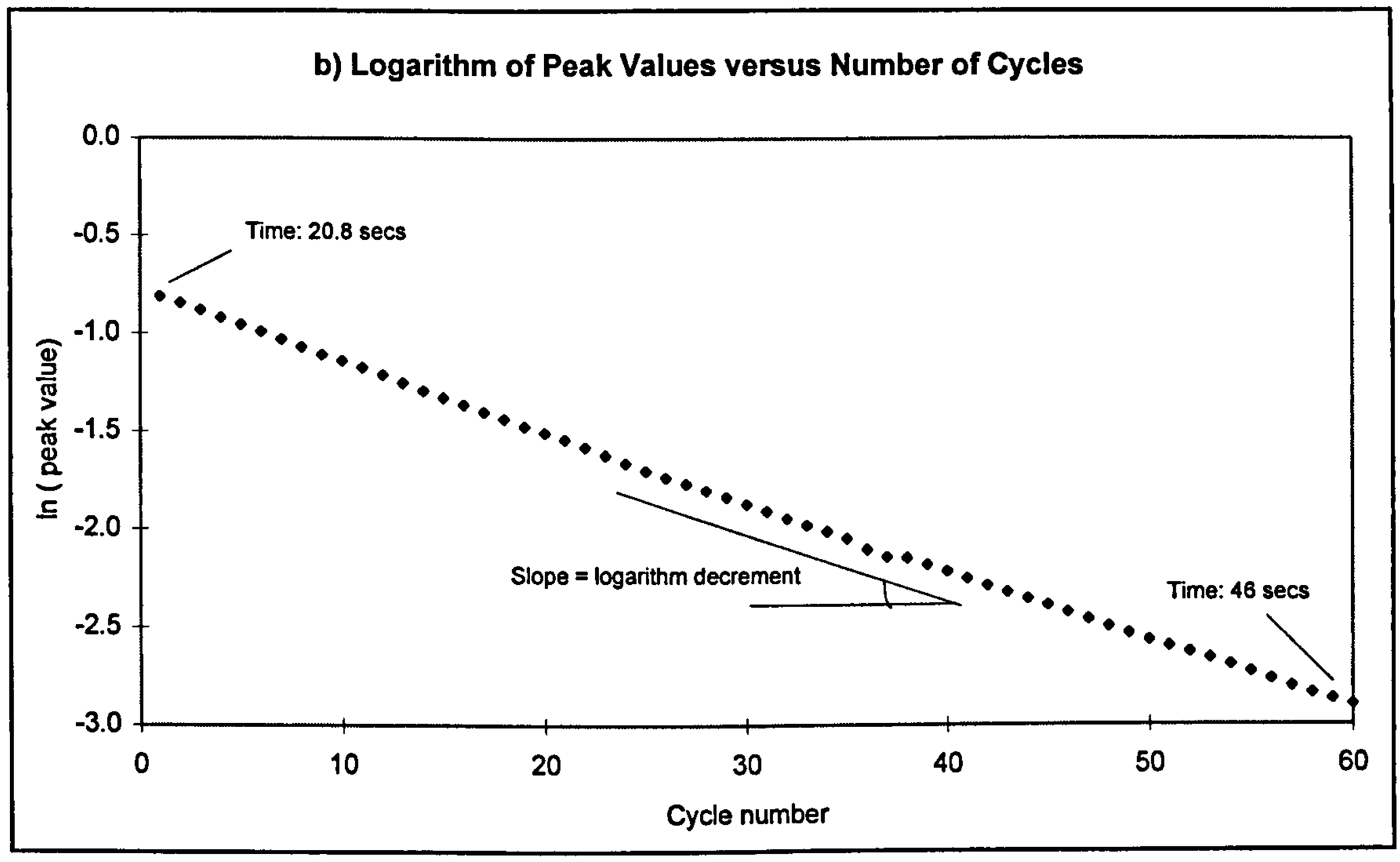

Figure 4.12 - Evaluation of damping from the free-vibration decay of walking tests

4.4.1 Analysis of Vibration Performance

The level of peak accelerations measured in controlled pedestrian tests may be considered acceptable when compared to the code limits. In support of this comment, it

should be remembered that the fundamental mode of vibration of the structure is almost antisymmetric, presenting a node at mid-span. This prevents the pedestrian-induced vibrations building up continuously during the crossing, reducing the time to which the pedestrian would be exposed to high accelerations.

The absence of a first symmetric mode shape is attributed to the catenary shape of the structure, which creates a membrane action similar in effect to the arch action observed in the composite footbridge, although remarkably more pronounced in this case. The combination of bending and catenary effects produced vibrations with mode shapes far different from those normally associated with a simply supported beam.

The handrails also had a more significant influence on the vibration characteristics of the structure. Their hollow cross section components had the following external dimensions: 101.6x50.8 mm for the top rail, and 88.9x38.1 mm for the bottom rail and post. Twelve solid steel infill bars were present per panel, having individual dimensions of 25x12.7 mm. Since the handrails followed the catenary shape of the deck and were firmly attached to it, it would be expected that they would contribute to increasing both bending and axial stiffness of the structure.

Indeed, an initial attempt was made in modelling the structure including the handrails simply as an added mass. The dimensions of the handrails were taken for calculations, together with the density of the steel of 7850 kg/m^3, resulting in a mass of 63.71 kg per handrail per panel, each panel being 1.95 m long. However, a high value of 55 GPa for the Young's modulus of the concrete and a barely reasonable correlation for some of the modes was obtained. The calculated natural frequencies obtained for this model are shown in Table 4.10, together with the calculated values modelling the handrails as an attached continuous frame. The measured natural frequencies are also shown for reference. The improvement obtained by modelling the handrails more precisely is evident.

In order to investigate in more detail the role of the axial effects on the modal properties, a FE model of the footbridge was prepared as if it was rectilinear. This resulted in a complete change of the modes of vibration, which were now similar to

those of a straight beam, as expected. The first mode presented a natural frequency of 0.9 Hz and was symmetric, as opposed to the first antisymmetric mode of 2.3 Hz measured on the actual footbridge. The difference in value between these fundamental frequencies shows the effectiveness of the catenary shape, for a given cross section, in increasing the stiffness of the structural system and therefore the natural frequencies.

Natural Frequencies (Hz)		
Calculated		Measured
Initial model: handrails modelled as added mass (E_c = 55 GPa)	Current model: handrails modelled as a frame (E_c = 42.5 GPa)	
2.1	2.3	2.3
3.6	3.6	3.6
5.0	4.7	4.6
6.4	6.2	6.3
9.2	8.8	8.9
12.6	11.9	11.7

Table 4.10 - Natural frequencies from different FE models

Natural frequencies from catenary shaped models (Hz)		Natural Frequencies from rectilinear models (Hz)	
Handrails modelled as added mass	Handrails modelled as a frame	Handrails modelled as added mass	Handrails modelled as a frame
1.9	2.3	0.7	0.9
3.2	3.6	1.9	2.2
4.5	4.7	3.6	4.0
5.7	6.2	5.7	6.2
8.2	8.8	8.2	8.8
11.2	11.9	11.2	11.9

Table 4.11 - Influences of the catenary shape and handrails

The natural frequencies for the rectilinear and current numerical models are presented in Table 4.11, together with results obtained for the analyses in which the handrails were modelled as added masses. For clarity of comparison, the elastic modulus of the concrete of 42.5 GPa was kept constant for all the numerical models. These results show that:

- The effect of the catenary shape is only present on the first three vibration modes; the latter three modes are pure bending modes.

- Modelling of the handrails as an attached frame contributed to increases at about 20% in the fundamental mode in both rectilinear and catenary models.

4.5 Modal Testing of a Glass Reinforced Plastic Footbridge

Among the new generation of ACM structures, the Aberfeldy glass reinforced plastic (GRP) cable-stayed footbridge was reported to have the largest span length in the world at the time it was built (Lee, 1993). It is a three-span structure, having a main span of 63 m and two side spans of approximately 25 m each. The towers were designed as A-frames and a total of forty aramid cables, twenty per tower, connected the towers to the 2.12 m wide deck (Plate 4.3). The innovative design received an award from the British Construction Industry (1993) and considerable international acclaim.

Plate 4.3 - Aberfeldy GRP cable-stayed footbridge

Details about the design, construction, materials and other properties of the structural components were presented by Lee (1993) and Harvey (1993). However, some points are worth mentioning since they will have an important bearing on the dynamic behaviour of the structure:

- The deck was built by joining three GRP planks by means of connectors and resin bonding. Each plank had external dimensions of 600 mm x 80 mm and was of cellular cross section. The plank is just one unit of a system called the Advanced Composite Construction System (ACCS) (Lee, 1993), and the main structural components were assembled by the association of units of ACCS. The cross section of the deck is variable and is shown in Fig. 4.13. Ballast material was used to fill some of the cells at the main span in order to prevent deck uplifting due to wind action. The attached handrails also shown in Fig. 4.13 were made of GRP; however, they were not conceived as having a structural function. To complete the deck, edge beams made by bonding altogether a variable number of box sections, and cross beams fully bonded along the width of the deck and spaced at 1.0 m centres, were provided. These cross beams were of a more robust cross section at the points at which they provided connection between the deck and cables. The deck surfacing was provided by thick conveyor belting, which was also beneficial in increasing the self weight of the structure.

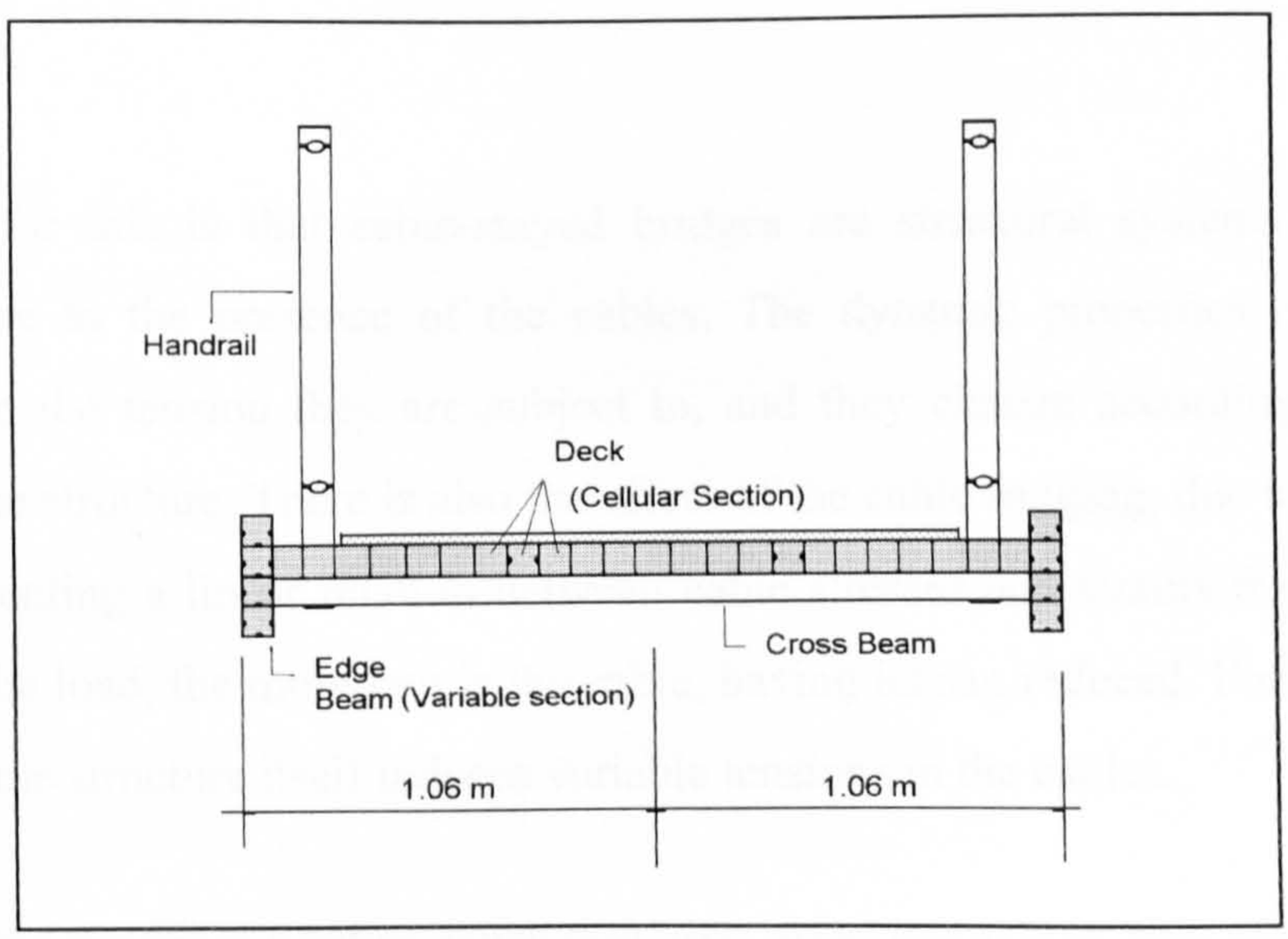

Figure 4.13 - Typical cross section of the deck

- The connections between the deck and towers in both the vertical and lateral directions and also at the abutments were made using friction bearings.

- Aluminium struts were provided on the side spans and also acted as tie-downs to each back-stay cable. This was reported to be necessary due to the high live/dead load ratio which could induce uplifting of the side spans.

The assessment of the dynamic performance of the footbridge involved six continuous days of testing in July 1994, and another five days in June 1995 under the same ambient conditions. The tests comprised a full modal survey for the determination of the modal properties of the structure, using ambient excitation, impulse response and free-vibration decay techniques. An investigation of the behaviour of the bridge under pedestrian-induced loads was also conducted.

Modal Survey

The challenge in conducting a modal survey of cable structures with the aim of calibrating a numerical model for the analysis of vibration performance goes beyond the complexity of the structural configuration and the presence of several structural connections of unknown properties. Indeed, there is the question of whether the assumption of linear behaviour of the structure is valid, which is necessary to carry out a modal survey.

The reason for this is that cable-stayed bridges are structural systems intrinsically nonlinear, due to the presence of the cables. The dynamic properties of cables are dependent on the tension they are subject to, and they change according to the load applied on the structure. There is also the effect of the cable sagging, due to its own self weight, preventing a linear relation between cable stresses and strains from occurring. The higher the load, the more taut is the cable, having its sag reduced. Furthermore, the vibration of the structure itself induces variable tensions in the cables.

Apart from the potential nonlinearities that arise from the cables, two other sources of nonlinearities have been identified (Gimsing, 1983; Troitsky, 1988):

- The effects of large displacements or geometric nonlinear effects: These account for changes in the geometry of the deformed structure, causing a redistribution of stresses. In particular, changes in the inclination of the cables will lead to a change of vertical and axial forces in deck and towers, which cannot be determined by linear analysis.

- Interaction between bending and axial effects: This occurs in both the deck and towers, the degree of nonlinearity due to this effect depending on the intensity of the compressive loads compared with the buckling load and on the magnitude of the deflections caused by bending action.

However, as was pointed out by Khan (1994), the extent of the nonlinear effects and their influence on the response of a given cable-stayed bridge needs to be evaluated before further attention is given to this subject since such effects might be negligible. Yiu and Brotton (1987) cited that, in relatively short span or stiff cable-stayed bridges, when deflections are relatively small and second order effects are negligible, a linear elastic analysis would produce a good approximation. This was the case in the works of Wilson and Gravelle (1991) and Vlahinos and Wang (1994). The former did not consider nonlinear effects in modelling a cable-stayed bridge and obtained a good correlation between a numerical model and the test results. The latter carried out further investigations on the same bridge and showed that the inclusion of nonlinear effects produced negligible changes in the natural frequencies and mode shapes. In another case study in which the dynamics of a cable-stayed bridge were investigated, a linear dynamic analysis using a tangent stiffness matrix obtained from a prior nonlinear static analysis under dead load was shown to be adequate (Fleming and Egeseli, 1980).

For carrying out modal tests and subsequent modal analysis, it is necessary to assume that the structure behaves linearly and seek the best linear approximation, or to abandon the approach altogether. However, as will be seen from the test results and corresponding numerical analysis, the nonlinear effects were not of significance in the case of the test footbridge in terms of analysis of vibration performance.

The ambient vibration survey (AVS) was the major technique adopted for obtaining the modal properties of the structure. The impulse response technique was also employed but the quality of the results was inferior to those obtained when applying this technique to testing the previous footbridges. A number of factors can be identified which contributed to the difficulties in obtaining good quality results while using this latter technique:

- The wind action, which produced more significant effects in terms of vibration than in the previous test footbridges. In order to eliminate this effect, a high number of averages, or hammer blows applied to each test point, was necessary. Use of ten averages as adopted in the tests of the stressed ribbon footbridge was found to be insufficient, and a higher number of averages would have prolonged the testing time. Attempts to reduce the influence of the wind by using a high decay coefficient for the exponential window did not produce the desired effect. The use of a decay coefficient of 10/16, as adopted in one of the previous tests, had already resulted in the overdamping of the first modes of vibration, which could hardly be detected in several test points.

- Part of the energy of the impact seemed to be absorbed locally through deformation of the cells of the GRP plank that was hit. This would contribute to a reduction in the amount of energy that was available to set the structure vibrating. On the other hand, trials made on a spare GRP plank showed that strong hits should be avoided since they could induce damage to the plank. These two factors combined were of little help in increasing the participation of the applied excitation on the response.

It has not been stated that hammer tests would definitely fail as a testing technique for this structure. A high number of averages and a lower decay coefficient for the exponential window could result, in the end, in good quality data. Nevertheless, the very good quality data obtained on initial attempts using ambient excitation discouraged pursuit of the use of hammer tests. The degree of separation between the resonance peaks on the response spectra made it possible to consider the modes as isolated, and phase angles very close to either 0 or 180 degrees in the region of the peaks confirmed the modes as real modes. These two pieces of experimental evidence assured the

validity of the hypotheses on which the AVS is based (see Sections 3.3.1 and 3.3.1.1). However, the FRFs obtained using the hammer tests could be employed to confirm the natural frequencies identified by ambient excitation.

The tests began by identifying the directions in which the structure would potentially present vibration problems caused by human-induced loads. Attempts to excite the structure revealed that potential vibration problems could arise in both the vertical and lateral directions. The structure seemed not to present problems in terms of torsional vibration. Therefore, effort was concentrated on obtaining the modal properties of the structure in the two former directions, and only a few additional measurements were carried out to establish the torsional natural frequencies.

The complexity of the structural system demanded a large number of test points to be selected, involving measurements on all structural components. Forty-five points were marked along the longitudinal axis of the footbridge, on the centreline of the deck. These points were selected to coincide with the nodes of a numerical model being developed. The test points were almost equally spaced, being located at each connection between deck and cables, and at the middle point between consecutive connections. Additional points, one on each cable and two on each tower, one of these at the tower top, resulted in a total of 89 test points. Throughout the tests, the footbridge was closed to pedestrian traffic.

The search for a reference station from which the modes of interest could be identified resulted in two distinct reference stations, one for the measurements in the vertical direction about one quarter along the main span, and the other for the measurements in the lateral direction about one third along the main span. The parameters adopted for data acquisition were an acquisition time of 16 secs and 2048 data samples, which are related to a frequency range of 50 Hz and a frequency resolution of 0.0625 Hz. It should be noted that the longer the acquisition time the better is the frequency resolution, although this would result in an increase in the testing time. The value of 16 secs was selected as a compromise between the two opposite requirements of higher frequency resolution and limited testing time. A detailed description of the measurements and results obtained for the various structural components follows:

(i) Measurement of the natural frequencies and mode shapes of the deck and towers in the vertical and longitudinal directions respectively

Vertical movements of the deck are coupled with the longitudinal displacements of the towers. The PSD of the reference station was taken to estimate the natural frequencies, and the curve-fitting procedure described in Section 3.3.1.1 was employed to improve the estimation of the lower modes. The determination of the mode shapes followed the procedure described in Sections 3.3.1.1 and 3.3.1.2, for which 10 and 20 averages at points on the main span and side spans, respectively, were adopted for determining each coordinate of the mode shape envelope. A plot of the Amplitude Spectrum of the reference point, the one at the mid-span and the respective Coherence plot between these test points are shown in Fig 4.14. Another plot of the Amplitude Spectrum of the reference point and of the point at the top of one of the towers, together with the respective phase plot, the latter evaluated from the Cross Spectrum between these two points, are shown in Fig. 4.15.

Figs. 4.14 and 4.15 illustrate some features of the dynamic behaviour of the footbridge and quality of the acquired data. The Amplitude Spectrum of the reference point in Fig. 4.14 or Fig. 4.15 shows nine resonance peaks identified as natural frequencies of the structure. The first vertical natural frequency of 1.59 Hz was identified being related to a symmetric mode shape. Correlation with numerical results showed that all first nine natural frequencies were identified as peaks in the aforementioned plots. On the other hand, the coherence plot shows values close to 1.0 in the region of the resonance peaks, this being an indication of the good quality of the acquired data.

Fig. 4.15 shows that the towers participate in lower vertical modes; however, their participation in the higher modes are negligible. A further measurement taken on the tower leg, at an intermediate point between the connection with the deck and the top, made it possible to conclude that the respective tower mode was of a cantilever type. The phase plot in Fig. 4.15 shows that the two test points referred in the Figure are vibrating in phase for at least all natural frequencies below 4.0 Hz (phase difference close to 0°).

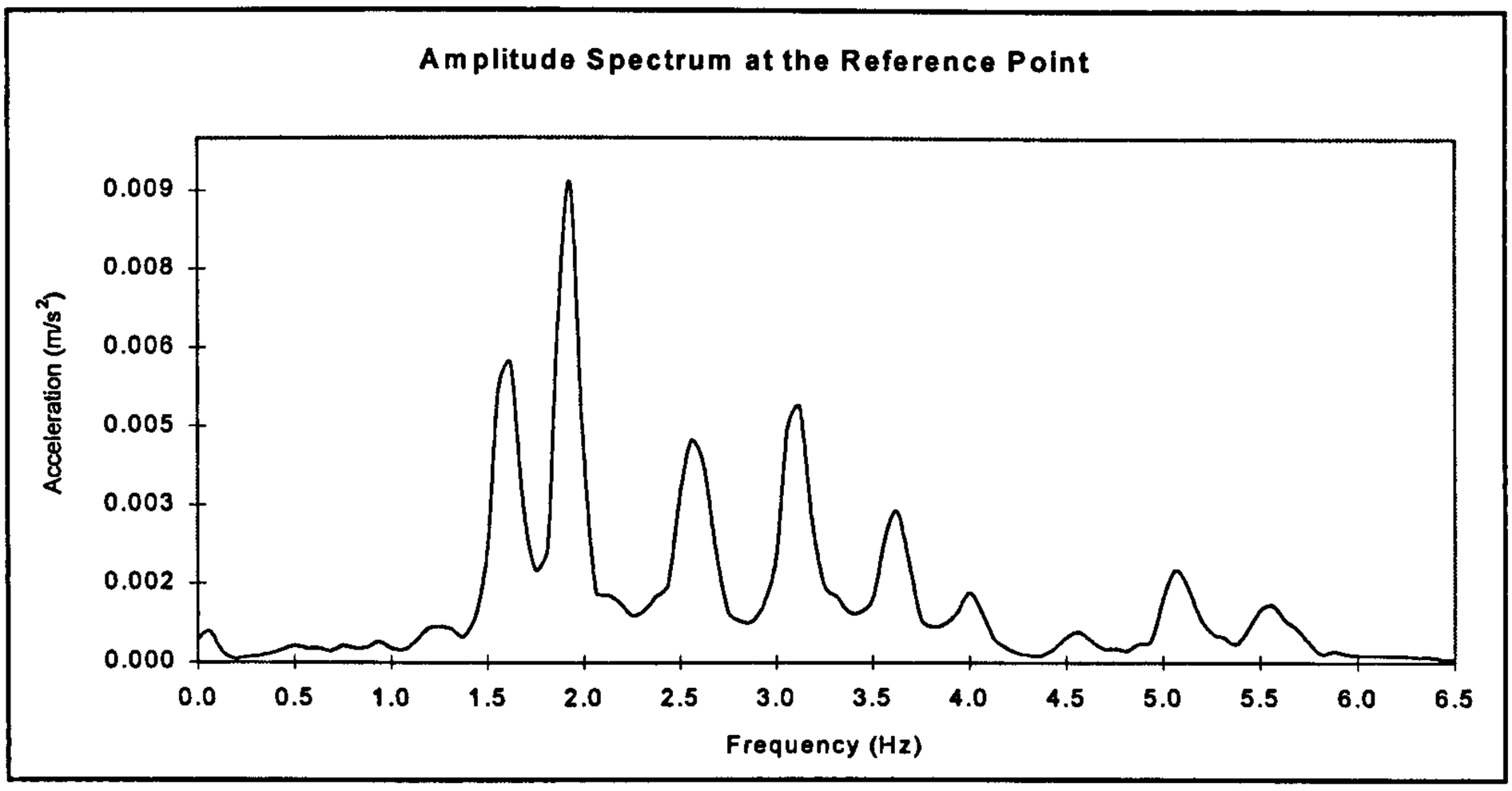

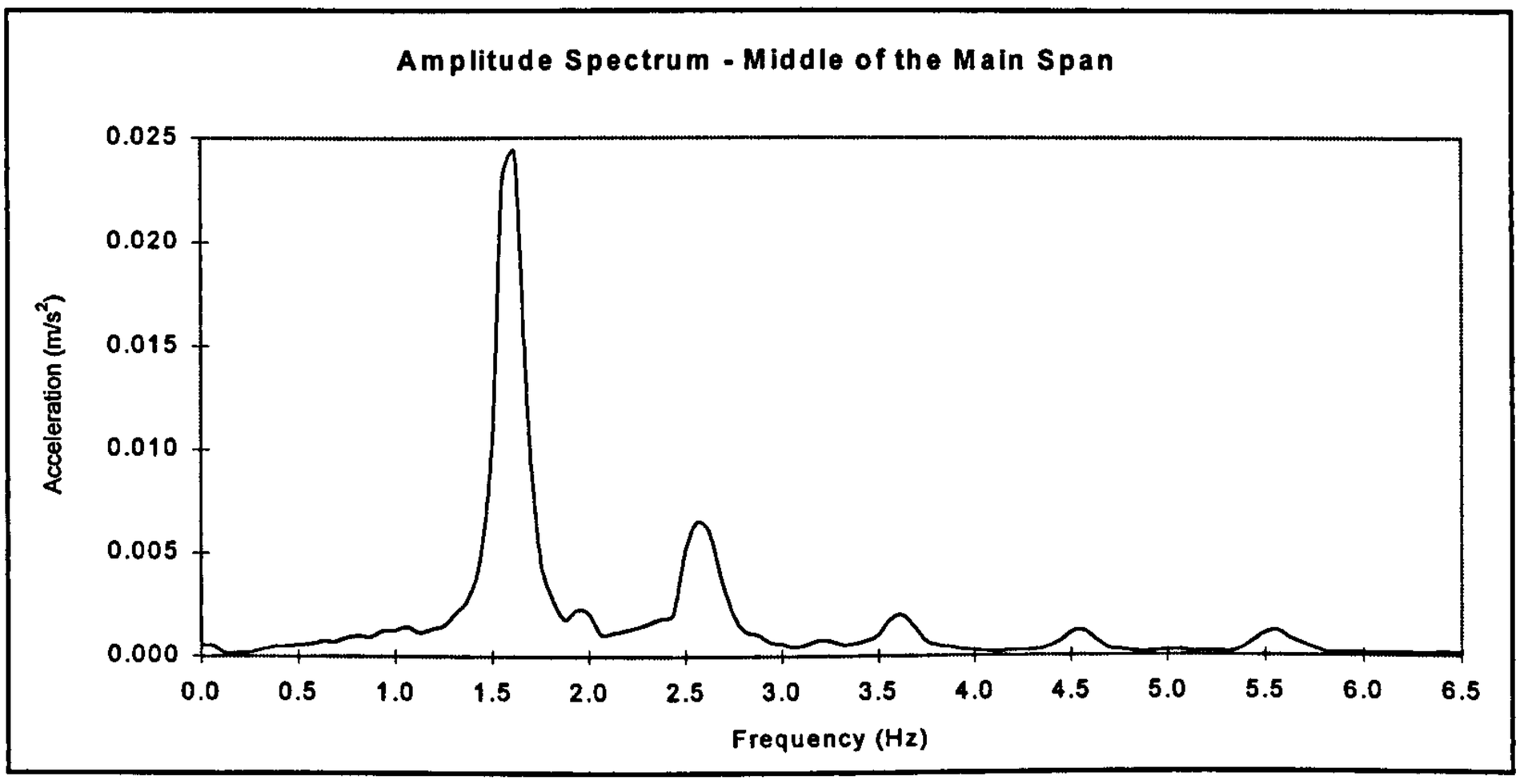

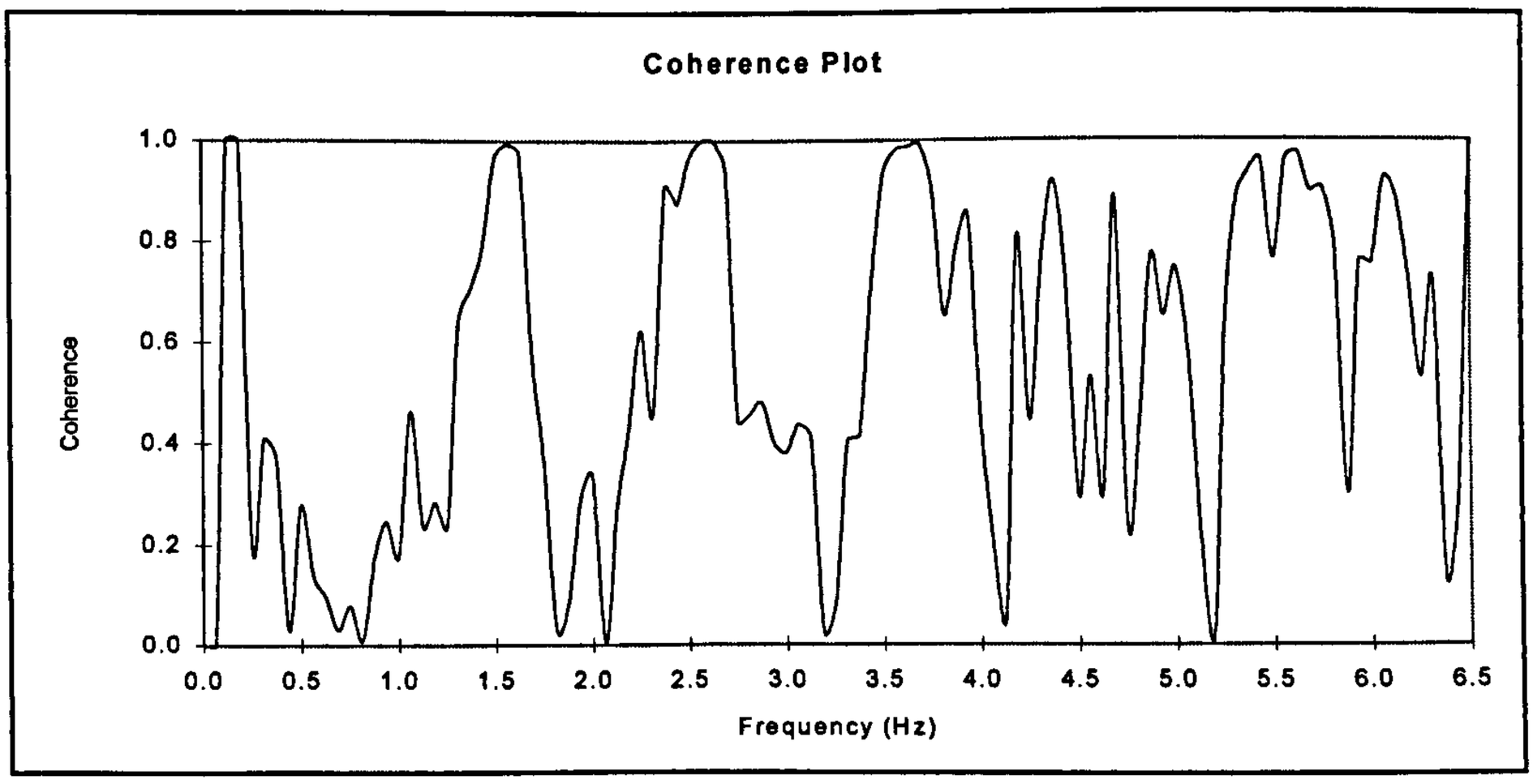

Figure 4.14 - Amplitude Spectra and Coherence between two points on the deck

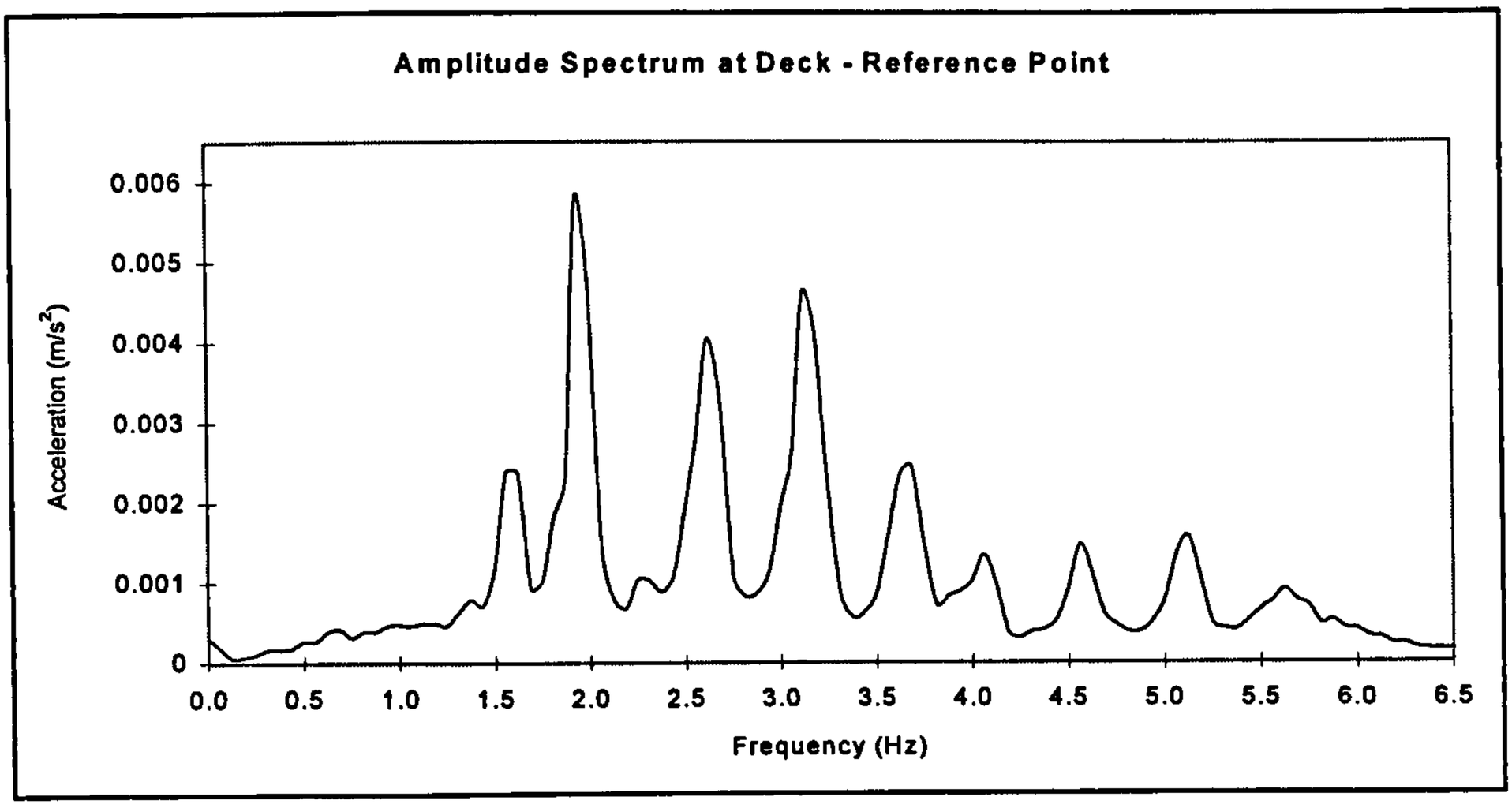

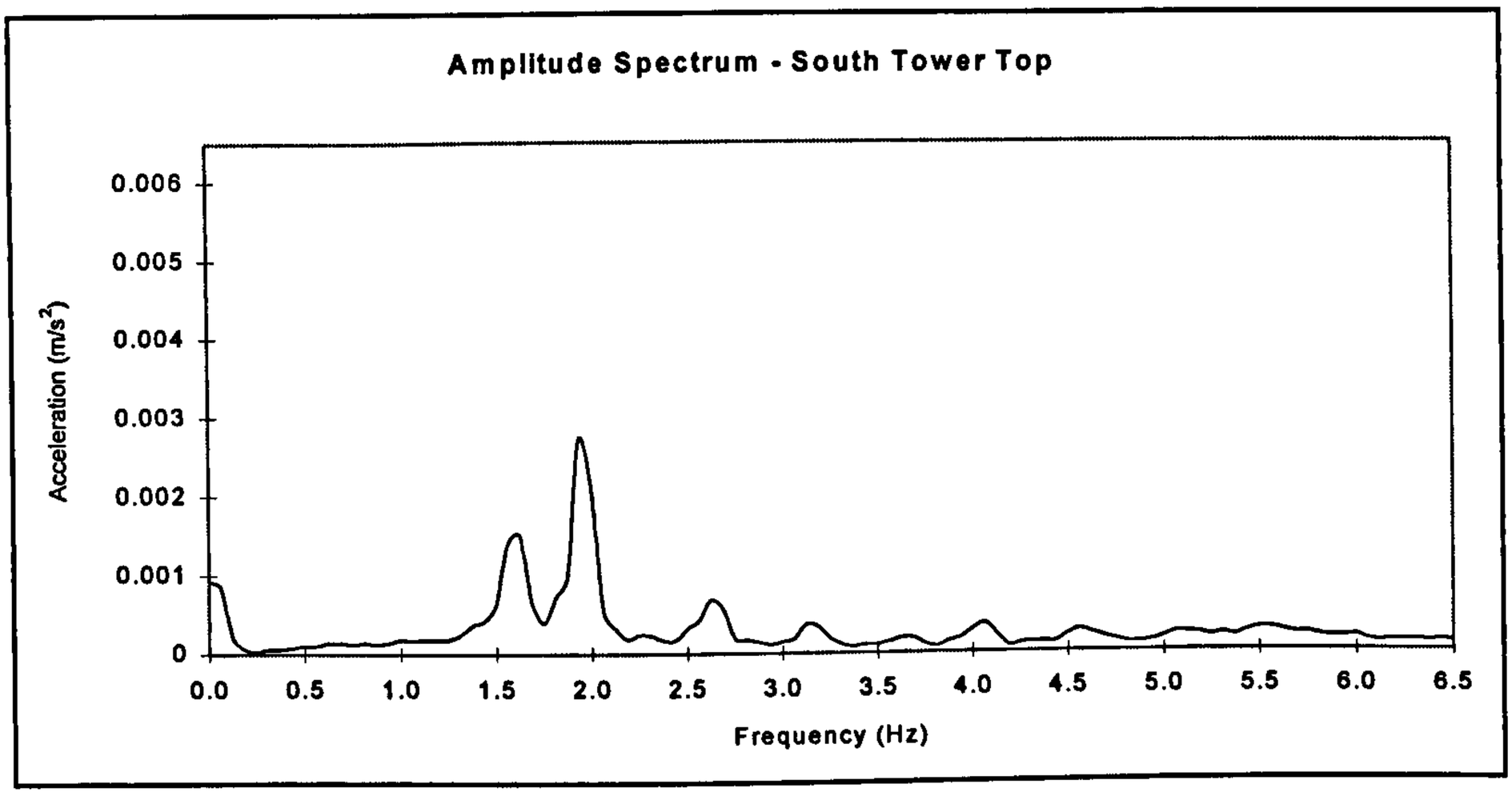

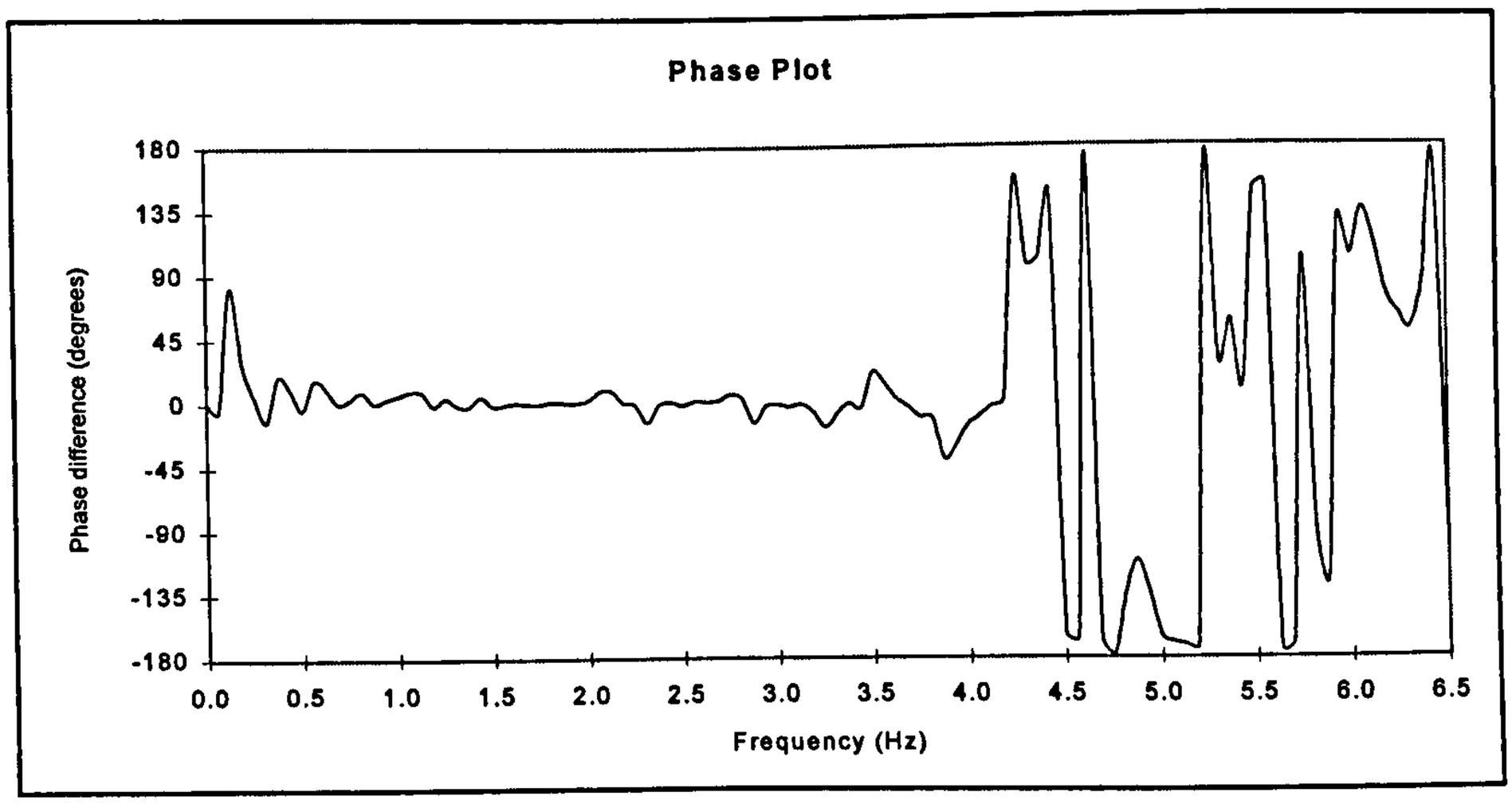

Figure 4.15 - Amplitude Spectra at the deck and tower and the respective phase plot

The first nine vertical natural frequencies identified are presented in Table 4.12. The determination of the mode shapes followed the procedure described in Section 3.3.1.1 and the first mode shapes are plotted in Fig. 4.16. It can be seen from these plots that the side spans essentially provided fixed supports for the main span at the towers. A slight asymmetry may also be observed comparing the mode shapes in the region of the towers, in which small displacements can be observed on the side span of the right hand side. Inspection carried out on site showed that some of the connections with the aluminium struts on that side were slack, enabling these struts to experience vertical displacements to some small extent.

Natural Frequency (Hz)	Mode	Direction
1.00	L1	lateral
1.59	V1	vertical
1.92	V2	vertical
2.59	V3	vertical
2.81	L2	lateral
3.14	V4	vertical
3.44	T1	torsional
3.63	V5	vertical
4.00	V6	vertical
4.31	T2	torsional
4.60	V7	vertical
5.10	V8	vertical
5.60	V9	vertical

Table 4.12 - Measured natural frequencies of the deck

(ii) Measurement of the lateral natural frequencies and mode shapes of the deck

These tests were conducted adopting the same array of points along the deck as the previous group of tests. The only differences were that the accelerometers were turned in the lateral direction and the reference station was changed. In addition, symmetry was assumed, in view of the negligible asymmetry presented in the vertical direction. The mode shapes were thus identified by taking measurements in only one half of the deck. The towers were expected to be much stiffer in the lateral direction due to their form, and no measurements were taken on them in this direction. Two natural frequencies were identified, the first being 1.0 Hz, which coincides with the typical value of the frequency of the lateral movement of a pedestrian while walking. These natural

frequencies are shown in Table 4.12 and the respective mode shapes are shown in Fig. 4.17. It can now be seen that the side spans present significant deflections in comparison with their behaviour in the vertical direction. This can be attributed to the design of the aluminium struts, which do not prevent movement of the deck in the lateral direction.

(iii) Measurement of the torsional natural frequencies of the deck

This was done placing two accelerometers either side of the centre line at the same cross section of the deck and obtaining the PSD and phase difference between the records. Two cross sections of the deck were chosen in order to measure natural frequencies related to both symmetric and antisymmetric modes. The peaks of the PSD that were out-of-phase corresponded to the torsional natural frequencies. The first torsional natural frequency of 3.44 Hz was found to be higher than several vertical and lateral natural frequencies, indicating that the footbridge is much stiffer in torsion than vertically or laterally (Table 4.12). The torsional mode shapes were not measured since the main focus of the dynamic assessment was the vibrations in the vertical and lateral directions.

(iv) Measurement of the natural frequency of the cables

An accelerometer was attached one at a time to each of the 40 cables of the footbridge. The cable was gently pulled and released, the acceleration time response was recorded and the Fourier amplitude spectrum calculated, from which the natural frequency of the cable was obtained. The reason for applying a gentle excitation was that this excitation already induced a high level of accelerations, close to the upper limit of the accelerometer (see Appendix A.1).

The Fourier spectrum revealed that the cables vibrated harmonically with a distinct fundamental frequency and harmonics at frequencies that were integral multiples of the fundamental, typical of vibration of strings (Humar, 1990) (Fig. 4.18). This provided evidence of the cables being taut, in agreement with site observations. Although being subject to a relatively small tension, since the constituent material of the bridge has a low weight, the constituent material of the cables is also of low weight. This contributes to the cables having a negligible sag, which has already been observed in other tests in cables of similar constituent material (Tuladhar *et al.*, 1996).

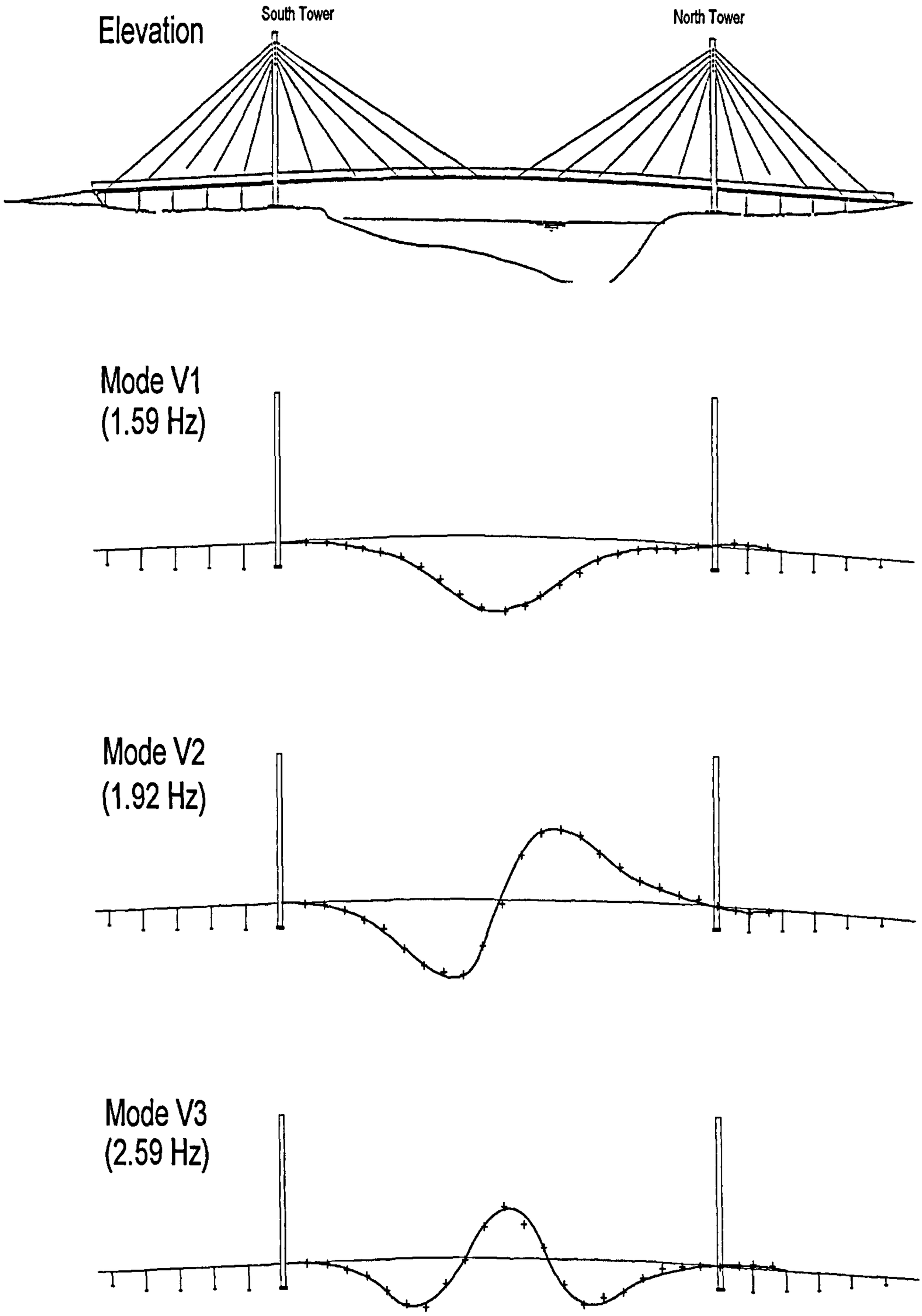

Figure 4.16 - First three measured mode shapes of the deck in the vertical direction

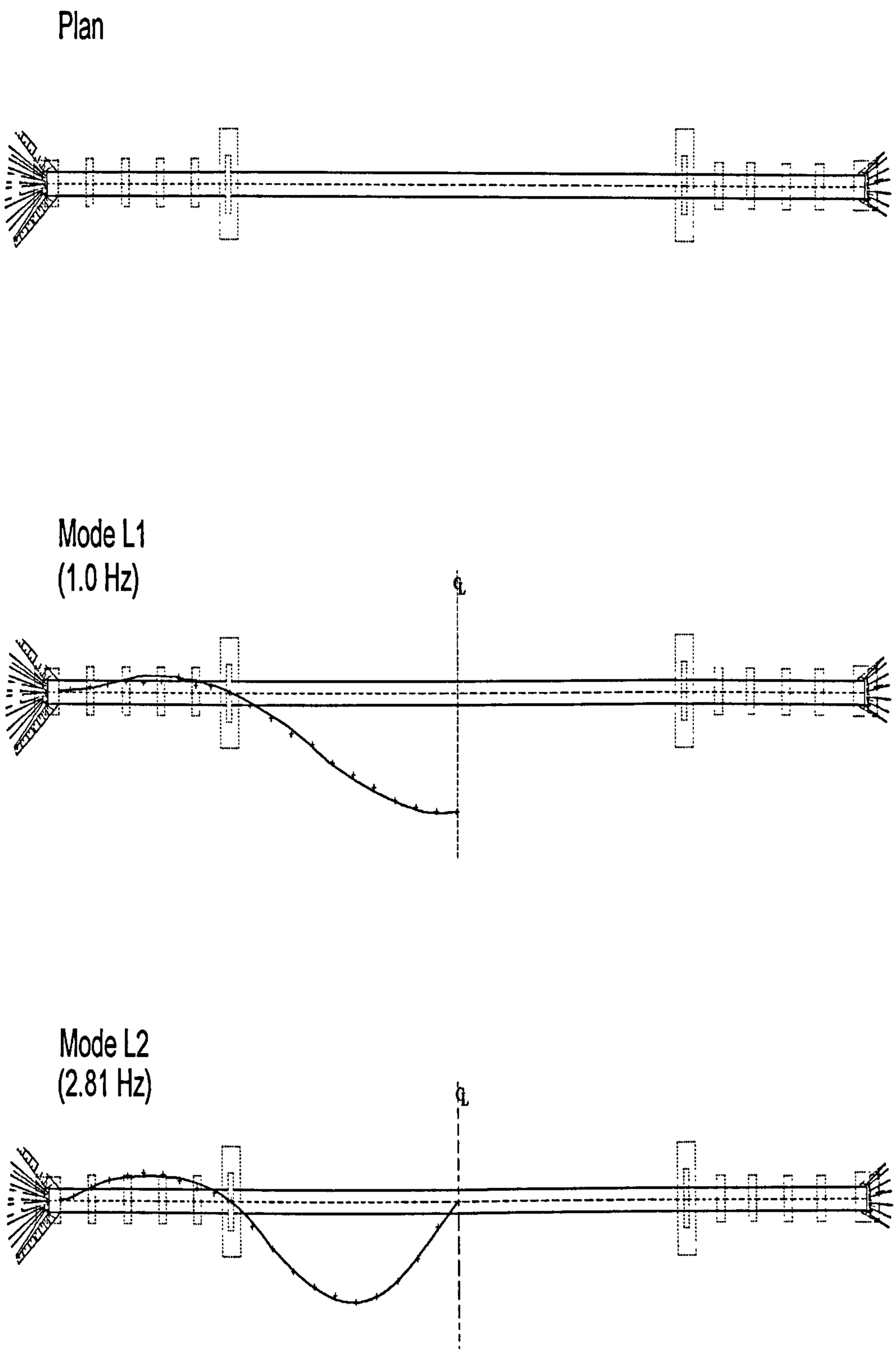

Figure 4.17 - First two measured mode shapes of the deck in the lateral direction

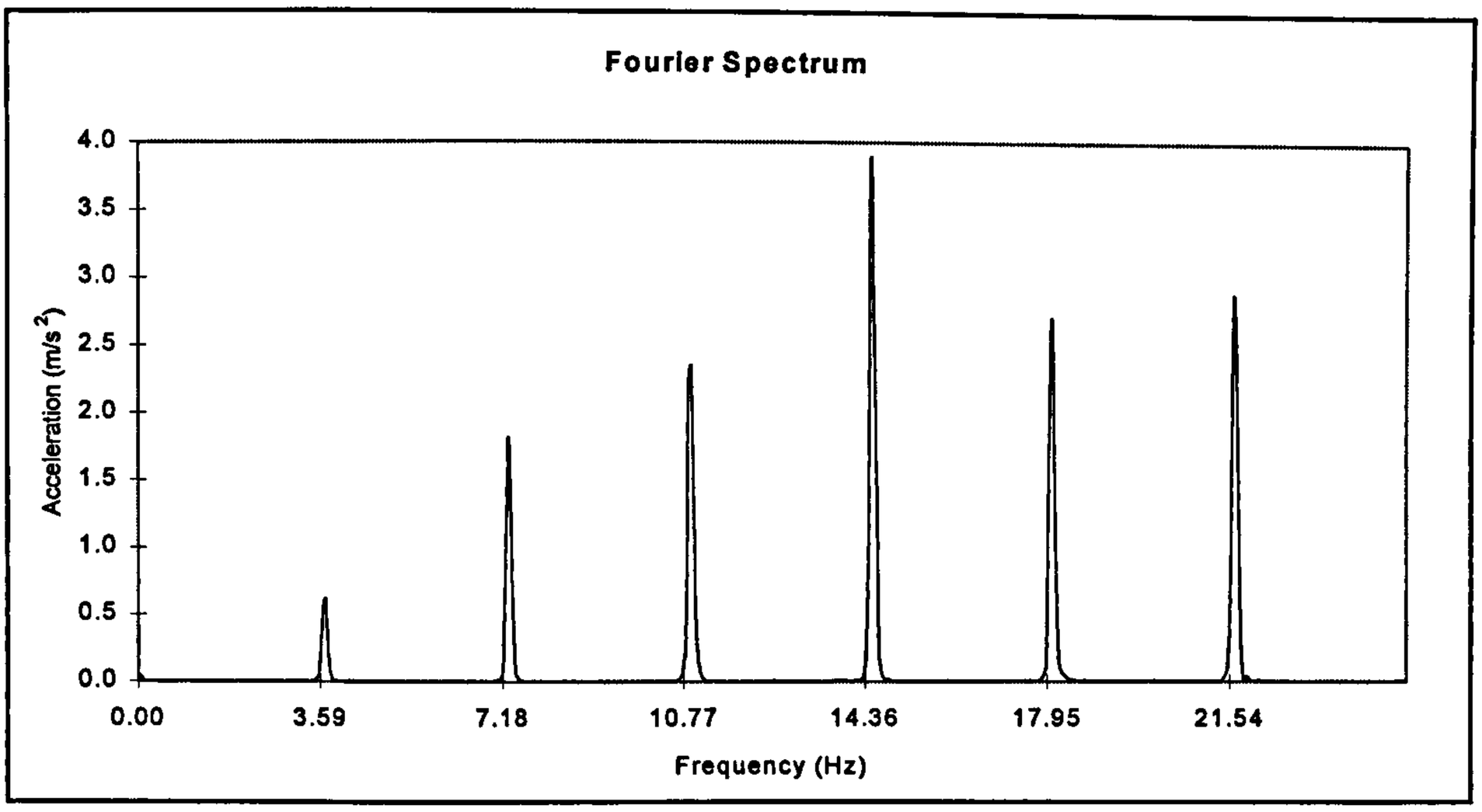

Figure 4.18 - Typical Fourier amplitude spectrum of a cable

For obtaining the fundamental frequency of each cable, the procedure adopted was to take an average of the difference between the frequencies of successive resonance peaks of the Fourier spectrum. This averaged value was usually very close to the frequency of the first peak. The tension in each cable was estimated using the string formula (Humar, 1990):

$$F_c = 4m_c f_{cab}^2 L_c^2 \tag{4.1}$$

were F_c is the cable tension, m_c and L_c its mass per unit length and length, respectively, and f_{cab} the estimated fundamental frequency of the cable. The fundamental frequencies and respective tensions for all cables are presented in Table 4.13, in which the notation for identifying the cables is in ascending numerical order starting from the south side of the bridge and using the identifiers L (left) and R (right) to identify the side of the deck, when observed from the south.

The natural frequencies of the cables were mostly higher than several natural frequencies of the deck in the vertical and lateral directions. Therefore, negligible induced vibrations of the deck due to the vibration of the cables and vice-versa (cable-deck interaction) in the lower modes of vibration are expected.

Cable	Natural Frequency (Hz)	Tension (N)	Cable	Natural Frequency (Hz)	Tension (N)
CA01L	3.59	12895	CA11L	3.11	11977
CA01R	3.53	12451	CA11R	3.34	13851
CA02L	3.75	10119	CA12L	3.66	11494
CA02R	3.77	10203	CA12R	5.03	21765
CA03L	4.19	5825	CA13L	measurement error	-
CA03R	4.78	7594	CA13R	measurement error	-
CA04L	6.86	10499	CA14L	measurement error	-
CA04R	5.81	7539	CA14R	5.20	6368
CA05L	6.83	7124	CA15L	5.54	4602
CA05R	5.35	4374	CA15R	6.67	6671
CA06L	6.02	5430	CA16L	3.08	1446
CA06R	6.58	6493	CA16R	4.39	2933
CA07L	5.56	7281	CA17L	3.59	2876
CA07R	5.38	6799	CA17R	5.22	6065
CA08L	4.36	7147	CA18L	5.22	9034
CA08R	4.27	6843	CA18R	5.05	8448
CA09L	3.58	11000	CA19L	3.73	10024
CA09R	3.47	10339	CA19R	4.41	13956
CA10L	3.19	12586	CA20L	3.89	15101
CA10R	3.13	12088	CA20R	3.64	13223

Table 4.13 - Estimated measured natural frequencies and cable tensions

(v) Measurement of damping

The frequency resolution of 0.0625 Hz adopted for the ambient excitation tests was not expected to provide accurate estimations for damping. The association of low natural frequencies with (expected) low damping led to quotients (B_e/B_r) being too high for using the PSDs for this purpose (see discussion in Section 3.3.1.2).

Equivalent viscous damping ratios were determined from heel drop tests and from the free-vibration decay part of jumping tests. In the case of the jumping tests, the test subjects were asked to bounce (by flexing their knees without their feet leaving the deck) instead of jump, as this was found to be an easy way to excite the structure at a pre-defined frequency. The test subjects, one at a time, bounced in the middle and close to a point one third along the main span. These positions corresponded to the antinodes of the first and third modes, and second mode respectively (see Fig. 4.16). The heel drops were also applied at these positions. Due to limitations of the equipment for the

acquisition of long records, the free-vibration decay part of the walking tests after the subject left the bridge was not recorded. These could also be used to assess damping.

The results for the damping ratios of the first three vertical modes together with the respective natural frequencies obtained from the free-decay measurements are presented in Table 4.14. It can be seen that the natural frequencies compare well with those obtained from the ambient excitation tests (Table 4.12), which is an indication of linear behaviour of the structure for different excitation levels. There was also no significant change in damping value along the free-vibration decay record, which is another indication of linear behaviour of the structure under normal usage.

Mode	Jumping Tests		Heel Drop Tests	
	Natural Frequency (Hz)	Damping Ratio (%)	Natural Frequency (Hz)	Damping Ratio (%)
1st Mode (V1)	1.56	0.84%	*	*
2nd Mode (V2)	1.88	0.94%	*	*
3rd Mode (V3)	2.56	1.20%	2.61	1.09%

* not possible to identify from the filtered response

Table 4.14 - Natural frequencies and equivalent viscous damping ratios from decay tests

Modelling and Correlation

A FE model was prepared using ANSYS 5.0, aiming to investigate further the vibration performance of the test structure. A 3-D skeletal FE model based on line elements was adopted, in which 3-D beam elements were employed to represent the deck, the cross beams at cable-deck connections, and the tower legs. As will be seen, the calculated modal properties using this model produced a very good correlation with the experimental results, confirming the adequacy of the model to represent the structure. However, the behaviour in torsion was misrepresented although this did not constitute a problem since no coupling was detected during the tests between torsional and lateral or vertical modes.

To complete the modelling, the connections between deck and tower and also between deck and abutments were modelled by elastic springs, the elastic constants of which

constituted variables to be calibrated. Additional elastic springs were placed at the supports of the aluminium struts beside the towers to model the vertical displacements detected at those points (see Fig. 4.16). With regard to the cables, each one was modelled as a truss element, with an equivalent modulus of elasticity. This approach has been extensively discussed in the literature and is actually the most simplified way of modelling cables. This modelling has been reported as not representing an interaction that may exist between cables and deck if the natural frequencies of the former are coincident with those of the latter (Abdel-Ghaffar and Khalifa, 1991). However, the results from the tests showed that cable-deck interaction is not an issue in the case under investigation.

The aforementioned equivalent modulus of elasticity (E_{eq}) aims to represent the variations in tension due to cable sagging, in such a way that an actual sagged cable is represented by a straight chord having an elastic modulus E_{eq} . The equivalent modulus is calculated for each cable using the following expression (Gimsing, 1983):

$$E_{eq} = \frac{E_{cab}}{1 + \frac{(\gamma_{cab} L_{ch})^2 E_{cab}}{12(\frac{F_c}{A_c})^3}} \qquad (4.2)$$

In Eq. 4.2, E_{cab} is the elastic modulus of the cable material, and γ_{cab} and A_c the specific weight and cross sectional area of the cable, respectively, whereas L_{ch} is the horizontal projected length of the cable. Values for E_{eq} are smaller than E_{cab}, the difference between them increasing with cable sag (or with reductions in the cable tension F_c, as can be seen directly in Eq. 4.2). However, the differences between the calculated values of E_{eq} for each cable and the material elastic modulus E_{cab} were found negligible for the case under study, confirming that the cables were very taut. This also made it possible to take E_{cab} as the elastic modulus of all cables, simplifying the calculations during the calibration of the FE model.

A feature of the FE package was employed, which is the option of including prestressing effects from a prior static analysis (e.g. under dead load conditions) into the modal analysis (ANSYS, 1992). This accounts for the interaction between axial forces and bending moments, previously reported as one of the potential sources of

nonlinearity in cable-stayed bridges. A comparison of natural frequencies obtained with and without the use of this option presented minor differences, which is evidence that a linear model was a good approximation of the actual behaviour of the test structure.

The variables taken for calibration were the elastic moduli of the GRP material (deck and towers) and of the aramid (cables), the mass added to fill some of the cells of the deck at main span, and also the aforementioned elastic constants of the spring elements to model the connections. Some features of the FE model are described as follows:

(i) 63 beam elements were placed on the centre line of the deck to represent the main span. Each had a length of 1.0 m, resulting in three times more nodes than the number of test points at that span. The mesh density was halved for the side spans since they predominantly presented deflections only in the lateral modes, the adopted coarser mesh density being sufficient to provide a good resolution for the first two lateral modes of vibration. Few elements were employed to model each tower leg since this would be sufficient to represent the cantilever mode shape of these components identified in the tests.

(ii) handrails and deck finishing were included as distributed added masses of 16.6 kg/m and 26 kg/m, respectively. Some elements, such as the several toggles used to connect the structural components of the deck, and also the cross beams other than those at the connection with the cables, were considered as non-structural elements and were included as an added mass of 10.4 kg/m. Adding to these figures the mass of 6.2 kg/m of the grout present in part of some cross beams gave a final added mass of 59.2 kg/m. All the aforementioned values were based on calculations using the design cross sections of the respective components and information from the design (Ripley, 1996).

(iii) at the tower tops, the degrees of freedom of the two separate tower legs were coupled to simulate the firm connection between them present on the actual structure.

(iv) constraint equations (ANSYS, 1992) were introduced to model the connection between the cross beams at the cables and the 'deck' beam. As was described at the beginning of this Section, the deck and cross beams were fully bonded to each other. In

order to represent this connection, the nodal degrees of freedom of the cross beams and the respective degree of freedom at the 'deck' beam were imposed the same longitudinal displacements.

The brief description of the FE mesh given above is the final product obtained through a long process of modifications, in order to improve the correlation between calculated and measured modal properties. The experience obtained during this process showed that in cases of complex structures like this, the hard work resides more in having a proper FE model to represent the structure than in calibrating the variables selected for adjustment in the correlation process. As opposed to the strategy adopted in the calibrations of the other test structures, in which the natural frequencies were correlated first leading to mode shapes almost correlated, in this case it was the observation of the mode shapes that guided where some of the changes were needed. A view of the model and modelling details is presented in Fig. 4.19, together with values obtained for the elastic constants of the supports that led to the best correlation with the experimental results.

Natural Frequencies (Hz)		MAC (%)
Calculated	Measured	
1.01	1.00 (L1)	98
1.61	1.59 (V1)	98
1.91	1.92 (V2)	98
2.56	2.59 (V3)	98
2.89	2.81 (L2)	96
3.06	3.14 (V4)	98
3.57	3.63 (V5)	98
3.98	4.00 (V6)	98
4.52	4.60 (V7)	96
5.03	5.10 (V8)	98
5.62	5.60 (V9)	97

Table 4.15 - Natural frequencies and mode shape correlation

A comparison between measured and calculated natural frequencies and mode shapes is shown in Table 4.15, confirming the accuracy of the FE model in representing the actual structure. The calibrated values of the variables were: 21 GPa and 113.9 GPa for the elastic modulus of the GRP and cable material, respectively, both presenting a

difference of less than 10% to the respective design values; variable constants for the several elastic springs, from $1.0*10^5$ N/m at the slack aluminium strut supports to $1.0*10^{20}$ N/m at the (rigid) connection between towers and deck in the vertical and lateral directions (Fig. 4.19); and 47.5 kg/m for the added mass at the main span, close to the estimated value of 46.1 kg/m for the amount of mass added shortly after erection of the bridge deck. This latter value was based on information from the design regarding the position and number of cells in which mass was added (Ripley, 1996) (see also Fig. 4.21). It was obtained by multiplying the density of the added material (baryte), obtained from the UK code (BS 648, 1964), by the area of the filled cells.

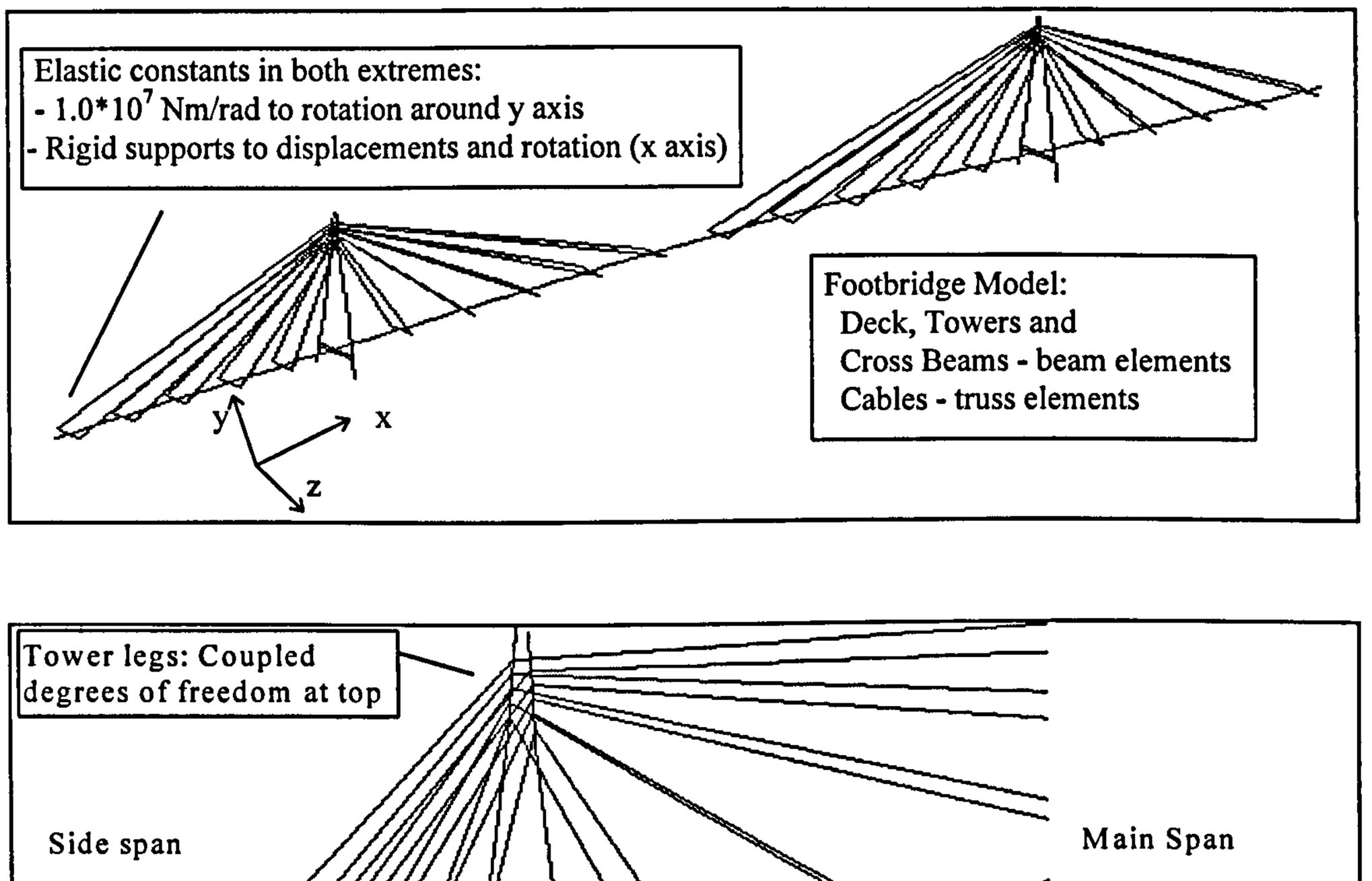

Figure 4.19 - Modelling details and calibrated elastic constants of the supports

Pedestrian Tests

The pedestrian tests aimed to check the serviceability of the structure against pedestrian-induced vibrations, according to the requirements of the UK code (BS5400, 1978). The first two vertical natural frequencies of 1.59 Hz and 1.92 Hz were both inside the range of excitation of the first harmonic of the walking load, and tests with subjects walking, one at a time, with a pacing rate coincident with these natural frequencies were carried out.

The filtered acceleration time-response of the footbridge at the antinode of the respective mode shapes was taken to determine the peak accelerations in each case. These are presented in Table 4.16, together with the respective acceptability limits of the UK code. In both cases, the measured peak accelerations are higher than the code limits, particularly for the first mode.

Natural Frequency Excited (Hz)	Average Peak Acceleration (m/s^2)	Code Limit (BS5400, 1978)
Mode V1 - 1.59 Hz	2.14	0.63
Mode V2 - 1.92 Hz	0.91	0.69

Table 4.16 - Measured peak accelerations in controlled pedestrian tests

4.5.1 Analysis of Vibration Performance

This was revealed to be a lively structure, having several natural frequencies below 5 Hz and some inside the range of normal pacing rates of pedestrians. The balance between its mass and stiffness is such that the first natural frequency of the bridge in the vertical direction compares very favourably with those measured in footbridges made of other materials (see Fig. 2.8). This indicates that the constituent material is much less important than span length in determining the natural frequency.

However, the much reduced mass of the structure due to the lightweight character of the GRP is certainly a contributing factor for higher accelerations to be experienced. The effect of mass on acceleration response can be visualised in Fig. 2.11, in which increases in mass are shown to produce reductions on acceleration levels of SDOF systems, particularly under resonance conditions. For two SDOF systems having the same natural frequency and damping, and submitted to a steady-state sinusoidal excitation in resonance condition, the one with less mass will experience higher accelerations. This can be shown by the mathematical expression for maximum acceleration a_{max} of a SDOF system under these conditions (Clough and Penzien, 1975):

$$a_{max} = \frac{P}{2m\zeta} \tag{4.3}$$

in which P is the amplitude of the sinusoidal excitation, ζ is the viscous damping ratio and m is the mass of the SDOF system appearing in the denominator of the expression. Thus, footbridges made of ACM lightweight constituent materials are potentially more lively than footbridges made of conventional materials, and great care should be taken in investigating their vibration performance.

In the particular case of the test structure, considering that the structure is in private ownership with very little pedestrian traffic, and that there have been no complaints regarding its excessive vibration, it does not seem necessary to take measures to improve its dynamic behaviour. However, the calibrated numerical model prepared can be used to investigate what improvements in terms of design would be effective for reducing the high acceleration levels, aiming to show that such structures can present satisfactory vibration performance despite their reduced mass. This means that the investigation will concentrate on changing/repositioning the mass and/or stiffness of the system rather than seeking for the application of tuned mass dampers (TMDs), since this is more appropriate for retrofitting (see Section 2.5).

As was discussed in Section 2.5, the overall strategy of making changes to mass and/or stiffness is to promote frequency tuning, removing the natural frequencies of the structure from the common range of frequencies of the source of excitation (i.e. the

walking load). Since the test structure presents several natural frequencies within the frequency ranges of both harmonics of the walking load in the vertical direction, massive changes would be necessary for the complete removal of the natural frequencies from this whole frequency range.

The strategy adopted for frequency tuning will thus be avoiding the frequency range of the first harmonic of the walking load, in which the magnitude of the walking load is higher, and also analysing the response of the structure at natural frequencies that eventually remain in the frequency range of the second harmonic. In addition, the presence of lateral natural frequencies within the critical range of 0.8 to 1.2 Hz has also to be taken into account since the bridge was easily excited in this direction. It should be noted that the approach of focusing attention on the critical frequency ranges excited by the walking load in both the vertical and lateral directions does not follow the recommendation of the UK code (BS5400, 1978) to the letter. Nevertheless, the approach adopted takes into account that the natural frequencies of the structure were precisely identified by tests. It also considers the research carried out so far into the definition of critical frequency ranges and the occurrence of case reports of lively footbridges, which are all concentrated in these ranges.

A useful feature of the ACCS system, being of cellular structure, is that it permits the addition of mass into its cells without changes in stiffness, creating more flexibility in terms of design for detuning the natural frequencies of the system out of the critical frequency ranges.

Low Tuning

Low tuning is carried out by adding or repositioning mass already added to the structure. Information from the original design indicated that mass was added uniformly into some cells along the main span of the structure, and the idea in repositioning this mass was to concentrate it in certain areas of the structure in such a way as to increase the modal mass of the modes intended to be detuned.

The concept of modal mass is described in books dealing with modal analysis (e.g. Clough and Penzien, 1975), and it can be understood in these terms: the participation of the mass of the system on the vibration in a given mode varies according to the position of the mass with respect to the respective mode shape. The regions of the structure which experience relatively large deflections in that mode are those in which the inertial effects of the mass are most significant. Therefore, the target locations to reposition and/or apply mass in order to increase the modal mass of a given mode of vibration are those in the regions of the highest relative ordinates of the mode envelope.

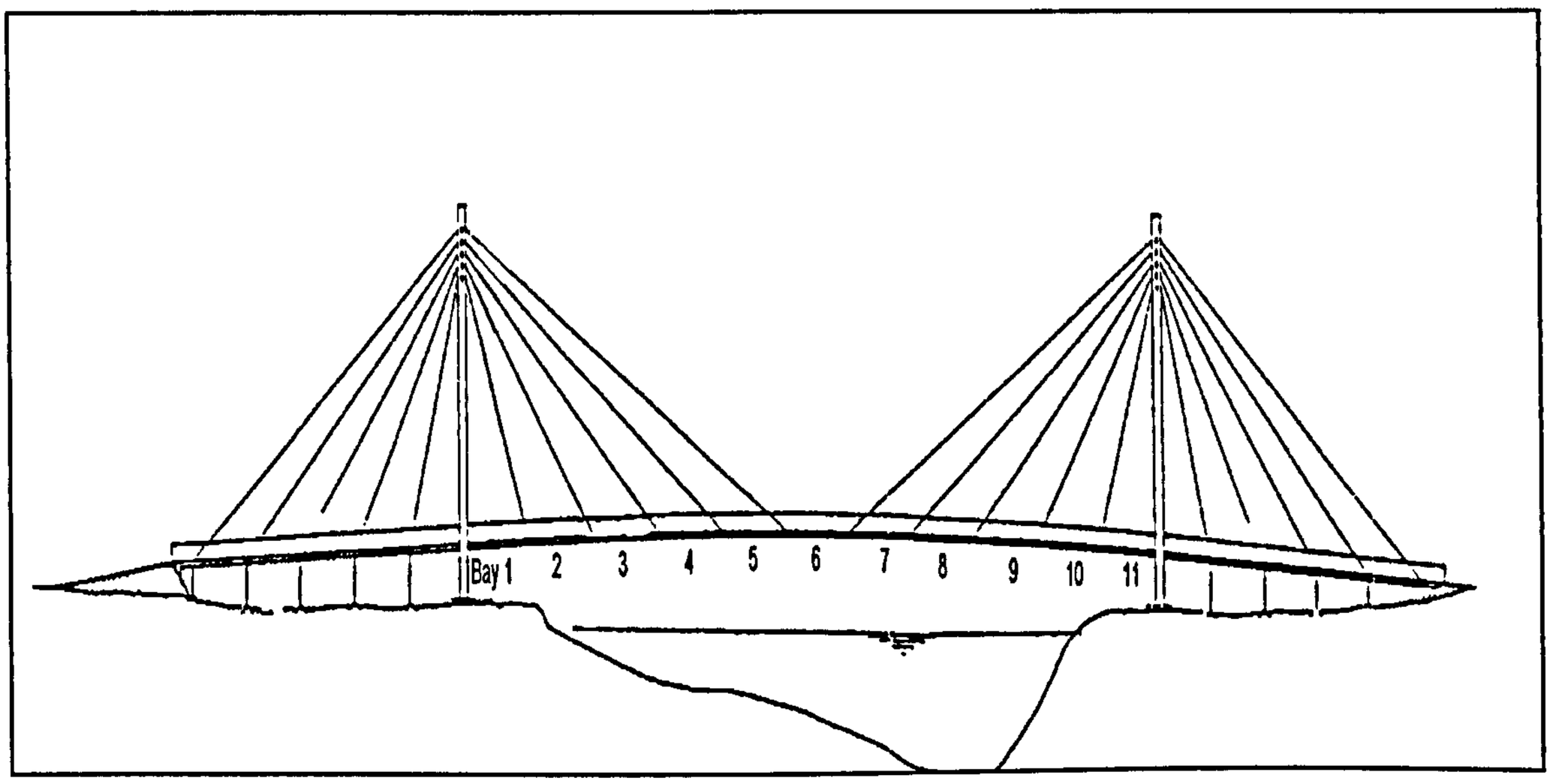

Figure 4.20- Identification of bays at the main span

Observing the envelopes of the first mode shape in the lateral direction and of the first and second mode shapes in the vertical direction, the strategy will then be to concentrate mass within the cells of the deck at the central bays of the main span. For reference, these bays are numbered and shown in Fig. 4.20. After several trials, a satisfactory solution was found, based on the following distribution of mass: a) move all the mass already present on bays 1 to 4 and 8 to 11 into the bays 5 to 7, resulting in a relocated mass of 126.7 kg/m, to be added to the distributed mass of 47.5 kg/m already present on the bays 5 to 7; and b) add 63.3 kg/m more mass into the cells of bays 5 to 7, which would fill up more four cells of the cross section. The final accommodation of mass within the cells of the central bays of the deck are shown in Fig. 4.21.

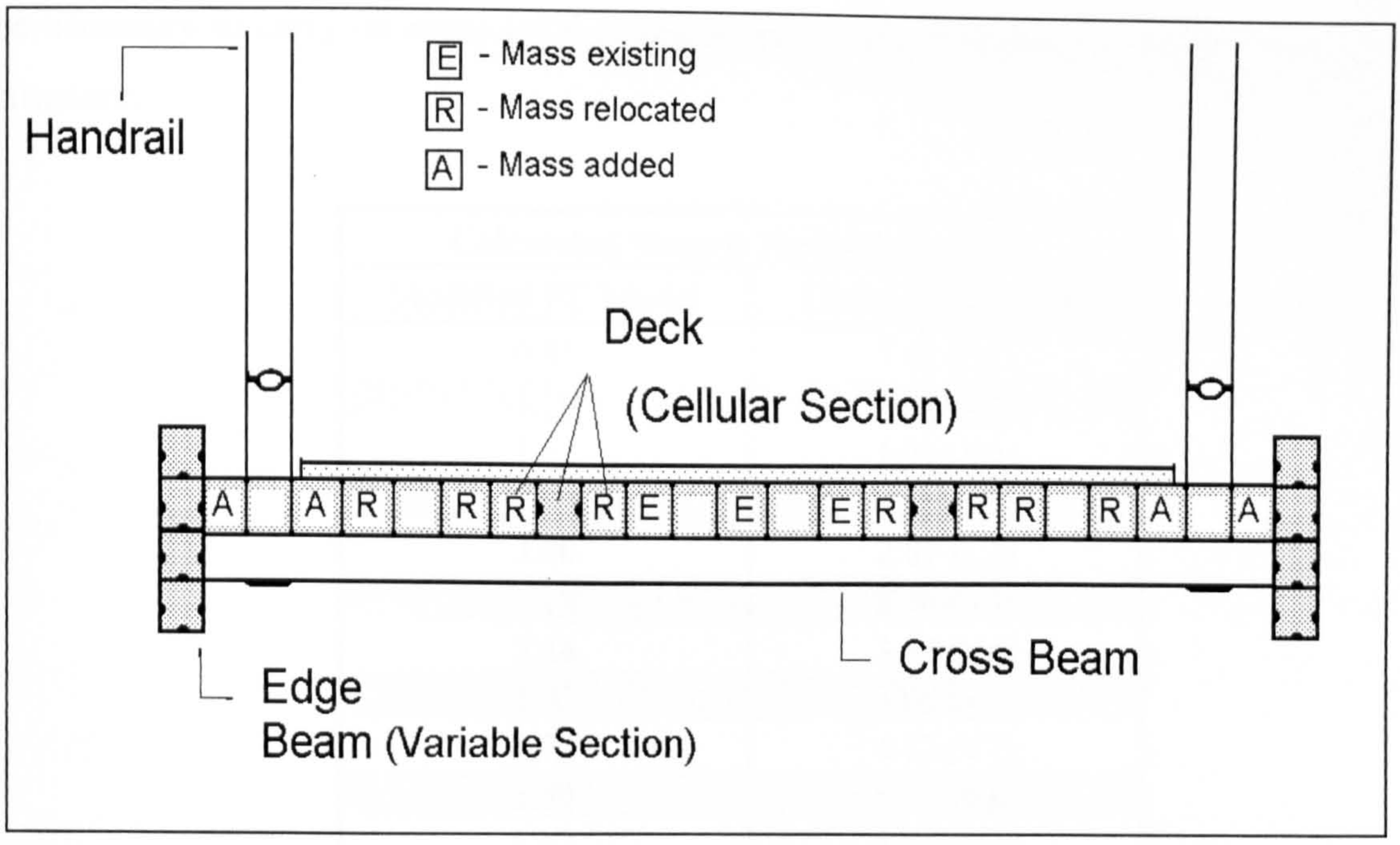

Figure 4.21 - Distribution of mass within the mid span cross section

The natural frequencies obtained are shown in Table 4.17 together with the ones of the current structure. It can be seen that the natural frequencies of the structure were removed (one remaining marginally) from the critical frequency ranges of 0.8 to 1.2 Hz in the lateral direction and from 1.6 to 2.4 Hz in the vertical direction. The natural frequencies of the structure within the frequency range of the second harmonic of the walking load in the vertical direction (from 3.2 to 4.8 Hz) are the fifth, sixth and seventh natural frequencies of 3.48, 4.32 and 4.73 Hz, respectively. It may be noted that the fifth mode of vibration is symmetric, having four nodes within the main span of the structure. This will naturally prevent vibrations from pedestrians crossing the structure building up, the same applying to the other two modes.

A final consideration is to compare the increase in the dead load within the central bays and on the whole main span due to the total added mass with the design live load of the footbridge. The latter was taken from the design (BS5400, 1978) as being 3.48 kN/m^2, which gives a total of 574 kg/m. This is more than double the total value of 237 kg/m for the added mass concentrated in the three central bays. However, for the whole span, the total added mass corresponds to 11% of the design live load. This analysis shows that this solution is feasible, particularly considering its low cost. Nevertheless, it may

be necessary to carry on some local strengthening within the three central bays of the structure.

Calculated Natural Frequencies (Hz)	
Modified FE Model	Current FE Model
0.83	1.01 (L1)
1.16	1.61 (V1)
1.52	1.91 (V2)
2.41	2.56 (V3)
3.00	2.89 (L2)
3.11	3.06 (V4)
3.48	3.57 (V5)
4.32	3.98 (V6)
4.73	4.52 (V7)
5.50	5.03 (V8)
5.83	5.62 (V9)

Table 4.17 - Natural frequencies of the footbridge with and without changes in mass

High Tuning

The success achieved by low tuning discourages further investigations into high tuning. This is particularly emphasised by the value of the natural frequencies to be detuned. If the second vertical frequency of 1.92 Hz is taken as an example, high tuning would imply increasing this frequency to a minimum value of 2.5 Hz, which gives an increase of 30%. However, strengthening the structure for detuning this mode would imply increases in the first vertical mode of 1.6 Hz, which could leave it in the more critical situation of being closer to the common value of 2.0 Hz of the pedestrian pacing rate. It should be noted that a selective stiffening of the second mode without affecting the first mode is not feasible due to contributions of the same structural components to these modes. Therefore, high tuning should be such that the first vertical mode should be increased to a minimum of 2.5 Hz, which gives a variation of 56% in its value. This is likely to be reached only with very substantial changes to the structure.

Nevertheless, some insight into these changes can be given using the calibrated numerical model. The adopted strategy adopted was to increase both the axial stiffness of the cables and to add new GRP components to the deck in order to achieve the

desired increase of the vertical natural frequencies and also of the first lateral natural frequency.

The first step was to investigate the effect of increasing the axial stiffness of the cables, which can be achieved by using cables of a larger diameter. An initial investigation showed that, as expected, increases on the axial stiffness of the cables did not promote significant changes of the first lateral natural frequency. This can be understood as the deck of the bridge vibrating in the lateral direction like a pendulum, in which the cables experience movements as rigid bodies with negligible further extension. Therefore, the improvements obtained by strengthening of the cables would be beneficial only for increasing the natural frequencies in the vertical direction.

As a second step, the cables in which increases in axial stiffness would be more effective for frequency detuning were identified. Observation of the vibration mode shapes was taken as a guide in the process of identification. It was realised that, for a common deflection at the tower top, the points on the deck experiencing higher deflection would indicate which cables were more extended while vibrating at those modes. The cables where changes could be more effectively made were identified as the central four pairs of cables.

The natural frequencies obtained by increasing the area of these central cables by 50% are presented in Table 4.18 together with the existing natural frequencies. As expected, negligible changes in the first lateral natural frequency took place. However, increases in the vertical natural frequencies occurred although not enough for the level desired for full detuning.

The side effect of increasing the area of the cables is a reduction of cable tension and consequently a deviation from the initial taut condition. Application of Eq. 4.2 shows that increases in axial stiffness due to increases in the area may be counteracted by reductions in the equivalent elastic modulus. These were taken into account in production of the results presented in Table 4.18.

Calculated Natural Frequencies (Hz)	
Modified FE Model	Current FE Model
1.02	1.01 (L1)
1.75	1.61 (V1)
2.04	1.91 (V2)
2.75	2.56 (V3)
2.90	2.89 (L2)
3.18	3.06 (V4)
3.75	3.57 (V5)
4.05	3.98 (V6)
4.56	4.52 (V7)
5.09	5.03 (V8)
5.65	5.62 (V9)

Table 4.18 - Natural frequencies of the footbridge with and without modified cables

This modified model was taken as the starting point to investigate further changes in other structural components, in order to achieve the desired degree of detuning. In order to investigate the influence of the structural components on the natural frequencies of the structure, particularly in the lower modes, some case studies were analysed:

Case 1 - Investigating the effect of stiffening the towers: the displacements of the tower tops were restrained in the longitudinal direction. This provided the upper limit, actually unattainable in practice, in terms of increases in the vertical natural frequencies of the deck that extremely stiff towers would produce. The results are presented in Table 4.19. It can be seen that the first natural frequency in the vertical direction was only marginally above the upper limit of the frequency range of the first harmonic of the walking load. Therefore, it does not seem feasible to think in terms of detuning by stiffening the towers since this degree of fixity is not achievable in practice. Indeed, the towers already seemed very stiff, presenting small relative displacements at the modes of interest. It may also be noted that little changes in the higher modes took place, showing that they are not influenced significantly by the towers.

Case 2 - Investigating the effect of stiffening the deck: observation of the cross section of the deck (Fig. 4.13) indicated that increases in stiffness for both the lateral and vertical directions would come by adding structural components at the soffit of the edge beams. In a first attempt, a total of 4 GRP cells (the components employed to build up

the edge beams) were added to each of the edge beams. The arrangement of the added cells followed the pattern adopted in the original design of the cross section of the deck in the neighbourhood of the towers. This cross section was already stiffened by addition of cells (Fig. 4.22). Adopting this modified cross section throughout the main span of the footbridge resulted in a reduction of the natural frequency of the first vertical mode (Table 4.19). However, it resulted in increases on the natural frequencies of the other modes. Albeit initially a surprising result, it may be noted that the addition of these GRP cells also represented an addition of mass to the main span. The pattern of changes in the natural frequencies indicates that, for the first vertical mode, the addition of the mass on the main span was more influential than the increase in stiffness. This can be understood by considering that the higher modes involve more local bending of the deck than the lower modes. These latter modes are more influenced by the towers and cables.

Natural Frequencies - Case 1 (Hz)	Natural Frequencies - Case 2 (Hz)	Natural Frequencies of the Initial (Modified) Model (Hz)	Natural Frequencies - Case 2a (Hz)	Natural Frequencies - Case 3 (Hz)
1.02	1.12	1.02 (L1)	1.19	1.04
2.46	1.67	1.75 (V1)	1.78	1.75
2.82	2.15	2.04 (V2)	2.30	2.04
2.98	3.19	2.75 (V3)	3.41	2.78
2.91	3.35	2.90 (L2)	3.55	2.91
3.27	4.08	3.18 (V4)	4.36	3.21
3.84	4.89	3.75 (V5)	5.23	3.73
4.21	5.88	4.05 (V6)	6.28	4.09
4.72	7.37	4.56 (V7)	7.84	4.92
5.21	9.10	5.09 (V8)	9.72	5.78
5.76	11.03	5.65 (V9)	11.79	6.14

Table 4.19 -Natural frequencies resulting from several numerical models

Case 2a - In order to confirm that the addition of mass that came with the addition of the GRP components was responsible for the reduction of the natural frequency of the first vertical mode, Case 2 was modified to include a mass compensation scheme. This was carried out by reducing the added mass in the model by the amount that was added by the GRP components. The results, also presented in Table 4.19, confirm that the addition of mass was the major cause of the reduction in the first vertical mode.

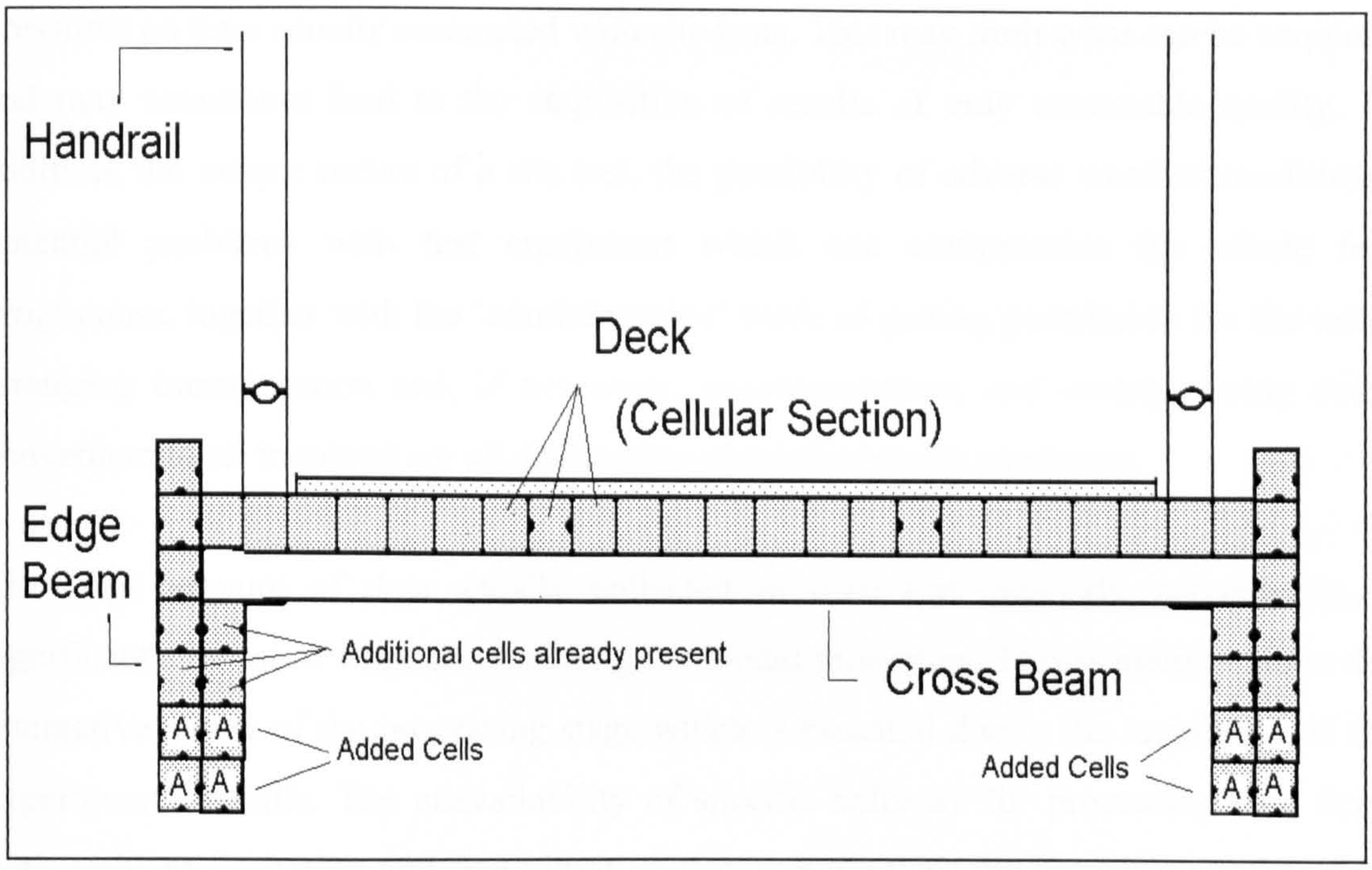

Figure 4.22 - Modified cross section of the deck

Case 3 - A final attempt was made by adding the GRP cells only to the first two bays of the main span adjacent to both towers (bays 1,2, 10 and 11, see Fig. 4.20). The idea was to avoid adding mass (GRP components) at the regions in which the first vertical mode presented higher relative displacements since this would increase the modal mass of that mode. Negligible variation was noticed in the first vertical mode (Table 4.19) and also in other higher modes.

The conclusion from these numerical cases is that high tuning is not a feasible alternative for this bridge.

4.6 Discussion of Results and Analysis

The very good correlation obtained between the experimental and numerical results for all footbridges have confirmed the appropriateness of both the experimental procedures and the numerical FE models developed. The good quality of the experimental results acquired confirmed the validity of the procedures outlined in Chapter 3 for acquiring and processing data. However, it is appropriate to call attention to the very high

pressures on time usually associated with site tests. This may limit what can be acquired and may sometimes lead to the acquisition of results of only reasonable quality. In addition, the unique nature of a site test, the possibility of adverse weather conditions, potential problems with test equipment which can compromise the whole test programme, together with the 'administrative' work of getting permission for the tests, arranging transportation and, if necessary, accommodation, and setting testing dates convenient to all involved are all difficulties which have to be overcome.

The large amount of data usually collected in each test demands, accordingly, a significant amount of work for obtaining the modal properties. This is mainly due to the interactive nature of the processing stage which is essential due to the variability of the experimental results. The unavailability of specific software for processing data from both ambient excitation and free-vibration decay made their processing a cumbersome task.

On the numerical side, simple models based on beam elements were shown to be sufficient for producing natural frequencies and mode shapes in good agreement with the ones obtained from the tests. This is in agreement with results presented in the literature, in which the use of such elements for modelling footbridges provided results which correlated well with test results (Brownjohn, 1997).

Uncertainty in material properties and particularly in support conditions implies that these should necessarily be taken as variables in the calibration process of the numerical model. The calibrated values of the elastic modulus of the constituent materials (concrete and GRP) of two test footbridges were close to the respective static design values, indicating that the latter can reasonably be taken as a reference for design calculations. Indeed, the static value of the Young's modulus of the constituent material is the value recommended for use in vibration serviceability calculations in both the UK (BS5400, 1978) and Ontario (OHBDC, 1991) codes. On the other hand, a significant discrepancy between the calibrated and the design values of the elastic constant of the bearings in one of the test footbridges was found. Laboratory tests reproducing the expected load to which the bearings are going to be submitted and also its actual

confinement condition could help in alleviating the uncertainty and produce more reliable values for inclusion in the design process.

However, the experience acquired during the calibration of the models showed that obtaining a realistic FE model capable of representing the actual structural behaviour was a crucial first stage before attempting to adjust the values of the chosen variables. For complex structures, such as the GRP cable-stayed footbridge tested, there is usually a need to include several additional parameters in the calibration process. Use of an automatic (software-based) model updating procedure using an initial 'manual' solution as a starting point may be useful in these cases to increase further the confidence in the results.

The following aspects of modelling are worth mentioning:

- The observation of the mode shapes of the structure for detection of unexpected structural displacements caused by incorrect modelling. This was found to be particularly important when using simple models to represent the structure, in which the connections between the structural components needed special attention.

- The modelling of the handrails as structural elements. A good representation of the dynamic behaviour of the structure was obtained by modelling handrails as an attached frame to the deck. The potential for the handrails to affect the vibration characteristics is considered in the UK code (BS 5400, 1978) by recommending their stiffness to be included in the analysis.

As was discussed in Section 2.5, the design alternatives to improve the vibration performance of a lively footbridge are increasing overall structural stiffness and/or addition of mass to reduce the response in resonance conditions. Frequency tuning aims avoiding the critical frequency range of the first harmonic of the walking load in which most vibration problems are concentrated. Features that can assist in high tuning are the use of stiff handrails suitably attached to the deck and membrane action due to a combination of a camber or catenary profile and horizontal stiffness at the bearings.

The tests of the GRP cable-stayed footbridge produced natural frequencies which were similar to those expected in structures made of conventional materials. This was due to the fact that the mass/stiffness ratio was similar for footbridges constructed from GRP and conventional materials. Damping values for this structure were higher than those measured in the other two test footbridges but are in the range of values generally expected for footbridges (Tilly *et al.*, 1984). Since the measured damping values are in the range of expected values for footbridges, the reduced mass implies higher accelerations being produced.

No reference has been found in the literature regarding vibration serviceability problems due to human-induced loads on the several prototype GRP bridges constructed to date (Meier, 1991). Green *et al.* (1994) and Johansen *et al.* (1996) reported that the dynamic behaviour of such structures is of concern and, indeed, included checks for vibration serviceability in their design calculations. However, the short 12.2 m span of the GRP footbridge analysed by Green *et al.* led to a reported fundamental frequency of 18 Hz, entirely out of the range of vibration serviceability problems. The design methodology reported by Johansen *et al.* aimed to design GRP footbridges to have a minimum natural frequency of 5.0 Hz to avoid human-induced vibration problems. This was attained by both GRP footbridges analysed which had span lengths of 12.3 and 24.6 m.

The absence of vibration problems is related to the short span lengths of the reported structures, which consequently would present natural frequencies above the common frequency ranges of pedestrian excitation (see Fig. 2.8 for a relation between natural frequency and span length). Conversely, the GRP footbridge tested here had a long span length, and the excessive level of vibrations presented in pedestrian tests has brought attention to the potential problems that GRP footbridges have in terms of vibration serviceability due to their low mass. A recent paper by Khalifa *et al.* (1996) discusses the design of a cable-stayed GRP pedestrian bridge having a main span of 122 m. Investigations are reported to be on course for reducing the unsatisfactory level of vibrations calculated in the initial design.

The addition and relocation of mass was found to be the best approach for frequency tuning of the natural frequencies of the test structure. In terms of stiffening the structure, the addition of new structural components on the deck was not found to be effective for

increasing the lower natural frequencies in the vertical direction. This was because the addition of new components also added mass to the deck, which was shown to counteract the increase of stiffness for these modes. Increasing the stiffness of the cables was shown to be useful for increasing the natural frequencies in vertical direction.

Chapter 5

Analysis of the Guidelines for Vibration Performance

5.1 Introduction

The chart presented in Fig. 2.8 reveals that the span length is a decisive factor in defining the natural frequencies of a footbridge, and that it is common to find footbridges having natural frequencies within the ranges of the harmonics of the walking load. They can be set vibrating in resonance under normal operational conditions, and it may be difficult or onerous to design such structures in order to avoid these critical frequency ranges. Moreover, tests of three potentially lively footbridges have shown that having natural frequencies within the critical frequency ranges does not necessarily mean that the footbridge is lively.

A critical review of the guidelines for vibration performance of footbridges due to human-induced loads is carried out in this Chapter. Topics have been selected in which research was found to be necessary, according to the discussions in Chapter 2. However, the availability of test results has limited the investigations to vibrations in the vertical direction only.

This Chapter is divided into Sections, as follows: in Section 5.2, an investigation into the pedestrian load is carried out, based on tests using pedestrians and analysis using the calibrated numerical models of the test footbridges; Section 5.3 is dedicated to the definition of frequency ranges of interest for vibration performance; in Section 5.4, the acceptability limits for vibration are discussed with the support of pedestrian tests that were carried out on the test footbridges; Sections 5.5 contains an analysis of vibrations with more than one frequency component; Section 5.6 concentrates on investigating vandal loading; and, in conclusion, guidelines for vibration performance are presented in Section 5.7 as a synthesis of what has been discussed in this Chapter.

5.2 Evaluation of the Pedestrian Load Models

The motivation for investigating the pedestrian load produced by an individual or a group comes from the different values to represent this load proposed in the literature and also from the way the investigations to obtain this load have been carried out. Three points can be highlighted and are investigated in this Section:

- The representation of the walking load of a single pedestrian. As was discussed in Section 2.3.3, the walking load is modelled as a sinusoidal load of constant amplitude (i.e. a constant dynamic load factor is adopted) in both the UK (BS5400, 1978) and Ontario (OHBDC, 1991) codes. It was also discussed that research into modelling the walking load has shown that variable amplitudes are more appropriate, according to which harmonic of the walking load is employed to excite the natural frequency of interest of the structure (see Table 2.1 for a summary of dynamic load factors from different sources). Nevertheless, there is a lack of investigation into potential alterations of the load while applied on actual vibrating footbridges, since the investigations so far have been carried out on rigid surfaces or platforms. This is the subject of the investigation in Section 5.2.1.

- Independent research into the effects of crowd loading have been conducted to obtain different crowd magnification factors (see Fig. 2.7). As was mentioned in Section 2.2.2, these factors are to be applied as multiplying factors of the response due to a single pedestrian. Therefore, use of magnification factors needs to be related to the procedure to obtain the response due to a single pedestrian. The applicability of crowd magnification factors as a magnifier of the response produced by a single pedestrian walking in resonance conditions is investigated in Section 5.2.2. The rationale for this investigation is that this latter condition of application of the pedestrian load is the one that has been adopted in the UK (BS5400, 1978) and Ontario (OHBDC, 1991) codes, which, conversely, do not consider the application of magnification factors.

- As discussed in Section 2.2.1, the interaction between pedestrians and the structure in the sense of how can this affect the dynamics of the system has not been fully investigated and is the subject of discussion in Section 5.2.3.

Attention is concentrated on investigating the load produced by walking, which is the major load case of interest in terms of vibration serviceability. The load produced by pedestrians jumping will be investigated in Section 5.6 as a potential source of deliberate excitation.

5.2.1 Load Model for an Individual

The walking load has usually been represented by the Fourier Series Eq. 2.1. For practical applications, the weight of a notional pedestrian is defined (e.g., 700 N (BS5400, 1978)), and it is the dynamic load factors and phase angles of the harmonics of the walking load that need to be obtained from tests.

It is worth first having a look at how these load factors have been obtained. The procedure adopted by Rainer and Pernica (1986) was to first obtain the time signatures for each harmonic of the load, from a force signal measured using a load cell. The load cell was installed on a support at the centre point of a platform on which a pedestrian was walking along. Isolating the contribution of each harmonic was carried out by digital band pass filtering in the frequency domain. Each filtered time signature shows the contribution of each harmonic of the walking load during the crossing. By taking the centre amplitudes of the time signature (i.e., the amplitudes of the filtered time signature when the pedestrian was in the neighbourhood of the measurement point) and normalising them by the weight of the test subject gives the respective dynamic load factor.

Rainer and Pernica also mentioned use of a correction factor to compensate for dynamic amplification effects of the test platform, although its lowest resonance frequency was 12 Hz. With regard to the phase angles (time shifts between the harmonics), they were reported as being obtained from the analysis of the filtered time signatures.

Despite using frequency domain techniques to isolate the contribution of each harmonic of the load, the aforementioned approach calculates the dynamic load factors and phase angles from response signatures in the time domain. Alternatively, Pernica (1990)

adopted a frequency domain approach for obtaining the dynamic load factors. Using the same experimental set-up of the aforementioned tests, the Fourier Spectrum of the force signal was calculated, and from the Fourier amplitudes at the frequencies of the excitation (i.e., the frequencies of the harmonics of the walking load), the load factors were obtained by normalising the spectral values by the weight of the test subjects. In more detail, this operation uses the Parseval theorem (Eq. 3.13), which relates each spectral amplitude to the root mean square (RMS) of the force time signal generated by the respective harmonic component of the load.

However, Eriksson (1994) pointed out that Pernica did not mention the spectral bandwidth adopted for obtaining the aforementioned RMS values from the Fourier Spectrum. This comment may be motivated by the fact that the power of a signal in a given frequency is spread over adjacent frequency lines of the actual discrete Fourier Spectrum obtained from the measurements. One also needs to take into account that the application of windows to prevent leakage, like the Hanning window, contributes to a broadening of the Spectrum. When trying to compare the results from his own measurements to those from Pernica, Eriksson (1994) showed that adopting different bandwidths around each spectral peak led to obtaining different dynamic load factors.

The approach adopted by Eriksson (1994) to represent the forces from walking differed from the ones previously mentioned. He aimed to obtain spectral representations of the force produced by pedestrians, i.e. a pedestrian load function in the frequency domain. To obtain this, he made use of the Power Spectral Density (PSD) of the response and the Frequency Response Function (FRF), evaluated at a point of a test platform having a fundamental frequency of 8 Hz and subject to loads resulting from walking. Application of Eq. 3.19 enables the PSD of the excitation at the measurement point to be obtained. A further conversion is necessary since the latter PSD is actually a generalised PSD as if the excitation was applied at that point at which the spectral functions were obtained and not from a moving person walking along. For obtaining the PSD or Fourier Spectrum of the applied force from the generalised PSD, use is made of the mode shape ordinates along the walking path, relating them to the mode shape ordinate at the measurement point.

The advantage of the latter approach is that the use of the FRF guarantees that the dynamic characteristics of the test structure do not affect the results. Indeed, the response of the structure is being used as a way to obtain the unknown excitation forces. However, the use of FRF assumes that a steady-state excitation is being applied.

A potential problem of assuming that a steady-state excitation is being applied is the transient effects of the moving load. The acceleration time response at a point of the structure during the crossing of a pedestrian usually presents the characteristics of a transient signal. If a steady-state vibration is reached, it would last only for a short period while the pedestrian was walking around the neighbourhood of the region of higher response (e.g., an antinode of the respective vibration mode shape). In addition, Timoshenko (1947) showed that a moving sinusoidal load (e.g. a pedestrian walking) generates responses in more than one frequency component. Taking as an example the case of a simply supported beam subject to a moving sinusoidal load $P\sin(2\pi ft)$, the expression of the generalised force for each mode of vibration r of this beam is given by:

$$P_r(t) = P \sin(2\pi ft) \sin(\frac{r\pi v}{l} t) = \frac{P}{2} [\cos((2\pi f - \frac{r\pi v}{l})t) - \cos (2\pi f + \frac{r\pi v}{l})t)] \qquad (5.1)$$

in which the last expression on the right-hand side is obtained using trigonometric identities. The generalised force P_r is the force applied to the mode r while decoupling the system on its modal components (modal superposition method (Clough and Penzien, 1975)). In Eq. 5.1, f is the frequency of the sinusoidal load, v is its speed, and l is the span length of the beam. Eq. 5.1 shows the appearance of two separate frequency components below and above the frequency of the sinusoidal load. As Smith (1988) pointed out, true resonance does not occur in this case.

It may be noted that the difference in value between the two frequency components of the generalised force depends on the speed that the load moves along the structure and the length of the span. As an example, for a test subject walking on a 20 m long beam-like footbridge, at a pacing rate f_p of 2.0 Hz and with a (reasonable) speed v of 1.8 m/s ($v = 0.9 f_p$, according to the UK code (BS5400, 1978)), the application of Eq. 5.1 leads

to a generalised force P_r with frequency components of 1.955 and 2.045 Hz. Indeed, for the order of magnitude of the pacing rate, speed of pedestrians and span length, the two frequency components will usually be close to each other.

This transient effect of the moving load also creates an additional complication in using Fourier spectra for obtaining dynamic load factors. It contributes to enlarging the peaks of the spectra since there will actually be two close frequency components in the response instead of the single frequency component of the excitation.

There is also the question of the effect of the structural vibrations in modifying the pedestrian load. Pedestrian tests carried out in the prototype footbridges presented in Chapter 4 and also on rigid surfaces showed evidence of the potential modifications to which the pedestrian load is subjected. A metronome was employed in all tests in which test subjects were asked to walk at a specified pacing rate. The first test was conducted with the purpose of comparing the time response of the body accelerations of a test subject walking on a rigid surface (ground floor) and on a footbridge in resonance conditions. An accelerometer was attached to the waist of the test subject using a L shape plate in such a way that it remained in a vertical position. The response signals were filtered in order to contain the contribution of the frequency of 2.3 Hz, which was the pacing rate of the pedestrian in each test, being also coincident with the fundamental frequency of the test footbridge (see Section 4.4 for a description of the structure). A third measurement was carried out on the test structure at the antinode of the vibration mode shape of interest, as a reference for the level of structural vibration during the crossing, producing a RMS value of 0.36 m/s^2. The two acceleration time signals taken on the body while crossing the footbridge and also while walking on ground are shown in Fig. 5.1, in which the time frame was selected so as to contain the whole signal measured during the crossing of the footbridge.

It may be noted that the measurements of acceleration on the body during the crossing corresponded to walking on a non-horizontal surface since the footbridge had a catenary shape. The higher amplitude values at the beginning of the crossing (Fig. 5.1a) may be due to the fact that the slope of the deck is also higher in this area. However, the consistently higher amplitude values throughout the bridge crossing when compared to

the amplitudes while walking on solid ground identified a possible interaction between the test subject and the footbridge, which was set vibrating by the test subject; otherwise the two acceleration response signals should present generally the same amplitude levels.

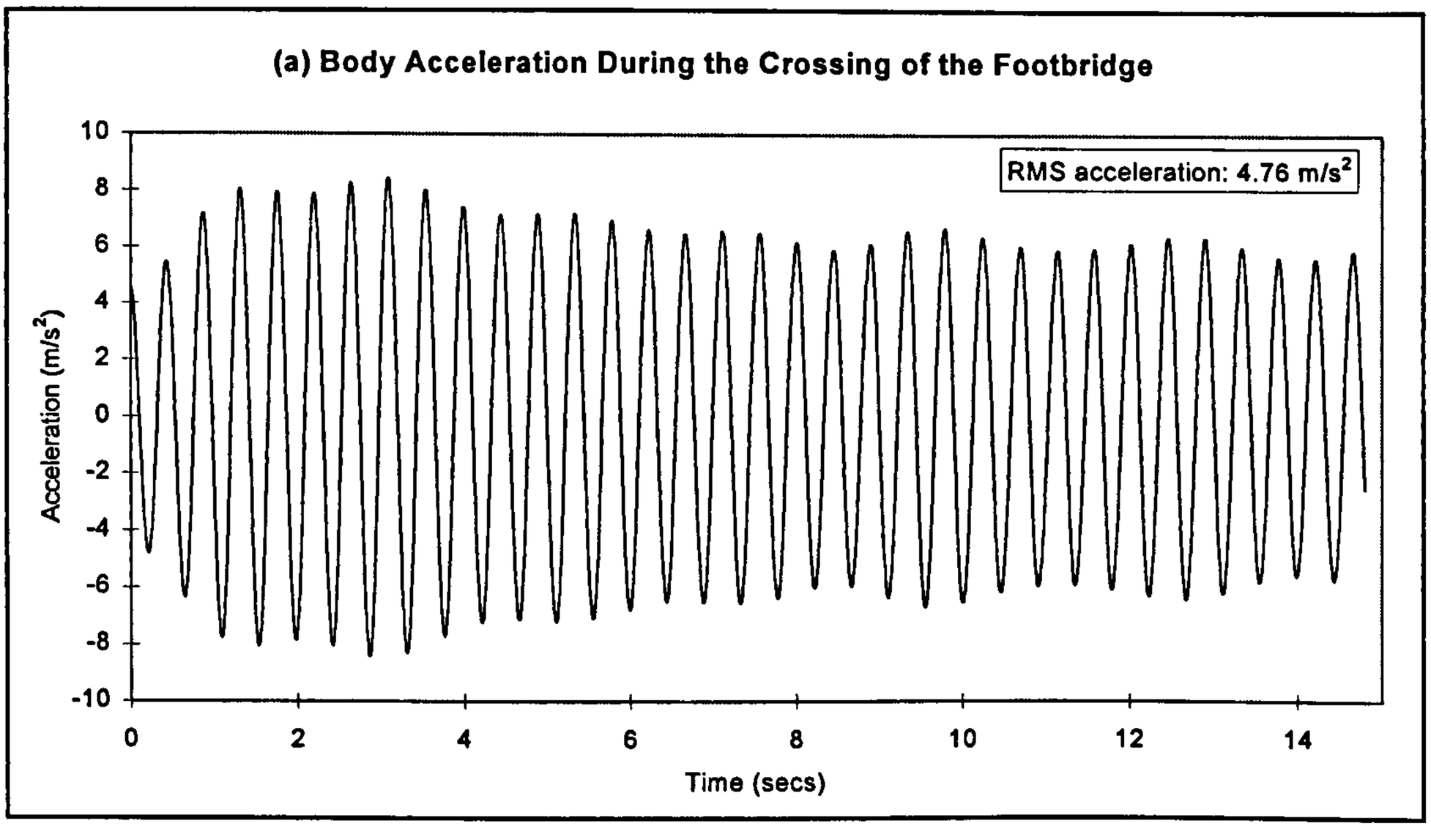

Figure 5.1 - Body accelerations (filtered) while walking on different surface conditions

Another pedestrian test was carried out aiming to investigate the effect that the vibration of the structure would present in terms of creating difficulties for a test subject to keep in phase with them. This was carried out by recording the accelerations in the mid span

of a footbridge tested in resonance conditions from two successive crossings of the same test subject. The test subject was walking at a pacing rate of 1.8 Hz, and the second harmonic of the walking load set the structure vibrating in resonance on its fundamental mode of 3.6 Hz (see details about the footbridge in Section 4.3). The superposition of the two measured time response signals in Fig. 5.2 shows that even in controlled conditions, it may be difficult to keep a steady pacing rate in phase with the vibration of the structure.

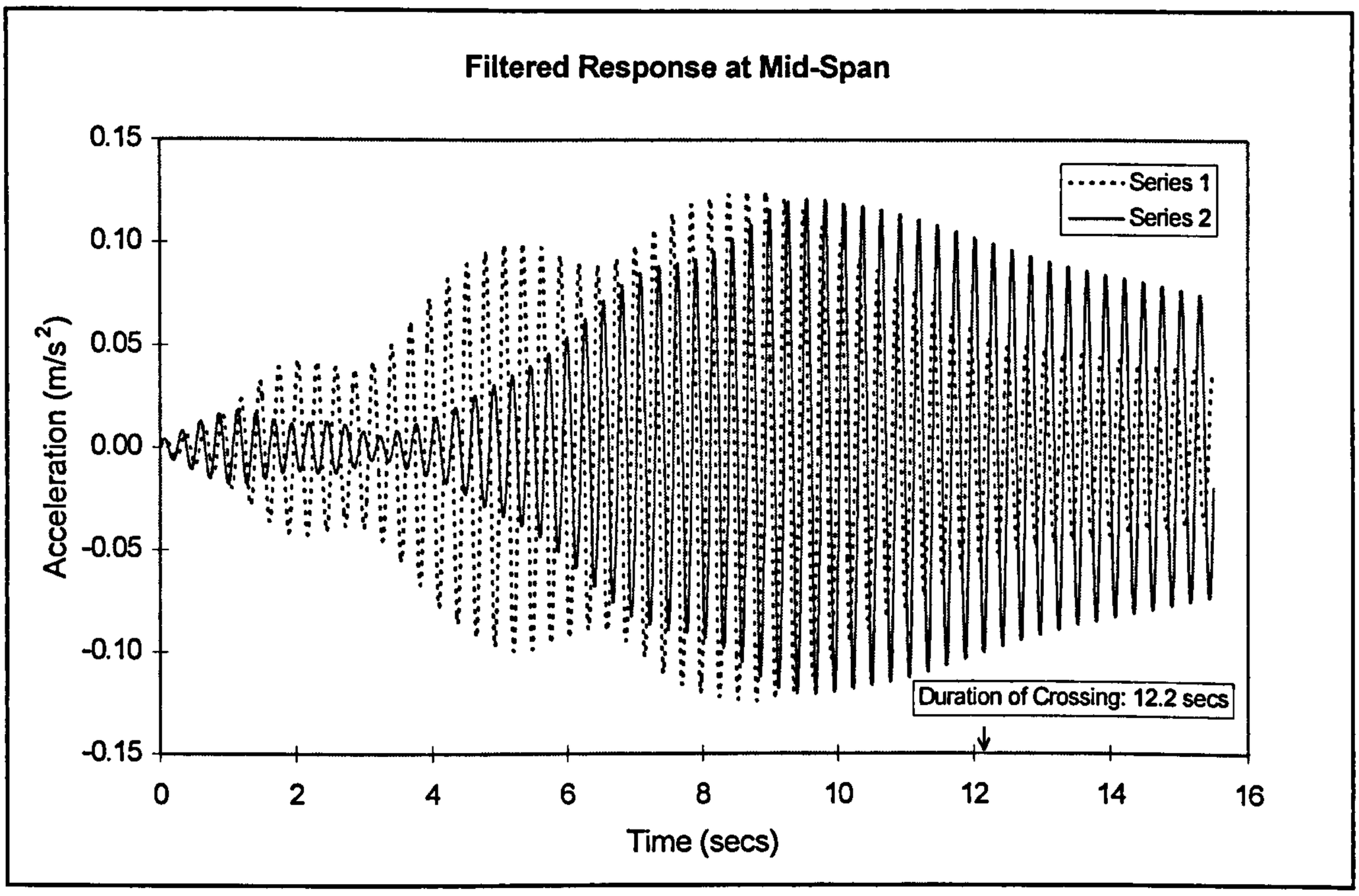

Figure 5.2 - Acceleration time response of a footbridge from two crossings of the same test subject

These effects show that changes occur in the load applied by a pedestrian while walking on vibrating structures when compared to that applied while walking on rigid surfaces. On the other hand, since the aim in defining such a load is usually to analyse the resonant response of structures, it seems more appropriate to obtain them from tests of prototype structures in resonance conditions. This was carried out focusing attention on obtaining the dynamic load factors of the first two harmonics of the load. Phase angles were not investigated. They would be of importance only if the effect of applying

simultaneously more than one harmonic of the pedestrian load was of interest. However, the analysis of vibration serviceability carried out in this study adopts only single frequency component excitations.

The procedure adopted for obtaining the dynamic load factors is based on a comparison between the results from pedestrian tests on footbridges and numerical simulations. The latter uses the theoretical load model (Eq. 2.1) and the calibrated FE model of each footbridge. In more detail, the procedure can be outlined in three stages:

1 - Controlled pedestrian tests were carried out on two footbridges. The test structures were a single span composite footbridge and a single span stressed ribbon footbridge, described in Sections 4.3 and 4.4, respectively. Two test subjects, who incidentally were the same weight, were employed. Their common weight varied slightly from 730 N to 740 N between the tests on the stressed ribbon and the composite footbridge, respectively. The pacing rate of the tests was set to excite the fundamental mode of vibration of each test footbridge. The acceleration responses of the footbridges during the crossing were measured at the antinodes of the mode shapes of the structure being excited, and were filtered to contain only the contribution of the harmonic of interest. The time spent during the crossing was measured using a stop watch. The number of samples per second varied according to the pacing rate and was set to guarantee an accurate evaluation of the amplitude of the accelerations (see comments about this in Section 4.2).

2 - Numerical simulations were performed using the calibrated FE models of the test footbridges, to obtain acceleration time responses at the same positions in which they were measured in the pedestrian tests. Details about the modal testing and calibration of the FE models of each test footbridge were described in the respective Sections of Chapter 4. The elastic modulus of the structure's constituent material was finely adjusted to ensure that the calculated and measured natural frequencies of interest were the same (to two decimal places). This was to avoid minor differences between the periods of the measured and calculated sinusoidal responses, which would be cumulative throughout the several cycles of vibration contained in both acceleration records.

The pedestrian forcing function defined by Eq. 2.1 was employed containing, however, only the term of the harmonic component of interest. The forcing function was applied at successive nodes of the FE model, one at a time, to simulate the pedestrian movement along the structure. The weight G was adjusted to the weight of the test subjects and the frequency of the excitation was set to the natural frequency of the test structure that was being excited. This frequency was either equal to the pedestrian pacing rate f_p, in the case of investigating the first harmonic of the load, or was equal to double the pacing rate, in the case of investigating the second harmonic of the load.

The length of time for which the load remained at each node was determined by dividing the average time spent by the test subject to cross the structure by the number of nodes to which the load was applied. The spacing of 0.9 and 1.0 m between the nodes of the FE models of the footbridges was reasonably compatible with the stride of the test subjects walking at pacing rates of 1.8 Hz and 2.37 Hz. These were the pacing rates of the pedestrian tests on each footbridge, respectively. The net result was that the duration of the load at each node was compatible with the time spent for each footstep.

At each node, the sinusoidal load was divided into approximately 40 load increments, corresponding to 20 increments per cycle. The mode superposition method was employed using the Newmark constant average acceleration scheme (ANSYS, 1992). A time step was adopted to be smaller than 1/100 of the period of the vibration in each case, to guarantee negligible period elongation (Bathe, 1982).

The suitability of this setting and also the accuracy of the subsequent calculation of the accelerations by the FE package (ANSYS, 1992) was assured by comparing the numerical calculations with the analytical results, for a simply supported straight beam of geometric and material properties similar to those of one of the test footbridges. In this case, the sinusoidal load was centrally applied to the beam. The numerical acceleration time response, produced by modelling the load as previously mentioned, was found to be in very good agreement with the analytical result (Rao, 1995), the difference in the peak acceleration being less than 0.25% (Fig. 5.3).

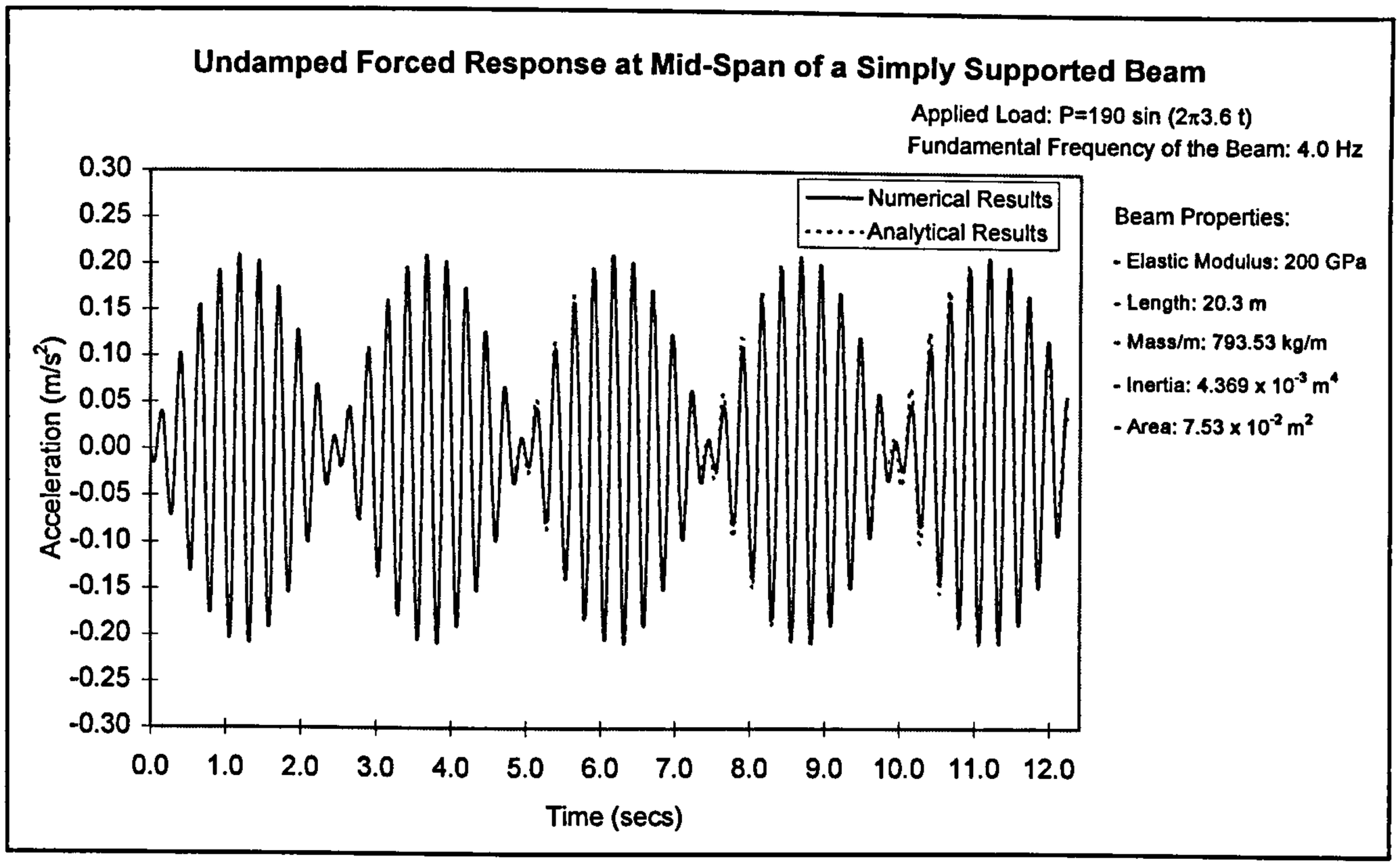

Figure 5.3 - Accuracy of the calculation of accelerations by the numerical procedure

Two aspects of the modelling of the load are worth mentioning. The first one is that the term in Eq. 2.1 that accounts for the static weight G of the pedestrian is not being applied together with the harmonic component of interest of the load. This is because the load is applied to successive nodes and is not gradually transferred from one node to the next, i.e. the transfer mechanism of the load between the feet is not being simulated. Therefore, if the static component G was being applied, there would be a sudden increase of the load from zero to the static weight G (a step load) in each node to which it was applied. This would generate a behaviour different from the actual way the load is applied by the test subject.

However, it is appropriate to note that Eq. 2.1 is conceived so as to represent the total load applied by a pedestrian walking, being a summation of the loads applied by each foot. It disregards how the load is applied by each foot and the transferring of the load between the feet. A remaining question is whether the absence of the static weight makes a significant difference in terms of the acceleration response of the structure. This was checked by comparing the numerical results obtained by this load model with one in which a gradual transfer of the load between the feet was modelled, with the inclusion

of the static weight *G*. The latter load model actually represented a pulse train of loads applied by the feet while walking. It was developed based on the sketch presented in Fig. 2.1, in which the increase of the load from each foot up to the static weight and back to zero was considered to vary linearly, and the fluctuating part in between was modelled by using the first harmonic component of Eq. 2.1. The contact duration of each foot and the duration of the overlap stage between the feet were taken from a chart presented by Inman *et al.* (1994) for an adopted pacing rate of 2.37 Hz, making it possible to construct a pulse train.

These load models were applied in the FE model of the stressed ribbon footbridge and accelerations were calculated at the antinode of the fundamental mode. They are shown in Fig. 5.4, in which the differences in RMS and peak accelerations were of the order of 9 %. The small differences obtained provided reassurance for the use of Eq. 2.1 without the inclusion of the static weight *G*.

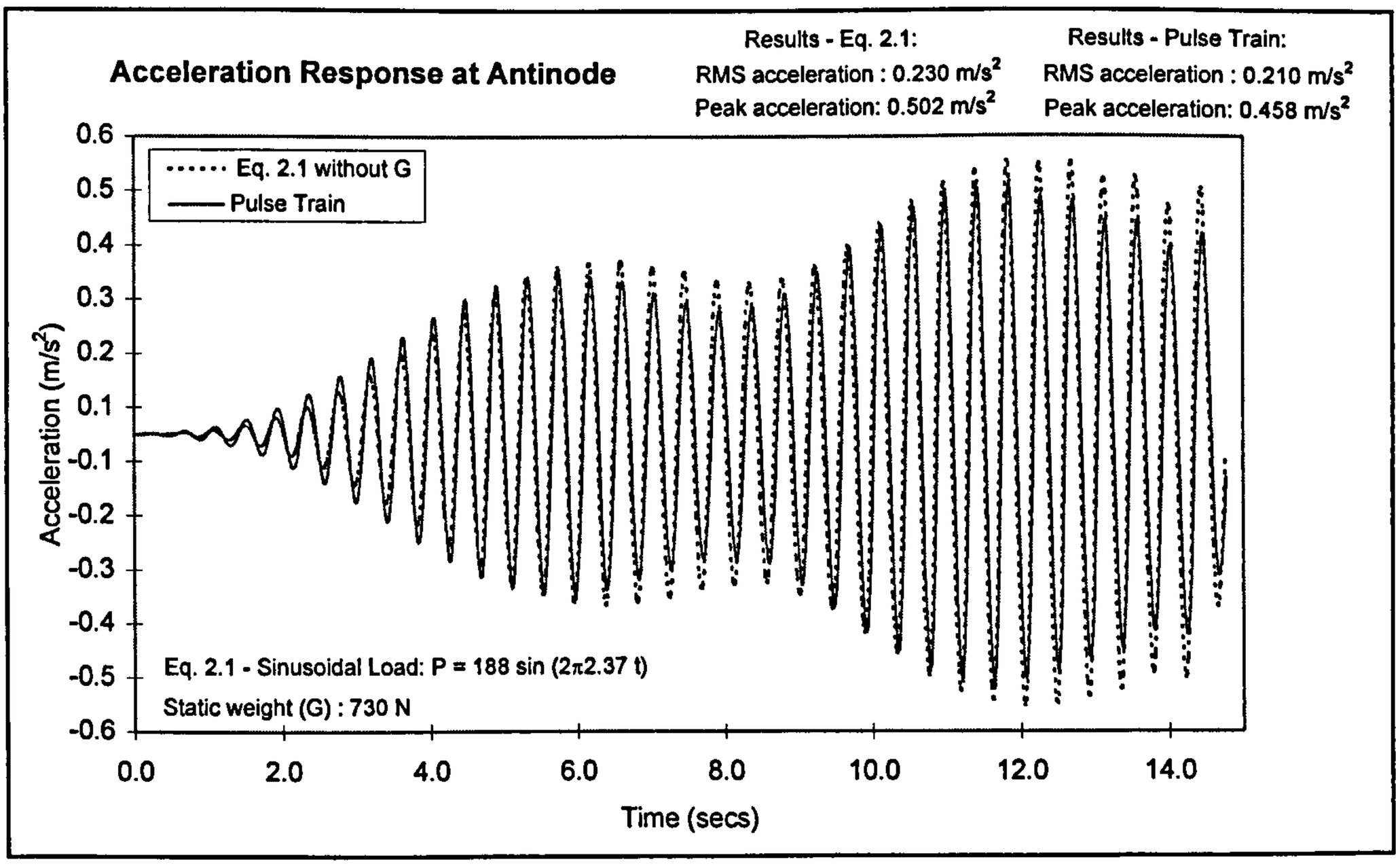

Figure 5.4 - Acceleration responses from different load models

The second aspect about modelling is whether the representation of the pedestrian as a load only is satisfactory, i.e., if the interaction between the pedestrian and the structure is such that, even for a single pedestrian, it may induce changes on the dynamics of the

system. It should be noted that changes possibly induced in the applied load by the pedestrian/structure interaction can be taken into account when comparing the numerical and experimental results. Nevertheless, changes in the structure, taking the pedestrian as a dynamic system, were not considered. This would imply that a dynamic nonlinear analysis was carried out because the system comprising both the structure and the pedestrian, both modelled as dynamic systems, would be changing during the crossing. However, as will be seen in Section 5.2.3, the level of changes in the structure induced by a single pedestrian or a small group walking can be considered negligible.

Finally, there is the question of which damping value should be adopted for the structure in the numerical calculations. The question arises because of the different values for damping obtained from the free-vibration decay tests, for the test subject staying on the bridge (after jumping tests) or leaving the bridge (following walking tests). The former were always higher than the latter. However, the actual damping value of the system during the crossing of pedestrians depends on the extent of the interaction between them and the structure. This is not a well understood phenomenon and the actual damping value during the crossing is expected to be within these two aforementioned values. For deciding which value to take, it should be noted that a reduction in the dynamic load factors obtained from tests on rigid surfaces is expected, to take into account the difficulties a test subject may experience keeping in phase with the vibrations. Therefore, in order to be conservative in adjusting the results of the numerical simulations to the measurements, the higher damping value from free-decay of jumping tests was adopted.

3 - The third stage of the procedure for obtaining the dynamic load factors consists of comparing the measured and numerical acceleration time responses. The first point to observe here is the alignment in time between the two sets of results since there was no electronic control to initiate the measurements on site. Therefore, the measurements were actually initiated before the test subjects had begun crossing the footbridges. The identification of the beginning of the crossing on the recorded measured time response was guided by the increase in response levels, and also by identifying the free-decay after the crossing. A comparison of the measured and calculated acceleration traces completed the process of aligning the two time signatures.

Ideally, the two time signatures would broadly coincide or would be different by a multiplying constant due to the use of an incorrect dynamic load factor in Eq. 2.1. The dynamic load factor would then be corrected in order to enable the calculated acceleration signature to be superimposed on to the measured one. Nevertheless, factors like the pedestrian-structure interaction or the pedestrian's difficulty in keeping in phase with the vibration of the structure can cause discrepancies between the two time signatures. Therefore, it is not expected that the two time signatures would possess an identical shape.

In order to obtain a dynamic load factor that can take into account the differences between the two signals and sensibly produce the same net effect of the load applied by the test subjects, it is suggested here that the RMS acceleration be adopted as a reference value in the calibration process. This is tantamount to saying that the Fourier Spectrum of both signals should present the same amplitudes, according to the Parseval theorem (Eq. 3.13).

This means that the dynamic load factor is adjusted until the RMS acceleration of the calculated time signature equals the average RMS acceleration obtained from the pedestrian tests. This process is facilitated by the fact that the two test subjects had the same weight and thus it is not necessary to repeat the numerical calculations twice. In addition, since the problem is linear, there is a proportionality between excitation and response which helps in finding a value of the dynamic load factor that promotes the required adjustment.

What follows are the results obtained using the recommended procedure. Two groups of results are presented, according to which harmonic of the walking load is being investigated.

(a) - Dynamic load factor of the first harmonic of the walking load

This was obtained from tests and numerical simulation of the stressed ribbon footbridge (see Section 4.4). The pacing rate of the test subjects and the frequency of the forcing function Eq. 2.1 in the numerical simulations were both set to 2.37 Hz. The pacing rate was very close to the fundamental frequency of 2.35 Hz of the structure, this being evaluated from the tail end of walking tests (Table 4.8).

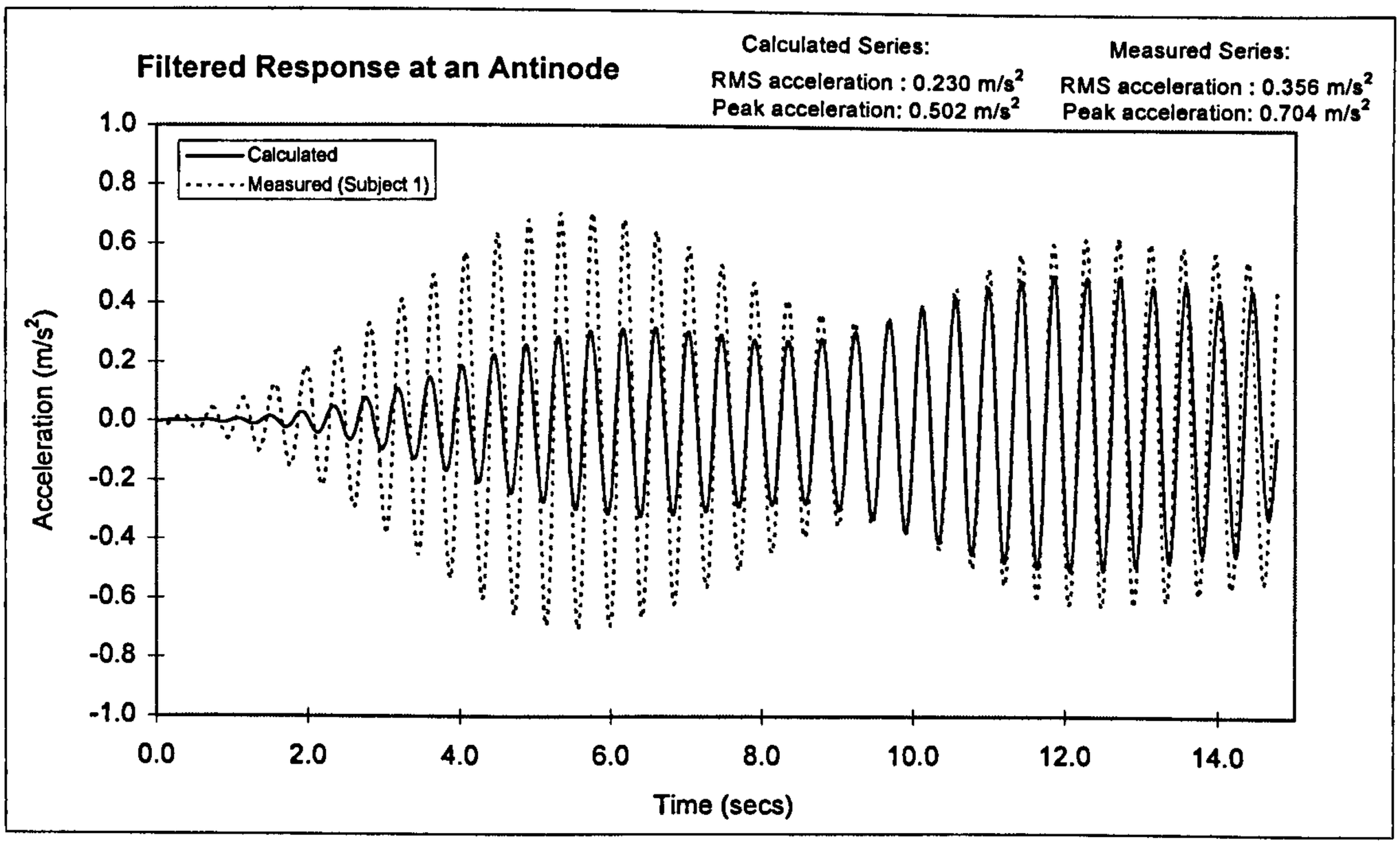

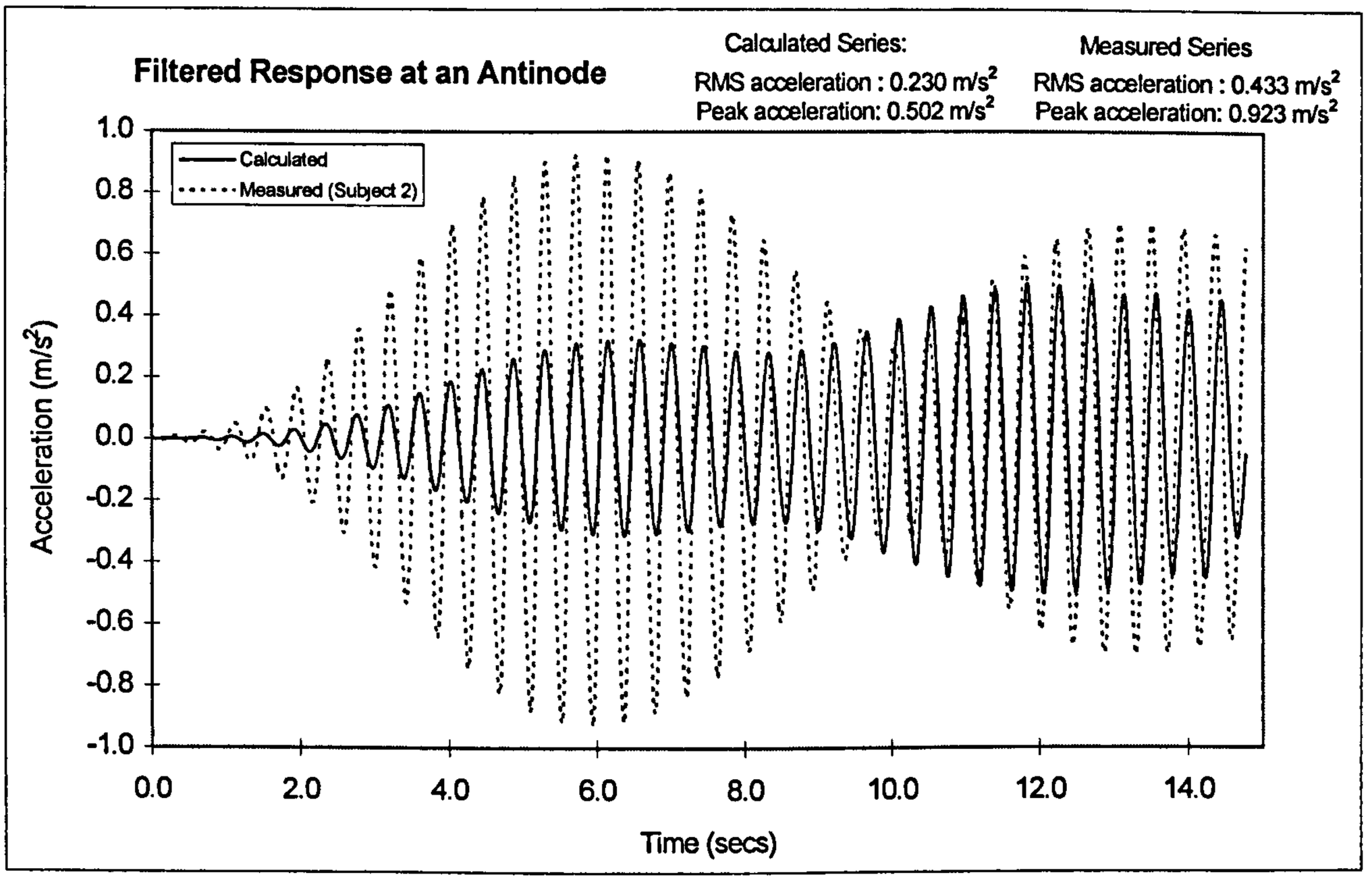

Figure 5.5 - Calculated ($\alpha_1 = 0.257$) and measured time response signals of each test

Comparisons were made between measured and calculated responses. In one of the calculated responses, the dynamic load factor (α_1) of 0.257 was adopted. This value is the one adopted in the UK (BS5400, 1978) and Ontario (OHBDC, 1991) codes (Fig. 5.5). In the other calculated response, the dynamic load factor of 0.49 was

employed (Fig. 5.6). This value was obtained from a linear interpolation between the load factors of 0.4 and 0.5 for pacing rates of 2.0 and 2.4 Hz, respectively (Bachmann and Ammann, 1987).

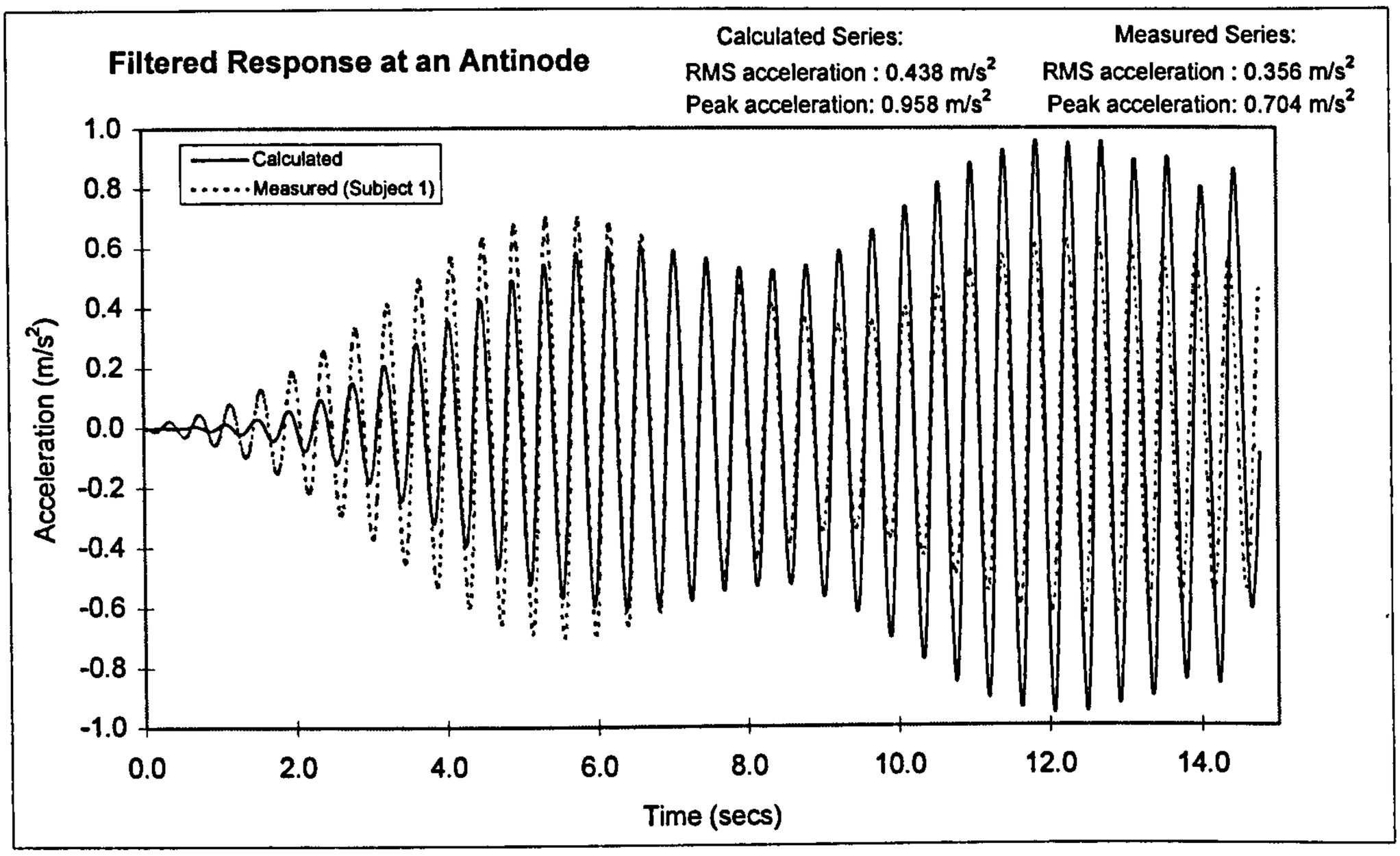

Figure 5.6 - Calculated ($\alpha_1 = 0.49$) and measured time response signals of each test

Figs. 5.5 and 5.6 show the acceleration response signatures during the crossing of the footbridge, which takes about 15 secs according to site measurements. Calculating the average RMS acceleration from tests with two pedestrians gave a value of 0.395 m/s^2. On the other hand, the RMS acceleration values of the two calculated time signatures were 0.230 m/s^2 and 0.438 m/s^2, for the dynamic load factors of 0.257 and 0.49, respectively. These calculated RMS values are proportional to the load factors adopted in the respective numerical exercises, keeping a ratio of (0.49/0.257) between them. Multiplying one of these calculated time signatures by a constant in order to adjust its RMS value to the average RMS measured value of 0.395 m/s^2 produced a dynamic load factor of 0.44. This implied a reduction at about 10% on the dynamic load factor of 0.49 suggested in the literature for this pacing rate. On the other hand, it is substantially higher than the value of 0.257 adopted by the codes.

It should be noted that in both Figs. 5.5 and 5.6, for both test subjects, the measured accelerations were higher than the calculated accelerations at the beginning of the record, even when the dynamic load factor of 0.49 was employed. This is thought to be due to the fact that the slope of the catenary shaped deck is also higher in this region, inducing an increase in the load applied by each foot. These measured results are consistent with the respective increases in acceleration measured at the waist level of a test subject while walking in this region of the footbridge (Fig. 5.1a). Therefore, the reduction on the dynamic load factor suggested above is expected to be conservative for footbridges having a horizontal deck.

(b) - Dynamic load factor of the second harmonic of the walking load

This dynamic load factor was obtained from tests and numerical simulations of the composite footbridge (see Section 4.3). The structure has a fundamental symmetric mode of 3.6 Hz, within the frequency range of the second harmonic of the walking load. The pacing rate of the test subjects was set to half of this value and so the fundamental frequency of the footbridge was excited by the second harmonic of the load. On the other hand, the frequency of the forcing function Eq. 2.1 was set at the fundamental frequency of 3.6 Hz since the frequency of the second harmonic of the load is double the pacing rate. Two load cycles are thus applied per node of the FE model, simulating the

desired 'pacing rate' of 1.8 Hz for the movement of the load over successive nodes. The duration of the crossing measured on site was of 12.2 secs.

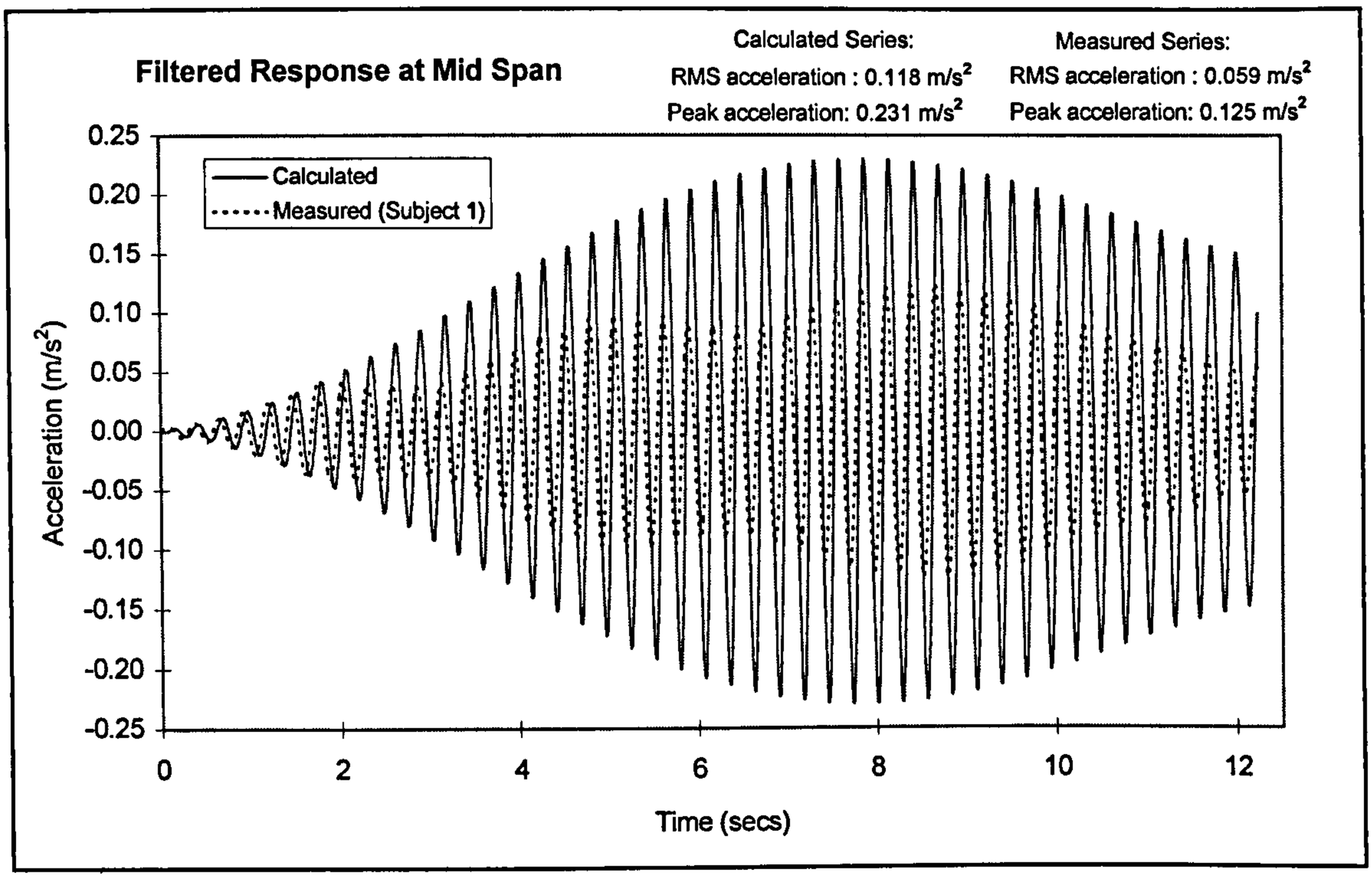

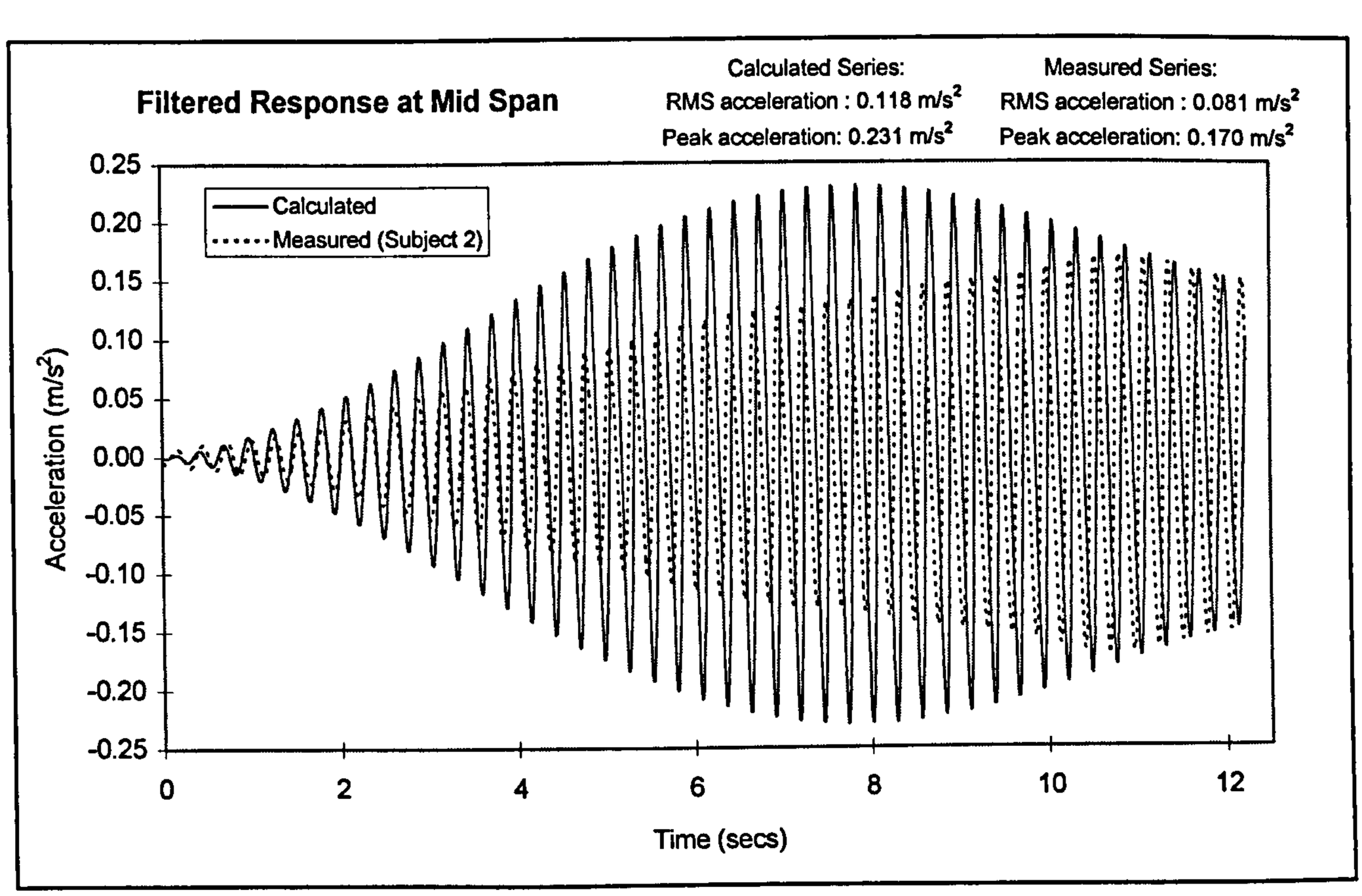

Figure 5.7 - Calculated ($\alpha_2 = 0.1$) and measured and time response signals of each test

A comparison was again made between measured and calculated responses. In the latter, the value of 0.1 was adopted as a dynamic load factor (α_2). This load factor was taken from the work of Bachmann and Ammann (1987) (see Table 2.1). The comparison between the numerical and the measured time signatures is presented in Fig. 5.7.

Following a similar procedure as to that adopted in the previous case, the average RMS acceleration from the tests with two pedestrians was calculated as 0.070 m/s^2, whereas a calculated RMS acceleration of 0.118 m/s^2 was obtained in the numerical exercise. Adjusting the dynamic load factor to produce a calculated time signature with this same RMS value led to a value of α_2 equal to 0.06 . This implied a reduction of 40% in the value of the dynamic load factor of 0.1 suggested in the literature.

The two investigations show that the adoption of a unique load factor of 0.257 by the UK (BS5400, 1978) and Ontario (OHBDC, 1991) codes is not appropriate. Use of the code value generates significant underestimates and overestimates of the response in the frequency range of the first and second harmonics of the walking load, respectively. This was expected in view of the values for dynamic load factors proposed in the literature for each of these frequency ranges (see Section 2.2.1).

However, the results showed that use of these latter values would result in an overestimation of the vibration response. Different reductions would apply for each of the frequency ranges, and the reason for this can be found by comparing the measured and calculated time signatures of Fig. 5.5 or 5.6 with Fig. 5.7. It can be seen that it is more difficult to keep in phase with vibrations the frequency of which are multiples of the pacing rate. Therefore, a more substantial reduction in dynamic load factors would apply for the frequency range of the second harmonic of the load.

5.2.2 Load Model for a Group

The usual approach for considering the effect of groups of people is by using a crowd magnification factor, as described in Section 2.2.2. An initial point for discussion is the treatment given to the effect of a group of people by the UK (BS 5400, 1978) and Ontario (OHBDC, 1991) codes. In both codes, the assessment of vibration serviceability

is based on the accelerations produced by a notional pedestrian exciting the structure in resonance conditions.

The use of a notional pedestrian was deemed to be sufficient based on the application of the procedures outlined in the codes to some existing footbridges (Blanchard *et al.*, 1977). Nevertheless, in several of the case reports of lively footbridges (Table 2.2), complaints were made in situations in which the structures were subject to excitation produced by several pedestrians.

Studies of the effects of groups of people walking have been presented in the literature, and several magnification factors of the response of a single pedestrian have been proposed (Fig. 2.7). As was discussed in Section 2.2.2, the validity of the theoretical magnification factor proposed by Matsumoto *et al.* (1978) (Eq. 2.3) was confirmed by Eriksson (1994), from tests using small groups of people in uncoordinated movements. Concern in applying it might arise from the fact that it implies a significant increase in the acceleration levels, which may, in turn, make the design too onerous to prevent the higher levels of accelerations that would result. As an example, for ten pedestrians simultaneously crossing a footbridge, the magnification factor to be applied to the response of a single pedestrian is approximately 3; for three pedestrians, the accelerations are to be increased by 73%.

Drawing a parallel between the application of Eq. 2.3 as a crowd magnification factor and the procedure recommended by the aforementioned codes, it may be noted that Eq. 2.3 represents a magnification to be applied to the mean vibration amplitude generated by a single pedestrian. However, if such a mean amplitude is obtained by a single pedestrian walking at a (coordinated) pacing rate equal to the fundamental frequency of the footbridge, it is expected that the net result of applying Eq. 2.3 would be an overestimation of the response of several uncoordinated pedestrians.

Some tests carried out with small groups of pedestrians have provided evidence of the potential overestimation that the application of Eq. 2.3 would produce, if the evaluation of the accelerations produced by a single subject is obtained using a controlled pacing rate equal to the fundamental frequency of the footbridge. In the first test, three

pedestrians were walking at leisure using pacing rates of their own choice (around 1.8 Hz) on the stressed ribbon footbridge (see Section 4.4 for details about the structure). The RMS acceleration obtained from this test was of 0.08 m/s^2, which is less than one fourth of the average RMS value of 0.395 m/s^2 obtained from controlled tests in resonance conditions using a single subject (Fig. 5.5 or 5.6). If Eq. 2.3 was applied as a multiplying factor to the average RMS acceleration of the controlled tests using a single pedestrian, it would result in a RMS acceleration of 0.68 m/s^2, against 0.08 m/s^2 actually measured on the test using three uncoordinated pedestrians.

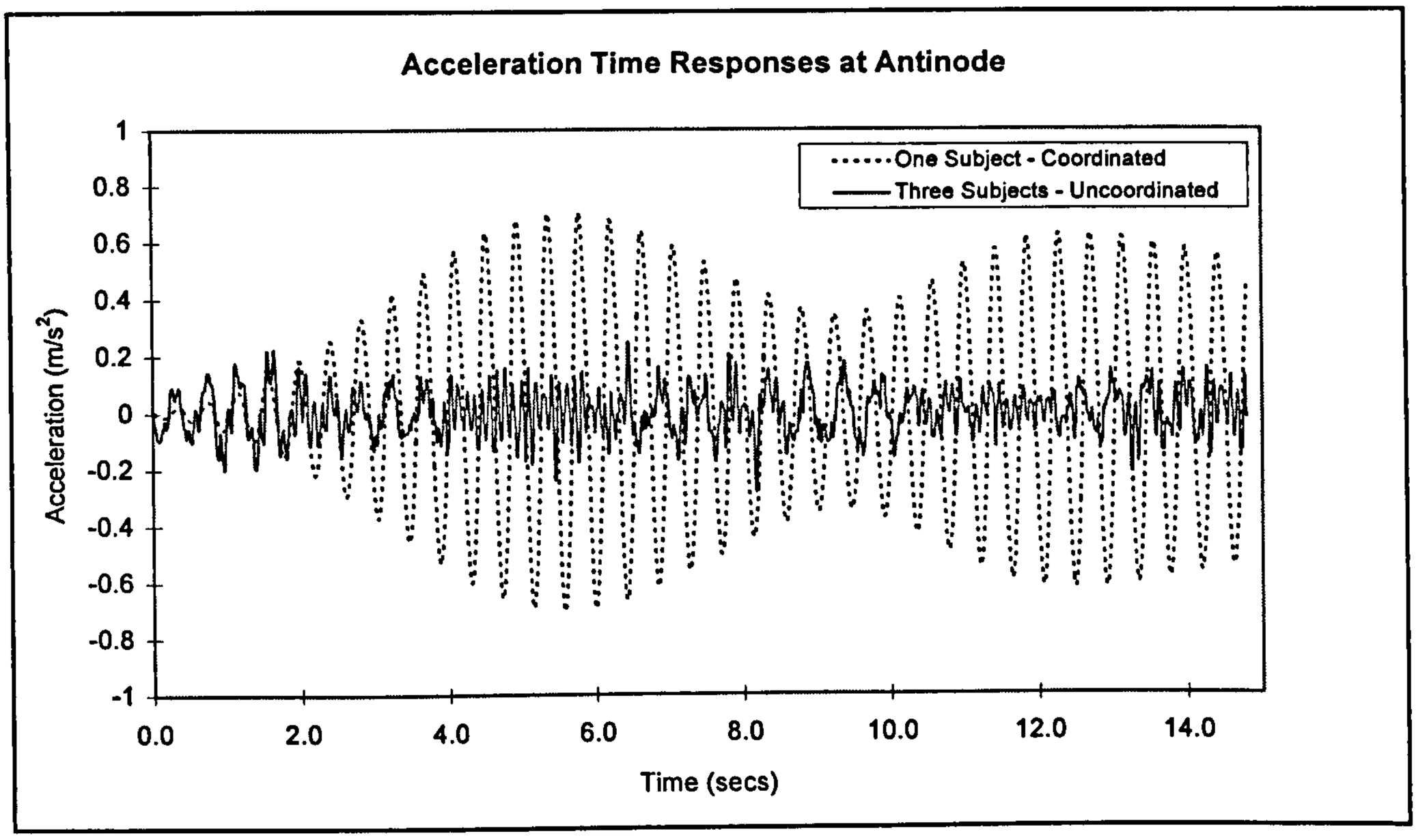

Figure 5.8 - Acceleration time signatures from pedestrian tests on the stressed ribbon footbridge.

The second test showed the same general trend. In this case three pedestrians were walking at leisure on the composite footbridge (see Section 4.3 for details about the structure). A comparison between the time signature produced by this test and one from a controlled pedestrian test using a single pedestrian is shown in Fig. 5.9. The application of the magnification factor Eq. 2.3 on the average RMS acceleration of 0.07 m/s^2 of the controlled tests using a single pedestrian (Fig. 5.7) would produce a RMS acceleration of 0.12 m/s^2, compared with 0.09 m/s^2 measured on the test using three uncoordinated pedestrians.

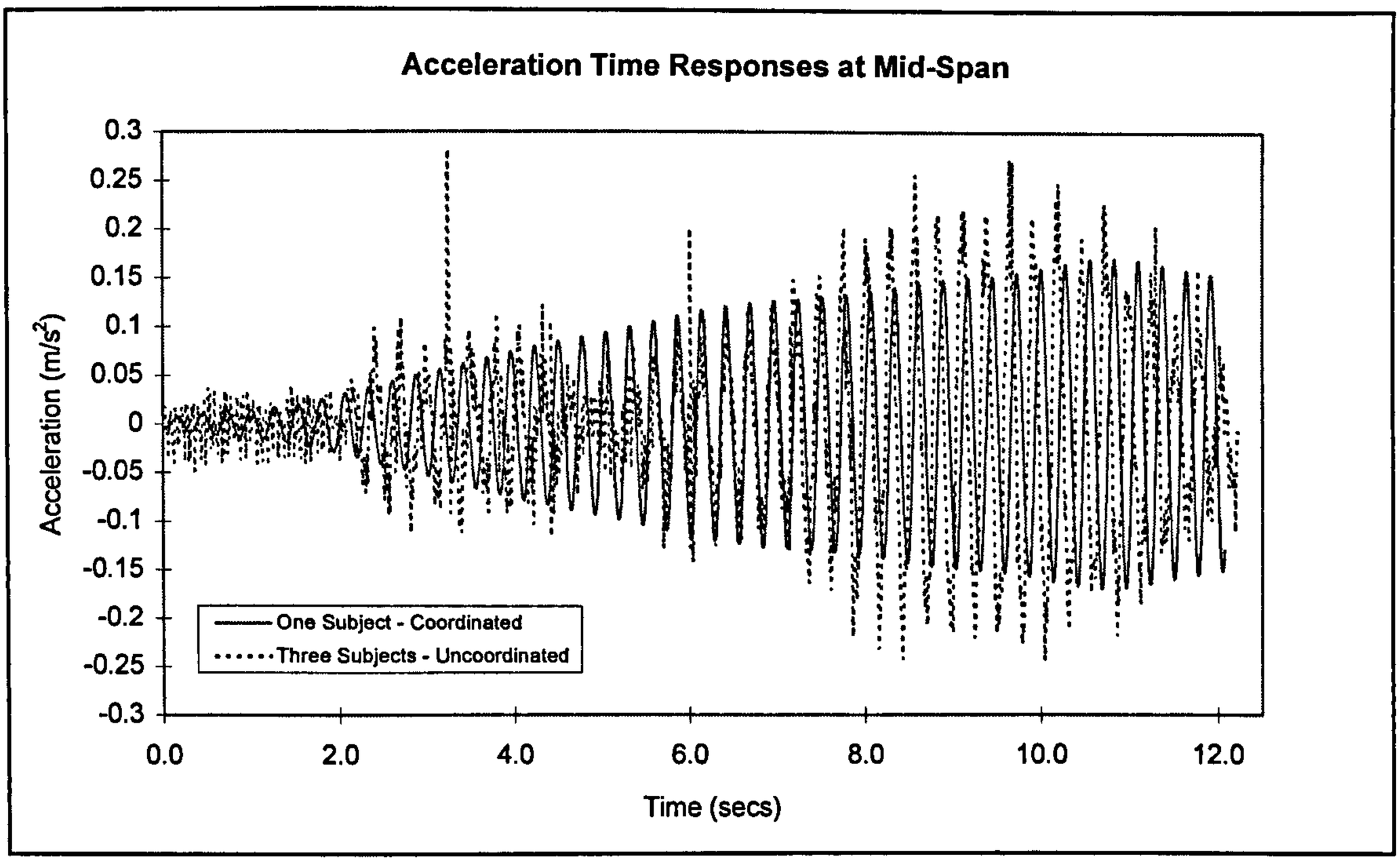

Figure 5.9 - Acceleration time signatures from pedestrian tests on the composite footbridge

The difference in magnification presented by the same number of test subjects with respect to that obtained by applying Eq. 2.3 can be explained by the difference between the pacing rates of the test subjects (around 1.8 Hz) and the natural frequency of the structure being excited. In the case of the tests carried out on the stressed ribbon footbridge, its fundamental frequency was 2.3 Hz and thus the excitation by uncoordinated pedestrians was out of resonance. On the other hand, in the case of the composite footbridge, its fundamental frequency of 3.6 Hz was excited by the second harmonic of the load produced by pedestrians walking at their own pacing rate.

An outcome of these results is that the application of the design procedure of either the BS5400 (1978) or Ontario (OHBDC, 1991) codes, in terms of using a single pedestrian in coordinated walking exciting a footbridge in resonance conditions, generally produces accelerations higher than those from a small group of pedestrians in uncoordinated walking.

Nevertheless, it is expected that there will be a point (i.e. a number of pedestrians) above which it would be necessary to apply a magnification factor to the response of a

single pedestrian, to take into account the effect of a crowd crossing the structure. A word of caution is, however, necessary: no experimental evidence was found regarding the validity of Eq. 2.3 for larger groups of pedestrians; in particular because the application of Eq. 2.3 does not take into account the synchronisation that may occur in larger groups.

With regard to synchronisation effects, the only relevant research found covering the topic was by Grundmann *et al.* (1993), which resulted in the proposal for a crowd magnification factor given in Eq. 2.4. Nevertheless, this factor actually resulted in smaller magnification than that proposed by Matsumoto *et al.* (1978) (Eq. 2.3) for any number of pedestrians up to 55 (obtained by equating Eqs. 2.3 and 2.4).

5.2.3 Pedestrian-Structure Interaction

A final point for consideration is the level of alteration to the modal properties of a footbridge due to the presence of several pedestrians walking. The scarce results presented in the literature on this subject in the case of pedestrians walking has provided some evidence that their effect in changing the dynamics of the system, if at all, would occur to a lesser degree than that caused by people standing still (see Section 2.2.1).

However, it is difficult to detect changes in the natural frequencies of a footbridge from measurements taken while the structure is being crossed by pedestrians. Measurements taken in this situation may indicate the frequencies of the excitation instead of the potentially modified natural frequencies of the structure. On the other hand, the effect of pedestrians in changing the dynamics of the system would be of significance only if reasonable vibration levels were attained; otherwise, the mobilisation of the dynamic forces of the bodies of the pedestrians would be negligible.

A test programme encompassing two different tests was prepared in an attempt to determine whether pedestrians walking could change the natural frequencies of a footbridge. The structure tested was the stressed ribbon footbridge (Section 4.4). However, during the days of these supplementary tests, the ambient temperature was significantly lower than it was during the major test programme described in

Section 4.4. The effects of temperature on this structure are such that the shortening due to a reduction in temperature leads to an increase on axial tension, since the structure is fully restrained at the supports. This would imply an increase in natural frequencies, as observed in the initial measurements carried out.

Two test subjects were used in this test programme. The longest acquisition time available on the spectrum analyser of 64 secs (see Appendix A.1) was adopted, being related to a frequency resolution of 0.015625 Hz. This would give some level of confidence in the evaluation of the frequencies up to two decimal places, since the level of variation of the natural frequencies of the structure amongst the tests was expected to be small.

Initially, the natural frequency of the structure was evaluated from the free-decay of jumping tests (two subjects staying at the antinode of the fundamental mode) and from the tail end of walking tests, after the test subject had left the bridge. The natural frequencies obtained were 2.39 and 2.44 Hz from the jumping and walking tests, respectively.

In sequence, two separate tests were carried out:

(a) Two test subjects were asked to walk together on the bridge during the whole acquisition time of 64 secs, at a pacing rate of 1.9 Hz. This pacing rate was reasonably far from the resonant frequency of 2.39 or 2.44 Hz previously mentioned. The Fourier Spectrum of the acceleration time response during the excitation at a point of the structure is shown in Fig. 5.10. It can be observed that, together with the higher peak around 1.9 Hz, corresponding to vibrations at the excitation frequency, two other peaks are present around 2.4 Hz, more precisely at 2.41 and 2.44 Hz.

(b) In a different test set-up, the same two test subjects were asked to, alternately, apply heel drops and walk side by side around the antinode of the fundamental mode of the footbridge using a pacing rate of their own choice that could keep the sequence of movements reasonably steady. The Fourier Spectrum of the acceleration time response is shown in Fig 5.11, where a higher peak at 2.41 Hz can be identified.

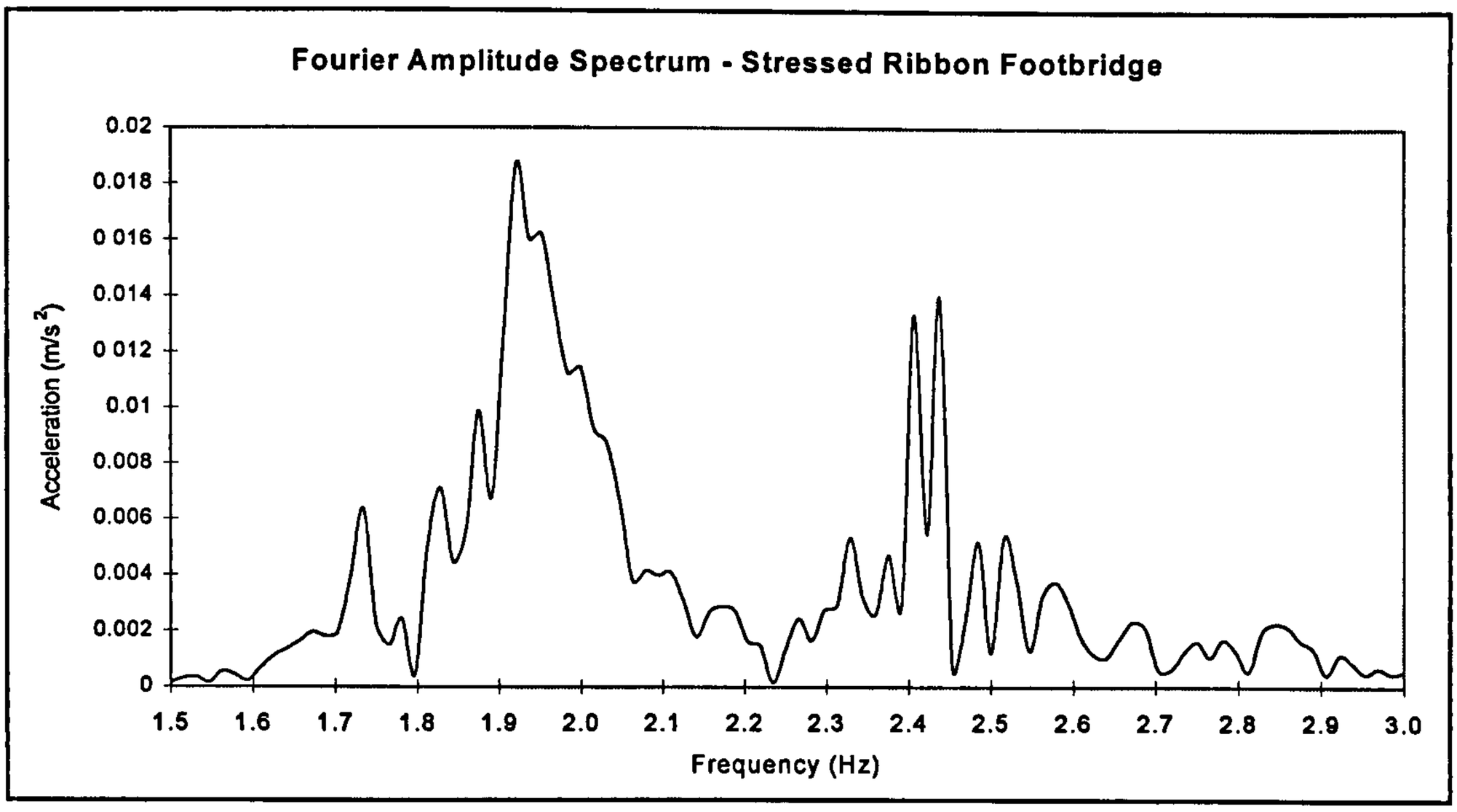

Figure 5.10 - Fourier Spectrum during walking tests - test set-up (a)

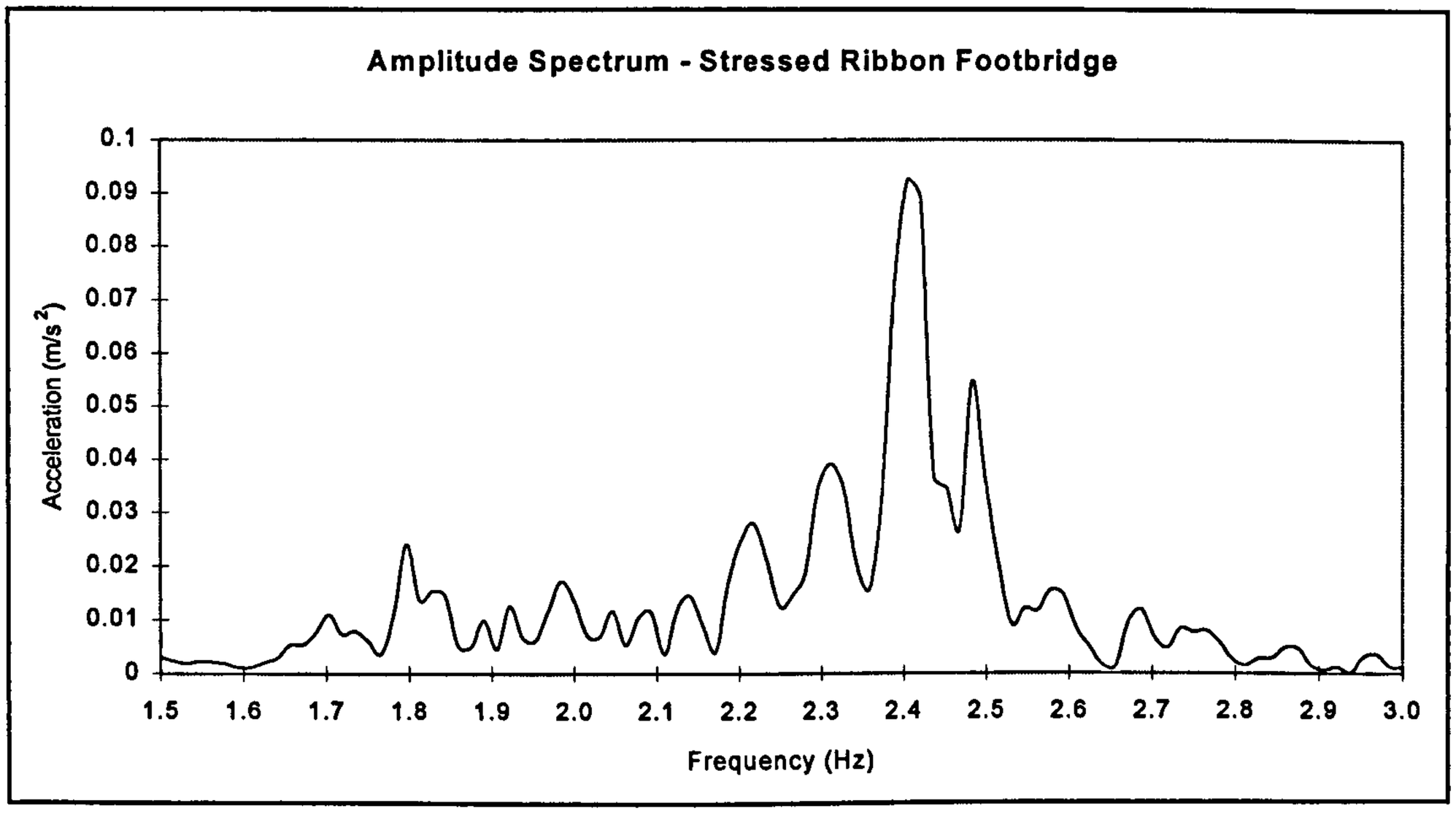

Figure 5.11 - Fourier Spectrum during walking test - test set-up (b)

A comparison between the structure's resonant frequency on these two tests and those obtained from the free-decay of walking and jumping tests shows that the natural frequencies of the structure during walking remained somewhere between those obtained from pedestrians standing still (after jumping tests) and without pedestrians (following walking tests). Nevertheless, it is not possible to quantify the level of variation due to the frequency resolution adopted in the test.

These results so far have shown that some variation of the dynamic properties of the structure takes place when pedestrians are walking over them, but to a lesser degree than those that would be produced by pedestrians standing still. The level of variation shown by the small group of pedestrians used in the tests was not of significance. However, a quantification of this effect would require a substantial test programme using different numbers of test subjects and structures with different ratios of dead to live load.

The reduction in natural frequencies observed during the tests may explain the occurrence of lively footbridges having natural frequencies closer to the upper limit of 2.4 Hz of the common range of pacing rates of pedestrians (Table 2.2). Such footbridges may have had their natural frequencies reduced by the presence of several pedestrians on them, which would more closely approximate the typical pedestrian pacing rate of 2.0 Hz. On the other hand, a compensating effect is the increase in damping arising from the presence of the pedestrians, which helps in reducing vibration levels.

The case of ACM footbridges would be more critical in this regard since the ratio of the live to dead load is higher in these structures than in those made of conventional construction materials.

5.3 Definition of Frequency Ranges of Interest

The very characteristic frequency ranges of the first two harmonics of the walking load in the vertical direction (Section 2.2.1) together with observation of case reports of lively footbridges (Table 2.2) show, without doubt, that these are the frequency ranges of interest for the assessment of vibration serviceability in this direction. Of the two frequency ranges of interest, from 1.6 to 2.4 Hz (first harmonic), and from 3.2 to 4.8 Hz (second harmonic), the former is the one of greatest interest since the amplitudes of the respective harmonic component of the walking load are much higher. Indeed, only one case report of a lively footbridge having its fundamental frequency within the frequency range of the second harmonic of the walking load has been found.

Another frequency range in the vertical direction worthy of attention is that associated with running, ranging generally from 2.5 to 3.5 Hz. The dynamic component of this

load within this frequency range was shown to have an amplitude which is more than three times that due to walking (see Section 2.2.1). Its consideration in terms of vibration serviceability would imply a much stricter design for footbridges having natural frequencies within this frequency range. Nevertheless, this is not supported by the case reports of lively footbridges, which leads to the conclusion that this is not a significant design loading case.

In the lateral direction, case reports of significant vibration within the frequency range of the first harmonic of this load make it necessary to consider such a frequency range (0.8 to 1.2 Hz) as one of interest for vibration serviceability.

Despite these observations, two factors need to be taken into account to define frequency ranges of interest to be used during design:

- The accuracy with which the modal properties of the structure (specifically, the natural frequencies) can be determined during design. The analysis of the prototype footbridges (see Chapter 4) revealed that aspects of modelling, such as whether or not the handrails have a structural function, and uncertainties in material properties and support conditions are factors expected to create discrepancies between natural frequencies calculated during design and present on the actual structure.

- The evidence of reduction on natural frequencies caused by the presence of pedestrians on a bridge, as was observed from the results presented in Section 5.2.3.

Therefore, despite the fact that the sources of excitation present very well defined frequency ranges, the definition of frequency ranges of interest for vibration serviceability should not be strictly limited to these ranges. The risk in doing this would be to have a footbridge with a calculated natural frequency outside these ranges and considered as presenting a satisfactory performance without further verification, whereas the actual structure when built could present natural frequencies within the critical ranges and be lively.

On the other hand, the level of uncertainty in the determination of such frequencies during the design stage cannot be predicted. A typical case was presented by

Deger *et al.* (1996), in which considerable differences between initially assumed foundation conditions of the pylon of a cable-stayed footbridge and actual conditions indicated from tests resulted in a difference of 37% in the fundamental frequency of vibration determined from design calculations and measurements.

Unfortunately, information is scarce about discrepancies between design and actual natural frequencies of footbridges. However, since it is necessary to consider extended frequency ranges of interest for design, the information available could provide guidance in defining extended frequency ranges.

5.4 Reviewing the Acceptability Limits to Vibration

Use of peak acceleration as a parameter to assess vibration serviceability in the vertical direction is adopted by the UK (BS5400, 1978) and Ontario (OHBDC, 1991) codes. The acceptability limits are defined by Eq. 2.5 and are based on independent tests carried out by Leonard (1966) and Smith (1969). The tests carried out by Kobori *et al.* (1974) (see Fig. 2.9) also resulted in a curve of similar shape.

There is a question of whether the use of peak acceleration represents adequately the variation of accelerations experienced by a pedestrian while crossing a footbridge and the human comfort while walking. This is because the maximum acceleration is experienced by the pedestrian only in the neighbourhood of the antinode of the respective vibration mode shape being excited. Besides, the duration of the exposure to vibrations while crossing the structure is not considered, and this was shown to be a parameter of crucial importance when assessing human comfort (Griffin, 1990).

One way ahead in defining proper acceptability limits to vibration in footbridges is by using a similar procedure as to those applicable to floors, which makes use of the RMS acceleration and/or the VDV (BS6472, 1992). The former parameter is an average of squared accelerations (Eq. 2.6), whereas the latter is based on the fourth power of the acceleration and also includes the time exposure to vibrations (Eq. 2.7).

However, the concept of comfort to vibrations for defining acceptability limits in terms of RMS acceleration or VDV considering the whole period of exposure to vibrations

may be not applicable to a situation in which a test subject is walking on a footbridge. Taking into account the effects of walking on human sensitivity to vibrations and the tests carried out by Smith (1969) to define acceptability limits for walking subjects (see Section 2.3.2), it may be the case that both the RMS and the VDV are not appropriate measures of exposure to vibration. This is because the sensitivity to vibrations while walking may be related solely to impairing of this movement, which would mainly be caused by the large vibrations experienced only in the regions of higher response during the crossing (i.e. the antinodes of the vibration mode shape). Therefore, the use of RMS or VDV taking into account the total exposure to vibrations during the crossing might lead to an incorrect evaluation of human response to vibration. How to take into account the time exposure to vibrations through the use of VDV, and also how to evaluate the actual importance of vibrations in regions other than the antinodes of the vibration mode shape deserve further study.

The variation of acceleration throughout the crossing for different mode shapes also seems to have a minor effect. Measurement of acceleration responses at antinodes of footbridges excited in modes of vibration of different shape had approximately the same crest factors (ratio peak/RMS acceleration) (Fig. 5.12). It should be noted that the acceleration signals shown in Fig. 5.12 are not actually those that would be experienced by a pedestrian since they are measured at a single point of the structure. However, the variation of the accelerations experienced by the pedestrian during the crossing would follow the vibration mode shape and have a similar shape to those presented in Fig. 5.12.

The results show a reasonably constant crest factor around 2.0, which can be useful for establishing relationships between peak and RMS accelerations in footbridges. However, until further studies are available, the continued use of peak acceleration as a parameter to assess exposure to vibrations in footbridges is recommended. In terms of acceptability limits, personal experience in carrying out tests (and experiencing the vibrations) on three footbridges, the first one presenting vibration levels below the limit established in the UK code (BS5400, 1978), the second marginally above the limit, and the third one significantly above the limit, provided reassurance that these limits are entirely suitable.

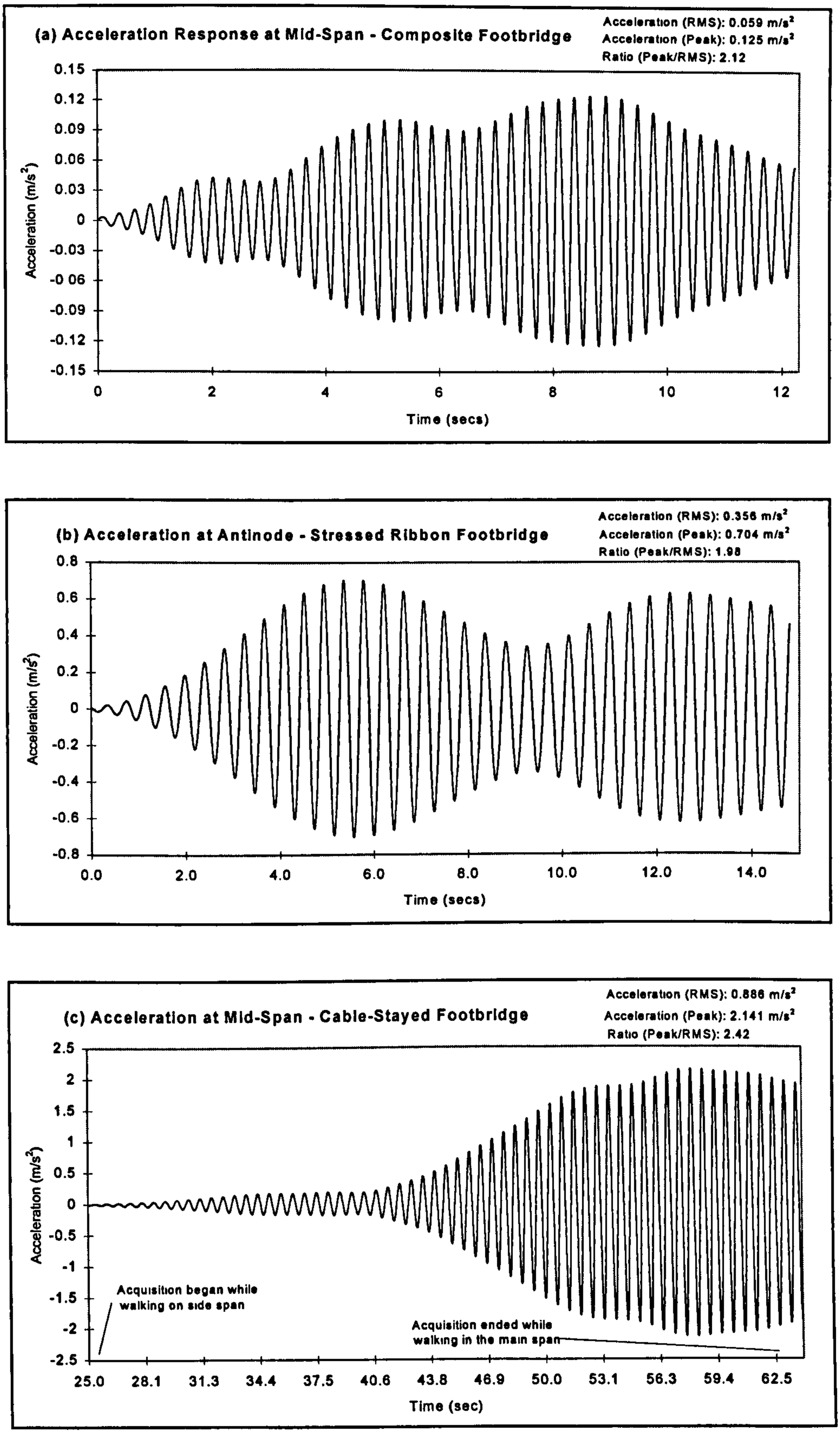

Figure 5.12 - Filtered acceleration time responses from controlled pedestrian tests in footbridges excited at their fundamental vertical mode

5.5 Vibrations with more than One Frequency Component

The procedures and acceptability limits available for evaluating footbridges for vibration serviceability in the vertical direction are related to single frequency motions. However, it is possible for a footbridge to have more than one of its natural frequencies within the specified frequency ranges of the harmonics of the walking load, as was the case in two of the footbridges tested. In cases like these, more than one natural frequency may be simultaneously excited by harmonics of the walking load. The response signal is thus composed of more than one frequency component.

Observing the behaviour of footbridges having different structural systems, for beam-like footbridges the natural frequencies are usually well separated. Taking as a reference a simply supported beam, the ratio between the n^{th} natural frequency and the fundamental frequency is the n^{th} term of the series (1, 4, 9, ... n^2 , ...) (Clough and Penzien, 1975). Therefore, it is not possible to have two or more natural frequencies within the frequency ranges of the harmonics of the walking load. The fundamental frequency is usually the one which may be within the critical ranges of the walking load. It should be noted that this is assumed in all the simplified expressions presented in Section 2.3.3 for assessing the vibration serviceability of beam-like footbridges.

However, for footbridges in which axial and bending effects are both significant (e.g. in arch, catenary and suspended bridges), a combination of these effects can result in closely spaced natural frequencies. In cases like these, a procedure to take into account vibrations with more than one frequency component would be required. Recent procedures for evaluating multi-frequency component vibrations have been proposed and are adopted for assessing vibrations in buildings (BS 6472, 1992). Nevertheless, developments of this criterion for footbridges would imply a definition of a new procedure to excite the structure as well as a new evaluation criterion since the current ones are based on a single frequency component excitation. Such a procedure would be more cumbersome in terms of design (e.g. by applying single notional pedestrians to excite each natural frequency of interest and superimposing the results).

However, by observing peculiarities in the excitation, acceptability limits and characteristics of some structural systems of footbridges, a simplified procedure is suggested. Initially, two situations of interest of multi-frequency component vibrations were identified: having more than one natural frequency within the same frequency range of an harmonic of the walking load (e.g., in the cable-stayed footbridge); and having natural frequencies in both frequency ranges of the first two harmonics (e.g. in both cable-stayed and stressed ribbon footbridges).

It should be noted that the magnitude of the second harmonic of the load excitation is seven times smaller than that of the first harmonic, according to the results presented in Section 5.2. Apart from this, excitations in the frequency range of the second harmonic have higher acceptability limits (see Eq. 2.5). Taking the central frequency of each frequency range as a reference leads to a ratio of 1.4 between the acceptability limits in each frequency range (by applying Eq. 2.5). Taking these ratios into Eq. 4.3 (response of a SDOF system) leads to a ratio of approximately ($7 \times 1.4 \approx 10$) between the modal masses of modes in the two frequency ranges. This is to say that the modal mass of a vibration mode within the frequency range of the second harmonic of the load would need to be one tenth of that for a mode within the frequency range of the first harmonic in order to be as critical for vibration serviceability.

On the other hand, the modal mass of each mode of vibration of a footbridge tends to be reasonably similar. Modal masses of simply supported beam-like footbridges have indeed the same value for all modes (Thomson, 1993). The modal masses of the test footbridges, having different structural systems, were calculated using their respective calibrated numerical models, and are presented in Table 5.1.

Apart from the second mode of the stressed ribbon footbridge (highlighted in the Table), it can be seen from Table 5.1 that the modal masses showed the same trend as that presented by a simply supported beam, i.e. they tended to be reasonably constant for each footbridge. This happens because in footbridges, the whole deck generally participates in all vibration modes. This is different from the vibrational performance of floors in which, for some modes, only a small portion of the floor may actively

participate in the vibration (Eriksson, 1994). The highlighted mode in Table 5.1 had a modal mass of about half of those for the other modes and was within the frequency range of the second harmonic of the walking load; however, it is still far from the ratio of 10 previously discussed.

Cable-Stayed Footbridge Total Mass: 20915 kg		Stressed Ribbon Footbridge Total Mass: 30157 kg		Composite Footbridge Total Mass: 20093 kg	
Mode	Modal Mass (kg)	Mode	Modal Mass (kg)	Mode	Modal Mass (kg)
V1	2547	V1	10791	V1	10230
V2	3330	V2	5666	V2	10652
V3	3466	V3	10369	V3	9721
V4	3511	V4	10024		
V5	3366	V5	11891		
V6	3633	V6	12128		
V7	2910				
V8	3679				
V9	4100				

Table 5.1 - Modal masses of the test footbridges

Therefore, if there are natural frequencies simultaneously present in both frequency ranges, since the ratio of the modal masses of the respective modes of vibration has been shown well below the reference value of 10, only those frequencies within the first frequency range would need to be considered.

The remaining case is to investigate how to consider two frequency components within the same frequency range, for which the excitation forces and acceptability limits are approximately the same. Pedestrians tests carried out on the cable-stayed footbridge provide evidence that, in this situation, the vibration mode shape has a significant influence in determining vibration levels. Plots of acceleration responses from crossings of the same test subject, in which the footbridge was set vibrating in resonance are presented in Fig. 5.13. In each case, the test subject adjusted his pacing rate to the natural frequency of interest, and the accelerations were measured at the antinodes of the respective modes.

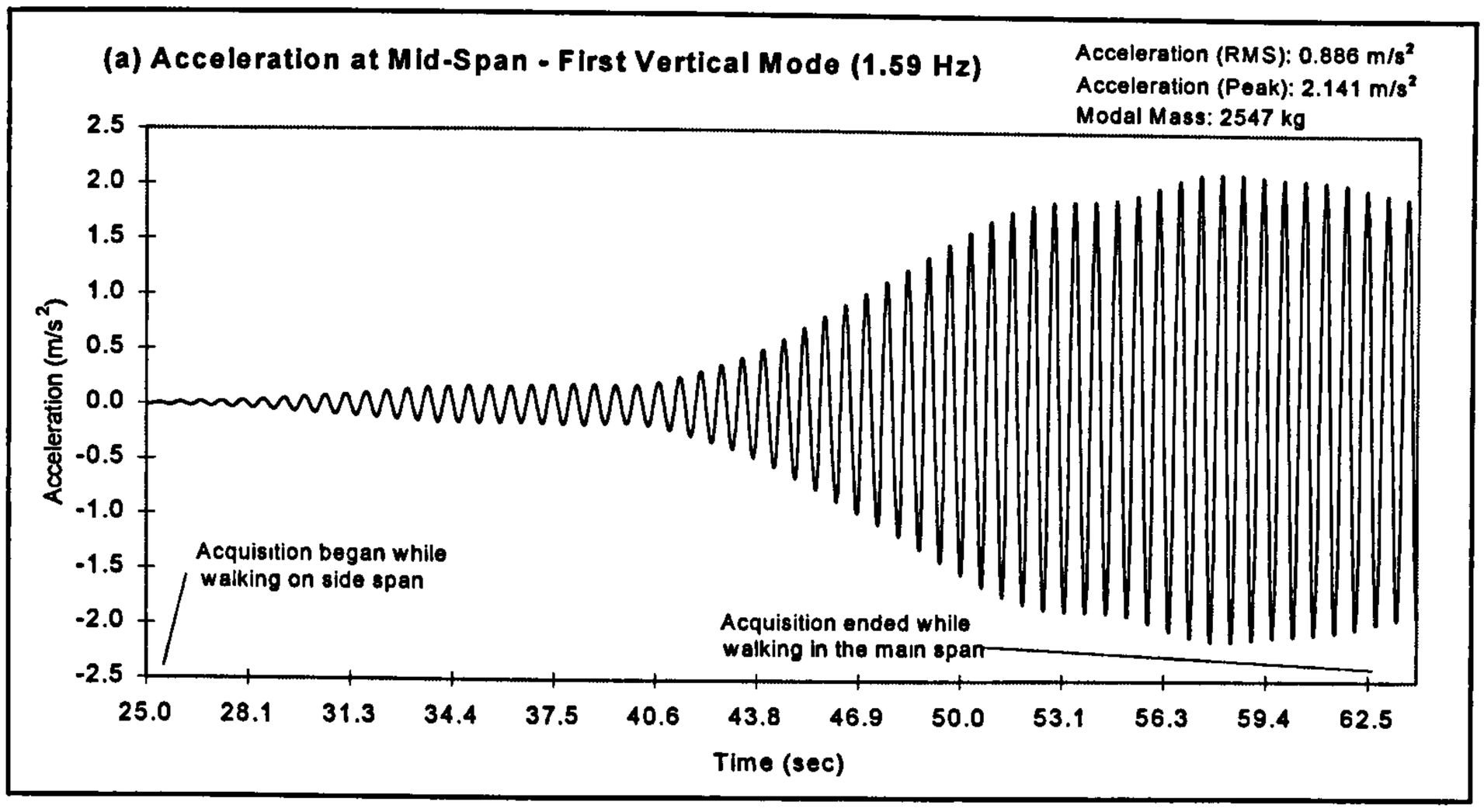

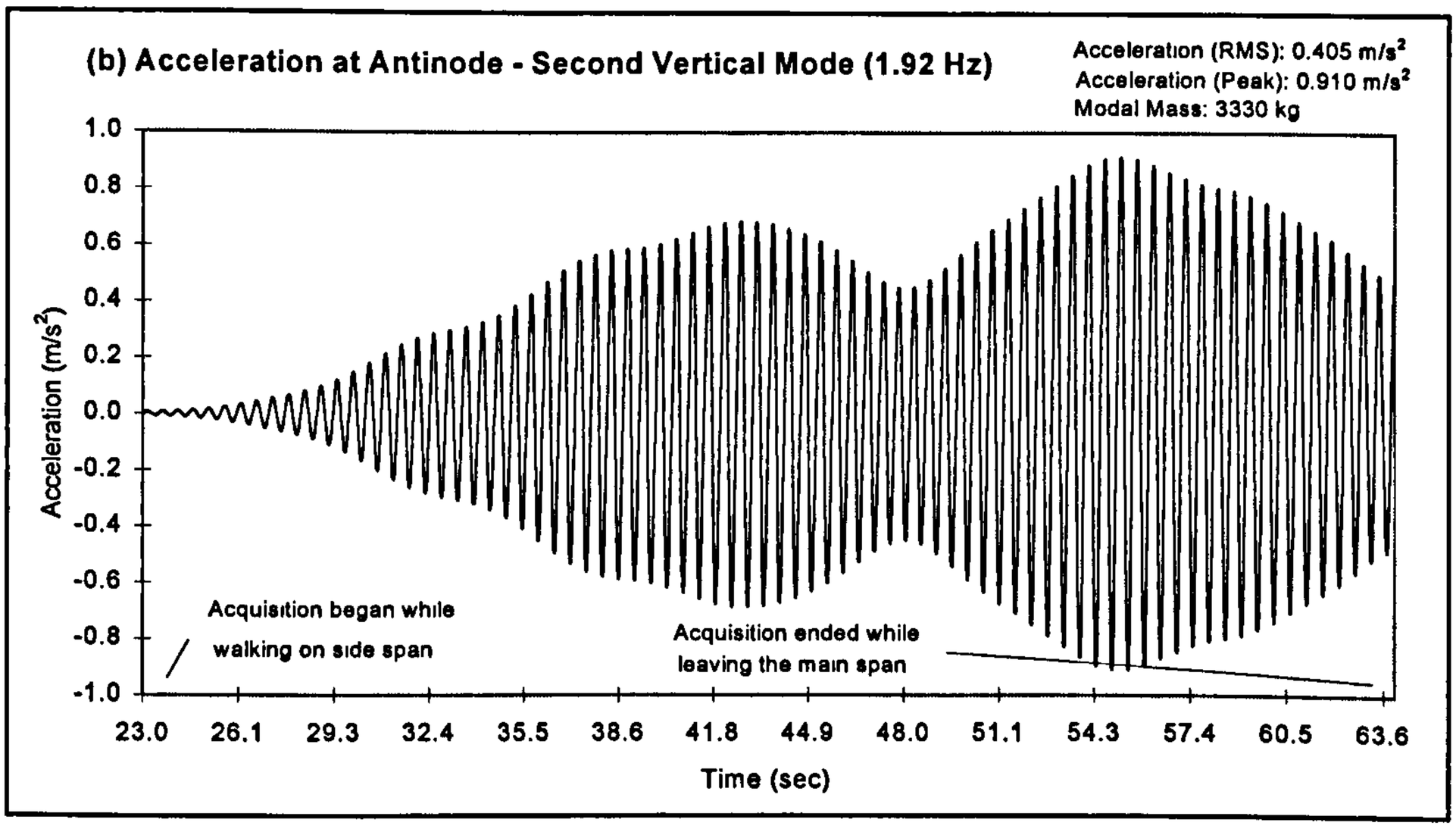

Figure 5.13 - Filtered acceleration response in each mode of vibration under resonance conditions

Fig. 5.13a is a reproduction, for comparison purposes, of the time response signal shown in Fig. 5.12c, and it presents the resonant response at the first vertical mode of 1.59 Hz. Fig. 5.13b shows a similar measurement for the second mode of vibration of 1.92 Hz. It should be noted that the amplitude of the excitation is expected to be higher in the latter case since the dynamic load factor increases with the pacing rate. On the other hand, this increase is expected to compensate a higher modal mass of the second mode when compared to the first mode.

The results show that the presence of nodes of vibration throughout the span prevent the build up of the vibration (Fig. 5.13b). Therefore, the mode with a smaller number of intermediate nodes tends to present higher accelerations and is the one on which to focus attention.

The suggested procedure cannot be taken as absolute since a case may occur which does not follow the pattern described above (e.g. if the modal masses of the modes within the same frequency range are significantly different). However, observation of frequency ranges, modal masses and mode shapes will help in reducing the vibration serviceability calculations usually to a single mode.

5.6 Vibrations Caused by Deliberate Excitation

The absence of case reports of damage amongst the reported lively footbridges reported in Table 2.2 makes the vibration induced by deliberate excitation a consideration only in so far as the potential risk it may cause to the integrity of the structure. Furthermore, it is unlikely that a footbridge which complies with vibration serviceability requirements would be sufficiently lively so as to attract the attention of vandals.

As was discussed in Section 2.4, recommendations regarding deliberate excitation are given as a general precaution (BS 5400, 1978). Investigations carried out within typical frequency ranges for individuals jumping and the effect of small groups of people jumping can be used to discuss this loading case further.

To begin with, it is necessary to define a frequency range of interest for the problem. From the studies of jumping loads (see Section 2.2.1), a broad frequency range between 1.5 and 3.5 Hz can be identified. However, since the liveliness of a footbridge is what potentially attracts attention for deliberate excitation, the frequency range of interest could be reduced, focusing on the range of the first harmonic of the walking load, in which the case reports of lively footbridges are most frequent.

Next, a procedure for applying the vandal loading is required. This load would be applied at the antinode of the respective vibration mode shape, with a frequency equal to

the natural frequency of the structure. It may be noted that the deflections and stresses generated during the vibration are to be added to those produced by the dead load.

Studies to obtain dynamic load factors in the vertical direction for an individual jumping were discussed in Section 2.2.1. The problem appears while trying to define the number of 'vandals' and the load applied by them. Pernica (1990) showed that the dynamic load increased almost linearly with group size for groups of up to four people. However, his tests with a group of eight people resulted in higher dynamic loads but not in proportion to the number of people.

Controlled tests were carried out using one and four people jumping in unison at the mid-span of the cable-stayed footbridge (see Section 4.5 for details of the structure). The jumping rate was set to excite in resonance the fundamental mode of 1.59 Hz. The subjects were actually bouncing by flexing their knees instead of jumping since it was found to be easy to excite the structure at this frequency in such a manner.

Number of People	Peak Acceleration (m/s^2)
1	2.62
4	8.27

Table 5.2 - Peak acceleration from Jumping Tests

The peak accelerations obtained in steady-state (resonance) conditions are shown in Table 5.2 for the two group sizes. It can be seen from the results that the ratio between the peak accelerations of the two groups is smaller than four, indicating difficulties in keeping a synchronised movement for a group of that size. Grouping together this result with those obtained by Pernica (1990) for a group of four and eight people, and rearranging them in terms of an equivalent number of fully synchronised people jumping is shown in Table 5.3.

By extending these results to larger groups suggests that a large number of equivalent people are in synchrony. Taking this hypothetical large group as the design loading case for deliberate excitation would result in a dynamic load of very high magnitude, and it is likely that damage would be unavoidable. This brings to mind the historical case of

damage induced to a bridge by soldiers marching in step mentioned in Chapter 1, a situation which it is not feasible to consider in design. On the other hand, it should be noted that the tests reported in Table 5.3 were controlled tests, in which either a metronome or a loudspeaker helped the group to keep the desired jumping rate. Moreover, the difference shown in Table 5.3 between the test results for a group of four people raises again the question of whether the difference in dynamic load is due to the vibration of the structure. The tests carried out by Pernica were on a rigid platform whereas the tests carried out in this study were on a lively footbridge, leading to a smaller number of synchronised pedestrians.

Number of People Participating	Equivalent Number of Fully Synchronised Pedestrians	
	Result from Table 5.2	After Pernica (1990)
Group of four	3.2	3.9
Group of eight	-	6.9

Table 5.3 - Results from groups of people jumping in controlled tests

A test programme involving groups of different sizes in uncontrolled conditions would be more realistic for defining an equivalent number of fully synchronised people jumping, which in turn could be taken as design loading case for deliberate excitation.

5.7 Guidelines for Vibration Performance

In this Section, it is intended to provide general guidance in tackling the problem of vibration performance of footbridges due to human-induced loads, based on the analysis of the literature and combining the results of the tests described in the previous individual Sections of this Chapter. Attention is concentrated on vibration serviceability since the analysis and suggestions to tackle the problem of deliberate excitation were discussed in the previous Subsection.

The problem of vibration serviceability of footbridges has not been widely studied. Variability is also to be expected among the various existing studies since it is the

characteristics of the (non-standardised) human body and forces produced by its movement that are central for defining the loading cases and acceptability limits to vibration. However, full advantage needs to be taken of the studies carried out so far without unnecessary simplifications.

In terms of the definition of acceptability limits for vibration while walking, independent tests have shown that such limits consistently increase with frequency as shown in Fig. 2.9. In the absence of further studies to consider the time exposure to vibrations, the continued use of peak acceleration is recommended. The nature of the exposure to vibration while walking on footbridges and its relationship to the impairment of this movement has been pointed out as a factor which favours the use of peak accelerations as the parameter to define acceptable vibration levels.

In terms of defining the load due to a pedestrian, the load factors obtained from tests on prototype footbridges under resonance conditions are suggested. The magnitude of the pedestrian load varies according to the frequency range covering the natural frequencies of the structure. The definition of these ranges and the respective intensity of the dynamic load is a central point of the investigation of vibration serviceability. Uncertainties need to be taken into account for defining these ranges, as was discussed in Section 5.3. This implied that, for design calculations, there is a need to enlarge the frequency ranges.

Taking as a reference the extreme natural frequencies of footbridges which have been reported as lively (Table 2.2), for the first harmonic of the walking load in the vertical direction, the natural frequencies of 1.8 Hz and 2.46 Hz are presented as upper and lower limits. A variation of 30% in these values to extend the frequency range is suggested, in order to take into account the uncertainties in the design calculations referred to earlier. The value of 30% is to some extent based on the reported variation of natural frequency between design and measurements by Deger *et al.* (1996). It is also convenient to cover the gap between the frequency ranges of the harmonics of the walking load, since it gives a broad frequency range from 1.3 Hz (equal to 0.7x1.8 Hz) to 3.2 Hz (equal to 1.3x2.46 Hz) for the first harmonic of the walking load.

With regard to the frequency range of the second harmonic of the walking load, a single case of a lively footbridge was reported, the natural frequency of which was 4.0 Hz. Since the frequency range below 3.2 Hz is already covered by the extended frequency range of the first harmonic of the load, applying a variation of 30% to extend the upper limit leads to a value of 5.2 Hz (equal to 1.3x4.0 Hz), which can be adjusted to 5.0 Hz, to make it the same as to the present upper frequency of interest of the UK code (BS5400, 1978) for vibration serviceability investigations.

For defining the dynamic load factors, the results obtained in Section 5.2 showed that selective reductions of 10% and 40% apply to dynamic load factors obtained from tests on rigid surfaces. The former reduction applies to dynamic load factors of the first harmonic of the walking load whereas the latter applies to load factors of the second harmonic. These reductions aim to take into account the variability on the pedestrian load while walking on vibrating surfaces. Bearing in mind the need to avoid discontinuities in the load factors within the extended frequency ranges of interest previously proposed, which would lack physical meaning, the following frequency ranges of interest for vibrations in the vertical direction and associated load factors are suggested:

- *Frequency range below 1.3 Hz:* investigations of vibration serviceability are not necessary.

- *Frequency range from 1.3 to 2.4 Hz:* a reduction of 10% applies to the dynamic load factors obtained from tests on rigid surfaces (see Table 2.1 for values obtained from tests on rigid surfaces). The value of 0.44 can be taken as the dynamic load factor at the upper frequency of this range, according to the results obtained in Section 5.2.

- *Frequency range from 2.4 to 3.2 Hz:* A linear decrease of the dynamic load factor applies, from 0.44 at the frequency of 2.4 Hz, to 0.06 at the frequency of 3.2 Hz. It should be noted that the latter value of 0.06 was actually evaluated from tests at a frequency of 3.6 Hz (see Section 5.2) but can be sensibly taken as a reference value at the frequency of 3.2 Hz, since this represents a conservative estimation.

- *Frequency range from 3.2 to 5.0 Hz:* a reduction of 40% applies to the dynamic load factors obtained from tests on rigid surfaces.

- *Frequency range above 5.0 Hz:* investigations of vibration serviceability are not necessary.

With regard to loads due to groups of people, the application of a magnification factor (e.g. Eq. 2.3) is suggested. Nevertheless, as was shown in Section 5.2, the application of Eq. 2.3 as a magnification factor of the accelerations produced by a notional pedestrian exciting the structure in resonance resulted in an overestimation of the response due to small groups of pedestrians. Since this equation does not take into account the synchronisation that may occur among pedestrians in large groups, which would enhance the vibration, this may compensate for the overestimation previously discussed. Therefore, in the absence of further studies, the use of Eq. 2.3 is suggested to be applied for footbridges in public areas where congested use is expected.

It is necessary to define a number of pedestrians for applying Eq. 2.3. Studies reported by Grundmann *et al.* (1993) and Ebrahimpour *et al.* (1996) mentioned that a density between 0.3 and 0.25 pedestrians per square metre, respectively, is the limit at which a pedestrian can walk, with an unrestricted choice of speed and pacing rate. Choosing one of these densities and multiplying this by the area of the deck gives the number of pedestrians at any one time on the bridge. It may be noted that higher densities would imply a reduction in the pacing rates, which would cause a reduction in the level of applied load.

The absence of test results for lateral excitations has prevented the extension of the investigation in this direction. However, significant vibrations in this direction have been reported (Table 2.2). The high excitation levels reported for footbridges may be due to the fact that the structure is not designed for gravity loads in this direction. The absence of studies of acceptability limits while walking and also the very limited studies to define excitation forces recommends a prudent avoidance of the frequency range of the first harmonic of the walking load in the lateral direction. This is the frequency range in which all case reports of lively footbridges in this direction are concentrated.

Based on the same line of thought used to define extended frequency ranges in the vertical direction, taking the extreme natural frequencies of lively footbridges in this direction (0.9 Hz and 1.1 Hz, see Table 2.2) and applying variations of 30% in these values give an extended frequency range from 0.6 Hz (equal to 0.7x0.9 Hz) to 1.4 Hz (equal to 1.3x1.1 Hz) which should be avoided in this direction.

The procedure of applying a pulsating moving load, following the recommendations of the UK (BS 5400, 1978) and Ontario (OHBDC, 1991) codes, reasonably reproduced the conditions of the pedestrian tests carried out. For beam-like footbridges, the expression proposed by Rainer *et al.* (1988) allows the introduction of variable dynamic load factors and could be used.

The situation in which more than one natural frequency may fall within the critical ranges of the pedestrian pacing rates should be considered. The suggestions presented in Section 5.5 can be adopted to tackle the problem until further studies, similar to those carried out for vibrations in buildings (BS 6472, 1992), are available to investigate multi-frequency component excitations in footbridges. It may be noted that the suggested avoidance of the critical frequency range in the lateral direction makes it unnecessary to consider the problem of investigating simultaneous excitation in different directions.

Guidelines for vibration serviceability as discussed here are fully applicable to ACM footbridges since the problem is governed by the excitation and frequency ranges rather than the construction material, which is assumed to behave linearly in all cases. However, the lightweight characteristic of ACM makes bridges made with this material more prone to excessive vibrations, which may require the avoidance of the critical frequency range of the first harmonic of the walking load.

Chapter 6

Conclusions

6.1 Summary of Findings

Needs for research into several aspects of vibration of footbridges due to human-induced loads have been identified in this thesis. Indeed, little research has been conducted in this area since the edition of the UK code in 1978 (BS 5400, 1978). Several topics in which research was found to be necessary have been covered in this thesis, based on tests carried out on three prototype footbridges and analysis using calibrated finite element models of these structures. The inclusion of an ACM footbridge in the test programme made it possible to investigate the peculiarities presented by this unconventional structure in terms of vibration performance.

Modal testing, encompassing three techniques, was employed as a tool to obtain the modal properties of the test structures. The applicability of such techniques was investigated, and the experience acquired in using them in site tests, together with a review of theoretical aspects on which the techniques are based, enabled some improvements in their application to be suggested. Practicalities in using the techniques and suggestions are summarised as follows, for each technique:

(a) Ambient Vibration Survey: Time pressure usually involved in site tests of civil engineering structures makes it difficult to fulfil theoretical requirements of frequency resolution and number of averages, to guarantee that the spectral functions calculated will present negligible bias and random errors, respectively. With regard to frequency resolution, bias (frequency resolution) error was shown not to be an issue for obtaining reliable mode shapes since its effect tended to cancel out when calculating the mode shape ordinates.

Regarding the number of averages, experience acquired in doing the tests and processing the results showed that, following the behaviour of the spectral functions

during the averaging process, while data is acquired, is a useful way of defining a satisfactory number of averages. In other words, a (satisfactory) number of averages can be defined in accordance with the specific testing conditions during data acquisition.

The procedure adopted for obtaining mode shapes aims to reduce the effects of random error, since the number of averages for obtaining each mode shape ordinate is usually small. The strategy required a few candidates for each mode shape ordinate to be calculated, by using points in the neighbourhood of the respective spectral resonance peak and averaging these results.

(b)Hammer Tests: A problem was identified in terms of finding a balance between having a proper frequency resolution and a sufficiently small time interval to enable the detection of the hammer peak. Evidence of this problem during data acquisition was presented as a sudden change in the profile of the FRFs during the averaging process, including the FRF 'jumping'. Practical measures were presented to overcome this problem like rejecting badly acquired records prior to their inclusion in the averaging process and/or properly setting the acquisition trigger. In terms of procedures for obtaining modal properties, an expression was suggested for removing the effects of the exponential window usually adopted in these tests. This expression was shown to be theoretically consistent, and the only simplification was to consider low structural damping, a requirement usually met in footbridges.

(c)Free-vibration decay: This technique was shown to be a reliable method of evaluating damping, since the alternative of evaluating damping by AVS demands a very fine frequency resolution to avoid bias error. This can only be attained by taking long acquisition records, a condition that may be difficult to fulfil due to testing time restrictions. On the other hand, obtaining damping from hammer tests resulted in an overestimation when compared to the evaluations from free-vibration decay. The reason for this was not completely clear but it may have something to do with the poor frequency resolution that can be achieved when using the hammer technique for testing low natural frequency footbridges. However, the different excitation levels at

which these two evaluations of damping were carried out may also cause differences between them.

The numerical models of the prototype footbridges were used to investigate modelling aspects and to help in finding ways of improving structural vibration performance. The calibration of these models was based on site measurements for obtaining the dynamic properties of each footbridge, using the aforementioned modal testing techniques. Based on the results of the tests and subsequent analysis, the following suggestions can be made for modelling and improving the design of footbridges in terms of vibration performance:

- Simple FE models based on beam elements were shown to be sufficient for producing natural frequencies and mode shapes in good agreement with the ones obtained from the tests. Use of the mode shapes to detect abnormal displacements occurring in the FE model and their subsequent correction is recommended.

- Material properties and support conditions should be included as variables in the calibration process of the numerical model. The calibrated values of the Young's modulus of concrete and GRP were close to the respective static design values.

- Handrails were shown to provide an opportunity for increasing the stiffness and thus the natural frequencies of a footbridge. In addition, a combination of a cambered or catenary profile together with horizontal restraint was also shown to be useful for increasing natural frequencies, since it induces some membrane action.

- Addition and relocation of mass was shown as an effective way of frequency tuning the GRP cable-stayed footbridge. Attempts to stiffen the structure by the addition of new GRP components were not effective.

Pedestrian tests carried out on the three footbridges and numerical simulations using the calibrated models have enabled suggestions to be proposed for improving the guidelines for vibration performance of footbridges. The aspects analysed involved the definition of the pedestrian load, frequency ranges of interest, acceptability limits to vibration,

multi-frequency component vibrations and vandal loading. Suggestions were presented in Section 5.8 regarding these topics, and are briefly summarised here:

- A reduction of 10% and 40% was proposed in the value of dynamic load factors associated respectively with the first and second harmonics of the walking load and obtained from tests in rigid surfaces. When considering the effect of groups of people, the use of a magnification factor (Eq. 2.3) is suggested on congested footbridges only.

- For defining the frequency ranges of interest, the uncertainties in obtaining modal properties of the structure during the design stage were taken into account. Extending the frequency ranges beyond the limits of the common frequency ranges of the harmonics of the walking load was proposed. Use of extended frequency ranges were also intended to cover the detected variation of the natural frequencies caused by the presence of people walking on the bridge, which may be more pronounced in ACM footbridges.

- The continued use of peak acceleration was suggested as the parameter to be adopted for defining acceptability limits to vibration, in the absence of (applicable) studies to take time exposure to vibrations into account.

- Vibrations with more than one frequency component within the frequency ranges of interest were shown to occur potentially in footbridges in which bending moments and axial forces were both significant. A procedure for treating vibrations with several frequency components was suggested. This was suggested as a provisional solution, due to the absence of a procedure for assessing multi-frequency component vibrations for footbridges such as those that already exist for assessing floors. The variation of the dynamic load factors, acceptability limits to vibration, modal masses and mode shapes were used in the analysis. It was shown that the analysis of vibration serviceability could be usually concentrated on a single mode, first choosing those modes with natural frequencies within the frequency range of the first

harmonic of the walking load, if there are any, and then choosing the mode with a smaller number of intermediate nodes.

- An investigation into the problem of vandal loading was carried out, considering the research advances in defining the load due to groups of people jumping. A procedure to treat the problem was suggested. Nevertheless, it was not possible to define a notional number of people to be used in design calculations.

- Guidelines for vibration serviceability are equally applicable to ACM footbridges since the problem is governed by the excitation and frequency ranges rather than by the particular properties of the construction material. However, the comparatively low mass of footbridges made of this material creates additional difficulties to comply with existing vibration serviceability guidelines.

6.2 Suggestions for Further Work

The following topics are suggested for further research in this area:

- Investigations of vibrations in the lateral direction are required, which involve studies to define dynamic load factors in a similar way to those obtained in the vertical direction, and a definition of acceptability limits to vibration in this direction for walking subjects. This research should also be extended to studies of vibration serviceability in torsion for those structures for which such vibrations may be coupled to those in the lateral direction.

- Research is needed to investigate the effects of groups of people involving synchronisation in crowd situations, the influence of pedestrians as dynamic systems, and the definition of a loading case for deliberate excitation. Special attention should be given to vibrations induced by crowds in the second harmonic of the walking load and also in the lateral direction, in which studies are scarce.

- A procedure is required to take into account the treatment of multi-frequency component vibrations, including the time exposure to vibrations, associated with the application of the Vibration Dose Value and frequency weighting.

- The use of automatic finite element modal updating techniques for calibrating numerical models of footbridges of complex geometry and a large number of parameters to be adjusted need to be investigated.

References

Abdel-Ghaffar, A. M. & Housner, G. W. (1978). "Ambient Vibration Tests of Suspension Bridge", *Journal of Engineering Mechanics Division, ASCE*, 104(5), pp. 983-999.

Abdel-Ghaffar, A. M. & Scanlan, R. H., (1985). "Ambient vibration studies of Golden Gate Bridge: I. Suspended Structure", *Journal of Engineering Mechanics Division, ASCE*, 111(4), pp. 463-482.

Abdel-Ghaffar, A. M. & Khalifa, M. A. (1991). "Importance of Cable Vibration in Dynamics of Cable-Stayed Bridges", *Journal of Engineering Mechanics*, ASCE, 117(11), pp. 2571-2589.

Allemang, R. J. & Brown, D. L. (1982). "A Correlation Coefficient for Modal Vector Analysis", *Proceedings of the 1st International Modal Analysis Conference*, Orlando, USA, pp. 110-116.

Allen, D. E. & Murray, T. M. (1993). "Design Criterion for Vibrations Due to Walking", *Engineering Journal, AISC*, 4(4), pp. 117-129.

ANSYS (1992). *User's Manual. Revision 5.0.*

Bachmann, H. & Ammann, W. (1987). "*Vibrations in Structures Induced by Man and Machines*". IABSE Structural Engineering Documents 3e.

Bachmann, H. (1992). "Vibration Upgrading of Gymnasia, Dance Halls and Footbridges", *Structural Engineering International, Journal of the IABSE*, 2(2), pp. 118-124.

Bachmann, H. (1992a). "Case Studies of Structures with Man-Induced Vibrations", *Journal of Structural Engineering, ASCE*, 118(3), pp. 631-647.

Bachmann, H. *et al.* (1995). *Vibration Problems in Structures - Practical Guidelines.* Basel, Switzerland: Birkhäuser Verlag.

Bathe, K. J. (1982). *Finite Element Procedures in Engineering Analysis*. Prentice-Hall, Inc.

BENCHmark. (1994). "Collapse of the Tacoma Narrows Bridge". March.

Bendat, J. S. & Piersol, A. G. (1986). *Random Data: Analysis and Measurements Procedures*. New York: John Wiley & Sons, 2nd ed.

Bendat, J. S. & Piersol, A. G. (1993). *Engineering Applications of Correlation and Spectral Analysis*. New York: John Wiley & Sons, 2nd ed.

Blanchard, J., Davies, B.L. & Smith, J.W. (1977). "Design Criteria and Analysis for Dynamic Loading of Footbridges", *Symposium on Dynamic Behaviour of Bridges*, TRRL Supplementary Report 275, pp. 90-106. Crowthorne, Berkshire.

British Construction Industry awards (1993).

Brownjohn, J. M. W., Dumanoglu, A. A. ; Severn, R. T. & Taylor, C. A. (1987). "Ambient Vibration Measurements of the Humber Suspension Bridge and Comparison with Calculated Characteristics", *Proceedings of the Institution of Civil Engineers*, Part 2, Vol. 83, September, pp. 561-600.

Brownjohn, J. M. W. (1988). "Assessment of Structural Integrity by Dynamic Measurements", *PhD Thesis*, University of Bristol, Department of Civil Engineering, University of Bristol, Department of Civil Engineering, Bristol, UK.

Brownjohn, J. M. W., Dumanoglu, A. A. & Severn, R. T. (1992). "Ambient Vibration Survey of the Fatih Sultan Mehmet (Second Bosporus) Suspension Bridge", *Earthquake Engineering and Structural Dynamics*, 21(10), pp. 907-924.

Brownjohn, J. M. W., Dumanoglu, A. A. & Taylor, C. A. (1994). "Dynamic Investigation of a Suspension Footbridge", *Engineering Structures*, 16(6), pp. 395-406.

Brownjohn, J. M. W. (1997). "Vibration Characteristics of A Suspension Footbridge", *Journal of Sound and Vibration*, 202(1), 29-46.

BS648 British Standards. (1964). Schedule of Weights of Building Materials.

BS5400 British Standards. (1978). Steel, Concrete and Composite Bridges: Specification for Loads, Part 2, Appendix C.

BS8110 British Standards. (1985). Structural Use of Concrete (Part 2) - Code of Practice for Special Circumstances.

BS6472 British Standards. (1992). Guide to evaluation of Human Exposure to Vibration in Buildings (1 Hz to 80 Hz).

Butler, A. A. W. (1977). "Stressed Ribbon Footbridge in the Peak District", *The Journal of the Institution of Highway Engineers*, March 1977, pp. 12-15.

Caetano, E. & Cunha, A. (1993). "Experimental Identification of Modal Parameters on a Full Scale Structure", *Proceedings of the 6th International Conference on Computational Methods and Experimental Measurements*, Brebbia, C. A. ; Carlomagno, G. M. (editors), Vol. 2. pp. 321-336.

Caverson, R. G. (1992). "Vibration Characteristics of Suspended Concrete Slabs", *MSc Thesis*, Department of Civil Engineering, University of Bristol, UK.

Cawley, P. (1984). "The Reduction of Bias Error in Transfer Function Estimates Using FFT-Based Analysers", *Journal of Vibration, Acoustics, Stress, and Reliability in Design*, Vol.106, January, pp. 29-35.

Cawley, P. (1986). "The Accuracy of Frequency Response Function Measurements Using FFT-Based Analysers with Transient Excitation", *Journal of Vibration, Acoustics, Stress, and Reliability in Design*, Vol.108, January, pp. 44-49.

CEB - Comite Euro-International Du Beton (1991). Bulletin D'Information No. 209, August.

CEB - Comite Euro-International Du Beton (1993). "CEB-FIP Model Code 90", In: *CEB Bulletin D'Information No. 213/214, May.*

Change, N. D. (1995). "Introduction to Impulse Hammers". In: Piezoelectric Sensors for Dynamic Measurements, *Dytran General Catalogue & Instrumentation Handbook.*

Cheung, J. T. (1984). *Vibration Analysis of Frame and Cable-Stayed Footbridges by 'VAFCAF'*. Transport and Road Research Laboratory (TRRL), Supplementary Report 824, Crowthorne, England: Transport and Road Research Laboratory.

Clark, R. L., Wicks, A. L. & Becker, W. J. (1989). "Effects on a Exponential Window on the Damping Coefficient", *Proceedings of the 7th International Modal Analysis Conference*, Vol. 1, Las Vegas, Nevada, pp. 83-86.

Clough, R. W. & Penzien, J. (1975). *Dynamics of Structures*. New York: McGraw-Hill, Inc.

Corelli, D. & Brown, D. L. (1984). "Impact Testing Considerations", *Proceedings of the 2nd International Modal Analysis Conference, IMAC*, Orlando, Florida, USA: SEM, Vol. 2, pp. 735-742.

Dally, J. W., Rilley, W. F. & McConnell, K. G. (1993). *Instrumentation for Engineering Measurements*, 2nd ed., USA: Wiley.

Deger, Y., Felber, A., Cantieni, R. & Smet, C. A. M. (1996). "Dynamic Modelling and Testing of a Cable Stayed Pedestrian Bridge", *Proceedings of the 14th International Modal Analysis Conference*, Dearborn, USA, Vol. 1, pp. 211-217.

Desforges, M. S., Cooper, J. E. & Wright, J. R. (1995). "Spectral and Modal Parameter Estimation from Output-Only Measurements", *Mechanical Systems and Signal Processing*, 9(2), pp. 169-186.

DI - Diagnostics Instruments (Undated) - FFT Analyser - Applications/Operating Manuals Revision 1.5.

Dobson, B. J. (1987). "A Straight-Line Technique for Extracting Modal Parameters from Frequency Response Data", *Mechanical Systems and Signal Processing*, 1(1), pp. 29-40.

DTA - Dynamic Testing Agency. (1993a). Handbook on Guidelines to Best Practice, Vol. 4, Non-Linearity in Dynamic Testing, Module 40 - Introduction to Non-Linearity.

DTA - Dynamic Testing Agency. (1993b). Handbook on Guidelines to Best Practice, Vol. 3, Modal Testing, Module 34 - Modal Parameter Estimation.

DTA - Dynamic Testing Agency. (1995). Handbook on Guidelines to Best Practice, Vol. 3, Modal Testing, Module 33 - Measurement of Frequency Response Functions.

Ebrahimpour, A. & Sack, R. L. (1989). "Modeling Dynamic Occupant Loads", *Journal of Structural Engineering, ASCE*, 115(6), pp. 1476-1496.

Ebrahimpour, A., Haman, A., Sack, R. L. & Patten, W. N. (1996). "Measuring and Modelling Dynamic Loads Imposed by Moving Crowds", *Journal of Structuring Engineering, ASCE*, 122(12), pp.1468-1474.

Ellingwood, B. & Tallin, A. (1984). "Structural Serviceability: Floor Vibrations", *Journal of Structural Engineering, ASCE*, 110(2), pp. 401-418.

Ellingwood, B. (1996). "Structural Serviceability Review and Standard Implementation", *Proceedings of the XIV Congress, ASCE*, Chicago, Illinois: Ghosh, S. K. and Mohammadi, J. (editors), Vol. 1, April 15-18, pp. 436-443.

Ellis, B. R. & Ji, T. (1994). "Floor Vibration Induced by Dance-Type Loads: Verification", *The Structural Engineer*, 72(3), pp. 45-50.

Ellis, B. R. & Ji, T. (1996). "Investigation of the Dynamic Characteristics of the Steel-Framed Building at the Cardington LBTF", In: Armer, G. S. T. & O'Dell, T.(editors), *Fire, Static and Dynamic Tests of Building Structures. Proceedings of the Second Cardington Conference,* London: E & FN SPON, pp. 181-191.

Ellis, B. R. & Ji, T. (1997). "Human-Structure Interaction in Vertical Vibrations", *Proceedings of the Institution of Civil Engineers, Structures & Buildings*, 122, February, pp. 1-9.

Endevco (Undated) - Shock and Vibration Measurement Technology: An Applications - Oriented Short Course P/H 29005.

Eriksson, P-E. (1994). "Vibration of Low-Frequency Floors - Dynamic Forces and Response Prediction", *PhD Thesis*, Unit for Dynamics in Design, Department of Structural Engineering, Chalmers University of Technology, Göteborg, Sweden.

Erki, M. A., Green, M. F., Wilson, R., Yantha, P. & Johansen, G. E. (1994). "Statics and Dynamics of an FRP Vehicle Bridge", In: Mufty, A. A., Bakht, B. & Jaeger, L. G. (editors), *Proceedings of the Developments on Short and Medium Span Bridges '94 International Conference*. Halifax, Nova Scotia, Canada, pp. 871-882.

Ewins, D. J. & Gleeson, P. T. (1982). "A Method for Modal Identification of Lightly Damped Structures", *Journal of Sound and Vibration*, 84(1), pp. 57-79.

Ewins, D. J. (1984). *Modal Testing: Theory and Practice*. England: Research Studies Press.

Eyre, R. & Cullington, D. W. (1985). "Experience with Vibration Absorbers on Footbridges", *TRRL Research Report No. 18*, Transport and Road Research Laboratory.

Felber, A. J. & Ventura, C. E. (1996). "Frequency Domain Analysis of the Ambient Vibration Data of the Queensborough Bridge Main Span", *Proceedings of the 14th International Modal Analysis Conference*, Vol. 1, pp. 459-465.

Fillod, R., Lallement, G., Piranda, J. & Raynaud, J. L. (1985). "Global Method of Modal Identification", *Proceedings of the 3th International Modal Analysis Conference*, Vol. 2, pp. 1145-1151.

Fladung, W. & Rost, R. (1997). "Application and Correction of the Exponential Window for Frequency Response Functions", *Mechanical Systems and Signal Processing*, 11(1), pp. 23-36.

Fleming, J. F. & Egeseli, E. A. (1980). "Dynamic Behaviour of a Cable-Stayed Bridge", *Earthquake Engineering and Structural Dynamics*, 8(1), pp. 1-16.

Fujino, Y., Pacheco, B. M., Nakamura, S. & Warnitchai, P. (1993). "Synchronization of Human Walking Observed During Lateral Vibration of a Congested Pedestrian Bridge", *Earthquake Engineering and Structural Dynamics*, 22(9), pp. 741-758.

Gade, S. & Herlufsen, H. (1987). "Windows to FFT Analysis (Part I)", *Technical Review*, No.3. Denmark: Brüel & Kjær.

Galbraith, F.W. & Barton, M.V. (1970). "Ground Loading from Footsteps", *Journal of Acoustical Society of America*, Vol. 48(5), Part 2, pp. 1288-1292.

Gardner-Morse, M. G. & Huston, D. R. (1993). "Modal Identification of Cable-Stayed Pedestrian Bridge", *Journal of Structural Engineering*, ASCE, 119(11), pp. 3384-3404.

Gaukroger, D. R., Skingle, C. W. & Heron, K.H. (1973). "Numerical Analysis of Vector Response Loci", *Journal of Sound and Vibration*, 29(3), pp. 341-353.

Gimsing, Niels J. (1983). *Cable Supported Bridges* - Concept and Design, New York: John Wiley.

Gray, H. L. & Odell, P. L. (1970). *Probability for Practicing Engineers*. PECDS - Professional Engineering Career Development Series, New York: Barnes & Noble.

Green, M. F., Heffernan, P. J., Johansen, G. E. & Wilson, R. (1994). "Dynamic Analysis of a FRP Footbridge", *Proceedings of the 12th International Modal Analysis Conference*, Honolulu, Hawaii, Vol. 1, pp. 718-723.

Griffin, M. J. (1990). *Handbook of Human Vibration*. London: Academic Press.

Grundmann, H., Kreuzinger, H. & Schneider, M. (1993). "Schwingungsuntersuchungen Für Fußgängerbrücken" (Dynamic Calculations of Footbridges), *Bauingenieur*, 68(5), pp. 215-225, (in German).

Halvorsen, W. G. & Brown, D. L. (1977). "Impulse Technique for Structural Frequency Response Testing", *Sound and Vibration*, pp. 8-21.

Harper, F.C. (1962). "The Mechanics of Walking", *Research Applied in Industry*, 15(Part 1), pp. 23-28.

Harvey, W. J. (1993). "A Reinforced Plastic Footbridge, Aberfeldy, UK", *Structural Engineering International*, Vol. 3, Part 4, pp. 229-232.

Humar, J. L. (1990). *Dynamics of Structures*. New Jersey, USA: Prentice-Hall.

ICATS - Imperial College Analysis, Testing and Software. (1995). Modent/Modesh - Reference Manual, Version 4.2B.

Imregun, M. & Ewins, D. J. (1995). "Complex Modes - Origins and Limits", *Proceedings of the 13th International Modal Analysis Conference*, Vol. 1, pp. 496-506.

Inman, V. T., Ralston, H. J. & Todd, F. (1994). "Human Locomotion", In: Rose, J. & Gamble, J. G. (editors), *Human Walking*. Baltimore, U.S.A.: Williams & Wilkins. 2nd ed., pp. 1-22.

ISO 10137 International Organisation for Standardization. (1992). Bases for Design of Structures - Serviceability of Buildings against Vibration.

ISO 7626-5 International Organisation for Standardization. (1994). Vibration and Shock: Experimental of Mechanical Mobility - Part 5: Measurements using impact excitation with an exciter which is not attached to the structure.

James III, G. H., Carne, T. G. ; Lauffer, J. P. & Nord, A. R. (1992). "Modal Testing Using Natural Excitation", *Proceedings of the 10th International Modal Analysis Conference*, San Diego, USA: SEM, Vol. 2, pp. 1209-1216.

Ji, T. & Ellis, T. (1994). "Floor Vibration Induced by Dance-Type Loads: Theory", *The Structural Engineer*, 72(3), pp. 37-44.

Johansen, G. E. *et al.* (1996). "Design and Construction of Two FRP Pedestrian Bridges in Haleakala National Park, Maui, Hawaii", *Advanced Composite Materials in Bridges and Structures*, M. M. El-Badry (editor), CSCE, Montreal, pp. 975-982.

Jones, R. T. & Pretlove, A. J. (1979). "Vibration Absorbers and Bridges", *The Highway Engineer, The Journal of the Institution of Highway Engineers*, January, pp. 2-9.

Kennedy, C. C. & Pancu, C. D. P. (1947). "Use of Vectors in Vibration Measurement and Analysis", *Journal of the Aeronautical Sciences*, 14(11), pp. 603-625.

Khalifa, M. A., Hodhod, O. A. & Zaki, M. A. (1996). "Analysis and Design Methodology for a FRP Cable-Stayed Pedestrian Bridge", *Composites: Part 27B*, pp. 307-317.

Khan, S. Z. (1994). "Aspects of Finite Element Modelling and Dynamic Seismic Analysis of Cable-Stayed Bridges", *Proceedings Cable-Stayed and Suspension Bridges - International Conference, AIPC-FIP*, Vol. 2, pp. 263-270.

Kobori, T. & Kajikawa, Y. (1974). "Ergonomic Evaluation Methods for Bridge Vibrations", *Transactions of JSCE*, Vol. 6, pp. 40-41.

Lee, D. J. (1993). "Project Linksleader': The First Major Cable-Stayed GRP Bridge", *FIP Symposium - Modern Prestressing Techniques and Their Applications*, Kyoto, Japan: FIP, Vol. 2, pp. 671-678.

Leonard, D. R. (1966). "Human Tolerance Levels for Bridge Vibrations", *Road Research Laboratory (RRL),* RRL Report No. 34.

Lieven, N. A. J. & Ewins, D. J. (1988). "Spatial Correlation of Mode Shapes, The Coordinate Modal Assurance Criterion (COMAC), *Proceedings of the 6th International Modal Analysis Conference (IMAC)*, Kissimmee, Florida- USA: SEM, Vol 1, pp. 690-695.

Littler, J. D. (1992). "Ambient Vibration Tests on Long Span Suspension Bridges", *Journal of Wind Engineering and Aerodynamics,* Vol. 41-44, pp. 1359-1370.

Littler, J. D. (1995). "An Assessment of Some of the Different Methods for Estimating Damping from Full-Scale Testing, *Journal of Wind Engineering and Industrial Aerodynamics*, Vol. 57, Part 2/3, pp. 179-190.

Maguire, J. R. & Severn, R. T. (1987). "Assessing the Dynamic Properties of Prototype Structures by Hammer Testing", *Proceedings of the Institution of Civil Engineers*, Vol. 83, Part 2, pp. 769-784.

Matsumoto, Y., Sato, S., Nishioka, T. & Shiojiri, H. (1972). "A Study on Dynamic Design of Pedestrian Over-Bridges", *Transaction of JSCE*, Vol. 4, pp. 50-51.

Matsumoto, Y., Nishioka, T., Shiojiri, H. & Matsuzaki, K. (1978). "Dynamic Design of Footbridges", IABSE Proceedings P-17/78, pp. 1-15.

McConnell, K. G. & Varoto, P. S. (1995). "The Effects of Window Functions and Trigger Levels on FRF Estimations form Impact Tests", *Proceedings of the 13th International Modal Analysis Conference*, SEM, Vol. 1, pp. 798-807.

McConnell, K. G. (1995). "Vibration Testing - Theory and Practice. New York: Wiley.

Meier, U. (1991). "Case Stories", In: Mufti, A. A., Erki, M-A. & Jaeger, L. G. (editors), *Advanced Composite Materials with Application to Bridges State-of-the Art Report, CSCE*, Montreal.

Meier, U. (1992). "Carbon Fiber-Reinforced Polymers: Modern Materials in Bridge Engineering", *Structural Engineering International, Journal of the IABSE*, 1(2), pp. 07-12.

Mouring, S. E. & Ellingwood, B.R. (1994). "Guidelines to Minimize Floor Vibrations from Building Occupants", *Journal of Structural Engineering, ASCE*, 120(2), pp. 507-526.

Mufti, A. A., Erki, M-A & Jaeger, L. G. (editors) (1991). "Advanced Composite Materials with Application to Bridges", *State-of-the-Art Report*, Canada: Canadian Society for Civil Engineering.

Newland, D. E. (1993). *An Introduction to Random Vibrations, Spectral & Wavelet Analysis*. New York: Longman Scientific & Technical, 3rd ed.

OHBDC - Ontario Highway Bridge Design Code. (1991). Ministry of Transportation and Communications, Highway Engineering Division, 3rd ed., Ontario, Canada.

Ohlsson, S. V. (1982). "Floor Vibrations and Human Discomfort", *PhD Thesis*, Division of Steel and Timber Structures, Chalmers University of Technology, Göteborg, Sweden.

Okubo, N. (1994). "Modal Analysis - Toward Virtual Design", *Proceedings of the 12th International Modal Analysis Conference*, Honolulu, Hawaii: Society for Experimental Mechanics, pp. xxiii-xxvii.

Pan, T-C. (1992). "Vibration of Pedestrian Overpass", *Journal of Performance of Constructed Facilities, ASCE*, 6(1), pp. 34-45.

Pavic, A., Williams, M. S. & Waldron, P. (1994). "Dynamic FE Model for Post-Tensioned Concrete Floors Calibrated Against Field Test Results", *International Conference on Engineering Integrity Assessment, Dynamic Testing Agency (DTA)*, Edwards, J. H., Kerr, J. & Stanley, P. (editors), Glasgow, Scotland, pp. 357-366.

Pavic, A., Crouch, R. S. & Waldron, P. (1995). "The Iterative Process of Linking Experimental Modal Testing & FE Modelling of a Full-Scale Concrete Structure", *BENCHmark*, October 1995, pp. 12-17.

Pavic, A., & Waldron, P. (1996). "Guidelines on Modal Testing of Full Scale Concrete Floors Using Instrumented Hammer Impact Excitation", *International Seminar Structural Assessment - The Role of Large and Full Scale Testing*. London: Paper P027.

Pavic, A. (1996). Personal Communication.

Pavic, A. (1997). "Vibration Serviceability of Long-Span in-Situ Concrete Floors in Buildings", *PhD Thesis*, Department of Civil & Structural Engineering, University of Sheffield, UK.

Pernica, G. (1990). "Dynamic Load Factors for Pedestrian Movements and Rhythmic Exercises", *Canadian Acoustics*, 18(2), pp. 3-18.

Petkovski, M. (1994). MMLDI - Data Processing Utilities

Rainer, J. H. & Pernica, G. (1986). "Vertical Dynamic Forces from Footsteps", *Canadian Acoustics*, Part 2, Vol. 14, pp. 12-21.

Rainer, J. H., Pernica, G. & Allen, D. E. (1988). "Dynamics Loading and Response of Footbridges", *Canadian Journal of Civil Engineering*, Vol. 15(1), pp. 66-71.

Randall, R. B. (1987). *Frequency Analysis*. Denmark: Brüel & Kjær, 3rd ed.

Rao, S. S. (1995). "Mechanical Vibrations", 3rd ed., USA: Addison-Wiley.

Richardson, M. H. & Formenti, D. I. (1982). "Parameter Estimation from Frequency Response Measurements Using Rotational Polynomials", *Proceedings of the 1st International Modal Analysis Conference*, Orlando, USA, pp. 167-181.

Ripley, G. (1996). Personal Communication.

Rogers, P. (1995). Personal Communication.

Ross, S. S. (1984). *Construction Disasters: Design Failures, Causes and Prevention.* New York: McGraw-Hill Book Company.

Schmidt, H. (1985a). "Resolution Bias Errors in Spectral Density, Frequency Response and Coherence Function Measurements, I: General Theory", *Journal of Sound and Vibration*, 101(3), pp. 347-362.

Schmidt, H. (1985b). "Resolution Bias Errors in Spectral Density, Frequency Response and Coherence Function Measurements, III: Application to Second-Order Systems (White Noise Excitation)", *Journal of Sound and Vibration*, 101(3), pp. 377-404.

Schmidt, H. (1985c). "Resolution Bias Errors in Spectral Density, Frequency Response and Coherence Function Measurements, IV: Comparison of Different Frequency Response Estimators", *Journal of Sound and Vibration*, 101(3), pp. 413-418.

Smith, J. W. (1969). "The Vibration of Highway Bridges and the Effects on Human Comfort", *PhD Thesis,* University of Bristol, UK.

Smith, J. W. (1988). *Vibration of Structures Applications in Civil Engineering Design*, UK: Chapman and Hall.

Smith, J. W. (1996). Personal Communication with respect to the article by Blanchard *et al.* (1977), "Design Criteria and Analysis for Dynamic Loading of Footbridges".

Sneddon, I. N. (1969). *Fourier Series*, Library of Mathematics, London: Routledge & Kegan Paul ltd.

Swiss Norm (1989) SIA 160. Effects of Loads On Structures.

Timoshenko, S. P. (1947). *The Collected Papers*. McGraw-Hill.

Thomson, W. T. (1993). *Theory of Vibration with Applications*. New Jersey: Chapman & Hall, 4th ed.

Thrane, N. (1980). " Zoom-FFT", *Technical Review*, No.2. Denmark: Brüel & Kjær.

Tilly, G. P., Cullington, D. W. & Eyre, R. (1984). "Dynamic Behaviour of Footbridges", *IABSE Surveys S-26/84*, pp. 13-24.

Trethewey, M. W. & Cafeo, J. A. (1992). "Signal Processing Aspects of Structural Impact Testing", *The International Journal of Analytical and Experimental Modal Analysis*, 7(2), pp. 129-149.

Troitsky, M. S. (1988). *Cable-Stayed Bridges*, Oxford, England: BSP Professional Books.

Tuladhar, R., El-Badry, M. M. & Dilger, W. H. (1996). "Seismic Response of Cable-Stayed Bridges with Carbon Fiber Reinforced Plastic Stay Cables", *Advanced Composite Materials in Bridges and Structures Conference*, M. M. El-Baldry (editor), CSCE, Montreal, pp. 367-374.

Vlahinos, A. & Wang, Y-C. (1994). "Nonlinear Dynamic Behaviour of Cable-Stayed Bridges", *Proceedings of the 12th International Modal Analysis Conference*, Honolulu, Hawaii : Society for Experimental Mechanics , Vol. 2, pp. 1335-1341.

Wheeler, J. E. (1981). "Crowd Loading on Footbridges". *Technical Report No. 23*, Western Australia: Main Roads Department.

Wheeler, J.E. (1982). "Prediction and Control of Pedestrian-Induced Vibration in Footbridges", *Journal of the Structural Division, ASCE*. 108 (9), pp. 2045-2065.

Willoughby, S. B. (1996). "The Ridgeway Footbridge", *The Structural Engineer*, Vol. 74(5), March 1996, pp.79-83.

Wilson, J. C. & Gravelle, W. (1991). "Modelling of a Cable Stayed Bridge for Dynamic Analysis", *Earthquake Engineering and Structural Dynamics*, Vol. 20, pp. 707-721.

Wright, D.T. & Green, R. (1959). "Human Sensitivity to Vibration". *Report No. 7*, Kingston, Ontario, Canada: Queen's University.

Wyatt, T. A. (1985). "Floor Excitation by Rhythmic Vertical Jumping", *Engineering Structures*, Vol. 7, pp. 208-210.

Wyatt, T. A. (1989). "Design Guide on the Vibration of Floors", *SCI Report 076*, England: The Steel Construction Institute.

Yiu, P. K. A. & Brotton, D. M. (1987). "Mathematical Modelling of Cable-Stayed Bridges for Computer Analysis", In: W. Kanok-Nukulchai (editor), *Proceedings of the International Conference on Cable-Stayed Bridges*, Bangkok, Thailand, Vol. 1, pp. 249-260.

Appendix

A.1 Equipment for Data Acquisition

The equipment for measuring, acquiring and processing data in all tests had been recently purchased and consists of an excitation device (instrumented hammer), response transducers (accelerometers), signal conditioners for the hammer and accelerometers, a spectrum analyser to acquire and process data, and a PC notebook, to which data was transferred for storage and further analysis. The equipment set-up followed the general layout for frequency response testing (Halvorsen and Brown, 1977) (Fig. A.1).

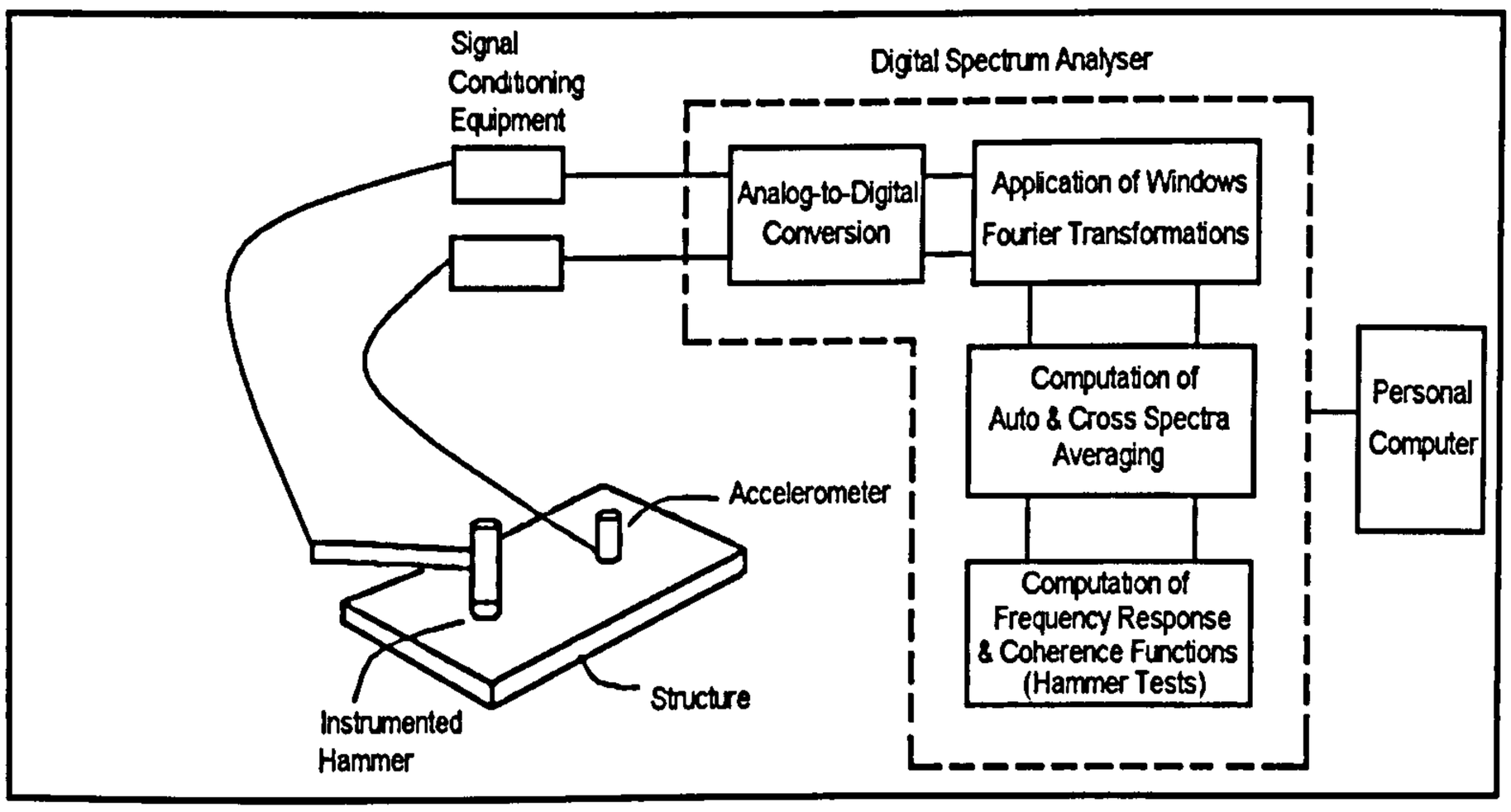

Figure A.1 - Equipment Set-up (after Halvorsen and Brown, 1977)

A description of each component and some of its features follows:

(a) 2 Endevco Isotron Piezoelectric Accelerometers Model 7754-1000 and Signal Conditioner Endevco Model 102

These accelerometers have a nominal sensitivity of 1 V/g and a resolution of 10^{-6} g. The sensitivity is the ratio of the output signal (in Volts) to the signal which is being measured (acceleration, expressed in units of gravity acceleration g). Great sensitivity is

necessary to measure the low level accelerations generated in vibrations at low frequencies. On the other hand, the resolution indicates the smallest acceleration that can be measured by the transducer. This means that below this value, it is not possible to distinguish the signal from the noise of the electronics of the accelerometer.

The accelerometers have a range of ± 5 g (i.e., they can detect accelerations up to these limits) and, in terms of their low frequency response, they present an error in amplitude of ± 5% and ± 5° in phase at a frequency of 0.2 Hz. The accuracy at this lower limit was satisfactory since the lowest natural frequency measured at the test footbridges was of 1.0 Hz.

The built-in electronics within the accelerometer case (identified by the trade name Isotron) are an important feature in transducers of this type intended for use in site tests. They reduce the high impedance of the piezoelectric sensor of the accelerometer, enabling long coaxial cables to be used without significant effects on the measured signal (McConnell, 1995). Further technical information about this transducer and its features can be found in the supplier's documentation (Endevco, undated) or in general textbooks about the subject (e.g., Dally *et al.* , 1993).

The accelerometers were mounted on levelled base plates and could be attached to measure accelerations in either the vertical or lateral direction (Plate A.1).

The accelerometers were powered by an Endevco Model 102 Signal Conditioner, having several user-defined amplitude magnification factors (gains). The nominal error of this unit at the lower frequency limit (lower cut-off frequency) was reported as a loss of 5% in amplitudes at a frequency of 0.1 Hz. Some measurements were carried out in the laboratory, in order to check the accuracy of the accelerometer and its signal conditioner in detecting low frequency vibrations. The accelerometers were placed in an actuator and subjected to sinusoidal excitations of different frequencies and amplitudes. The ratio between the calculated (theoretical) and measured peak accelerations are plotted in Fig. A.2, indicating that the accelerometers and signal conditioner could be used for detecting vibration signals having frequencies as low as 0.5 Hz.

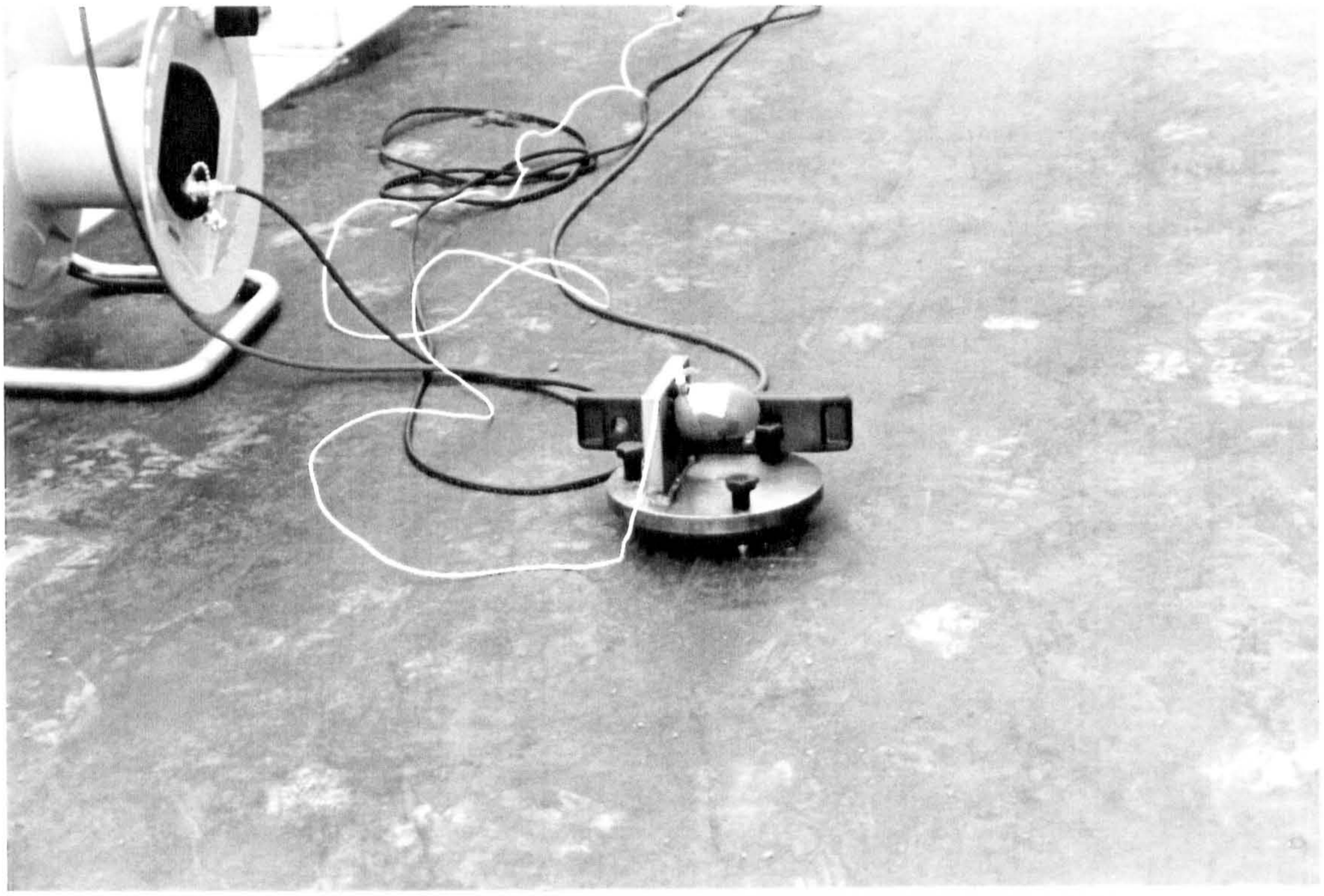

Plate A.1 - Accelerometer (with a protective capsule) mounted for measurements in the lateral direction

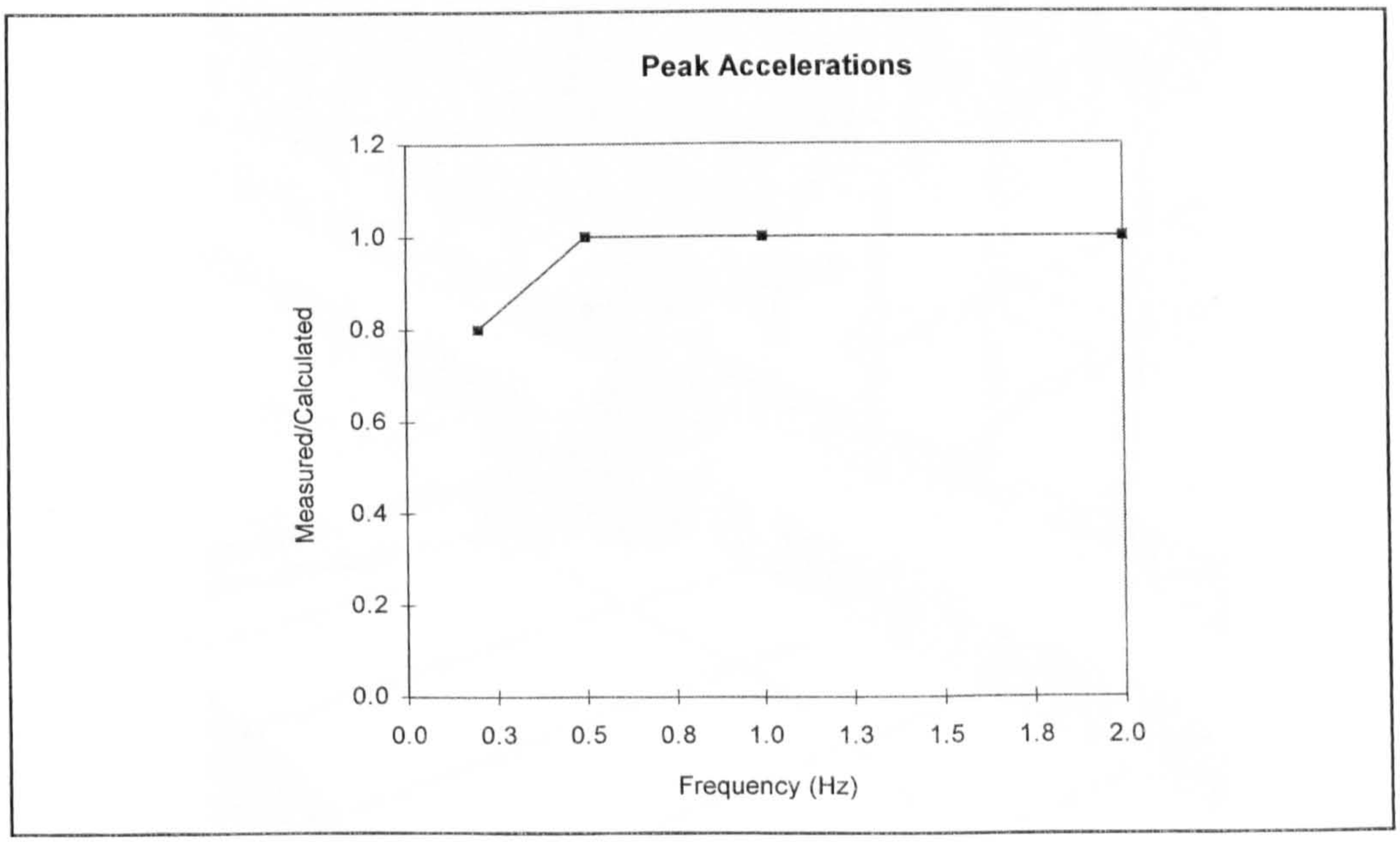

Figure A.2 - Losses on peak accelerations as a function of frequency

(b) Instrumented Hammer Dytran Model 5803A and Power Unit Dytran Model 4102B

A 5 kg instrumented hammer was adopted to excite the structure (Plate A.2). It has a force transducer installed within the hammer head, with a nominal sensitivity of 1 mV/Lb-f (0.22 mV/N). The input range of the device is 5V, giving a maximum impact of approximately 22 kN. Impact tips of different stiffness are provided, the softest tip (brown coloured) being the one preferably used since the energy of the impact is more concentrated in the low frequency range (Change, 1995). The hammer was powered by a unity gain battery-operated Power Unit.

Plate A.2 - Instrumented 5 kg Hammer

(c) Dual Channel Diagnostic Instruments PL-202 FFT Spectrum Analyser

This Spectrum Analyser was used to acquire and process data from all the tests carried out. It is a portable instrument, being easily operated by pressing buttons on its panel (Plate A.3). Time domain signatures and frequency domain functions can be obtained upon selection. The equipment operates with a bandwidth range up to 40 kHz.

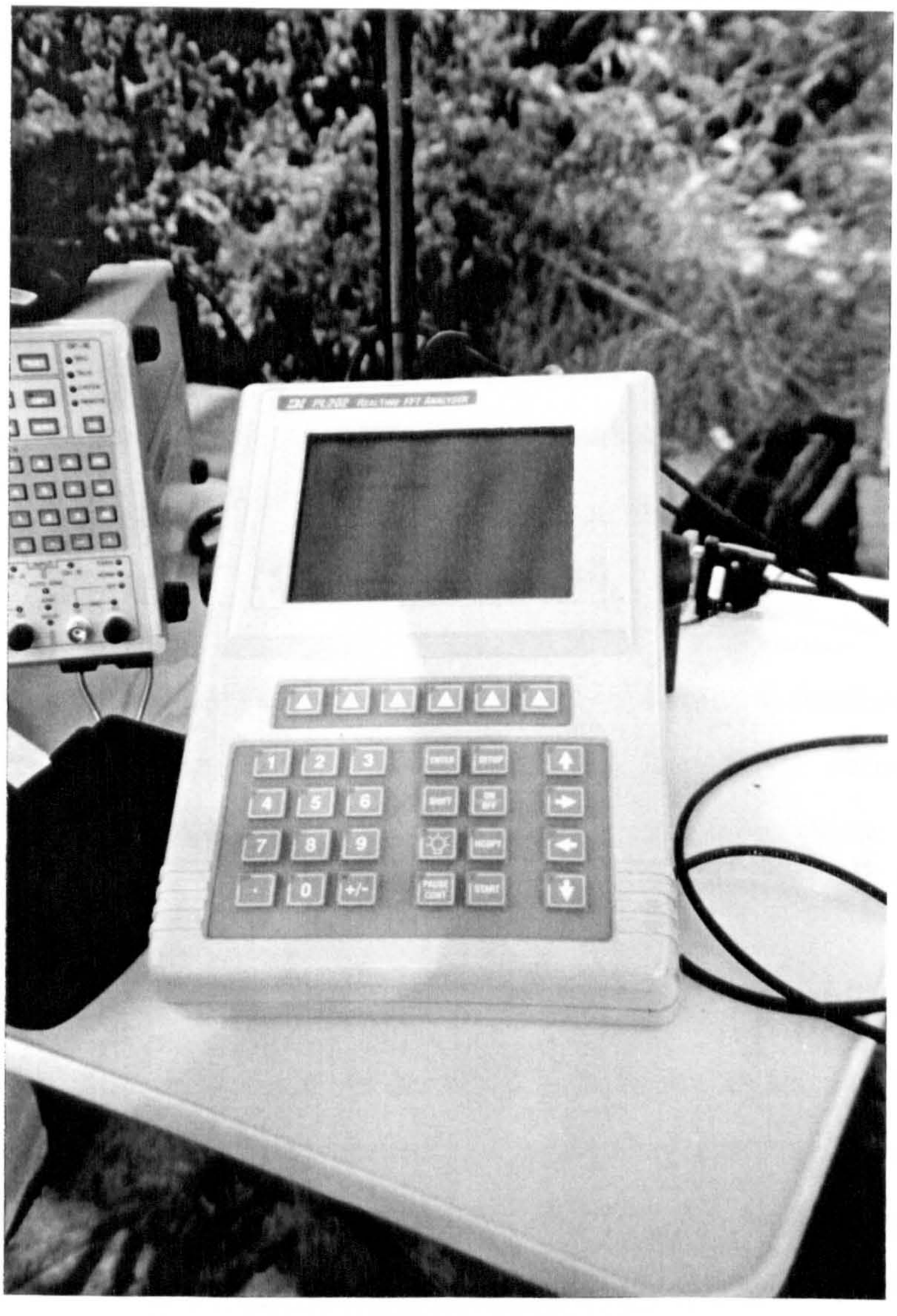

Plate A.3 - DI PL-202 Spectrum Analyser

The following parameters are of most interest for the acquisition of time domain signals: the longest acquisition time is 64 secs, with a maximum of 4096 points per channel. This gives a time interval of 0.015625 secs, related to a non-aliased frequency range f_c

of 25 Hz (Eq. 3.24). This proved to be a limitation during the acquisition of long time domain records from pedestrian tests.

Several spectral functions can be calculated. The Fourier Spectrum of each channel is the basic spectral function calculated, from which the other spectral functions are obtained. The amplitude of this one-sided Spectrum has units of RMS of the time domain input signal (DI Applications, undated). It may be noted that this is in accordance with the application of Eq. 3.13 and thus the calculation of the Fourier Spectrum by using Eq. 3.7.

The Power Spectral Density (PSD) is calculated from the Fourier Spectrum using Eq. 3.14. However, the actual display is the root square of the PSD, in order to keep the unit of the time domain input signal. A scaling (multiplying) factor is applied for the calculations of the root square of the PSD only, and for the Hanning window, it has a value of $\sqrt{2/3}$ (Rogers, 1995). This indicates that the adopted Hanning window is defined by multiplying Eq. 3.25 by two (see Section 3.2.2).

As can be noted, the identification of the aforementioned spectral functions and window were achieved by drawing a parallel between their theoretical definition with the information obtained from the references cited above. They were confirmed by experimentation, using a signal generator as a source of input signal to the spectrum analyser.

Several features of this instrument are described in its operating Manual (DI Operations, undated). Some of them are emphasised here since they are extremely important for using the spectrum analyser in hammer tests. The first one is the equipment trigger which can be set in a variety of ways. The trigger is set as a percentage of the maximum input range, this in turn also being defined by the user. A positive slope was adopted since the hammer impact generated an acquired peak having a positive value. A positive slope means that the acquisition will be initiated when the input signal increases in value, after it reaches the specified trigger level. A number of pre-trigger points can be selected, in order to begin the acquisition before the trigger level is reached and thus include the whole hammer peak in the acquired signal.

The second feature is the force/exponential window. The force window is specified as a percentage of the total acquisition time, defining the region of the hammer input signal which is preserved (see Fig. 3.7). The exponential window is applied to both channels, being defined as an exponential function $e^{-\gamma_e t}$. The parameter γ_e is given by the ratio of a user defined input value (varying from 1 to 10) to the acquisition time.

Finally, there is also the possibility of rejecting badly acquired signals from the averaging process. Nevertheless, as was discussed in Section 3.3.2.1, this would make it difficult to follow the changes in the frequency response function during the averaging process.

(d) 486 DX33 MHz Dual PC Notebook

This portable PC was part of the site test equipment since data needed to be downloaded occasionally from the spectrum analyser when its memory was full.